DOCTORAL THESIS

CONTRIBUTION OF SUMO TO THE REPLICATION OF EBOLA VIRUS

Santiago Vidal Freire

ESCOLA DE DOUTORAMENTO INTERNACIONAL DA
UNIVERSIDADE DE SANTIAGO DE COMPOSTELA
PROGRAMA DE DOUTORAMENTO EN MEDICINA MOLECULAR

SANTIAGO DE COMPOSTELA
2021

DECLARACIÓN DO AUTOR/A DA TESE

D./Dna. **Santiago Vidal Freire**

Título da tese: **Contribution of SUMO to the replication of Ebola virus**

Presento a miña tese, seguindo o procedemento axeitado ao Regulamento, e declaro que:

1) A tese abarca os resultados da elaboración do meu traballo.

2) De ser o caso, na tese faise referencia ás colaboracións que tivo este traballo.

3) Confirmo que a tese non incorre en ningún tipo de plaxio doutros autores nin de traballos presentados por min para a obtención doutros títulos.

4) A tese é a versión definitiva presentada para a súa defensa e coincide a versión impresa coa presentada en formato electrónico

E comprométome a presentar o Compromiso Documental de Supervisión no caso de que o orixinal non estea na Escola.

En **Santiago de Compostela**, **14 de Outubro de 2021**.

Sinatura electrónica

AUTORIZACIÓN DO DIRECTOR/TITOR DA TESE

D./Dna.**M. Carmen Rivas Vázquez**

En condición de: **Director/a**

Título da tese: **Contribution of SUMO to the replication of Ebola virus**

INFORMA:

Que a presente tese, correspóndese co traballo realizado por D/Dna Santiago Vidal Freire, baixo a miña dirección/titorización, e autorizo a súa presentación, considerandoque reúne os requisitos esixidos no Regulamento de Estudos de Doutoramento da USC, e que como director/titor desta non incorre nas causas de abstención establecidas na Lei 40/2015.

En **Santiago de Compostela**, **13 de October de 2021**

Sinatura electrónica

Yo, Santiago Vidal Freire, declaro no tener ningún conflicto de interés en relación con la tesis doctoral.

Santiago de Compostela, 14 de octubre de 2021

Esta tesis fue desarrollada en el Centro de Investigación en Medicina Molecular y Enfermedades Crónicas de la Universidad de Santiago de Compostela gracias a los proyectos (BFU-2017-88880-P), del Ministerio de Ciencia e Innovación y al proyecto (ED431G 2019/02) de la Xunta de Galicia. Tambien gracias al Contrato de iniciación a la investigación primera convocatoria 2017 del CiMUS y al contrato predoctoral (ED481A-2018/110) concedido por la Xunta de Galicia a través de la Consellería de Cultura, Educación y Ordenación Universitaria

AGRADECIMIENTOS

Antes de presentar el cuerpo del trabajo me gustaría poder tomarme unas líneas en las que poder dar las gracias.

Primero agradecer a mi directora de tesis y mentora científica por la oportunidad que me dio hace tiempo y por todo lo que me ha enseñado, la paciencia que ha tenido y la motivación continua que ha supuesto. Carmen jamás podría llegar a ser doctor sin tu ayuda y mi agradecimiento será eterno.

A mis padres y hermanas por todo el apoyo durante todos los años y por la confianza ciega que siempre han demostrado en mí. Por querer siempre que sacara la mejor versión y por ser un apoyo más grande de lo que creéis.

A mi abuelo por querer siempre entenderme.

A Lara por llegar a mi vida y darme una motivación más para hacer que alguien se sienta orgulloso de mí.

A Sandra por todo lo que has pasado y compartido conmigo, las noches, las tardes, las comidas en silencio y el verme sufrir. Por sacarme todas las sonrisas, por hacerme todos los planes, por cuidarme y entenderme como nadie, por tu compañía, por ser tú y por dejarme ser yo contigo. Gracias, un pedazo enorme de esta tesis te pertenece.

A Pablo y Dani por saber sacarme el laboratorio de la cabeza y hacerme disfrutar.

A mis compañeros de laboratorio: a Rocío por ser una persona increíble con la que es tan fácil compartir. A Ahmed por ser un guía magnífico del que solo he aprendido sin parar. A Yanis por estar siempre ayudando.

A todas las personas que habéis estado y que estaréis.

Gracias

Gracias al desarrollo de esta tesis se ha podido publicar la siguiente relación de artículos:

Expression of the Ebola virus VP24 protein compromises the integrity of the nuclear envelope and induces a laminopathy-like cellular phenotype.

Autores: Santiago Vidal[a] Maite Sánchez-Aparicio[b,c] Rocío Seoane[a] Ahmed El Motiam[a] Emily V. Nelson[d,e] Yanis H. Bouzaher[a] Maite Baz-Martínez[a,d] Isabel García-Dorival[f] Susana Gonzalo[g] Enrique Vázquez[h] Anxo Vidal,a César Muñoz-Fontela[d,e] Adolfo García-Sastre[b,c,i,j] Carmen Rivas[a,k]

[a]Centro de Investigación en Medicina Molecular (CIMUS), Universidade de Santiago de Compostela, Instituto de Investigaciones Sanitarias (IDIS), Santiago de Compostela, Spain. [b] Department of Microbiology, Icahn School of Medicine at Mount Sinai, New York, New York, USA. [c]Global Health and Emerging Pathogens Institute, Icahn School of Medicine at Mount Sinai, New York, New York, USA. [d] Bernhard Nocht Institute for Tropical Medicine, Hamburg, Germany. [e] German Center for Infection Research (DZIF), Partner Site Hamburg, Germany. [f]Institute of Infection, Veterinary and Ecological Sciences, University of Liverpool, Liverpool, UK. [g]Department of Biochemistry and Molecular Biology, Saint Louis University, School of Medicine, Saint Louis, Missouri, USA. [h]Centro Nacional de Investigaciones Cardiovasculares (CNIC) Carlos III, Madrid, Spain. [i]Division of Infectious Diseases, Department of Medicine, Icahn School of Medicine at Mount Sinai, New York, New York, USA. [j]The Tisch Cancer Institute, Icahn School of Medicine at Mount Sinai, New York, New York, USA. [k]Centro Nacional de Biotecnología, CSIC, Cantoblanco, Madrid, Spain.

Publicado en mBio (open acces) en julio de 2021. doi.org/10.1128/mBio.00972-21.

Índice de impacto: 7.867 (Q1); ISSN 2150-7511

Contribución de Santiago Vidal Freire: diseño e investigación experimental, escritura, análisis de resultados y preparación de figuras.

Los resultados publicados en este artículo son reproducidos en los capítulos resultados y discusión.

Regulation of the Ebola Virus VP24 Protein by SUMO.

Autores: Santiago Vidal,[a,b] Ahmed El Motiam,[a,b] Rocío Seoane,[a,b] Viktorija Preitakaite,[a] Yanis Hichem Bouzaher,[a,b] Sergio Gómez-Medina,[c,d] Carmen San Martín,[e] Dolores Rodríguez,[f] María Teresa Rejas,[g] Maite Baz-Martínez,[a,b,c] Rosa Barrio,[h] James D. Sutherland,[h] Manuel S. Rodríguez,[i,j] César Muñoz-Fontela,[c,d] Carmen Rivas[a,b,f].

[a]Centro de Investigación en Medicina Molecular (CIMUS), Universidade de Santiago de Compostela, Santiago de Compostela, Spain. [b]Instituto de Investigaciones Sanitarias (IDIS), Santiago de Compostela, Spain. [c]Berhard Nocht Institute for Tropical Medicine, Hamburg, Germany. [d]German Center for Infection Research (DZIF), Partner Site Hamburg, Hamburg, Germany. [e]Departamento de Estructura de Macromoléculas, Centro Nacional de Biotecnología-CSIC, Madrid, Spain. f Departamento de Biología Molecular y Celular, Centro Nacional de Biotecnología-CSIC, Madrid, Spain. [g]Centro de Biología Molecular Severo Ochoa (CSIC-UAM), Universidad Autónoma de Madrid, Madrid, Spain. [h]CIC bioGUNE, Derio, Spain. [i] Advanced Technology Institute in Life Sciences (ITAV) CNRS-USR3505, Toulouse, France. [j]IPBS-University of Toulouse III-Paul Sabatier, Toulouse, France.

Publicado en Journal of Virology en octubre de 2019 doi: 10.1128/JVI.01687-19CE. 2019.

Índice de impacto: 4.501 (Q1). ISSN: 1098-5514

Contribución de Santiago Vidal Freire: diseño e investigación experimental, escritura, análisis de resultados y preparación de figuras.

Los resultados publicados en este artículo son reproducidos en los capítulos resultados y discusión.

INDEX

TABLE OF CONTENTS

FIGURE INDEX

1. ABREVIATIONS

A549: human lung epithelial carcinoma cells
ATG: autophagy-related protein
ATP: adenosine triphosphate
ATPase: adenosine triphosphatase
BAF: barrier to autointegration factor
BiFC: bimolecular fluorescence complementation
BSA: bovine serum albumin
BSL4: biosafety level 4
BSRT7: baby hamster kidney (BHK-21)-derived cell line stably expressing T7 RNA polymerase
CARDS: caspase activation and recruitment domains
cDNA: complementary DNA
cGAS: cyclic GMP-AMP synthase
CHX: cycloheximide
cRNA: complementary positive-stranded RNA
CSF: colony stimulating factor
DAMP: damage-associated molecular pattern
DAPI: 4',6'-diamidino-2-phenylindole
DMEM: Dulbecco's modified Eagle's medium
DNA: deoxyribonucleic acid
dsRNA: double stranded RNA
EBD: Ebola virus disease
EBV: Epstein-Barr virus
EBOV: Ebola virus
eIF2α: eukaryotic initiation factor 2-α
ERK: extracellular signal-regulated kinase
EYFP: enhanced yellow fluorescent protein
FAT-10: human leukocyte antigen-F adjacent transcript 10
FUB1: fusaric acid biosynthesis protein 1
GAPDH: glyceraldehyde-3-phosphate dehydrogenase
GFP: green fluorescent protein
GP: glycoprotein
HA: hemagglutinin
HAUSP: herpesvirus-associated ubiquitin-specific protease
HCMV: human cytomegalovirus
HEK 293: human embryonic kidney 293 cells

Hela: human cervical adenocarcinoma cells
HHV-8: human herpesvirus-8
HIV: human immunodeficiency virus
hnRNP C1/C2: heterogenous nuclear ribonucleoprotein complex C1/C2
HSV-1: herpes simplex virus type 1
HTLV-1: human T-cell leukemia virus type 1
HUB1: homologous to ubiquitin 1
HUH-7: human-derived hepatoma cells
IAV: Influenza A virus
ICP0: infected cell protein 0
IFN: interferon
IFNAR: interferon α/β receptor
IRF3: interferon regulatory factor 3
IRF7: interferon regulatory factor 7
IKK: IκB kinase
IP: immunoprecipitation
ISG: interferon stimulated gene
ISRE: IFN-stimulated response elements
JAK: janus kinase
kb: kilobase
kDa: kilodalton
KPNA: Karyopherin α
L: EBOV RNA-dependent RNA polymerase
LAP: lamina-associated proteins
LB: Luria Bertani
LCMV: lymphocytic choriomeningitis virus
LEM: LAP2–Emerin–MAN
LGP2: laboratory of genetics and physiology 2
MAPK: mitogen activated protein kinase
MAVS: mitochondrial antiviral-signaling protein
MDA5: melanoma differentiation-associated protein 5
MOI: multiplicity of infection
NEDD8: neural precursor cell expressed developmentally down-regulated protein 8

NF-κB: nuclear factor kappa-light-chain-enhancer of activated B cells
NLS: nuclear localization signal
NP: nucleoprotein
NP40: Nonidet-P-40
NPC: nuclear pore complex
NPC-1: Nieman-Pick C1
OD: optical density
ORF: open reading frame
PACT: IFN-inducible dsRNA-dependent protein kinase activator A
PAGE: polyacrylamide gel electrophoresis
PAMP: pathogen-associated molecular patterns
PBS: phosphate buffer saline
PEI: polyethylenimine
PCR: polymerase chain reaction
PKR: protein kinase R
PML: promyelocytic leukemia protein
PML-NBs: PML nuclear bodies
PRRs: pattern recognition receptors
qRT-PCR: real time quantitative reverse transcription PCR
RIG-I: retinoic acid-inducible gene I
RIPA buffer: radioimmunoprecipitation assay buffer
RLRs: RIG-I-like receptors
RNA: ribonucleic acid
SAE: SUMO activating enzyme
SDS: sodium dodecyl sulfate
SENP: SUMO specific protease
sGP: soluble glycoprotein
sh: short hairpin
SIM: SUMO interacting motif
ssGP: small soluble glycoprotein
STAT: signal transducer and activator of transcription
SUMO: small ubiquitin-like modifier
TBK1: tank-binding kinase-1
TTBS: tween tris-buffered saline

TYK2: tyrosine kinase 2
U2OS: human bone osteosarcoma epithelial cells
UBLs: ubiquitin-like proteins
UbKO: ubiquitin with all lysines mutated to arginine
UFM1: ubiquitin-fold modifier 1
URM1: ubiquitin-related modifier 1
USP7: ubiquitin specific protease 7
Vero: African green monkey kidney epithelial cells
VLP: viral-like particles
VP24: viral protein 24
VP30: viral protein 30
VP35: viral protein 35
VP40: viral protein 40
WCE: whole cell extract

2. SUMMARY

2.1. RESUMO

O virus do Ébola (EBOV) descubriuse no ano 1977 e dende entón causa gromos de forma recorrente en rexións do centro e do oeste do continente africano. Aínda que normalmente o virus non sae deste continente, conseguiu chegar a rexións de Europa e América nos anos 2013-2016 poñendo en relevancia a súa capacidade de ser unha ameaza a nivel mundial e de se converter nun problema de saúde pública. EBOV é o axente causante da enfermidade do virus do Ébola (EBD). A EBD é unha febre hemorráxica asociada a alta letalidade, podendo chegar a una tasa de mortandade arredor do 90%. No gromo acontecido entre os anos 2013 e 2016 faleceron 28640 persoas por mor da infección por EBOV. Aínda que xa se aprobou unha vacina fronte ao virus, non existen fármacos efectivos para o tratamiento das persoas infectadas. O coñecemento dos mecanismos de patoxenicidade do virus é fundamental para o descubremento de dianas terapéuticas que permitan o control efectivo da enfermidade.

EBOV é un virus envolto, cunha apariencia filamentosa e cun xenoma de ácido ribonucleico (ARN) non segmentado de cadea simple e orientación negativa. O xenoma do virus codifica para 7 proteínas estruturais: a nucleoproteína (NP), a proteína viral (VP) 35 (VP35), VP40, a glicoproteína (GP), VP30, VP24, e a polimerase dependente de ARN (L). EBOV entra nas células por endocitose e macro-pinocitose e unha vez no interior da mesma o virus desprega toda unha batería de estratexias moleculares para evitar que os mecanismos antivirais da célula podan impedir a súa replicación no organismo e a súa dispersión na poboación.

As células recoñecen virus e axentes invasores a través de receptores de recoñecemento de patróns (PRR). Estes receptores son capaces de recoñecer moléculas que aparecen de forma recorrente en patóxenos, denominados patróns moleculares asociados a patóxenos (PAMPs) ou moléculas liberadas dende células infectadas ou danadas denominadas patróns moleculares asociados a dano (DAMPs). A activación destes receptores desemboca na síntese de interferón (IFN) e na activación e síntese de xenes estimulados por interferón (ISGs). O material xenético de microbios invasores é un dos PAMPs máis comúns. O xenoma destes microbios, independentemente da súa natureza, ARN

ou ácido desoxirribonucleico (ADN), é recoñecido por distintas proteínas citoplasmáticas coma o xen inducible por ácido retinoico (RIG) I, a proteína asociada á diferenciación a melanoma (MDA) 5 ou a proteína laboratorio de xenética e fisioloxía (LGP) 2. Unha vez detectan o xenoma de microbios invasores, estes sensores son capaces de activar a ruta de sinalización que desembocará na fosforilación dos factores reguladores do interferón (IRF) 3/7. Estas proteínas son factores de transcripción encargados de promover a síntese do IFN. Outras proteínas citoplásmicas tamén son capaces de recoñecer material xenético invasor. Un exemplo é a proteína quinase r (PKR), que recoñece o ARN de dobre cadea (dsRNA) o que leva á dimerización e fosforilación da proteína e a consecuente fosforilación do factor de iniciación da tradución de eucariotas 2 (eIF2)-α e desta maneira impide a síntese de proteínas nas células infectadas. O IFN sintetizado en resposta á infección viral actúa de forma paracrina nas células da contorna promovendo así o desencadeamento de vías de sinalización molecular antivirais nas células próximas á infectada. O IFN é recoñecido polo receptor do interferón α/β (IFNAR). A unión do IFN a estes receptores induce a activación das quinases janus (JAK) que a súa vez inducen a fosforilación das proteínas transdutoras de sinais e activadoras de transcrición (STAT), que unha vez fosforiladas son capaces de interactuar con proteínas da familia das importinas, encargadas de transportar estas proteínas do citoplasma ao núcleo da célula. Unha vez no núcleo celular, os factores de transcrición STAT fosforilados únense a rexións do ADN coñecidas como elementos de resposta estimulados por interferón (ISREs) e inducen a síntese de xenes estimulados polo interferón.

As proteínas VP35 e VP24 do EBOV son as encargadas de protexer ao virus da actividade antiviral da célula. Impedir que a célula recoñeza o material xenético do EBOV tras a infección e bloquear a ruta de sinalización que promove a síntese de IFN son actividades descritas para a proteína viral VP35. Esta proteína recoñece o dsRNA que se produce no transcurso da infección e interactúa con el para desta maneira ocultalo dos sensores celulares e evitar que a ruta RIG-I-MDMA5 promova a produción do IFN. VP35 é capaz tamén de inducir a modificación post traduccional de IRF3/7 pola proteína pequena

similar a ubiquitina (SUMO) e desta forma impedir a inducción da transcrición do IFN dependente destas proteínas. A interacción de VP35 có dsRNA tamén é crucial á hora de inhibir a actividade de PKR e desta forma impedir a inhibición da síntese de proteínas por dita quinase. A proteína VP24 do EBOV tamén leva a cabo distintas actividades coa fin de inhibir a sinalización do IFN e desta maneira impedir que se propague o estado antiviral. Por un lado, VP24 únese ás importinas α da célula e interfire coa unión de STAT fosforilado coas importinas e desta forma impide a traslocación da proteína fosforilada dende o citoplasma ao núcleo. Os factores de transcrición STAT non son as únicas proteínas afectadas pola interacción de VP24 coas importinas α. Así, VP24 tamén impide a translocación do complexo heteroxéneo ribonuclear C1/C2 dende o citoplasma ao núcleo da célula. Ademais, VP24 tamén pode interaccionar de forma directa con STAT1 e desta forma inhibir a síntese de IFN tipo III. Recentemente tamén se ten descrito que VP24 interacciona de forma directa con STAT3 demostrando un novo nivel de regulación do sistema inmune levado a cabo por esta proteína multitarea. Estudar os mecanismos de regulación das proteínas VP24 e VP35 do EBOV e identificar os seus interactores celulares pode permitirnos coñecer novas dianas terapéuticas de utilidade para combatir a infección por EBOV.

Un dos mecanismos máis importantes da regulación de proteínas é a través de modificacións post traducionais con proteínas da familia das ubiquitinas. As proteínas tipo ubiquitina (UBLs) son modificadores post traducionais que presentan o pregamento de suxeción tipo β característico da proteína ubiquitina. Esta familia de proteínas son reguladores chave dos procesos celulares esenciais. O proceso de conxugación das UBLs aos seus substratos é un proceso enzimático altamente regulado. A UBL máis estudada é a ubiquitina, que está encargada, entre outras funcións, da reciclaxe de proteínas. As enzimas encargadas de deconxugar a ubiquitina dos seus substratos son as deubiquitinases. Unha das deubiquitinases máis estudadas é a protease específica de ubiquitina (USP) 7. Esta proteína regula vías moleculares celulares esenciais como a replicación do ADN ou o ciclo celular e tamén xoga un papel moi importante no proceso de infección do virus do herpes simplex 1 así coma de outros virus. É importante destacar que

USP7 ten tamén a capacidade de funcionar coma una SUMO-deubiquitinase. As proteínas SUMO poden unirse de forma covalente a diferentes substratos nun proceso coñecido como SUMOilación. Este é moi dinámico e reversible grazas a acción de proteases específicas de SUMO (SENPs). As proteínas modificadas post traducionalmente por SUMO tamén poden interactuar con SUMO ou con outras proteínas SUMOiladas a través de unións non covalentes grazas aos dominios de interacción con SUMO (SIM). A interacción de SUMO cos seus substratos pode ter distintas consecuencias entre as que podemos citar a regulación da localización subcelular, modular a estabilidade do substrato modificado ou a interacción con outras proteínas. SUMO está implicado en diferentes procesos celulares coma pode ser a reparación do DNA, a transcripción, a inmunidade innata ou a división celular. Existen varios parálogos de SUMO pero son as proteínas SUMO1 e a SUMO2/3 as que se expresan en todos os tipos celulares e tecidos. As proteínas SUMO e sobre todo SUMO2/3 teñen un papel chave na resposta celular ao estrés. SUMO xoga un papel tan importante para a célula que unha alteración dos procesos de SUMOilación ou dos niveis de SUMO na célula soen ir ligados a diferentes condicións patolóxicas como poden ser cancros, enfermedades neurodexenerativas ou infección viral.

Entre as función esenciais de SUMO atopamos a regulación da resposta inmune da célula. SUMO modifica post traducionalmente numerosas proteínas antivirais entre as que atopamos diferentes compoñentes da ruta RIG-I-MDMA5 ou da ruta JAK-STAT. De feito, a SUMOilación parece ser esencial para a correcta propagación do estado antiviral. É por ista razón que un gran número de virus coma poden ser o virus *Influenza*, os rotavirus, os rubulovirus ou os enterovirus evolucionaron para poder interactuar con SUMO ou coa maquinaria de SUMOilación das células e aproveitarse desta interacción. No caso do EBOV dous estudos diferentes demostraron que este virus é capaz de afectar á SUMOilación de proteínas celulares e tamén de sacar proveito de SUMO para modificar as súas proteínas e desta forma aumentar a replicación viral. Coma mencionamos antes, a proteína VP35 do EBOV induce a SUMOilación de IRF3/7 para impedir a síntese de interferón. Ademais, a proteína de matriz VP40 do

EBOV emprega a maquinaria de SUMOilación para modificarse e desta forma favorecer a súa estabilidade. Ademais a proteína VP40 secuestra á proteína SUMO nas partículas tipo virión (VLPs) formadas por ela. Estudar a interacción de SUMO coas diferentes proteínas do EBOV pode resultar na descuberta dos mecanismos que as regulan e a identificación de novas dianas terapéuticas que permitan controlar a patoxenicidade do virus.

SUMO ten un papel moi importante na regulación da proteína da leucemia promielocítica (PML). PML é unha proteína inducida en resposta ao IFN e é o compoñente esencial dos corpos nucleares (NBs). Os PML-NBs son unha agrupación de proteínas con funcións reguladoras de diversos procesos coma a apoptose, a senescencia, a transcrición ou a estabilidade xenómica das células. A proteína PML tamén promove a SUMOilación de diversos substratos coma o supresor de tumores p53. PML tamén exerce actividade antiviral, razón pola que moitos virus desenvolveron mecanismos dirixidos contra esta proteína coa fin de impedir a súa actividade e así favorecer a súa replicación ou infectividade. Se EBOV posúe algún mecanismo para modular a actividade antiviral de PML descoñécese.

Debido a relevancia de VP24 na patoxenicidade do EBOV e coa finalidade de descubrir novos interactores desta proteína dous grupos de investigación levaron a cabo sendos estudos de proteómica. Nestes estudos a proteína de membrana emerina aparece formando parte do interactoma de VP24. Emerina é una proteína que interactúa con outras proteínas da membrana nuclear coma lamina A/C, lamina B e a proteína chamada barreira do factor de autointegración (BAF). A proteína emerina leva a cabo distintas funcións coma contribuir á estabilidade da membrana nuclear, regular diferentes rutas de sinalización ou funcionar como rexións de anclaxe dos telómeros. Estas proteínas son estruturalmente interdependentes, se unha destas falta as outras dúas non son capaces de ensamblarse de forma correcta. A relevancia da estrutura formada por estas proteínas ponse en evidencia tras a demostración de que mutacións en calquera dos xenes que codifican para estes compoñentes da membrana nuclear está ligado ao desenrolo de enfermidades moi severas que está agrupadas baixo o nome de laminopatías.

Unha das funcións da membrana nuclear é actúar coma unha barreira que impide a libre difusión de proteínas entre o núcleo e o citoplasma. Coma os virus necesitan frecuentemente gañar acceso a proteínas nucleares ou a diferentes componentes do núcleo das células, moitos deles desenvolveron mecanismos para atacar e comprometer a estabilidade da membrana nuclear. Estudar a posible interacción de VP24 coa proteína emerina e as consecuencias moleculares desta interacción podería ser de utilidade para descubrir novos mecanismos que axuden a entender a patoxenicidade do EBOV e podería servir para identificar novas dianas contra as que dirixir posibles terapias antivirais para o tratamento da EBD.

En base a todo o exposto, neste traballo propuxémonos como obxectivos estudar a modulación por SUMO das proteínas do EBOV VP24 e VP35, confirmar se VP24 interacciona con emerina e estudar os mecanismos e as consecuencias funcionais da interacción entre VP24 e dita proteína da membrana nuclear.

Os nosos resultados demostran que a proteína VP24 de EBOV se SUMOíla. SUMO conxúgase á lisina 14 de VP24. Ademais VP24 tamén interactúa con SUMO de forma non covalente grazas a presenza dun dominio SIM localizado entre os residuos 198 e 201 da proteína viral. A interacción de VP24 con SUMO é necesaria para que VP24 poda interactuar de forma eficiente coa proteína importina α e desta forma conseguir impedir a acumulación nuclear da proteína STAT fosforilada e bloquear a sinalización do IFN. Ademais, a SUMOilación de VP24 aumenta a estabilidade da proteína viral mentras que a interacción non covalente de VP24 con SUMO modula negativamente a súa mono-ubiquitinación. Neste traballo demostramos que VP24 se mono-ubiquitina en diferentes residuos sendo un deles a lisina 206. Esta mono-ubiquitinación é regulada pola deubiquitinase USP7 que interacciona có dominio SIM de VP24 e deconxuga a ubiquitina da proteína viral. A interacción de USP7 con VP24 a través do dominio SIM levounos a hipotetizar que a propia deubiquitinase USP7 podería ser un substrato de SUMO. Ensaios de SUMOilación in vivo confirmaron esta hipótese. Ademais, o estudo dun mutante de VP24 no residuo 206 revelou que a proteína era aínda máis efectiva á hora de bloquear a sinalización do IFN que a proteína silvestre o que nos leva a

suxerir que a mono-ubiquitinación de VP24 funciona como un regulador negativo da actividade da proteína viral sobre a sinalización do IFN.

Neste traballo tamén demostramos que a proteína VP24 interacciona cós compoñentes da membrana nuclear emerina, lamina A/C e lamina B. Esta interacción non depende de se a proteína exprésase fusionada a outras proteínas nin se ve afectada pola expresión de outras proteínas do EBOV. A interacción de VP24 con estas proteínas reduce a interacción emerina-lamina A/C e como consecuencia desta reducción promóvense a disrupción da membrana nuclear, cambios morfolóxicos nas células que expresan VP24, a activación da ruta da proteína quinase activada por mitóxeno (MAPK), a acumulación de dano no ADN e un aumento dos niveis da proteína xen estimulado por interferón 15 (ISG15). Ademais, a expresión de VP24 conleva unha diminución e translocación ao citoplasma da proteína nuclear BAF e a unha alteración da transcrición celular. Así, as células que expresan a proteína VP24 de EBOV presentan un aumento transcricional de xenes pro-inflamatorios e unha diminución de xenes regulados por BAF coma o factor estimulador de colonias (CSF), necesario para a correcta maduración de células dendríticas.

Outra nova actividade da proteína VP24 identificada neste traballo é a de promover a translocación ao citoplasma da proteína PML. Esta translocación de PML vai asociada con unha diminución na súa SUMOilación. VP24 tamén afecta á modificación por SUMO do supresor de tumores p53 inducida por PML e a unha alteración do ciclo celular. Demostramos que o dominio SIM en VP24 é esencial para inducir a translocación de PML ao citoplasma das células pero non se require para a interacción de PML con VP24, dado que o mutante no dominio SIM segue a interactúar con PML. Por último demostramos tamén que a traslocación de PML ao citoplasma inducida por VP24 favorece a interacción entre PML e a proteína de EBOV NP.

Os estudos levados a cabo neste traballo coa proteína VP35 do EBOV demostran que VP35 interacciona covalentemente con SUMO2 pero non con SUMO1. Ademais, VP35 interacciona con SUMO1 de forma non covalente. Observamos que tanto SUMO1 coma SUMO2 co-localizan con VP35 no citoplasma celular, pero que esta co-localización

viuse reducida en presenza da proteína de EBOV NP. Aínda que son necesarios máis estudos coa fin de identificar os residuos de VP35 que interaccionan con SUMO, o análise in silico da proteína parece indicar que estes localizaríanse no dominio C-terminal coincidindo có dominio de unión a dsRNA na proteína viral. Ademais, os nosos resultados indican que a presenza de SUMO podería favorecer a interacción de VP35 có dsRNA.

A identificación das proteínas SUMO coma reguladoras de VP35 e VP24 e da súa actividade sobre o sistema inmune lévanos a suxerir á interacción entre estas proteínas virais e SUMO como potenciais dianas terapeúticas para o tratamento da EBD. Os nosos resultados tamén revelan que a conxugación de ubiquitina a VP24 ten un efecto negativo sobre a actividade moduladora da vía do IFN. Estes resultados xunto con resultados previamente publicados que proban a utilización da maquinaria de SUMOilación da célula por parte do virus lévanos a propor que a regulación da conxugación de proteínas da familia da ubiquitina ás proteínas do EBOV podería ser explotada con fins terapéuticos.

Confirmando os resultados dos diferentes estudos de proteómica previamente publicados, neste traballo probamos que VP24 interacciona con emerina pero tamén con outros compoñentes da membrana nuclear coma lamina A/C e lamina B. Isto ten coma consecuencia unha alteración da interacción entre lamina A/C e emerina e a conseguinte rotura da membrana nuclear. Todo isto resulta nun dano na envolta nuclear e á inducción dun fenotipo celular similar ao que acontece nas laminopatías, caracterizado por un aumento na fosforilación da proteína quinase regulada por sinais extracelulares (ERK), a acumulación de dano no ADN ou a alteración da transcrición celular. Dacordo con este fenotipo celular que recorda as laminopatías, VP24 tamén induce a localización citoplásmica de PML. O impacto deste fenotipo na replicación, infectividade ou patoxenicidade do EBOV debe ser aínda estudado pero as novas actividades de VP24 identificadas neste traballo poderían axudar a comprender mellor os mecanismos de patoxenicidade do EBOV.

Hai que destacar que unha das consecuencias que resultan da expresión de VP24 e que podería estar ligada coa rotura da membrana

nuclear, a translocación de PML ao citoplasma da célula, tamén require da integridade do dominio SIM na proteína viral o que volve a indicar o importante papel que SUMO ten na regulación da actividade de VP24. Novos estudos son necesarios para poder identificar as consecuencias funcionais de esta translocación de PML ao citoplasma pero facilitar a súa interacción coa nucleoproteína NP do EBOV podería ser una delas.

En resumo, neste traballo demostramos a relevancia de SUMO e ubiquitina á hora de modular as proteínas VP24 e VP35 do EBOV. Tamén identificamos novas actividades da proteína VP24 que poderían explicar o fenotipo altamente inflamatorio observado nos pacientes infectados con EBOV así como a falta de maduración das células dendríticas infectadas có virus. Algúns interactores e rutas de sinalización identificadas neste estudo aparecen coma prometedoras dianas terapéuticas. Ademais os nosos descubrementos axudan a incrementar o coñecemento e entender mellor a infección por EBOV e a súa patoxenicidade.

2.2. SUMMARY

Ebola virus (EBOV) was discovered in the year 1976 and since then it has been caused recurrent outbreaks in the west and central regions of the African continent. Although usually the outbreaks are restricted to this continent, there were reported cases in the United States of America and Europe during the 2013-2016 outbreak, highlighting EBOV as a potential public health problem. EBOV is the causing agent of ebola virus disease (EBD). EBD is a hemorrhagic fever with a high lethality rate (up to 90%). During the 2013-2016 outbreak more than 28000 people died as a result of the infection by EBOV. Although a vaccine has been already approved against EBD, there is no effective drugs to treat infected people. Understanding the mechanisms of EBOV pathogenicity is fundamental to unveil novel therapeutic targets that may useful to control the disease.

EBOV is an enveloped, non-segmented negative-strand ribonucleic acid (RNA) virus with a filamentous appearance. The EBOV genome encodes for 7 structural proteins: the nucleoprotein (NP), the viral protein (VP) 35 (VP35), VP40, glycoprotein (GP), VP30, VP24, and the RNA-dependent RNA polymerase (L). EBOV enters the cells by endocytosis and macro-pinocytosis and once inside of the cell the virus uses multiple strategies to avoid the antiviral mechanisms of the host innate immune system.

Cells recognize invading and replicating viruses and agents through patterns recognition receptors (PRRs). These receptors are able to recognize molecules that are often found in pathogens, named pathogen-associated-molecular patterns (PAMPs) as well as molecules released from infected or damaged cells (damage-associated-molecular patterns (DAMPs). Activation of these receptors lead to the synthesis of interferon (IFN) and to the activation of interferon stimulated genes (ISGs). Genetic material from invading microbes is one of the most common PAMPs. RNA and deoxyribonucleic acid (DNA) genomes are recognized by distinct cytoplasmic sensors such as the retinoic acid-inducible gene (RIG) I, the melanoma-associated protein 5 (MDA5) and the laboratory of genetics and physiology (LGP) 2. Once they detect the genome from invading microbes, these sensors activate the signaling pathways that promote the activation of the interferon

regulatory factors (IRF) 3 and 7 leading to transcriptional activation of type I IFN. Other cytoplasmic proteins are also able to recognize genetic material from invading viruses. An example is the protein kinase r (PKR), that interacts with double stranded RNA (dsRNA). This interaction leads to the dimerization and phosphorylation of the protein and consequently to the phosphorylation of the eukaryotic initiation factor 2 (eIF2)-α and the inhibition of protein synthesis in the infected cells. The IFN synthesized is released from the cells and acts in a paracrine way promoting antiviral signaling in the surrounding cells. IFN is recognized by interferon α/β receptors (IFNAR). The union of IFN to these receptors induces the activation of members of the janus kinase (JAK) family. The JAK proteins then phosphorylate signal transducer and activator of transcription (STAT) factors inducing their homo or heterodimerization. P-STAT dimers then interact with proteins of the importin alpha family allowing their translocation from the cytoplasm to the nucleus of the cell. Once in the nucleus, STAT transcription factors bind to IFN-stimulated response elements (ISREs) in ISGs promoters modulating inflammation, cell cycle arrest, protein synthesis or recruitment of immune cells thus impeding viral infection or replication.

Two EBOV proteins, VP35 and VP24, have the ability to counteract host innate immune responses. VP35 protein blocks both dsRNA and virus-induced phosphorylation and activation of IRF3 inhibiting IFN transactivation. VP35 also induces the post-translational modification of IRF3/7 by small ubiquitin-like modifier (SUMO) proteins and in this way abolishes IFN transcription. The interaction of VP35 with dsRNA is also crucial to inhibit the activity of PKR and to avoid the inhibition of protein synthesis resulting from phosphorylation of eIF2α. EBOV VP24 protein also regulates immune responses. VP24 binds to importin α proteins and interferes with the interaction between phosphorylated STAT1 and the importins, inhibiting the translocation of the phosphorylated protein from the cytoplasm to the nucleus. The STAT transcription factors are not the only proteins affected by the interaction of VP24 with importins α. VP24 also avoids the translocation of heterogeneous nuclear ribonuclear complex C1/ C2. Besides, VP24 can also interact directly with STAT1 inhibiting the

synthesis of type III IFN. Recently, it has been described that VP24 can also interact with STAT3. Studying the mechanisms of regulation of VP24 and VP35 proteins and identifying their cellular interactors may help to discover new therapeutic targets for EBOV infection.

One of the most important mechanisms for protein regulation is the post-translational modification with proteins of the ubiquitin family. Ubiquitin-like proteins (UBLs) are post-translational modifiers that adopt the beta grasp-fold that is characteristic of the ubiquitin protein. UBLs are key regulators of essential cellular processes. Conjugation of UBLs to their substrates is an enzymatic process tightly regulated. Ubiquitin can be conjugated to substrates as a monomer (monoubiquitination) or it can be polymerized to form a chain (polyubiquitination). Deubiquitinases are the enzymes that deconjugate ubiquitin from their substrates. One of the most abundant deubiquitinating enzymes is ubiquitin specific peptidase 7 (USP7)/Herpesvirus-associated ubiquitin-specific protease (HAUSP). This protein regulates essential cellular pathways like replication of the DNA or cell cycle and it plays a very important role in the infection of herpes simplex type-1 virus. It is important to highlight that USP7 can also work as a SUMO-deubiquitinase.

SUMO proteins covalently bind to their substrates through a process known as SUMOylation. This is very dynamic and reversible process thanks to action of SUMO specific proteases (SENPs). SUMOylated proteins can also interact with SUMO or with other SUMOylated proteins in a non-covalent manner through SUMO interacting motifs (SIM). The interaction of SUMO with their substrates can have different consequences such as regulation of their subcellular localization, modulation of their stabilities or of their interaction with other proteins. SUMO is involved in different cellular processes including DNA repair, transcriptional regulation, innate immunity or cell division. There are five different SUMO paralogs but only SUMO1 and SUMO2/3 are expressed in all cell types. SUMO proteins, and especially SUMO2/3, have a key role in the cellular response to stress. Equilibrated SUMO levels and normal function of the SUMOylation machinery is essential for the correct function of cells. Therefore, a

deregulation of the SUMOylation pathway is linked to different pathological conditions such as cancer or viral infection.

SUMO plays an essential role in the regulation of innate immunity. SUMO modifies numerous antiviral proteins including different components of the RIG-I-MDMA5 and of the JAK-STAT pathways. In fact, SUMOylation seems to be essential for the correct establishment of antiviral state. That is why a big number of viruses such as influenza A virus, rotavirus, rubulovirus or enterovirus have evolved in order to interact with SUMO or the cellular SUMOylation machinery and take advantage of this interaction. In the case of EBOV two different studies showed that this virus is able to exploit the SUMOylation machinery to modify its own proteins and to increase viral replication. As we mentioned above, VP35 protein induces SUMOylation of IRF3/7 to inhibit IFN synthesis. Besides, the major matrix protein (VP40) of EBOV is a substrate for SUMO conjugation and this modification favors its stability. Moreover, SUMO protein has been detected inside viral-like particles (VLPs) formed by VP40. It has been then proposed that SUMO may be essential for EBOV life cycle. Targeting the interaction of SUMO with the EBOV proteins may represent a novel therapeutic strategy to block EBOV infection.

SUMO plays a crucial role in the regulation of the promyelocytic leukemia protein (PML). PML is a protein induced in response to IFN and it is an essential component of the nuclear bodies (NBs). The PML-NBs are dynamic structures enriched in SUMOylated proteins involved in the regulation of innate immunity during viral infection, apoptosis, senescence, transcription and genome stability. PML protein also promotes SUMOylation of different substrates such as the tumor suppressor p53. The relevance of PML in both intrinsic and innate immunity explains why viruses have evolved mechanisms to modulate PML or PML-NBs associated proteins. Whether EBOV modulates the antiviral activity of PML is still unknown.

Due to the relevance of VP24 in EBOV pathogenicity two research laboratories carried out different proteomic analyses in order to discover new interactors for this viral protein. In these studies emerin protein was identified as part of the interactome of VP24. Emerin is a nuclear membrane component that interacts with other nuclear

membrane proteins such as lamin A/ C, lamin B and the protein barrier to autointegration factor (BAF). These proteins are structurally inter-dependent, if one of them is missing or altered, the other two fail to assemble correctly. The relevance of the nuclear envelope is evidenced by the demonstration that mutations in any of the genes that codify for these components of the nuclear membrane are linked to the development of severe diseases grouped as laminopathies.

Nuclear membrane forms a barrier that avoids free diffusion of proteins between cytoplasm and nucleus. Since viruses frequently need access to nuclear proteins or to different nuclear components, many of them have developed mechanisms to attack and engage the stability of the nuclear membrane. Studying the possible interaction of VP24 with the protein emerin and the molecular and functional consequences of this interaction may be useful to better understand the pathogenicity of EBOV and to identify new druggable targets.

Altogether these results led us to propose the following objectives: to study the modulation by SUMO of the proteins VP24 and VP35 of EBOV, to evaluate the potential interaction of VP24 with emerin and to study the mechanisms and the functional consequences of this interaction.

Our results show that VP24 protein is SUMOylated. SUMO is conjugated to lysine 14 of VP24. Moreover, VP24 also interacts with SUMO in a non-covalent manner through a SIM domain (198-201 amino acid residues of the viral protein). VP24-SUMO interaction is facilitating the interaction of the viral protein with importin α and it is essential to avoid nuclear accumulation of p-STAT protein and to inhibit IFN signaling. In addition, VP24 SUMOylation also increases its stability while non-covalent interaction of VP24 with SUMO negatively modulates its mono-ubiquitination. In this work we show that VP24 is mono-ubiquitinated in different residues including the lysine residue 206. Mono-ubiquitination of VP24 is negatively regulated by the deubiquitinase USP7. USP7 interacts with VP24 through its SIM domain and deconjugates ubiquitin from the viral protein. USP7-VP24 interaction through the SIM domain led us to hypothesize that USP7 could be a SUMO substrate. *In vivo* SUMOylation assays confirmed this hypothesis. Moreover, the study of

a VP24 mutant protein in residue 206 revealed that this protein is more effective blocking IFN signaling than the wild-type protein which led us to suggest that to mono-ubiquitination negatively regulates the ability of VP24 to block IFN signaling.

In this work we also show that VP24 protein interacts with the nuclear membrane components emerin, lamin A/C and lamin B. This interaction was not affected by the expression of other EBOV proteins. Importantly, binding of VP24 with these proteins reduces emerin-lamin A/C interaction and, consequently, it promotes the disruption of the nuclear membrane. Furthermore, expression of VP24 induces morphological changes, activation of the mitogen activated kinase (MAPK) pathway, accumulation of DNA damage and upregulation of interferon stimulated gene 15 (ISG15) levels. Together with these changes, expression of VP24 induces the cytoplasmic translocation of the nuclear protein BAF and its downmodulation, as well as an alteration of the cellular transcription. Cells expressing VP24 protein showed transcriptional upregulation of pro-inflammatory genes and downmodulation of genes regulated by BAF, including the colony stimulator factor (CSF), involved in the correct maturation of dendritic cells.

Here we also demonstrate that VP24 promotes the nucleus to cytoplasm translocation of PML. This translocation was associated with a decrease in PML SUMOylation and with a reduction of the SUMOylation of p53 tumor suppressor protein induced by PML. Finally, our data revealed that the SIM domain in VP24 is essential to induce the translocation of PML to the cytoplasm of the cells but it is not required for the PML-VP24 interaction. Interestingly, the PML cytoplasmic translocation induced by VP24 favors the interaction between PML and EBOV NP protein.

Our studies with the EBOV VP35 protein revealed that VP35 interacts covalently with SUMO2 but no with SUMO1. In addition, VP35 interacts with SUMO1 in a non-covalent way. We observed that SUMO1 and SUMO2 co-localize with VP35 in the cell cytoplasm but this co-localization was reduced in presence of EBOV NP protein. More studies are necessary in order to identify the VP35 residues interacting with SUMO. However, *in silico* analysis of the protein seems to indicate

that this interaction occurs through the dsRNA binding domain in VP35. Furthermore, our results indicate that the presence of SUMO could favor the VP35-dsRNA interaction.

Identification of SUMO proteins as regulators of VP35 and VP24 proteins and of their immunomodulatory activities led us to suggest that the interaction of these viral proteins with SUMO may be therapeutic targets for the treatment of EBD. Our results also reveal that the conjugation of ubiquitin to VP24 has a negative effect on its modulatory activity on the IFN signaling pathway. These results together with previously published data reveal the relevance of UBLs for EBOV and led us to propose that regulation of the conjugation of UBLs to EBOV proteins may have therapeutic applications.

Confirming the results of the different proteomic analysis previously published, in this work we demonstrated that VP24 interacts with emerin but also with other components of the nuclear membrane such as lamin A/C and lamin B. As a consequence of this binding, the interaction between lamin A/C and emerin is reduced and nuclear membrane is disrupted, resulting in the induction of a laminopathy-like cellular phenotype, characterized by an increase in phosphorylation of the extracellular signal-regulated kinase (ERK), accumulation of DNA damage and alterations in cellular transcription. In agreement with the induction of a laminopathy-like phenotype, VP24 also promotes the cytoplasmic localization of PML. The impact of this cellular phenotype in the replication, infectivity or pathogenicity of EBOV needs to be further studied but the novel activities of VP24 identified in this work have help us to better understand the pathogenicity of EBOV.

Importantly, one of the consequences that result of the expression of VP24 and that could be linked to nuclear membrane disruption, the translocation of PML to the cytoplasm, also requires of the integrity of the SIM domain in the viral protein which indicates the important role of SUMO in the regulation of VP24 activity. New studies are necessary to identify the functional consequences of this PML translocation but facilitating PML interaction with EBOV nucleoprotein NP could be one of them.

In summary, here we show the relevance of SUMO and ubiquitin as modulators of VP24 and VP35 proteins of EBOV. In addition, we

identified novel activities for VP24 protein that could explain the inflammatory phenotype observed in the patients infected with EBOV and the lack of maturation of dendritic cells infected with EBOV. Interactors and signaling pathways identified in this study are promising therapeutic targets. Finally, our findings increase our knowledge on EBOV infections and pathogenicity.

3. INTRODUCTION

3.1. EBOLAVIRUS HISTORY

Ebola virus (EBOV) is a highly pathogenic virus causing regular outbreaks since its discovery in 1976 (Bowen et al., 1977; Johnson et al., 1977). EBOV is responsible for the ebola virus disease (EBD), characterized as a hemorrhagic fever with a high lethality rate (up to 90%) (Emond et al., 1977). *Ebolavirus* is one of the six genera, together with *Marburgvirus, Cuevavirus, Dianlovirus, Striavirus, and Thamnovirus*, belonging to *Filoviridae* family in the order Mononegavirales (Kuhn et al., 2019). The genus *Ebolavirus* has six species among which the species *Zaire ebolavirus, Sudan ebolavirus*, and *Bundibugyo ebolavirus* have caused a highly fatal disease in people. *Tai Forest ebolavirus* is reported to cause just one case of severe but non-fatal disease. In contrast, *Reston ebolavirus* has never been identified to cause disease in people. *Bombali ebolavirus* pathogenicity in humans has still to be addressed (Kuhn et al., 2019; Martell et al., 2019). The first EBOV outbreak was detected in the Democratic Republic of Congo and in South Sudan (Bowen et al., 1977; Johnson et al., 1977). The proximity both geographically and temporally between them led the scientific community to believe that both outbreaks were caused by the same specie, but it turned out to be caused by two different EBOV species, *Sudan ebolavirus*, and *Zaire ebolavirus* (McCormick et al., 1983; Richman et al., 1983). In the following years, ecological studies were carried out to understand how these two different species emerged so rapidly in the human population. All of these studies pointed out that humans can become infected with EBOV after direct contact with blood or bodily fluids from an infected person or animal. The virus can infect other primates, but they are likely dead-end hosts for the virus and not reservoir species. So far Old World fruit bats, predominant in tropical rainforest areas, are suspected to be the most likely reservoirs for EBOV as they carry the virus but do not succumb to it (Leroy et al., 2005). Most outbreaks in history affected central and west Africa. The largest outbreak so far took place during 2013-2016 and affected more than 28640 people, with cases reported in the United States of America, Spain, Italy and the United Kingdom. The last outbreak started in 2020 and it was declared over in June it was

declared over in June 2021 (Figure 1). Molecular studies to better understand host-virus relations are needed in order to develop therapies to reduce the mortality ratio in forthcoming outbreaks.

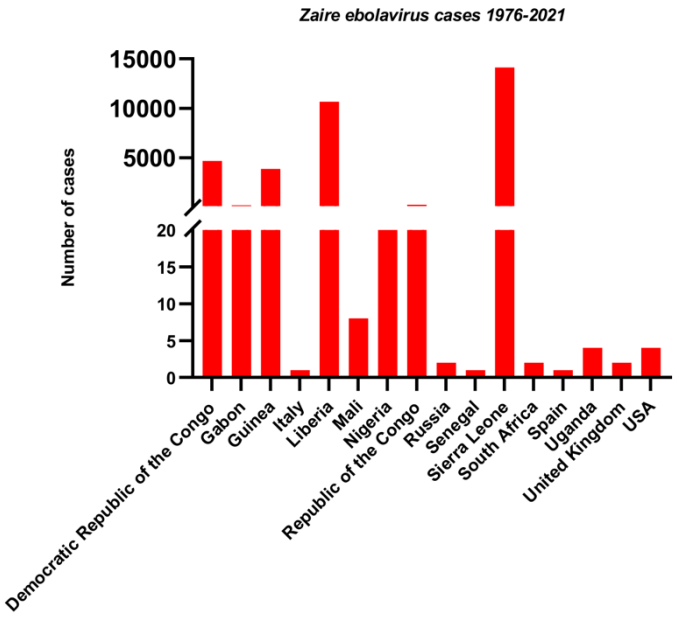

Figure 1. Geographical distribution of EBOV cases in the world according to World Health Organization reports. Own elaboration.

3.2. EBOLA VIRUS GENOME AND CYCLE OF INFECTION

EBOV is an enveloped, non-segmented negative-strand ribonucleic acid (RNA) virus (Geisbert, 2015) with a filamentous appearance. EBOV genomes are about 19 kilobases (kb) and encode for 7 structural proteins. The order of the EBOV genes is: 3'-leader-nucleoprotein (NP)-viral protein (VP) 35 (VP35)-VP40-glycoprotein (GP) -VP30-VP24- RNA-dependent RNA polymerase (L)-trailer-5'(Geisbert, 2015; Kiley et al., 1988). The GP gene encodes for three different products due to transcriptional editing by L: the full-length envelope protein GP, the nonstructural soluble glycoprotein (sGP) and the small soluble GP (ssGP) The majority of GP gene transcripts are

unedited and encode sGP. Full-length GP is encoded by two different open reading frames (ORFs) by RNA editing and forms a trimer on the virion surface being essential for the entry of virus into the cell. Although the function of sGP is still unclear, it has been reported its ability to neutralize anti-GP antibodies (Ito et al., 2001; Mohan et al., 2012; Sanchez et al., 1996; Volchkov et al., 2005, 1995). The ribonucleoprotein complex of EBOV is formed by NP, VP30, VP35 and L proteins (Geisbert, 2015). VP40 serves as the matrix protein and mediates viral particle formation (Hoenen et al., 2010; Jasenosky et al., 2001; Timmins et al., 2001). VP24 is a multifunctional structural protein first described as needed for plasma membrane interaction (Han et al., 2003) but recently it has been demonstrated that it lacks direct lipid binding properties, discarding this classical role for VP24 (Su and Stahelin, 2020).

EBOV requires endocytosis and macro-pinocytosis for viral entry (Nanbo et al., 2010; Saeed et al., 2010). As many other filoviruses, EBOV uses a wide range of receptors for attachment to target cells (Alvarez et al., 2002; Kondratowicz et al., 2011; Matsuno et al., 2010; Shimojima et al., 2006; Simmons et al., 2003), which can explain its broad tissue tropism. After EBOV enters the cell, releases its genetic material into the cytoplasm by fusion of the viral membrane envelope with the membrane of a late endosomal compartment. Within the acidic environment of the endosome GP protein is processed by proteolytic cleavage to yield a protein able to recognize the late intracellular endosome receptor Niemann-Pick C1 (NPC-1). In fact, fibroblasts derived from patients lacking NPC-1 receptor are resistant to EBOV infection (Carette et al., 2011). Moreover, small molecules inhibiting NPC-1 binding to GP inhibit EBOV infection (Côté et al., 2011). Recently, crystal structure of GP bound to NPC-1 has been obtained (Wang et al., 2016). After viral fusion, the ribonucleoprotein complex is released from the virion and used as a template for synthetizing complementary positive stranded RNA (cRNA) in the form of a ribonucleoprotein. cRNA then generates viral genomic RNA to be packaged into the virions. GP, VP40, and VP24 proteins show a critical role in orchestrating virion packaging (Hoenen et al., 2006; Huang et al., 2002; Ito et al., 2001; Johnson et al., 2006; Licata et al., 2004).

Assembly of the viral particles begins with the nucleocapsids formation which accumulate in the perinuclear region and are transported to the budding sites at the plasma membrane. The coordinator of the virus assembly and budding is VP40, the most abundant protein in the virions that when expressed alone is able to assemble into viral-like particles (VLPs) morphologically indistinguishable from authentic virions that are released from the cells (Jasenosky et al., 2001; Timmins et al., 2001).

3.3. EBOLA VIRUS EVASION OF INNATE IMMUNITY

Invading and replicating viruses are recognized by the host via cellular pattern recognition receptors (PRRs). These proteins are capable of recognizing molecules often found in pathogens, (pathogen-associated-molecular patterns, PAMPs) and molecules released from infected or damaged cells (damage-associated-molecular patterns, DAMPs) (Jounai et al., 2013). This recognition is crucial for activation of the innate immune system and the propagation of an antiviral state through interferon (IFN) synthesis or via induction of IFN stimulated genes (ISGs). Genetic material from invading microbes is one of the major PAMPs. Nucleic acid sensors are present in different subcellular compartments and are able to differentiate between deoxyribonucleic acid (DNA) and RNA genomes (Jounai et al., 2013). One of the most relevant sensors for RNA is the helicase retinoic acid-inducible gene I (RIG-I). The other two components of the family of RIG-I-like receptors are melanoma-associated protein 5 (MDA5) and laboratory of genetics and physiology 2 (LGP2) (Rehwinkel and Gack, 2020). These proteins have a central helicase domain, and a C-terminal RNA binding domain (Leung and Amarasinghe, 2012). MDA5 and RIG-I comprise the tandem caspase activation and recruitment domains (CARDs) in the N-terminus of the protein which is required for their association with the adapter molecule mitochondrial antiviral-signaling protein (MAVS). This association leads to the recruitment of downstream signaling molecules such as tank-binding kinase-1 (TBK1) and IκB kinase ε (IKKε) to activate the IFN regulator factor 3 (IRF3) and 7 (IRF7), leading to transcriptional activation of type I IFN (Brisse and Ly, 2019). This CARD domain is absent in LGP2 allowing LGP2 to negatively

modulate RIG-I and MDA5 signaling (Rodriguez et al., 2014). Once IFN is synthesized and released from the cells it acts in a paracrine way promoting antiviral signaling in the surrounding cells (Samuel, 2001). Type I IFN is recognized by the IFN α/β receptors (IFNAR) 1 or 2. These receptors interact with members of the janus kinase (JAK) family. The JAK proteins JAK1 and tyrosine kinase 2 (TYK2) then phosphorylate signal transducer and activator of transcription (STAT) factors inducing their homo or heterodimerization (Horvath, 2004). P-STAT dimers interact with proteins of the importin alpha family allowing their nuclear import (Platanias, 2005). Then, STAT transcription factors bind to IFN-stimulated response elements (ISREs) in ISGs promoters modulating inflammation, cell cycle arrest, protein synthesis or recruitment of immune cells thus impeding viral infection or replication (McNab et al., 2015). IFN signaling is not restricted only to the JAK-STAT pathway. Another relevant cytoplasmic protein and sensor for double stranded RNA (dsRNA) is the protein kinase R (PKR). PKR is activated after binding to dsRNA through its dsRNA-binding

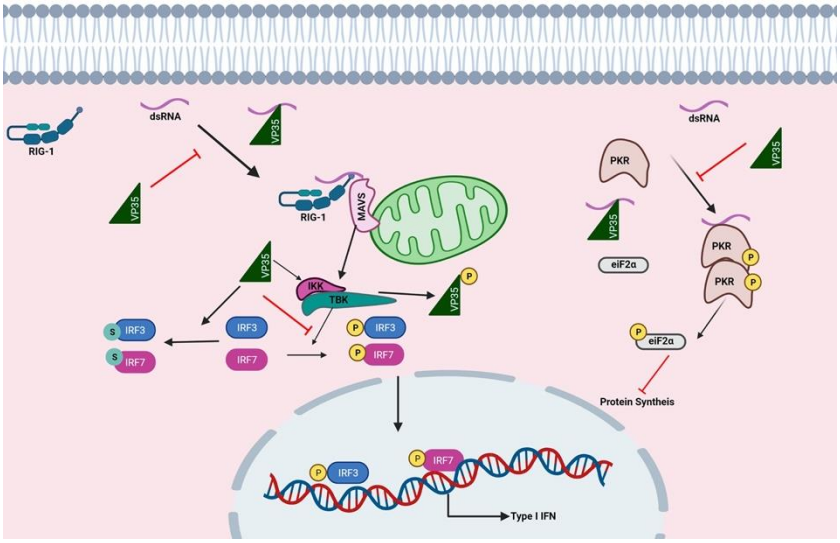

Figure 2. Inhibition of the IFN signaling pathway by VP35. Designed with biorender.com

domain (Mayo and Cole, 2017). This interaction induces its autophosphorylation and the phosphorylation of the α-subunit of

eukaryotic initiation factor 2 (eIF2α) and consequently its inactivation and the shut-down of protein synthesis (Proud, 2005). This inhibition of protein synthesis contributes to the control of viral replication by PKR. In addition, it has been proposed that the activation of the nuclear factor kappa-light-chain-enhancer of activated B cells (NF-κB) pathway by PKR also contributes to its antiviral activity (Pindel and Sadler, 2011).

The ability of EBOV to counteract host innate immune responses is considered an important component of viral pathogenesis. So far, two out of the 7 EBOV structural proteins, namely VP35 and VP24, have been demonstrated to be linked to the inhibition of both type I and type II IFN responses in target cells, resulting in a defect in dendritic cell maturation, diminished activation and proliferation of T cells and lymphopenia, a key characteristic of EBOV disease (Gupta et al., 2001; Harcourt et al., 1998). VP35 was the first EBOV protein described to abolish IFN induction (Basler et al., 2000) (figure 2). VP35 has been reported to downmodulate IFN-β transcription and to inhibit both virus and dsRNA-induction of IFN (Basler et al., 2000). Several molecular mechanisms mediate the inhibition of IFN transactivation by VP35. VP35 protein blocks both dsRNA and virus-induced phosphorylation and activation of IRF3 (Basler et al., 2003). The molecular mechanism by which VP35 inhibits IRF3 phosphorylation is linked to its ability to bind and sequester dsRNA intermediates and RIG-I-like receptors (RLRs) activity. In addition, VP35 binds to the IFN-inducible dsRNA-dependent protein kinase activator A (PACT), inhibiting PACT-RIG-I interaction and PACT-induced RIG-I adenosine triphosphatase (ATPase) activity (Luthra et al., 2013). Other VP35 interactors are the IRF kinases TBK-1 and IKKe. VP35 interacts with TBK-1 and IKKε and inhibits the interaction between these kinases and their substrates, IRF3 and IRF7 (Prins et al., 2009). But IRF3 and IRF7 activities are also regulated by other post-translational modifications. Thus, it has been proposed that activation of Toll-like receptor and RIG-I-like receptor signaling pathways induce the post-translational modification of IRF3 and IRF7 by small-ubiquitin modifier (SUMO) as a mechanism contributing to post-activation attenuation of IFN production. It is not then unexpected that some viruses have developed strategies to induce

the modification of IRF3 or IRF7 by SUMO (Kubota et al., 2008). Induction of conjugation of IRF7 and IRF3 to SUMO is another mechanism employed by VP35 to repress IFN transcription (Chang et al., 2009). Moreover, VP35 counteracts the antiviral action of IFN in infected cells thanks to its ability to suppress the pathway activated by PKR (Feng et al., 2007). Although the N-terminal domain of VP35 is required for several VP35-mediated functions, residues that are critical for dsRNA binding in VP35 are sufficient for IFN inhibition (Cárdenas et al., 2006; Di Palma et al., 2019; Leung et al., 2009).

As mentioned before, VP24 is the other key EBOV protein for regulating immune response. IFN binding to their receptors led to the activation of JAKs, which phosphorylate STATs transcription factors leading to their dimerization, importin-mediated nuclear translocation,

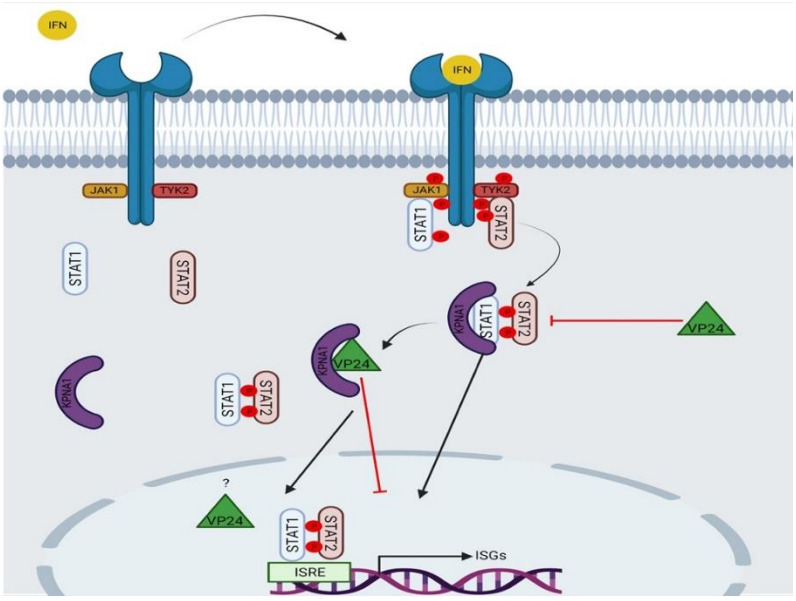

Figure 3. Ebola virus VP24 inhibition of IFN signaling. Designed with biorender.com

and activation of their transcriptional activity (McBride et al., 2002, 2000; Sekimoto et al., 1997; Stark et al., 1998). Expression of EBOV VP24 does not abolish STAT1 phosphorylation but inhibits its nuclear

accumulation (Reid et al., 2006). The ability of VP24 to inhibit p-STAT1 nuclear translocation correlates with its ability to interact with the components of the karyopherin alpha (KPNA) family KPNA1, KPNA5, and KPNA6, and to inhibit their interaction with phosphorylated-STAT1 (Reid et al., 2007). Mutational and structural studies revealed that VP24 recognizes a non-classical nuclear localization signal (NLS) binding site in the karyopherin that is required for the nuclear transport of p-STAT1 (Reid et al., 2007, 2006). In addition, although VP24 does not alter the nuclear import of the vast majority of karyopherin cargos (Xu et al., 2014), other karyopherin substrates may be affected. Thus, VP24 prevents the binding of heterogenous nuclear ribonuclear protein complex C1/C2 (hnRNP C1/C2) (Shabman et al., 2011) to karyopherin, negatively modulating its nuclear import (figure 3). The interaction of VP24 with karyopherin is not only critical for modulating the host immune system but it is also important for maintaining the stability of VP24 (Schwarz et al., 2017). There are other molecular mechanisms by which VP24 contributes to immune suppression. Thus, VP24 can directly interact with STAT1 (Zhang et al., 2012) and this interaction is essential for the inhibition of type III IFN gene expression by the viral protein (Guito et al., 2017; Schwarz et al., 2017). Furthermore, VP24 interacts with STAT3 in a karyopherin-independent manner and antagonizes STAT3 signaling by an unclear mechanism (Harrison et al., 2021). Therefore, VP24 and VP35 are considered perfect targets for drug development against Ebola virus infection. A better understanding of the regulation of their activities is critical for the development of antiviral therapies to improve the survival of infected patients. Post-translational modifications are key regulators of biological functions of proteins and may be used as novel therapeutic targets in EBOV infection.

3.4. UBIQUITIN AND SUMO

Ubiquitin-like proteins (UBLs) are post-translational modifiers that adopt the beta grasp-fold that is characteristic of the ubiquitin protein (van der Veen and Ploegh, 2012). Many UBL proteins have been described including neural precursor cell expressed

developmentally down-regulated protein 8 (NEDD8), human leukocyte antigen-F adjacent transcript 10 (FAT-10), ISG15, SUMO1, 2, 3, 4, 5, autophagy-related protein (ATG) 8, ATG12, fusaric acid biosynthesis protein 1 (FUB1), homologous to ubiquitin 1 (HUB1), ubiquitin-related modifier 1 (URM1) and ubiquitin-fold modifier 1 precursor (UFM1) (Hochstrasser, 2009). All UBLs are covalently coupled to target proteins via isopeptide bonds between C-terminal diglycine motifs and ε-amino groups in lysine residues of target proteins through the sequential action of evolutionary related enzymes named E1, E2, and E3. This process can be reversed through the action of UBL-deconjugating enzymes that remove UBLs from substrates (Kerscher et al., 2006). Conjugation of UBLs to target proteins regulate their activity, stability, subcellular localization, and macromolecular interactions (van der Veen and Ploegh, 2012). Modification of proteins by UBLs plays an important role in many cellular processes such as differentiation, cell cycle progression, cell division and modulation of innate immunity (Kerscher et al., 2006; van der Veen and Ploegh, 2012).

Ubiquitin can be conjugated to substrates as a monomer or it can be polymerized to form a chain. A monomer of ubiquitin can be conjugated to one or more sites on a substrate, referred as mono-ubiquitination or multi-mono-ubiquitination, respectively. The variety of functions associated with protein ubiquitination requires exquisite regulation (Komander and Rape, 2012; Swatek and Komander, 2016). The precise control of deubiquitination is a critical component of the ubiquitin signaling cascade. One of the most abundant deubiquitinating enzymes is ubiquitin specific peptidase 7 (USP7)/Herpesvirus-associated ubiquitin-specific protease (HAUSP). USP7 was first described as an interactor of the infected cell protein 0 (ICP0) from herpes simplex virus type-1 (HSV-1) (Everett et al., 1997). Later on, it was found that USP7 has many sustrates and plays a key role in cell cycle, DNA repair and chromatin remodeling, among other biological activities (Al-Eidan et al., 2020). Interestingly, USP7 also can deubiquitinate SUMO and by doing so it contributes to modulate levels of SUMO (Lecona et al., 2016).

In vertebrates there are five functional forms of SUMO proteins: SUMO1, SUMO2, SUMO3, SUMO4 and SUMO5. SUMO2 and SUMO3 share almost 97% sequence identity but they are only 50% identical in sequence to SUMO1. These 3 isoforms are ubiquitously expressed whereas SUMO4 and SUMO5 are expressed in specific tissues such as kidney, lymph node, and spleen and they are poorly characterized (Bohren et al., 2004; Guo et al., 2005; Owerbach et al., 2005). The process of covalent conjugation of SUMO proteins to their

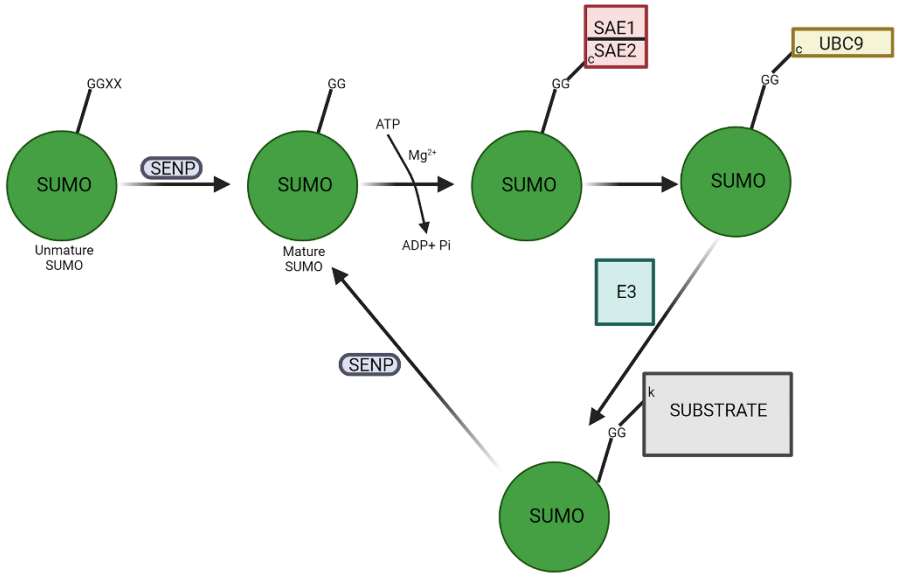

Figure 4. Scheme of the SUMO conjugation pathway. Designed with biorender.com

substrates is called SUMOylation. SUMO proteins are translated as immature precursors that must be processed by a SUMO specific protease (SENP) to generate the mature form. The cleavage of the C-terminal portion of SUMOs by SENPs exposes a diglycine motif which can then form a thioester bond with the catalytic cysteine of the E1 activating enzyme (SAE1/2). Activated SUMO is then conjugated to the E2 conjugating enzyme UBC9. UBC9 is the only E2 enzyme described for SUMOylation. In the final step, an isopeptide bond is formed between SUMO proteins and substrates through the action of

UBC9 and E3 SUMO ligases. SUMOylation is a highly dynamic process and it can be reversed by SENP proteins (figure 4). The target lysine where SUMO is attached is usually located within the ψKxE motif (where ψ is a hydrophobic residue and x stands for any amino acid) of the target protein (Geiss-Friedlander and Melchior, 2007). However, an increasing number of proteins are SUMOylated in non-consensus SUMOylation sites. Interestingly, many SUMOylated proteins interact with SUMO or SUMOylated proteins in a non-covalent way through SUMO-interacting motifs (SIMs). SIMs are typically composed of a hydrophobic core (V/I/L)x(V/I/L)(V/I/L) flanked by acidic residues, and it has been proposed to contribute to SUMO binding affinity and orientation, and paralog selection. SUMO-SIM interactions can be modulated by post-translational modifications such as phosphorylation or acetylation. Interestingly, efficient SUMOylation of some substrates requires functional SIMs (Kerscher, 2007; Minty et al., 2000).

SUMO has important functions in several cellular processes including DNA repair, transcription, innate immunity, and cell division (Wilkinson and Henley, 2010). In addition, SUMO has a critical role in the cellular stress response and many cellular stresses result in increased SUMOylation (Flotho and Melchior, 2013; Hay, 2005). Consequently, dysregulated SUMOylation has been linked to several pathological conditions such as cancer, viral infection, and neurodegeneration.

3.5. INTRINSIC AND INNATE IMMUNITY AND SUMO

Once a cell is infected by an RNA virus, the viral cytoplasmic RNA is recognized by cellular sensors triggering a signaling cascade that will end with type I IFN synthesis. The host immune system employs a wide variety of mechanisms including post-translational modifications by SUMO proteins to combat the pathogen. Several host proteins involved in intrinsic and innate immunity are regulated through SUMO interaction. SUMO1 conjugation to RIG-I increases RIG-I stability and facilitates its interaction with MAV5, increasing IFN production. Similarly, conjugation of SUMO1 to MDA5 also leads to an increase in IFN levels (Fu et al., 2011). However, SUMOylation can also have a negative effect on IFN synthesis. Thus, SUMO1

modification of the NF-κB inhibitor IkBα increases its stability and inactivates NF-κB (Desterro et al., 1998). In addition, SUMO conjugation to IRF7 or IRF3 protects these proteins from ubiquitination and degradation (Kubota et al., 2008) but represses its transcriptional activity with the consequent downmodulation of type I IFN gene expression (Kubota et al., 2008; Ran et al., 2011).

The relevance of SUMO in the JAK-STAT pathway has been also described. STAT1 is modified by SUMO and this covalent interaction downmodulates the phosphorylation of STAT1. In addition, phosphorylation of STAT1 inhibits its SUMOylation (Begitt et al., 2011; Grönholm et al., 2012; Ungureanu et al., 2005; Zimnik et al., 2009). Consequently, SUMO proteins impair IFN-induced biological consequences (Maarifi et al., 2015).

The antiviral state is then regulated by SUMO interaction and SUMOylation has been shown essential for the correct antiviral activity of different proteins such as p53, promyelocytic leukemia protein (PML), and PKR (El Motiam et al., 2020). The relevance of SUMO in innate immune response explains why many viruses have evolved strategies to modulate the SUMO pathway. Unveiling the role of SUMO and its regulation in EBOV infection is needed for understanding EBOV pathogenesis.

3.6. SUMO AND EBOV

As mentioned above, SUMOylation of host proteins greatly impacts host innate immunity. Consequently, viruses have evolved to hijack the SUMO machinery. Viruses can inhibit or induce host protein SUMOylation to ensure their survival and propagation. In addition, the SUMO pathway is widely exploited by viral pathogens to modulate their own proteins. Consequently, SUMOylation is essential for the successful replication of different viruses (El Motiam et al., 2020; Everett et al., 2013; Lowrey et al., 2017; Wilson, 2016). One RNA virus that exploits the SUMOylation pathway in its own benefit is influenza A virus (IAV) which infection extensively modulates SUMOylation and exploits SUMOylation changes (Domingues et al., 2015; Han et al., 2014; Pal et al., 2011; Schmidt et al., 2019; Wu et al., 2011; Xu et al.,

2011). Similarly, SUMOylation positively regulates rotavirus replication and viral protein production (Campagna et al., 2013). Numerous viral proteins are modulated by SUMO including different IAV or rotavirus proteins, the RNA polymerase P protein of Rubulavirus which SUMO1 modification improves viral gene expression (Sun et al., 2011), and the polymerase 3D of enteroviruses which SUMOylation increases its stability (Liu et al., 2016). In the case of EBOV, two different reports show that this filovirus exploits SUMO in its own benefit. As mentioned before, VP35 is able to induce IRF3/7 SUMOylation and, by doing so, inhibits IFN synthesis (Chang et al., 2009). In addition, the major matrix protein VP40 was reported to be SUMOylated and this modification increases VP40 stability (Baz-Martínez et al., 2016) Interestingly, SUMO can be included into the VLPs formed by VP40 suggesting that SUMO has a relevant role in VP40 functions (Baz-Martínez et al., 2016). It has been then proposed that SUMO may be essential for EBOV life cycle. Targeting the interaction of SUMO with the EBOV proteins may represent a novel therapeutic strategy to block EBOV infection.

3.7. VIRAL TARGETING OF PML-NUCLEAR BODIES

SUMO is required for the intrinsic antiviral activity of some factors such as PML or PKR proteins. PML is a protein induced by IFN

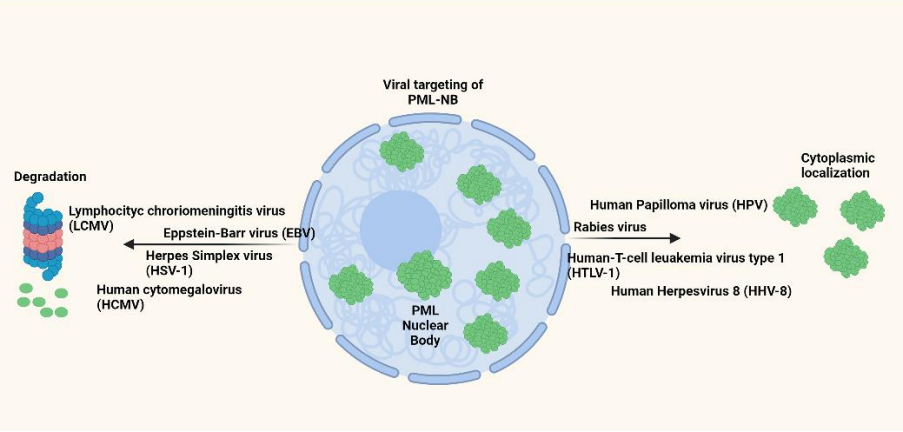

Figure 5. Viral targeting of PML-NBs. Designed with biorender.com

and it is the organizer of the PML-nuclear bodies (PML-NBs) (Shen et al., 2006), dynamic structures enriched in SUMOylated proteins and involved in the regulation of innate immune signaling during viral infection. The few permanent residing proteins that form the PML-NBs are PML, SUMO and Sp100 (Szostecki et al., 1990). Conjugation of SUMO to PML regulates its subcellular localization, stability, and ability to interact with other proteins, and it is required for the formation of the PML-NBs. Many cellular proteins are recruited to PML-NBs, depending on the stimuli and cell context (Ishov et al., 1999). So far, seven different isoforms of PML have been described (PML I to VII) that differ in their C-terminal region, and in their specific functions (Nisole et al., 2013). PML-NBs are functionally linked to different cellular processes including control of apoptosis, senescence, transcription, and genome stability (Bernardi et al., 2008; Bernardi and Pandolfi, 2007). PML has SUMO E3 ligase activity, which can mediate the SUMOylation of different PML partners such as p53. The relevance of PML in both intrinsic and innate immunity explains why viruses have evolved mechanisms to modulate PML or PML-NBs associated proteins.

Some viral proteins such as ICP0 protein from HSV-1 induce PML-NBs disruption through proteasome degradation of PML and Sp100 proteins (Cuchet-Lourenço et al., 2012; Everett et al., 2006). Human cytomegalovirus (HCMV) (Müller and Dejean, 1999), Epstein-Barr virus (EBV) or lymphocytic choriomeningitis virus (LCMV) (Bonilla et al., 2002) infection also induce PML-NBs disruption although through unclear mechanisms (Xu et al., 2001). Other viruses including human T-cell leukemia virus type 1 (HTLV-1), human immunodeficiency virus (HIV), papilloma virus, human herpesvirus-8 (HHV-8), and rabies virus promote the translocation of PML to the cytoplasm (Blondel et al., 2002; Desbois et al., 1996). In the case of papilloma virus or HHV-8, cytoplasmic mislocalization of PML has been proposed to help virion assembly (Day et al., 1998; Katano et al., 2001) (figure 5). However, in the case of HIV infection, the cytoplasm translocation of PML is considered an antiviral response that interferes with HIV-mediated transduction (Turelli et al., 2001). EBOV infection has been shown to induce cytoplasmic translocation of PML (Björndal

et al., 2003). Moreover, an inverse correlation between EBOV infection and the overall expression levels of PML in the cells has been reported (Björndal et al., 2003). However, the molecular mechanism mediating this PML translocation, and its consequences are unknown.

3.8. VIRAL TARGETING OF THE NUCLEAR ENVELOPE

The critical role of VP24 for EBOV pathogenesis led to search for potential novel interacting partners for VP24 using proteomic analyses (Batra et al., 2018; García-Dorival et al., 2014). These studies identified emerin as a putative VP24 interactor. Emerin is a transmembrane

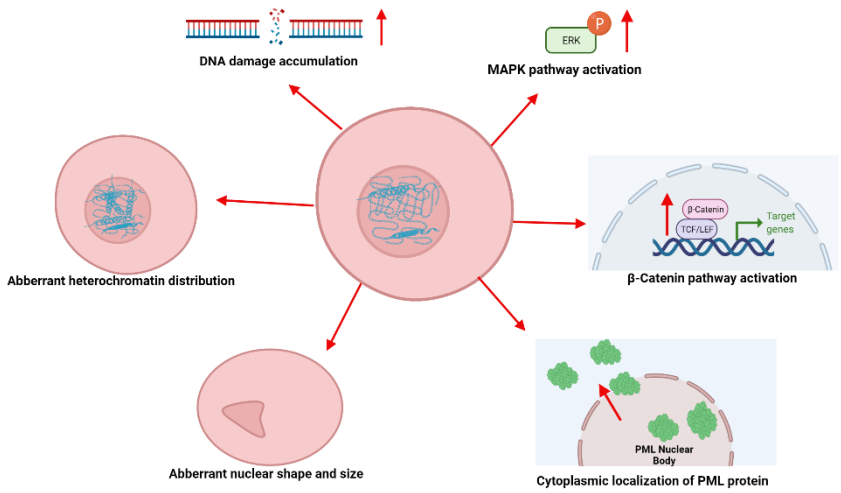

Figure 6. Molecular features associated with laminopathies. Designed with biorender.com

protein that most often localizes in the inner nuclear membrane. It belongs to the family of nuclear lamina-associated proteins (LAPs) and it is characterized by presenting a (LAP2)–Emerin–MAN (LEM) domain that allows proteins to directly interact with both the barrier to autointegration factor (BAF) and lamins (Lin et al., 2000; Margalit et

al., 2007). BAF is a small, abundant, and highly conserved protein able to bind double-stranded DNA, histones, transcription factors and the LEM family of proteins (Margalit et al., 2007). BAF is required for the assembly of emerin into the reforming nuclear envelope (Haraguchi et al., 2001) and it has been identified as a key regulator of retrovirus infection since it modulates its genome integration, chromatin organization and structure (Segura-Totten and Wilson, 2004). Lamins are intermediate filament proteins that are divided into two different groups, A-type lamins (lamin A and lamin C) encoded by LMNA gene, and B-types lamins (lamin B-1 and lamin B-2) encoded by LMNB1 and LMNB2 genes, respectively. Lamins line the the inside of the nuclear membrane. These filaments are crucial for the assembly, structure, shape and mechanical stability of eukaryotic nuclei (Dechat et al., 2009, 2008; Wilson and Foisner, 2010). Emerin, BAF and lamins are structurally interdependent. Therefore, if any of these three proteins is missing the other two fail to assemble correctly (Liu et al., 2003; Qi et al., 2015; Samson et al., 2018). Moreover, mutations in any of these genes result in a disorganization of nuclear envelope, nuclear morphological abnormalities, induction and accumulation of DNA damage, aberrant heterochromatin distribution and altered signaling such as the activation of beta-catenin and mitogen activated protein kinase (MAPK) pathways (Schreiber and Kennedy, 2013) (figure 6). These alterations are characteristic of many diseases collectively known as laminopathies (Piekarowicz et al., 2019).

Nuclear envelope acts as a physical barrier that separates nucleus from cytoplasm and impedes free diffusion of proteins (Feldherr and Feldherr, 1960) with the consequent impact on protein function. Indeed, aberrant localization of proteins contributes to the pathogenesis of many human diseases (Rodriguez et al., 2004). This barrier needs to be overcome by many viruses in order to establish a productive infection. Different viruses enter the nucleus through Nuclear Pore Complex (NPC), using the host transport machinery (Cohen et al., 2011; Kobiler et al., 2012). NPCs are large multiprotein complexes, which are embedded in the nuclear envelope, and which allow transportation of molecules across the nuclear envelope (Lin and Hoelz, 2019). Other viruses enter the nucleus during mitosis, when the nuclear envelope is

temporarily disassembled, and some other viruses transiently disrupt the nuclear envelope to enter the nucleus through the resulting gaps. Although some RNA viruses do not require nuclear entry of their genome to replicate, they require viral proteins found in the nucleus to disrupt the host-cell transcription and innate anti-viral responses (Flather and Semler, 2015). In addition, some nuclear envelope components play an important role in virus infection. In the case of HIV infection, both emerin and BAF have been shown to be crucial for complementary DNA (cDNA) integration into the host's genome (Chen and Engelman, 1998; Jacque and Stevenson, 2006). In addition to its proviral activity, BAF can also act as an antiviral effector (Wiebe and Jamin, 2016) and regulation of BAF and emerin by viruses have been reported. HSV infection induces hyperphosphorylation of emerin, resulting in nuclear lamina disorganization (Leach et al., 2007). EBV infection or the expression of the EBV protein BRF1 also induces emerin hyperphosphorylation and its delocalization (Yadav et al., 2017). So far, whether these cellular proteins play a role in EBOV infection is unknown. However, the identification of two different lamina proteins, emerin and lamin B, as potential interactors of VP24 led us to hypothesize that they may play an important role in EBOV pathogenesis.

4. OBJECTIVES

EBOV is a highly pathogenic virus and EBD outbreaks tend to rely on supportive care measures remaining a public health problem. Key to developing effective treatments for this frequently deadly disease is understanding the mechanisms of the infection process and pathogenesis of EBOV. Two of the EBOV proteins, VP24 and VP35, are known as type I interferon antagonists and they are thought to play key roles in EBOV pathogenicity. In addition, the potential interaction between VP24 and nuclear membrane components suggest that VP24 may have novel functions at the nuclear envelope. How these proteins are regulated is incompletely understood. Often viruses hijack the SUMOylation machinery of the cell for modification of their own proteins and effective replication. SUMO plays an important role at the nuclear envelope and many viruses need to overcome the nuclear membrane barrier to alter cellular gene expression. Whether EBOV VP24 protein enters the nucleus to facilitate virus replication is unknown.

The main objectives of this thesis have been the following:

1. To study the putative modulation of EBOV VP24 protein by SUMO
2. To study the putative modulation of EBOV VP35 protein by SUMO
3. To evaluate the mechanisms and functional consequences of the interaction between EBOV VP24 and nuclear membrane components

5. MATERIAL AND METHODS

5.1. CELL CULTURE

5.1.1. Cell lines

In this study we used human embryonic kidney 293 (HEK 293) cells, human cervical adenocarcinoma (Hela) cells, African green monkey kidney epithelial (Vero) cells, human-derived hepatoma cells (HUH-7), baby hamster kidney (BHK-21)-derived cell line stably expressing T7 RNA polymerase (BSR-T7), human lung epithelial carcinoma (A549) cells, and human bone osteosarcoma epithelial (U2OS) cells.

5.1.2. Cell culture media

HEK 293, Hela, Vero, BSR-T7, A549, and U2OS cells were cultured in Dulbecco's Modified Eagle's Medium (DMEM) (Sigma) supplemented with 10% fetal bovine serum (Thermo Fisher), 10 U/mL of penicillin/streptomycin (Sigma), and 2 mM L-Glutamine (Sigma). Cells were passaged upon reaching 80-90% confluency

5.1.3. Cell transfection

Cells were transfected with DNA plasmids using 1mg/mL polyethilenimine (PEI) (Polysciences, Inc, Hirschberg an der Bergstrasse, Germany). The appropriate amount of DNA plasmid and the optimal volume of PEI (3:1 ratio of PEI to total DNA) were diluted in serum and antibiotic-free DMEM in two sterile tubes. The diluted PEI was mixed with the DNA solution, left for 30 min at room temperature, and added directly to the cells.

5.2. BACTERIA TRANSFORMATION AND COMPETENT CELLS

5.2.1. Competent bacteria production

First *Escherichia coli* DH5α were grown overnight on LB agar plates. The next day a single colony was picked and grown in 10 mL Luria Bertani (LB) broth overnight at 37ºC with shaking (225 rpm). The following day, bacteria were refreshed into 1 L of LB, and incubated at 37ºC with shaking until they reached an optical density (OD) at 600 nm

of 0.35-0.4. The culture was then chilled in ice for 20 min and harvested by centrifugation (3000 x g for 15 min at 4ºC). Pelleted cells were resuspended in 100 mM $MgCl_2$ and then centrifugated (2000 x g for 15 min at 4ºC). Pelleted cells were resuspended in 100 mM $CaCl_2$ and incubated in ice for 20 min. Cells were then again harvested by centrifugation (2000 x g for 15 min at 4ºC). Pellet was resuspended in 85 mM $CaCl_2$ with 15% glycerol and harvested by centrifugation (1000 x g for 15 min at 4ºC). Finally, pelleted cells were resuspended in 2 mL of 85 mM $CaCl_2$/15% glycerol, aliquoted and snap frozen with liquid nitrogen. Bacteria were stored at -80ºC.

5.2.2. Bacteria transformation

Competent bacteria were thawed on ice, the plasmid DNA was mixed with chilled cells and incubated on ice for 30 min. The mixture was then heat shocked by incubation for 40 s at 42ºC. The mixture was cooled immediately in ice. The bacteria were then grown for one h at 37ºC with shaking (500 rpm) in 1mL of LB. Finally, the culture was harvested by centrifugation (4500 x g for 5 min), resuspended in 100 µl of LB and plated on LB agar plates containing the appropriate antibiotic.

5.2.3. Purification of plasmid DNA

Plasmid DNA was purified from bacteria using different commercial kits: GeneJET Plasmid Miniprep kit from Thermo Fisher Scientific and DNA purification midiprep kit from Macherey-Nagel. Briefly, a colony was picked and grown in LB broth supplemented with the appropriate antibiotic overnight at 37ºC with shaking (225 rpm). The culture was then harvested by centrifugation (6800 x g for 30 min at 4ºC), the pelleted bacteria were resuspended in resuspension buffer, lysed with a lysis buffer and neutralized with a neutralization buffer. The cell debris was then pelleted by centrifugation and the plasmid-containing supernatant was loaded onto a silica column. Columns were washed with washing buffer, plasmid DNA was eluted using elution buffer, and precipitated using isopropanol. Finally, DNA was washed with 70% ethanol and resuspended in sterile Milli-Q H2O.

5.3. PLASMIDS

HA-VP24: plasmid expressing Hemagglutinin (HA)-tagged VP24 protein was generated by subcloning VP24 cDNA into pCMV5-HA vector using oligos listed in table 1. The different VP24 mutants were generated using oligos listed in table 1.

pcDNA3.1: empty vector (Invitrogen).

pcDNA3.1-v5-UBC9: plasmid expressing SUMO conjugating enzyme UBC9 fused to V5 tag. Kindly provided by Manuel S Rodríguez (Rodriguez et al., 2001).

pcDNA-His6-SUMO1: plasmid expressing Histidine-tagged SUMO1 protein. Kindly provided by Manuel S Rodríguez (Rodriguez et al., 1999).

pcDNA-His6-SUMO2: plasmid expressing Histidine-tagged SUMO2 protein. Kindly provided by Manuel S Rodríguez (Vertegaal et al., 2006).

ISG54-luc: plasmid harboring a luciferase reporter gene under the control of the ISG54 promoter.

pcDNA-beta-gal: plasmid expressing β-galactosidase protein.

pcDNA-His6-UbKO: plasmid expressing an Histidine-tagged Ubiquitin protein with all lysine residues mutated to arginine (UbKO). Kindly provided by Manuel S Rodríguez (Hjerpe et al., 2009).

GFP-USP7: plasmid expressing Green Fluorescent Protein (GFP)-tagged USP7 protein.

MYC-USP14: plasmid expressing MYC-tagged USP14 protein.

pQHA-USP7: plasmid expressing HA-USP7 WT. Kindly provided by Goedele Maertens & Gordon Peters through addgene #46753 (Maertens et al., 2010).

YN-VP24, YC-lamin A, YC-emerin, and YN-emerin: were obtained by cloning the coding region of lamin A (YC-lamin A) or emerin (YC-emerin and YN-emerin) into the vectors pCAGGS-eYN or pCAGGS-eYC (Sánchez-Aparicio et al., 2017) using the oligonucleotides listed in table 1.

EGFP-C1: vector expressing enhanced GFP protein (Clontech).

GFP-VP24: plasmid generated by subcloning VP24 cDNA into the EGFP-C1 vector using the oligos listed in table 1.

pTRIP-SFFV-EGFP-NLS: plasmid expressing EGFP protein fused to a NLS. Kindly provided by Nicolas Manel through Addgene #8667 (Raab et al., 2016).

pTRIP-CMV-GFP-Flag-cGAS: plasmid expressing GFP-tagged cyclic GMP-AMP synthase (cGAS) protein. Kindly provided by Nicolas Manel through Addgene # 86675 (Raab et al., 2016).

pLKO-sh-lamin A: Plasmid expressing short hairpin (sh) against Lamin A. Kindly provided by Susana Gonzalo (Redwood et al., 2011).

pLKO-sh-luciferase: plasmid expressing short hairpin against Luciferase. Kindly provided by Susana Gonzalo (Redwood et al., 2011).

pREP4-CSF1-luciferase: plasmid harboring a luciferase reporter gene under the control of the colony stimulating factor (CSF) 1 promoter. Kindly provided by Keji Zhao (Liu et al., 2001).

Plasmids of the Zaire EBOV Makona minigenome system VP35, NP, VP30, and L. Kindly provided by Julian Hiscox (García-Dorival et al., 2016).

HA-VP35: plasmid expressing HA-tagged VP35 protein. Kindly provided by César Muñoz-Fontela.

GFP-PML: plasmid expressing GFP-tagged PMLIV protein.

NP: plasmid expressing EBOV NP. Kindly provided by César Muñoz-Fontela.

5.4. CLONING

Coding sequence of the gene of interest was amplified by polymerase chain reaction (PCR) using specific primers (listed in table 1) containing sites for restriction enzymes and a high-fidelity DNA Polymerase (Phusion High-Fidelity Polymerase, Thermo Fisher Scientific), following manufacturer's instructions. The resulting PCR product was then purified from an agarose gel using GeneJet Gel Extraction Kit (Thermo Fisher Scientific) and digested with the required restriction enzymes following the indications of the manufacturer (FastDigest, restriction enzymes, Thermo Fisher Scientific). The digestion product was then purified from an agarose gel using GeneJet Gel Extraction Kit. Digested insert and vector were

ligated by T4 DNA ligase for 1 h at room temperature. Finally, competent bacteria were transformed with the ligation reaction. The resulting colonies were analyzed by restriction enzyme analysis. The positive ones were sent for sequencing.

5.5. MUTAGENESIS

All mutants generated in this work were obtained using site-directed mutagenesis and Phusion High-Fidelity DNA Polymerase (Thermo Fisher Scientific) or the quick-change site-directed mutagenesis kit (Agilent) and the primers listed in table 1, following manufacturer's instructions. After amplification, the PCR products were incubated with 2 µl of Dpn1 restriction enzyme for 2 h at 37ºC. The resulting mutagenesis products were transformed into competent bacteria. The resulting colonies were grown and the plasmid DNA was purified and sent for sequencing.

5.6. ANTIBODIES

Monoclonal mouse anti-HA (#901503) antibody was purchased from BioLegend. Goat anti-HA (#A190-138A) antibody was purchased from Bethyl Laboratories. Anti-tubulin (#2146), anti-MYC tag (#2276S), and anti-SUMO2 (#4971), anti-gH2AX (#9718), and anti-extracellular signal-regulated kinase (ERK) (#9102) antibodies were from Cell Signaling. Anti-glyceraldehyde-3-phosphate dehydrogenase (GAPDH) (#32233), anti-Y701 phosphorylated STAT1 (#8394), anti-ubiquitin (#8017), anti-lamin B (#365962), anti-RANGAP (#28322), anti-RANBP (#74518), anti-FLAG (#166355), anti-PML (#377103), and anti-phospho-ERK (#16982-R) antibodies were from Santa Cruz Biotechnology. Anti-VP24 (#362919) antibody was from Biorbyt. Anti-GFP antibodies were from Abcam (#1218) and BioLegend (#902601). Anti-USP7 antibody (#A300-034A) was purchased from Bethyl Laboratories and Sigma (#PLA0009). Anti-emerin and anti-lamin A/C antibodies were from Abcam (#40688) (#108595) and Cell Signaling (#30853) (#4777). Anti-BAF antibody (#29184) was from Abcam. Anti-KPNA5 antibody (#PA529460) was from Invitrogen.

Anti-VP35 (#GTX134032) and anti-NP (#GTX134031) were from Genetex.

5.7. *IN VITRO* TRANSLATION

TNT quick coupled transcription/translation system (Promega) was used for *in vitro* translation of the desired proteins, following the manufacturer´s instructions. Briefly, plasmid DNA was incubated with the TNT-coupled reticulocyte lysate system and in the presence of [^{35}S]-labeled methionine for 90 min at 30ºC. 1 µl of the resulting protein was analyzed by sodium dodecyl sufate (SDS)-polyacrilamide gel electrophoresis (PAGE). The remaining protein was kept at -80ºC until further use.

5.8. *IN VITRO* SUMOYLATION ASSAY

0.3 µg of SAE1/2 (Biomol, Enzo Life Sciences), 2 mM adenosine triphosphate (ATP), 50 mM Tris pH 7.5, 5 mM $MgCl_2$, 10 mM Creatine Phosphate, 3.5 U/mL of creatine kinase, 0.6 U/mL of inorganic pyrophosphate, 600 ng of UBC9, 10 µg of SUMO1 or SUMO2, and the *in vitro* translated protein were incubated for 90-180 min at 37ºC. The reaction was stopped by adding SDS-sample buffer and boiling for 5 min at 100ºC. Finally, the samples were loaded on a SDS-PAGE gel and detected by autoradiography.

5.9. *IN VITRO* DESUMOYLATION ASSAY

In vitro deSUMOylation assays were performed using recombinant GST-SENP1 protein (Biomol). Briefly, SUMOylated proteins were incubated with 2 µg of GST-SENP1 for 1 h at 37 °C. The reaction was stopped by adding SDS-sample buffer and boiling for 5 min at 100ºC. Reaction products were then analyzed on an SDS-PAGE gel and detected by autoradiography.

5.10. PROTEIN ELECTROPHORESIS AND WESTERN BLOT

Purified proteins or cell extracts were boiled in SDS-sample buffer for 5 min and loaded on SDS-PAGE gels. Separated proteins were then transferred to nitrocellulose membranes and blocked in 5% non-fat dry milk in Tween Tris-buffered saline (TTBS) (150 mM NaCl, 10 mM Tris pH 8.0, 0.1 % v/v Tween20) for 30 min. Blocked membranes were incubated with the primary antibody diluted in 5% non-fat dry milk or 5% bovine serum albumin (BSA) in TTBS (following antibody manufacturer's indications) overnight with shaking at 4ºC. The membranes were then washed 3 times (10 min each wash) with TTBS and incubated with the secondary antibody diluted in 5% non-fat dry milk in TTBS for 1 h with shaking at room temperature. Finally, the membranes were washed four times with TTBS (10 min each), incubated with ECL solution, and exposed to X-ray film.

5.11. PURIFICATION OF HISTIDINE-TAGGED PROTEINS

Cells were washed twice with phosphate buffer saline (PBS) and recovered by scraping in PBS. 10 % of the cell suspension was centrifuged at 1000 xg for 5 min and the cell pellet was resuspended in SDS-sample buffer and boiled for 5 min at 100ºC (input). The remaining cells were centrifuged, and the cell pellet was lysed in buffer G (6 M guanidine HCl, 0.1 M Na_2HPO_4, 6.8 mM NaH_2PO_4, 25 mM Tris HCl pH 8). To break the DNA, the lysate was passed through a 0.3 X 13 mm needle several times. The protein extracts were then incubated with TALON® Nickel Affinity Resin (Clontech) and rotated for 2 h at room temperature. The nickel beads were then washed 4 times with 1 mL of buffer U (8 M Urea, 100 mM Tris HCl pH 8, 93.2 mM Na_2HPO_4, 6.8 mM NaH_2PO_4). Finally, the Histidine-tagged purified proteins were resuspended in SDS-sample buffer and boiled for 5 min at 100ºC.

5.12. VIRAL INFECTION

90% confluent Hela cells were infected with EBOV (NC_002549.1) at a multiplicity of infection (MOI) of 1. All infection experiments were carried out by experienced personnel wearing

positive pressure protection suits at the biosafety level 4 (BSL4) laboratory of the Bernhard Nocht Institute for Tropical Medicine in Hamburg.

5.13. LUCIFERASE REPORTER ASSAY

Cells were co-transfected with the luciferase reporter plasmid of interest together with pcDNAbeta-gal co-reporter (at a 10:1 ratio), and the expression plasmids for ebola virus proteins. For IFN reporter assay, 24 h after transfection cells were treated with 1,500 U/mL human IFN-α for 16 h. Cells were then harvested following the instructions of the luciferase assay kit "Luciferase Reporter Gene Assay, high sensitivity kit" from Roche (11814036001), and the luciferase levels were measured using Berthold Mithras LB 940 luminometer. Firefly luciferase values were normalized to beta-galactosidase values. The relative light values were normalized to obtain a fold change with respect to the control samples.

5.14. IMMUNOFLUORESCENCE

Cells were grown on coverslips and transfected as indicated in each experiment. At the indicated time post-transfection, cells were fixed in 2% paraformaldehyde in PBS and permeabilized with 0.25% Triton X-100 or digitonin in PBS. Upon permeabilization, nonspecific binding sites were blocked with 2% BSA in PBS, and samples were incubated with primary antibodies overnight at 4ºC. Coverslips were extensively washed with PBS and further incubated with the appropriate Alexa-conjugated secondary antibodies for 1 h at room temperature. Nuclei were then stained with 4',6'-diamidino-2-phenylindole (DAPI), and preparations were mounted with ProLong Diamond antifade mounting medium (P36970) (Thermo Fisher) and analyzed with a confocal Leica SP5 microscope.

5.15. GST-PULLDOWN ASSAY

Pulldown experiments were performed using [^{35}S] methionine-labeled *in vitro*-transcribed/translated proteins. Recombinant proteins were incubated in GST-binding buffer (20 mM Tris-HCl pH 8.8, 200 mM NaCl, 1 mM EDTA pH 8.0, 0.5% Nonidet-P-40 (NP40)) with GST or GST-SUMO1 proteins immobilized on glutathione sepharose beads (GE Healthcare (#17-0756-01)) for 2 h at 4ºC. The resin was then washed 4 times in the same buffer. Finally, sepharose beads were resuspended in SDS-loading buffer and boiled for 5 min at 100ºC. GST-bound proteins were analyzed by SDS-PAGE and autoradiography.

5.16. IMMUNOPRECIPITATION (IP) ASSAY

Cells were lysed by incubation for 15 min on ice in radioimmunoprecipitation assay (RIPA) (1% NP40, 1% sodium deoxycholate, 0.1% SDS, 150 mM NaCl, 20 mM Tris HCl pH 8.0, 2 mM EDTA pH 8.0) or BC-100 buffer (20 mM Tris HCl pH 7.4, 100 mM NaCl, 10% glycerol, 0.2 mM EDTA, 0.1% Triton x-100) buffer. Lysates were centrifuged at 15,800 × g for 10 min, and the supernatant, containing the protein extract, was incubated with the antibody of interest together with 30 µl of 50% protein G-sepharose beads (Invitrogen (#101242)) overnight at 4°C. Beads were then washed four times with lysis buffer, resuspended in 30 µl of SDS-loading buffer and boiled for 5 min at 100ºC.

5.17. *IN VITRO* UBIQUITINATION ASSAY

[^{35}S]methionine-labeled *in vitro*-transcribed/translated proteins were incubated in a 10 µl reaction mixture containing 50 mM Tris pH 7.6, 5 mM $MgCl_2$, 2 mM ATP, 10 mM creatine phosphate, 3.5 U/mL of creatine kinase, 0.6 U/mL of inorganic pyrophosphatase, 10 ng human E1, 12 ng E2 (UbcH5), and 10 µg recombinant UbKO for 120 min at 37°C. The reaction products were then separated by SDS-PAGE and analyzed by autoradiography.

5.18. BIMOLECULAR FLUORESCENCE COMPLEMENTATION

Cells grown on cover slides were transfected with two non-fluorescent protein fragments of enhanced yellow fluorescent protein (EYFP) fused respectively to the proteins of interest, and 36 h after transfection the cells were incubated for 3 h at 30°C. After incubation, cells were fixed and permeabilized with cold 100% methanol, blocked with 2% BSA in PBS, and incubated with the primary antibodies overnight at 4ºC. Coverslips were then washed extensively with PBS and further incubated with the appropriate Alexa-conjugated secondary antibodies for 1 h at room temperature. Nuclei were stained with DAPI, and preparations were mounted with ProLong Diamond antifade reagent and analyzed using a confocal Leica SP5 microscope.

5.19. REAL TIME QUANTITATIVE REVERSE TRANSCRIPTION PCR

Total RNA was purified with the RNeasy mini kit (Qiagen), and reverse transcription was performed using random primers and a reverse transcription kit (Promega). qRT-PCR was performed using NZYSpeedy qPCR Green Master Mix, NzyTech (MB22303) in a RealPlex 4 thermocycler (Eppendorf). The oligonucleotides used are listed in table 2.

5.20. RNA-SEQ

RNA-seq was carried out at the CNIC Genomics Unit. RNA quantity was measured using a Nanodrop (Thermo Scientific), and RNA integrity was measured with an Agilent 6000 Pico kit and Bioanalyzer. Total RNA (200 ng) was used to generate barcoded RNA-seq libraries using the NEBNext Ultra RNA library preparation kit (New England Biolabs). Briefly, poly A+ RNA was purified using poly T oligo-attached magnetic beads followed by fragmentation and then first and second cDNA strand synthesis. Next, cDNA 3′ ends were adenylated, and the adapters were ligated followed by PCR library amplification. Finally, the size of the libraries was checked using the Agilent 2100 Bioanalyzer DNA 1000 chip, and library concentration was determined using the Qubit fluorometer (Life Technologies).

Libraries were sequenced on a HiSeq2500 (Illumina) to generate 60 base single reads and processed with RTA v1.18.66.3. FastQ files for each sample were obtained using bcl2fastq v2.20.0.422 software (Illumina). Sequencing reads were trimmed of Illumina adapters using cutadapt 1.16 and then aligned to the African green monkey reference transcriptome (ChlSab1 v92) and quantified with RSem v1.3.1 (101, 102). Raw counts were normalized with transcripts per million (TPM) and trimmed mean of M values (TMM) methods, transformed into log2 expression (log2 [rawCount + 1]), and compared to calculate fold change (FC) and corrected P values. The two groups were too similar, so we could not detect any significant differential expressed with the limits of a log2 FC of >1 (2×) and a corrected P-value of <0.05. We reduced the limits to a log2 FC of >0.4 (1.32×) and a P-value of <0.05 and tested some of the candidates by qRT-PCR. Only mRNAs detected in almost 3 samples were used in the analysis. Heat maps were created with the Morpheus web app from the Broad Institute.

5.21. DSRNA BINDING ASSAY

[^{35}S] methionine-labeled *in vitro*-translated proteins, proteins subjected to an *in vitro* SUMOylation assay or proteins expressed in cells were mixed in binding buffer (50 mM Tris-HCl, pH 7.5, 150 mM NaCl, 1 mM EDTA, 1% NP40) with 30 µl of poly(I:C)-agarose beads and incubated overnight at 4ºC. Beads were then washed with 500 µl of binding buffer four times. Beads-bound proteins were analyzed by SDS-PAGE followed by autoradiography or fluorography.

5.22. IMAGE PROCESSING

Confocal images were processed using Adobe Photoshop CC 2019. Western blots were quantified by ImageJ software. Confocal images were analyzed for nuclear area and circularity (=4 π [area/perimeter2]) using ImageJ software.

5.23. PREDICTION OF SUMOYLATION AND UBIQUITINATION SITES

To predict the SUMOylation sites we used the SUMOsp software (**http://sumosp.biocuckoo.org/online.php**). To predict the ubiquitination sites we used the ubpred software.

5.24. CREATION OF FIGURES

Images were created using Biorender software

5.25. STATISTICAL ANALYSIS

Statistical analysis was performed using GraphPad Prism software

6. RESULTS

6.1. UBIQUITIN-LIKE PROTEINS AND VP24

6.1.1. EBOV VP24 protein is modified by SUMO

Previous reports demonstrated that EBOV hijacks the host SUMO system to undermine innate immunity (Kubota et al., 2008) and that the EBOV major matrix protein VP40 usurps the cellular SUMOylation machinery to increase its stability (Baz-Martínez et al., 2016), We then decided to explore whether the EBOV minor matrix protein VP24 is also a substrate for SUMO modification.

To evaluate whether VP24 protein could be modified by SUMO we first translated the protein using a coupled transcription/translation rabbit reticulocyte system and in the presence of ^{35}S-methionine. Then we performed an *in vitro* SUMOylation assay with the *in vitro* translated protein and in the presence of SUMO1 or SUMO2. As shown in figure 7a, the molecular weight of VP24 was around 28 kilodaltons (kDa). After incubation with SUMO1 or SUMO2, we can see the appearance of a band with the predicted molecular weight for VP24-SUMO (around 40 kDa). These results indicated that VP24 can be modified by SUMO1 and SUMO2 *in vitro*. Interestingly, in the reaction incubated with SUMO1, we observed the appearance of a double band, suggesting that the VP24-SUMO1 protein may be additionally modified. To further confirm that the 40 kDa bands detected in the *in vitro* SUMOylation reactions correspond to VP24 protein conjugated to SUMO, we carried out a deSUMOylation assay. First, VP24 protein was subjected to an *in vitro* SUMOylation assay and then the SUMOylated product was incubated with the SUMO specific protease SENP1. A shown in figure 7b, the 40 kDa band disappeared after the incubation with SENP1 confirming that this band corresponds to SUMOylated VP24 protein. To evaluate whether SUMO can modify VP24 in cells, we transfected HEK 293 with HA-VP24 plasmid in combination with pcDNA or with His6-SUMO1 or His6-SUMO2, and UBC9 expression plasmids. 36 h after transfection cells were collected,

lysed in denaturing buffer G, and the Histidine-tagged proteins were

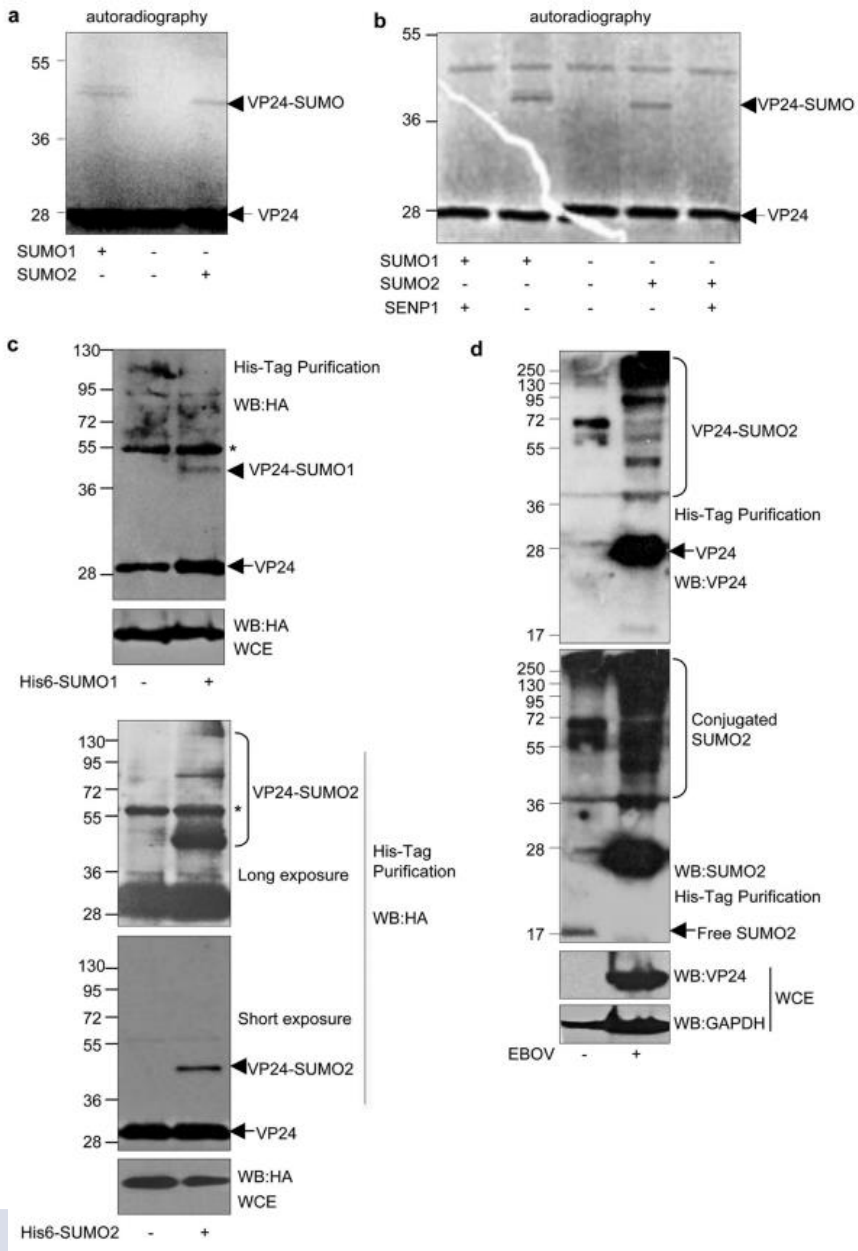

Figure 7. EBOV VP24 protein is modified by SUMO. a, *In vitro* SUMOylation assay in the presence of SUMO1 or SUMO2 using ^{35}S methionine labeled *in vitro*-translated VP24 protein. b, Incubation of VP24-SUMO1 or VP24-SUMO2 proteins with SENP1. c, HEK 293 cells were transfected with HA-VP24 in combination with pcDNA, His6-SUMO1 and UBC9 (upper panel) or His6-SUMO2 and UBC9 (lower panel). 36 h after transfection whole-cell extracts and Histidine-tagged purified proteins were analyzed by Western blot with the indicated antibodies. Asterisks mark unspecific bands. d, Hela cells that stably express His6-SUMO2 were infected with EBOV or left uninfected. 5 days after infection whole-cell extracts and Histidine-tagged purified proteins were analyzed by Western blot with the indicated antibodies. WCE, whole-cell extracts

purified using Ni^{2+} columns. Then, the whole protein extract and the Histidine-tagged purified proteins were analyzed by Western blot using anti-HA antibody. A band of 40 kDa was detected only in the cells co-transfected with SUMO1 or SUMO2 (figure 7c), indicating that VP24 protein is modified by SUMO1 and SUMO2 in transfected cells. In those cells co-transfected with SUMO2, we also observed the appearance of an additional higher molecular weight band likely corresponding to SUMO chains conjugated to VP24 (figure 7c). Finally, to evaluate whether VP24 protein is SUMOylated in the context of viral infection, Hela cells that stably express His6-SUMO2 were infected with EBOV and 5 d after infection, the Histidine-tagged proteins were purified using Ni^{2+} columns under denaturing conditions. Whole cell extracts and purified proteins were analyzed by Western blot using anti-VP24 antibody. We detected bands corresponding to the size of SUMOylated VP24 protein (figure 7d), indicating that VP24 protein is modified in infected cells. Altogether, we can conclude that VP24 can be modified by SUMO *in vitro*, in transfected cells, and in infected cells.

6.1.2. SUMOylation increases VP24 stability and its ability to block IFN signaling

In order to identify the lysine residues involved in SUMO conjugation, VP24 amino acid sequence was analyzed using the SUMOsp software. The analysis revealed lysine 14 (K14) and lysine 142 (K142) as the most probable SUMOylation sites in VP24 (figure 8a). We then generated the single mutants VP24-K14R, VP24-K142R or the double mutant VP24-K14RK142R using site directed mutagenesis and the primers listed in table 1. Then we performed *in*

vitro SUMOylation assays with *in vitro* translated VP24 wild-type (WT) or the indicated VP24 mutants and in the presence of SUMO1. As seen in figure 8a, VP24-K142R protein is modified by SUMO1. However,

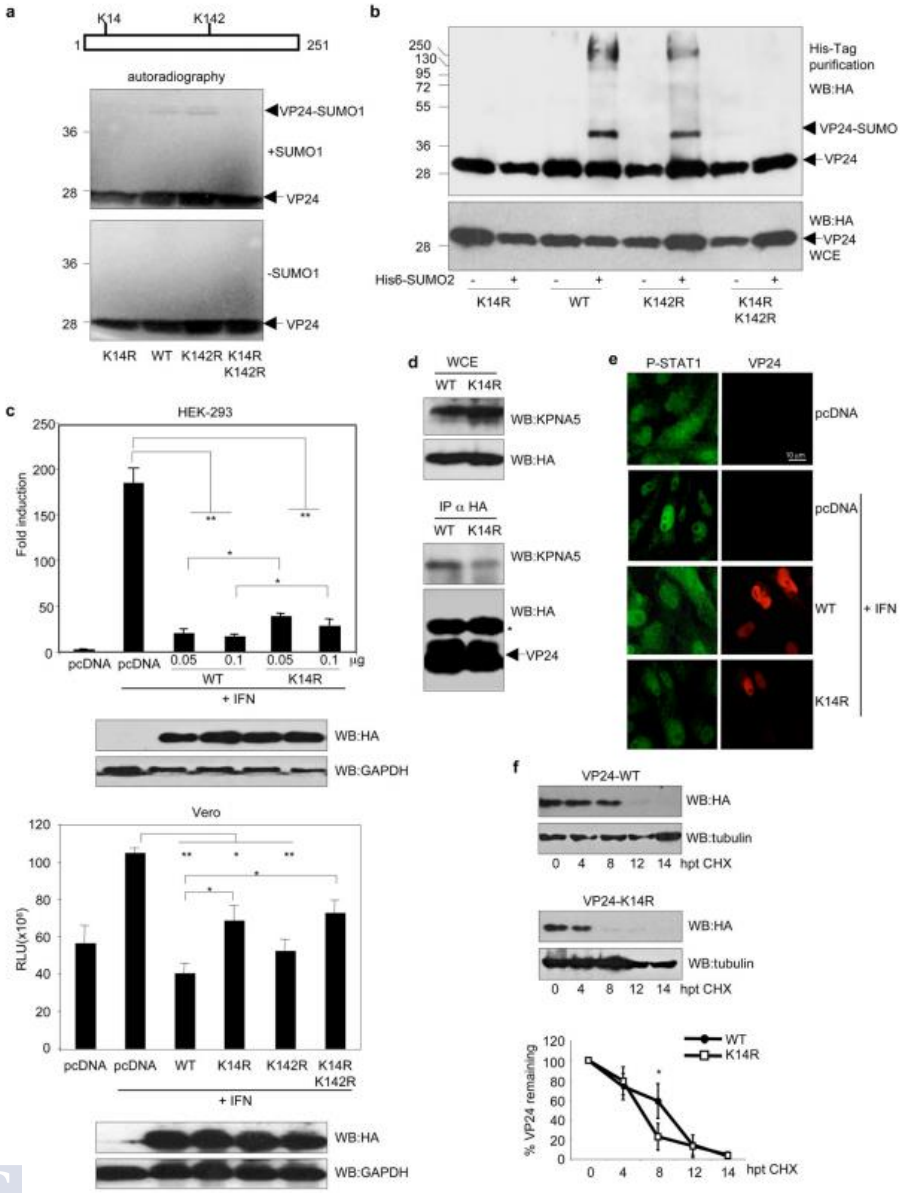

Figure 8. SUMOylation increases VP24 stability and its ability to block IFN signaling. a, i*n vitro* SUMOylation assay using ^{35}S methionine labeled *in vitro*-translated VP24 WT, VP24-K14R, VP24-K142R or VP24-K14R-K142R proteins and in presence of SUMO1. b, HEK 293 cells were co-transfected with HA-VP24-WT, HA-VP24-K14R, HA-VP24-K142R or HA-VP24-K14R-K142R, and pcDNA or His6-SUMO2 and UBC9 expression plasmids. 36 h after transfection whole cell lysates and Histidine-tagged purified proteins were analyzed by Western blot using the indicated antibodies. c, HEK 293 cells (upper panel) were transfected with ISG54-luc, pcDNA-beta-gal and the indicated doses of HA-VP24-WT or HA-VP24-K14R plasmids. 24 h after transfection cells were treated with 1,500 U/mL of IFN α and 16 h after treatment luciferase activity was measured. Columns are representative of means, and error bars represent standard deviations of results from three biological replicates. Statistical significance was assessed by a Student's t test. Cell lysates from the experiment were analyzed by Western blot for HA-VP24 expression. Vero cells were co-transfected with the luciferase reporter ISG54-luc and the pcDNA-beta-gal plasmids together with the indicated plasmids. 24 h after transfection cells were treated with 1500 U/mL of IFN α and luciferase production was analyzed 16 h after treatment. Columns are representative of means, and error bars represent standard deviations of results from three biological replicates. Statistical significance was assessed by a Student's t test. Cell lysates from the experiment were analyzed by Western blot for HA-VP24 expression. d, HEK 293 cells were transfected with HA-VP24 WT or HA-VP24-K14R, and 36 h after transfection, immunoprecipitations (IP) were performed with anti-HA antibody, and the immunoprecipitated proteins were analyzed by Western blot with anti-HA or anti-KPNA5 antibodies, as indicated. The asterisk indicates the immunoglobulin. e, Vero cells were transfected with the indicated plasmids, and 24 h after transfection, cells were serum starved for 4 h and then treated with 1,000 U/mL of human IFN α for 30 min or left untreated. Cells were then fixed and immunostained using primary goat anti-HA and mouse anti-Y701 phosphorylated STAT1 (P-STAT1) antibodies and secondary Alexa-488 chicken anti-mouse and Alexa-594 donkey anti-goat antibodies. f, HEK 293 cells were transfected with HA-VP24-WT or HA-VP24-K14R, and 24 h after transfection, cells were treated with cycloheximide (CHX). At the indicated h after CHX treatment, protein extracts were analyzed by Western blot with anti-HA antibody. VP24 protein intensity bands were quantified using ImageJ software. VP24 bands intensity were normalized to tubulin from each respective time point and plotted. Data represent means and error bars of results from 3 independent experiments. Statistical analysis was assessed by a Student's t test.

we did not observe conjugation of SUMO1 to VP24-K14R or VP24-K14RK142R (figure 8a), indicating that K14 is involved in SUMO conjugation. To confirm this result, we transfected HEK 293 cells with HA-VP24 WT or the different VP24 mutants, together with pcDNA or

His6-SUMO2 and UBC9. 36 h after transfection cells were collected, lysed in denaturing buffer G and the Histidine-tagged proteins were purified with Ni^{2+} columns. Analysis of the samples by Western blot using anti-HA antibody revealed that VP24-K14R and VP24-K14RK142R mutants did not conjugate to SUMO2 (figure 8b), confirming that K14 is the acceptor of SUMO in VP24. We then decided to evaluate the impact of SUMOylation on the activity of VP24 protein. VP24 inhibits IFN signaling by binding KPNA proteins and thereby preventing the nuclear translocation of phosphorylated STAT1. Therefore, HEK 293 cells were co-transfected with ISG54-luc, pcDNA-beta-gal, and the indicated amount of VP24-WT or VP24-K14R plasmids. 24 h after transfection we treated the cells with IFN α and 16 h after treatment we collected the cells and analyzed the luciferase activity. IFN treatment induced the transactivation of the reporter (figure 8c) and expression of VP24-WT inhibited this transactivation, as expected (figure 8c). The levels of luciferase detected in cells transfected with VP24-K14R were significantly higher than the levels detected in the VP24-WT transfected cells but significantly lower than the levels observed in the pcDNA transfected cells (figure 8c), suggesting that conjugation of SUMO to K14 in VP24 contributes to the inhibition of IFN signaling by the viral protein. These results were confirmed in Vero cells. As shown in figure 8c, IFN treatment induced the transactivation of the reporter and VP24 WT abolished this transactivation, as expected. We did not observe significant differences in the abilities of VP24-WT and VP24-K142R to block luciferase transactivation (figure 8c). However, the inhibition of the reporter activity by VP24-K14R was significantly lower than the reduction caused by the WT protein (figure 8c). A significant inhibition of the IFN pathway was not observed in those cells transfected with VP24-K14RK142R (Figure 8c). These results suggested that conjugation of SUMO to K14 in VP24 is needed for the inhibition of IFN signaling by the viral protein. The reduced ability of VP24-K14R to block IFN signaling could be due to the loss of interaction between the mutant viral protein and KPNA. Therefore, we decided to evaluate the interaction between both proteins. We transfected cells with HA-VP24-WT or HA-VP24-K14R, 48 h after transfection we carried out IP assay

with anti-HA antibody, and finally, we evaluated the immunoprecipitated proteins by Western blot with anti-HA or anti-KPNA5 antibodies. The levels of KPNA5 protein co-immunoprecipitating with VP24-K14R were slightly lower than the levels of importin interacting with VP24-WT protein (figure 8d), suggesting that conjugation of SUMO to lysine residue K14 in VP24 contributes to its interaction with karyopherin. The interaction of VP24 with KPNA5 has been reported to inhibit the nuclear translocation of phosphorylated STAT1 (Reid et al., 2006). We therefore decided to evaluate whether the nuclear translocation of phosphorylated STAT1 in response to IFN treatment was altered by VP24-K14R. We transfected Vero cells with pcDNA, HA-VP24-WT or HA-VP24-K14R, and 24 h after transfection cells were treated or not with IFN-α. Cells were then stained with anti-phosphorylated-STAT1 and anti-HA antibodies and immunostained cells were analyzed by confocal microscopy. As shown in figure 8e IFN treatment induced the accumulation of phosphorylated-STAT inside the nucleus in 88% of the control cells (n=69). Phosphorylated STAT1 was detected inside the nucleus in only 4% of the VP24-WT expressing cells (n=72). In contrast, we observed translocation of phosphorylated-STAT to the nucleus in 36% of the cells expressing HA-VP24-K14R (n=79). These results suggested that SUMOylation of VP24 is required for an effective inhibition of the nuclear translocation of STAT1 by the viral protein.

The interaction of VP24 with karyopherin 5 has been reported to increase the stability of the viral protein (Schwarz et al., 2017). We then decided to evaluate the stability of the VP24-K14R mutant. We transfected HEK 293 cells with HA-VP24 or HA-VP24-K14R. 24 h after transfection cells were treated with cycloheximide (CHX) and collected at the indicated time points after treatment. Samples were analyzed by Western blot with anti-HA antibody. We observed that the stability of VP24-K14R is significantly lower than the stability of the WT protein (figure 8f), suggesting that conjugation of SUMO to K14 in VP24 increases its stability.

6.1.3. VP24 interacts in a non-covalent manner with SUMO through a SIM domain and this interaction is critical for modulation of the IFN signaling by the viral protein

Many SUMOylated proteins interact with SUMO in a non-covalent manner through a SUMO interacting motif (SIM). In order to test whether VP24 could also interact non-covalently with SUMO, we performed GST-pulldown assays using *in vitro* translated VP24 protein

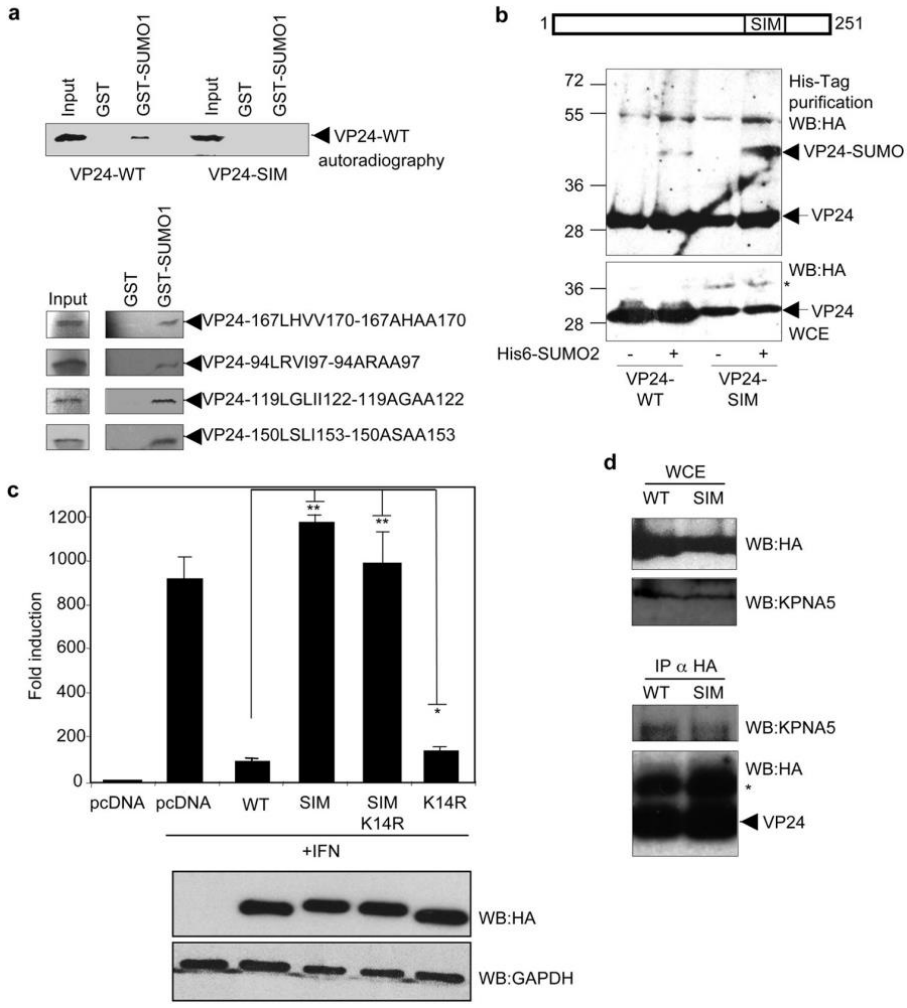

Figure 9. VP24 interacts in a non-covalent manner with SUMO through a SIM domain and this interaction is critical for modulation of the IFN signaling by the viral protein. a, GST-pulldown assay using ^{35}S methionine labeled *in vitro*-translated VP24-WT or the indicated VP24 mutants and GST or GST-SUMO1. b, HEK 293 cells were co-transfected with HA-VP24-WT or HA-VP24-SIM mutant, and pcDNA or His6-SUMO2 and UBC9. 36 h after transfection whole cell lysates (WCE) and Histidine-tagged purified proteins were analyzed by Western blot with the indicated antibodies. Asterisk indicates the band corresponding to SUMO conjugated VP24-WT or VP24-SIM proteins. c, HEK 293 cells were co-transfected with the luciferase reporter ISG54-luc and pcDNA-beta-gal co-reporter together with the indicated plasmids. 24 h after transfection cells were treated with 1,500 U/mL of IFN α. Luciferase levels were analyzed 16 h after treatment (upper panel). Columns are representative of means of results, and error bars represent standard deviations of results from three biological replicates. Statistical significance was assessed by a Student's t test. Cell lysates were analyzed by Western blotting with anti-HA antibody (lower panel). d, HEK 293 cells were transfected with HA-VP24-WT or HA-VP24-SIM. 36 h after transfection we performed IP assays with an anti-HA antibody. Immunoprecipitated proteins were analyzed by Western blot with anti-KPNA5 and anti-HA antibodies as indicated. Asterisk indicates immunoglobulin.

labeled with ^{35}S-methionine and GST or GST-SUMO1. As shown in figure 9a, VP24 can interact in a non-covalent manner with SUMO1. An *in silico* analysis of the amino acid sequence of VP24 using GPS-SUMO software pointed to the presence of 5 different potential SIM domains (94-LRVI-97, 114-LGLI-119, 1450-LSLI-153, 167-LHVV-170, and 198-LVEL-201). We then generated mutants of VP24 in the putative SIM domains and analyzed their non-covalent interaction with SUMO1 using GST- pull-down assays. Only the mutant protein VP24-198-LVEL-201-198AAEA-201 (VP24-SIM) was unable to interact with SUMO1 (figure 9a). It has been reported that SIM domains can be important for efficient substrate SUMOylation. To evaluate the potential role of the SIM domain in the SUMOylation of VP24 protein, we co-transfected HEK 293 cells with HA-VP24-WT or HA-VP24-SIM, together with pcDNA, or His6-SUMO2 and UBC9. 36 h after transfection cells were lysed in buffer G and Histidine-tagged proteins were purified using Ni^{2+} columns. Then samples were analyzed using by Western blot with anti-HA antibody. As shown in figure 8b, mutation of the SIM domain in VP24 did not alter the SUMOylation of HA-VP24-WT protein. To unveil the possible role of the SIM domain

in the modulation of the IFN signaling pathway by VP24, we performed luciferase reporter assays. We transfected HEK 293 cells with ISG54-luc, pcDNA-beta-gal, and the plasmids indicated in figure 9c. 24 h after transfection cells were treated with IFN and 16 h after transfection cells were collected and luciferase activity was measured. As shown in figure 9c, IFN treatment induced transactivation of the reporter and this transactivation was blocked by HA-VP24-WT but not by HA-VP24-K14R, confirming our previous results. Surprisingly, HA-VP24-SIM and HA-VP24-SIM-K14R were completely unable to block IFN signaling (figure 9c), suggesting that the non-covalent interaction with SUMO is essential for the inhibition of the IFN signaling by VP24. Finally, to address whether the failure of VP24-SIM to block IFN signaling was related to its inability to interact with KPNA, we performed IP analysis. HEK 293 cells were transfected with HA-VP24-WT or HA-VP24-SIM. 36 h after transfection cells were collected, protein extracts were immunoprecipitated with an anti-HA antibody and analyzed by Western blot with both anti-KPNA5 and anti-HA antibodies. As shown in figure 9d, the levels of KPNA5 protein co-immunoprecipitating with VP24-SIM were lower than the levels of KPNA5 interacting with VP24-WT, suggesting that the non-covalent interaction of VP24 with SUMO1 facilitates its interaction with KPNA5.

6.1.4. The SIM domain in VP24 regulates both deubiquitination of VP24 and its interaction with USP7 protein

Western blot analysis of HA-VP24-SIM using anti-HA antibody revealed the appearance of a band of around 10 kDa higher molecular weight than VP24 detected in the cells transfected with VP24-SIM (asterisk in figure 9b). We hypothesized that this band might correspond to mono-ubiquitinated VP24 protein. To evaluate this hypothesis, HEK

293 cells were transfected with pcDNA or HA-VP24-SIM. 36 h after

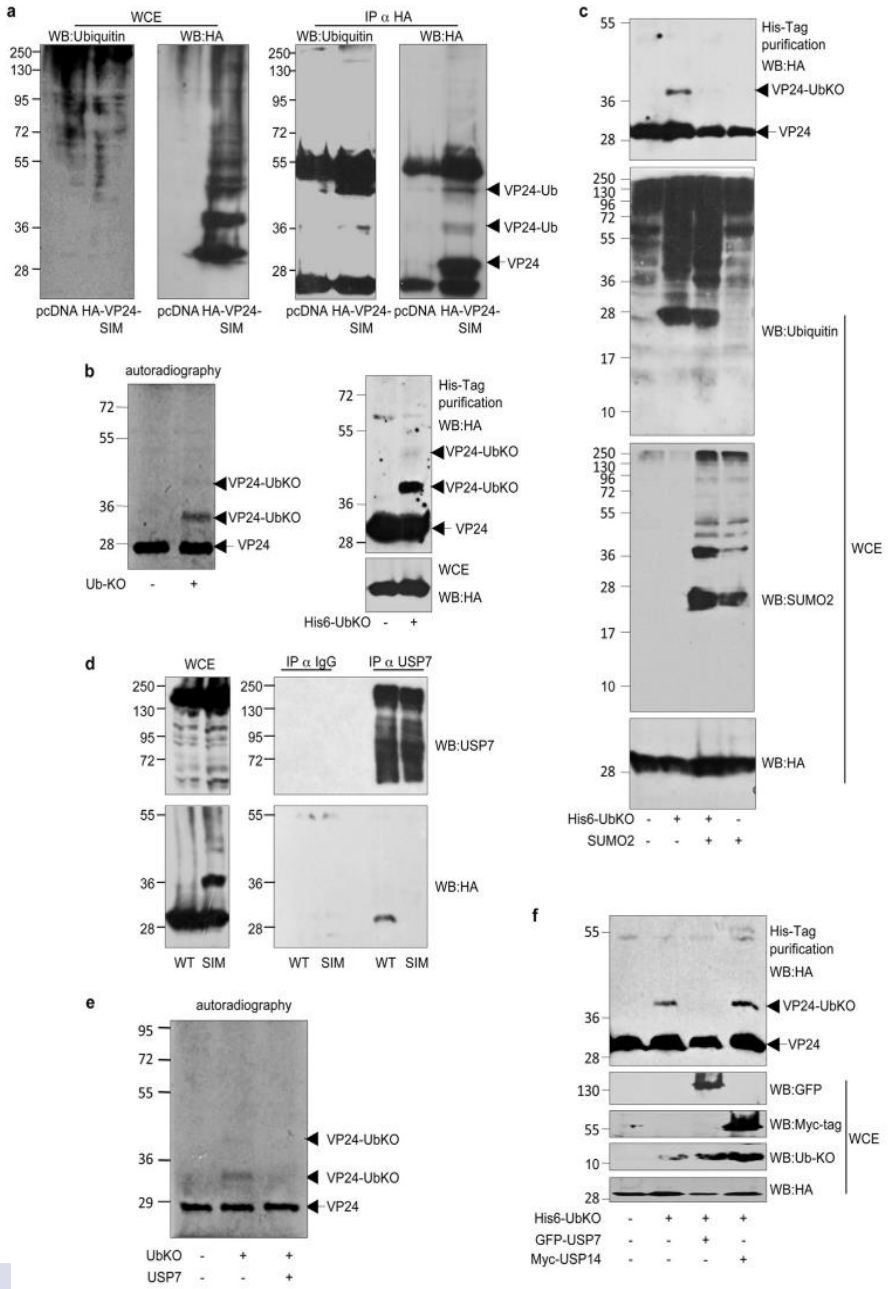

Figure 10. The SIM domain in VP24 regulates both its deubiquitination and the VP24 interaction with USP7 protein. a, HEK 293 cells were transfected with pcDNA or HA-VP24-SIM. 36 h after transfection protein extracts were immunoprecipitated with anti-HA antibody. Immunoprecipitated proteins were analyzed by Western blot with anti-ubiquitin or anti-HA antibodies. b, In vitro ubiquitination assays in presence of the lysine-less ubiquitin mutant (UbKO) using 35S-methionine-labeled in vitro translated VP24-WT protein (left panel). HEK 293 cells were transfected with HA-VP24-WT, pcDNA and His6-UbKO expression plasmids. 36 h after transfection whole cell extracts and Histidine-tagged purified proteins were analyzed by Western blot with anti-HA antibody (right panel). c, HEK 293 cells were co-transfected with HA-VP24-WT, pcDNA, His6-UbKO, SUMO2 or His6-UbKO and SUMO2. 36 h after transfection whole cell extracts and Histidine-tagged purified proteins were analyzed by Western blot with anti-HA antibody. d, HEK 293 cells were transfected with HA-VP24-WT or HA-VP24-SIM. 36 h after transfection protein extracts were immunoprecipitated with anti-USP7 antibody. Immunoprecipitated proteins were analyzed by Western blot using anti-HA antibody. e, Incubation of in vitro ubiquitinated in vitro translated 35S-methionine-labeled VP24-WT protein in presence of UbKO and recombinant USP7 protein. f, HEK 293 cells were transfected with HA-VP24-WT and pcDNA, His6-UbkO, His6-UbKO and GFP-USP7 or His6-UbKO and MYC-USP14. 36 h after transfection whole cell extracts and Histidine-tagged purified proteins were analyzed by Western blot with anti-HA antibody.

transfection cells were collected and protein extracts were immunoprecipitated with an anti-HA antibody. Analysis of the immunoprecipitated proteins by Western blot with anti-ubiquitin antibody revealed a band at the predicted molecular weight of monoubiquitinated VP24 in the cells transfected with HA-VP24-SIM (figure 10a), and this band was identified also with the anti-HA antibody (figure 10a), suggesting that mutation of the SIM domain in VP24 promoted its mono-ubiquitination. We then decided to evaluate the ubiquitination of the VP24-WT protein by carrying out *in vitro* ubiquitination assays using *in vitro* translated VP24 protein labeled with ^{35}S-methionine and a lysine-less ubiquitin mutant (UbKO). Incubation of VP24 with UbKO led to the appearance of two bands of around 38 and 48 kDa molecular weight (figure 10b left panel), indicating the presence of at least two different ubiquitin-conjugation sites in VP24 protein. To evaluate whether VP24 protein could be mono-ubiquitinated in cells, HEK 293 cells were co-transfected with HA-VP24-WT and pcDNA or His6-UbKO. 36 h after transfection cells were collected and Histidine-tagged proteins were purified under

denaturing conditions. Analysis of the purified proteins by Western blot with anti-HA antibody revealed the presence of two bands of around 38 and 48 kDa molecular weight in those cells transfected with His6-UbKO (figure 10b right panel), indicating that at least two lysine residues in VP24 can serve as ubiquitin acceptor sites in cells. These results suggested that the non-covalent interaction between VP24 and SUMO modulated the ubiquitination of VP24. To test this hypothesis, we evaluated the ubiquitination of VP24-WT in HEK 293 cells after overexpressing or not SUMO2. We detected a clear decrease in the levels of monoubiquitinated VP24 protein in those cells overexpressing SUMO2 (figure 10c). It has been recently proposed that the ubiquitin-specific protease USP7, involved in virus-host interactions processes, binds to SUMOylated proteins through an hypothetical SIM domain and reverses its ubiquitination(Lecona et al., 2016). Therefore, we decided to evaluate the putative interaction of USP7 with VP24-WT or VP24-SIM. HEK 293 cells were transfected with HA-VP24-WT or HA-VP24-SIM. 36 h after transfection protein extracts were immunoprecipitated with anti-USP7 antibody and samples were analyzed by Western blot with anti- HA or anti-USP7 antibodies. We observed co-immunoprecipitation between USP7 and VP24-WT protein (figure 10d). However, we did not detect interaction between USP7 and VP24-SIM (figure 10d). We then decided to evaluate the potential deubiquitination of VP24 by USP7. We first carried out *in vitro* ubiquitination assays using *in vitro* translated VP24 protein labeled with ^{35}S-methionine. Then, the ubiquitination reaction was incubated with recombinant USP7 protein. At least two bands corresponding with monoubiquitinated VP24 protein were detected in the ubiquitination assay (figure 10e). Those bands disappeared after incubation with USP7 (figure 10e), indicative of the deubiquitination of VP24 by USP7. To further demonstrate that USP7 is the deubiquitinase of VP24 we performed similar experiments in cells. In addition, to evaluate the specificity in the deubiquitination, we analyzed the effect of the ubiquitin-specific protease USP14 on ubiquitinated VP24. HEK 293 were co-transfected with HA-VP24-WT and pcDNA, His6-UbKO, His6-UbKO and GFP-USP7, or His6-UbKO and MYC-USP14. 36 h after transfection cells were collected, Histidine-tagged proteins were

purified under denaturing conditions and samples were analyzed by Western blot with the indicated antibodies. We detected HA-VP24 mono-ubiquitinated bands in those cells co-transfected with His6-UbKO (figure 10f). We did not observe bands corresponding with mono-ubiquitinated VP24 protein in those cells co-transfected with GFP-USP7 (figure 10f), confirming that USP7 can deubiquitinate VP24. However, we did not observe any change in the ubiquitination of HA-VP24 in those cells co-transfected with MYC-USP14 (figure 10f). These results indicated that USP7 interacts with VP24 through the SIM domain and induces its de-ubiquitination.

6.1.5. USP7 interacts covalently with SUMO2

Our results showing that VP24 interacts with USP7 through a SIM domain led us to propose the hypothesis that USP7 could be a SUMO substrate. So far, no SUMOylation of USP7 has been demonstrated; however, USP7 has been identified as a putative substrate for SUMO in proteomic studies (Lumpkin et al., 2017). We then decided to analyze the SUMOylation of USP7. HEK 293 cells were transfected with HA-USP7 together with pcDNA or His6-SUMO2. 36 h after transfection cells were collected and Histidine-tagged proteins were purified under denaturing conditions. Samples were analyzed by Western blot using and anti-HA antibody. As shown in figure 11a, USP7 protein was detected as a band of around 130 kDa molecular weight, as expected. In addition, we detected a band of higher molecular weight corresponding with the predicted size of SUMOylated USP7 protein in those cells co-transfected with His6-SUMO2 (figure 11a), indicating that USP7 is modified by SUMO. In order to confirm the SUMOylation of USP7, we performed an *in vivo* SUMOylation assay with endogenous USP7 protein. HEK 293 cells were transfected with pcDNA or His6-SUMO2. 36 h after transfection cells were collected and Histidine-tagged proteins were purified under denaturing conditions. Samples were analyzed by Western blot using and anti-USP7 antibody. As shown in figure 11b, we detected a band with higher molecular weight in those cells co-transfected with SUMO2, suggesting USP7 is a substrate for SUMOylation, and

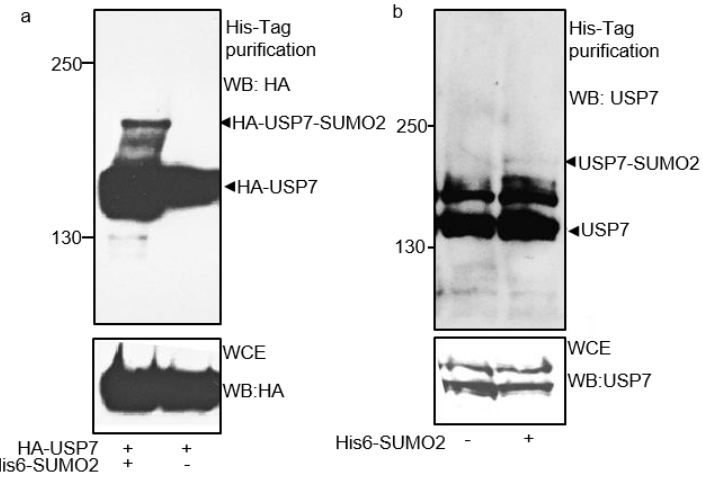

Figure 11. USP7 interacts covalently with SUMO2. a, HEK 293 cells were co-transfected with HA-USP7 together with pcDNA, or His6-SUMO2. 36 h after transfection whole cell extracts and Histidine-tagged purified proteins were analyzed by Western blot with anti-HA antibody. b, HEK 293 cells were transfected with pcDNA or His6-SUMO2. 36 h after transfection whole cell extracts and Histidine-tagged purified proteins were analyzed by Western blot with anti-USP7 antibody.

reinforcing the hypothesis that SUMO mediates the interaction of VP24 with USP7.

6.1.6. Ubiquitin conjugation to K206 in VP24 has a negative impact on its IFN-signaling inhibitory activity

In silico analysis of VP24 protein using the Ubpred program pointed out to lysine 206 (K206), a residue just five amino acids away from the SIM domain 198-LVEL-201 as the unique putative ubiquitination site in VP24 (figure 12a, schematic representation). To evaluate the involvement of this lysine residue in ubiquitin conjugation, we first generated the mutants VP24-K206R and VP24-SIM-K206R. Then we transfected HEK 293 cells with HA-VP24-WT, HA-VP24-SIM, or HA-VP24-SIM-K206R, and 36 h after transfection, the cells were analyzed by Western blot with anti-HA antibody. Interestingly, the intensity of the band corresponding to VP24 monoubiquitinated protein detected in the cells transfected with HA-VP24-SIM was clearly reduced after mutation of K206 in VP24 (figure 12a), suggesting that

K206 is involved in VP24 ubiquitination (figure 12a). In addition, we

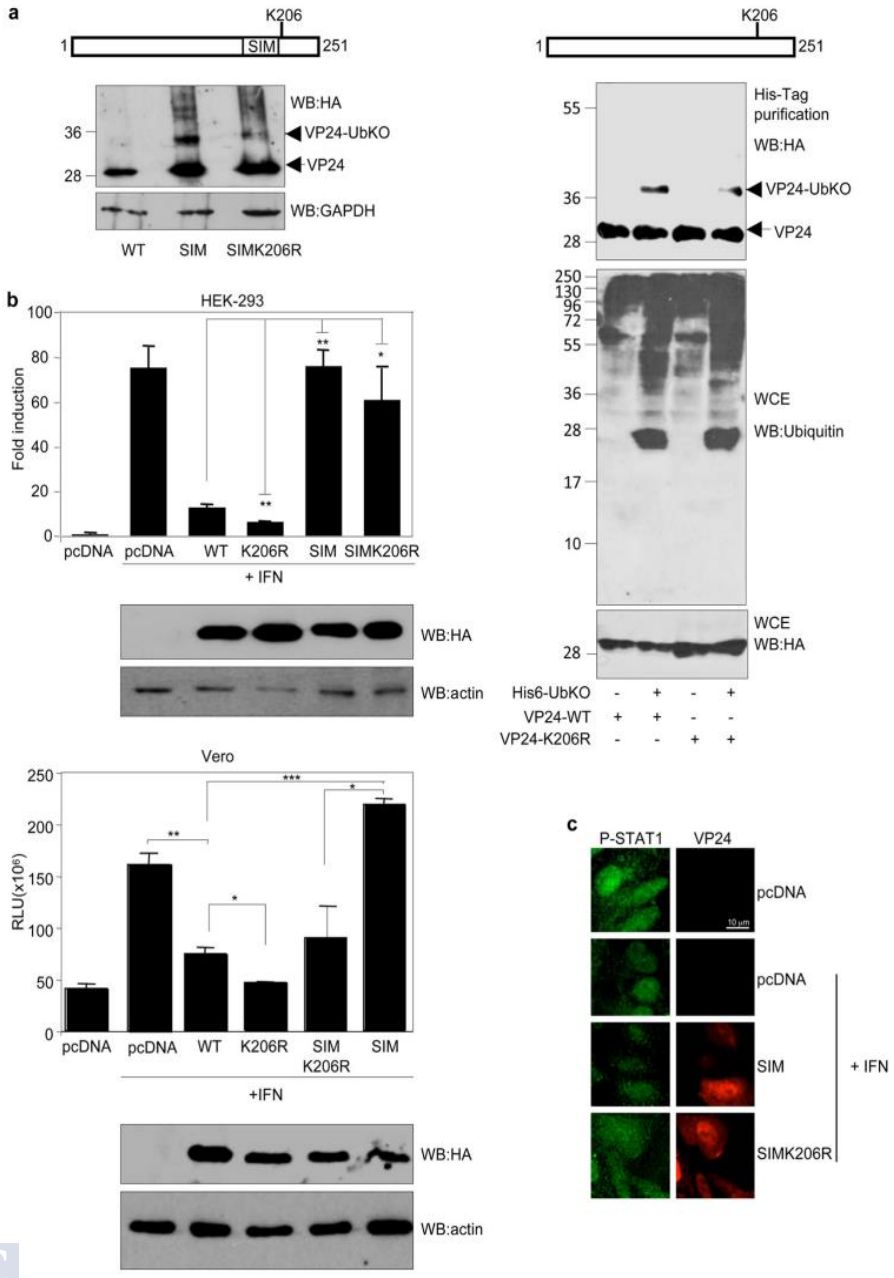

Figure 12. Conjugation of ubiquitin to K206 in VP24 has a negative impact in VP24 modulation of innate immune system. a, HEK 293 cells were transfected with HA-VP24-WT, HA-VP24-SIM or HA-VP24-SIM-K206R. 24 h after transfection whole cell lysates were analyzed by Western blot with anti-HA antibody, left panel. HEK 293 cells were transfected with HA-VP24-WT or HA-VP24-K206R and His6-UbKO. 36 h after transfection whole cell lysates and Histidine-tagged purified proteins were analyzed by Western blot with the indicated antibodies. b, HEK 293 cells, upper panel, or Vero cells, lower panel, were co-transfected with the luciferase reporter ISG54-luc and pcDNA-beta-gal together with the indicated plasmids. 24 h after transfection cells were treated with 1500 U/mL of IFN α and luciferase production was analyzed 16 h after treatment. Columns are representative of means of results, and error bars represent standard deviations of results from three biological replicates. Statistical significance was assessed by a Student's t test. Cell lysates from the experiment were analyzed by Western blotting for HA-VP24 expression. c, Vero cells were transfected with pcDNA, HA-VP24-SIM or HA-VP24-SIM-K206R. 24 h after transfection cells were serum starved for 4 h and treated with 1,000 U/mL of IFN α for 30 min or left untreated. Then cells were fixed and immunostained with mouse anti-Y701 phosphorylated-STAT1 (anti-p-STAT1) and goat anti-HA primary antibodies followed by secondary Alexa-488 chicken anti-mouse and Alexa-594 donkey anti-goat antibodies.

also co-transfected HEK 293 cells with HA-VP24-WT or HA-VP24-K206R together with pcDNA or His6-UBKO. 36 h after transfection cells were collected, Histidine-tagged proteins were purified under denaturing conditions and samples were analyzed by Western blot using an anti-HA antibody. As shown in figure 12a, ubiquitination of VP24 was reduced after K206R mutation, confirming that K206 in VP24 is an ubiquitin acceptor site. Finally, in order to decipher whether ubiquitin conjugation modulates the inhibition of IFN signaling by VP24 we performed a luciferase reporter assay. We co-transfected HEK 293 cells with ISG54-luc, pcDNA-beta-gal, and VP24-WT, VP24-SIM, VP24-K206R or VP24-SIM-K206R. 36 h after transfection cells were treated with IFN and 16 h after treatment luciferase activity was measured. Treatment with IFN led to an increase in the luciferase levels (figure 12b), as expected. Transactivation of the reporter was abolished after expression of VP24-WT while transfection of VP24-SIM did not have effect on the transactivation, as we previously observed (figure 12b). Interestingly, expression of the VP24K206R mutant induced a stronger inhibition of the reporter than the WT protein (figure 12b), suggesting that ubiquitination is a negative modulator of the IFN

signaling inhibitory activity of VP24. Similar results were obtained in Vero cells. As shown in figure 12b, mutation of K206 in VP24-WT or VP24-SIM significantly potentiated the inhibition of the reporter. To confirm these results, we decided to analyze the translocation of phosphorylated STAT1 in Vero cells transfected with HA-VP24-SIM or HA-VP24-SIM-K206R upon treatment with IFN. Phosphorylated STAT1 was detected in both nucleus and cytoplasm of untreated cells and accumulated in the nucleus of cells treated with IFN, as expected. Expression of VP24-SIM did not inhibit the translocation of phosphorylated STAT1 to the nucleus (90% of the cells expressing VP24-SIM shown nuclear phosphorylated STAT1 (n=96)). The translocation of phosphorylated STAT1 to the nucleus in cells expressing the VP24-SIM-K206R mutant was reduced (73% of the cells expressing VP24-SIM-K206R shown nuclear phosphorylated STAT1 (n=49)) (figure 12c.) These results suggested that ubiquitin negatively modulates the ability of VP24 to avoid STAT1 nuclear accumulation in response to IFN treatment while SUMO positively modulates this VP24 activity.

6.2. EBOV VP24 INDUCES A LAMINOPATHY-LIKE PHENOTYPE BY PROMOTING DISRUPTION OF NUCLEAR MEMBRANE

6.2.1. VP24 interacts with emerin

Two different proteomic studies to identify novel VP24 partners pointed out to emerin as a potential VP24 interactor (Batra et al., 2018;

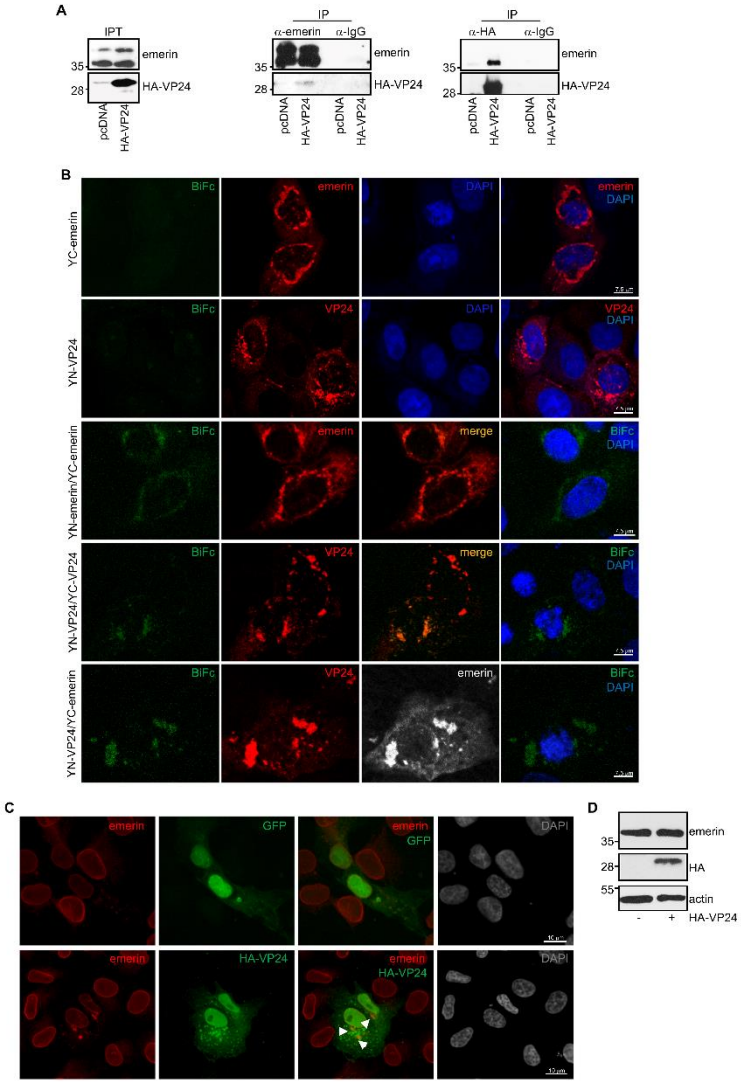

Figure 13. VP24 interacts with emerin. a, Vero cells were transfected with pcDNA or HA-VP24 expression plasmids. 36 h after transfection protein extracts were immunoprecipitated with anti-emerin or anti-HA antibodies. Samples were analyzed by Western blot with anti-emerin or anti-HA antibodies, as indicated. b, Vero cells were transfected with the indicated BiFC constructs (C-terminal part of the yellow fluorescent protein (YFP) fused to the N-terminus of full-length emerin, YC-emerin; N-terminal part of YFP fused to the N-terminus of full-length emerin, YN-emerin; N-terminal part of YFP fused to the N-terminal part of full length VP24, YN-VP24; C-terminal part of YFP fused to the N-terminal part of full length VP24, YC-VP24). Cells were fixed, permeabilized and stained with anti-emerin and/or anti-VP24 primary antibodies. Chromosomes were stained with DAPI (blue). c, Vero cells were transfected with GFP or HA-VP24 expression plasmids. 36 h after transfection, cells were fixed, permeabilized and stained with anti-emerin and anti-HA primary antibodies. Chromosomes were stained with DAPI (grey). White arrows indicate emerin-HA-VP24 co-localization. d, Vero cells were transfected with pcDNA or HA-VP24 expression plasmids. 36 h after transfection whole cell extracts were analyzed by Western blot with anti-emerin, anti-HA and anti-actin antibodies.

García-Dorival et al., 2014). We then decided to evaluate the potential interaction between VP24 and emerin. First, we performed IP assays. Vero cells were transfected with HA-VP24 or pcDNA and 36 h after transfection, protein extracts were immunoprecipitated with an anti-HA or anti-emerin antibodies. Immunoprecipitated proteins were analyzed by Western blot using the same antibodies. We observed that VP24 co-immunoprecipitated with emerin (figure 13a). To further characterize the interaction of VP24 with emerin, we performed bimolecular fluorescence complementation (BiFC) assays. Vero cells were transfected with plasmids encoding emerin or VP24 fused to the two complementary halves of the yellow fluorescent protein (YFP) (N-terminal, YN- or C-Terminal, YC-). We observed that cells expressing only one-half of YFP did not show fluorescence signal (figure 13b). Cells co-transfected with VP24 or emerin fused to the two halves of YFP showed YFP fluorescence signal (figure 13b) indicative of emerin or VP24 oligomerization, as previously reported (Berk et al., 2014; Han et al., 2003). When cells were co-transfected with YC-emerin and YN-VP24 expression plasmids, we also observed recovery of YFP fluorescence (figure 13b), indicative of emerin-VP24 interaction. Interestingly, the fluorescence signal was detected mainly outside the

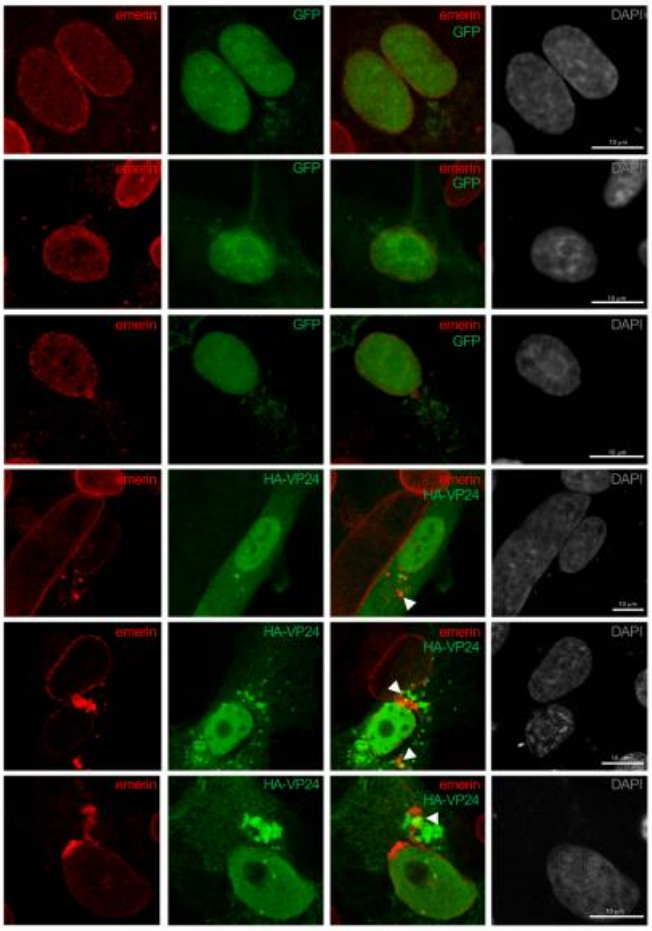

Figure 14. HA-VP24 co-localizes with endogenous emerin. a, Vero cells were transfected with GFP or HA-VP24 expression plasmids. 36 h after transfection cells were fixed, permeabilized and stained with anti-emerin and anti-HA primary antibodies. Chromosomes were stained with DAPI (grey). White arrows indicate emerin-HA-VP24 co-localization.

nuclear membrane. We then decided to evaluate the interaction of VP24 with endogenous emerin using immunofluorescence assays. Vero cells were transfected with GFP or HA-VP24 expression plasmids. 36 h after transfection cells were fixed and immunostained using anti-emerin and anti-HA antibodies. Confocal analysis revealed the localization of VP24 protein in both nucleus and cytoplasm, as reported before (He et

al., 2017). Endogenous emerin protein was detected in the nucle ar ring of those cells co-transfected with pcDNA, as expected (figure 13c and figure 14). We observed some cytoplasmic aggregates of emerin as well as partial emerin-VP24 co-localization in the cells expressing HA-VP24 (figure 13c and figure 14). To determine whether VP24 alters emerin protein levels, we transfected Vero cells with HA-VP24 or pcDNA. 36 h after transfection whole cell protein extracts were analyzed by Western blot with anti-emerin antibody. We did not detect any alteration in emerin levels upon expression of HA-VP24 (figure 13d).

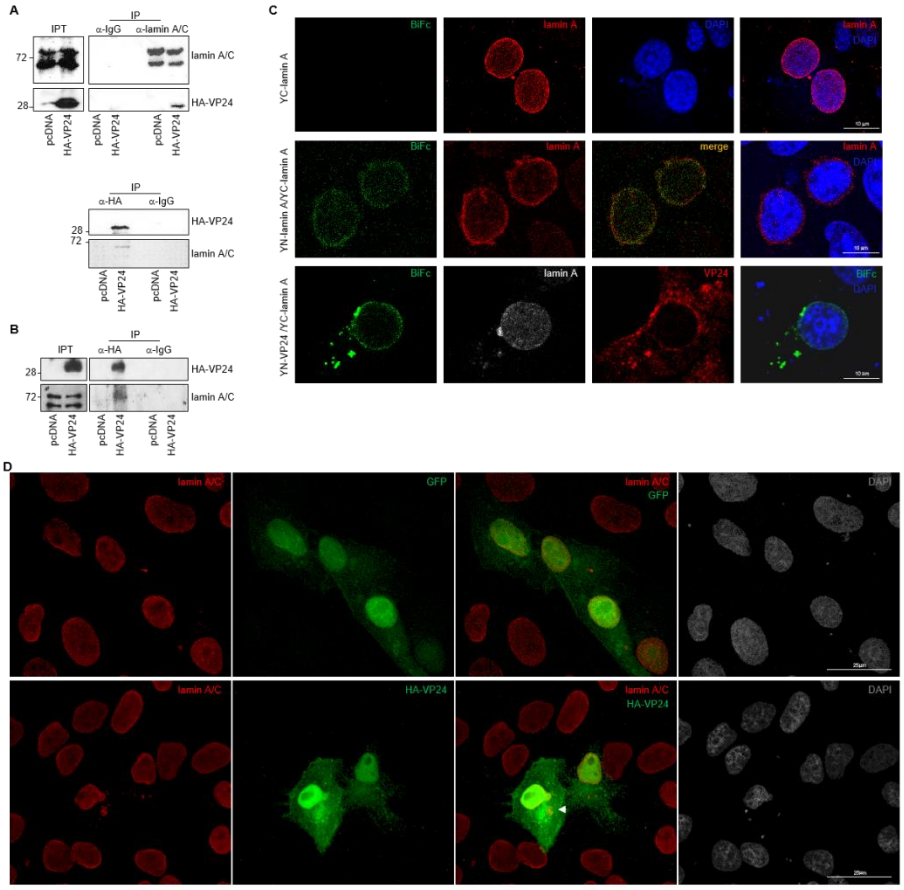

Figure 15. VP24 interacts with lamin A/C. a, Vero cells were transfected with pcDNA or HA-VP24 expression plasmids. 36 h after transfection, protein extracts were immunoprecipitated with anti-lamin A/C or anti-HA antibodies. Immunoprecipitated proteins were analyzed by Western blot with anti-lamin A/C and anti-HA antibodies. b, HUH-7 cells were transfected with pcDNA or HA-VP24 expression plasmids. 36 h after transfection protein extracts were immunoprecipitated with anti-HA antibody. Immunoprecipitated proteins were analyzed by Western blot with anti-lamin A/C and anti-HA antibodies. c, Vero cells were transfected with the indicated BiFC constructs (C-terminal part of the yellow fluorescent protein (YFP) fused to the N-terminus of full-length lamin A, YC-lamin A; N-terminal part of YFP fused to the N-terminus of full-length lamin A, YN-lamin A; N-terminal part of YFP fused to the N-terminal part of full length VP24, YN-VP24). Cells were fixed, permeabilized and stained with anti-lamin A/C and/or anti-VP24 primary antibodies. Chromosomes were stained with DAPI (blue). d, Vero cells were transfected with GFP or HA-VP24. 36 h after transfection cells were fixed, permeabilized and stained with anti-lamin A/C and anti-HA primary antibodies. Chromosomes were stained with DAPI (grey). White arrow indicates lamin A/C-HA-VP24 co-localization.

6.2.2. VP24 interacts with nuclear membrane components lamin A/C and lamin B

Emerin interacts with other components of the nuclear membrane such as lamin A/C and lamin B. In fact, emerin depends on lamin A for localization at the nuclear envelope (Samson et al., 2018). Therefore, we decided to evaluate the putative interaction of VP24 with the nuclear membrane components lamin A/C and lamin B. First, we analyzed the potential interaction between VP24 and lamin A/C using co-IP assays. Vero cells were transfected with pcDNA or HA-VP24 and 36 h after transfection protein extracts were immunoprecipitated with anti-lamin A or anti-HA antibodies. Western blot analysis of the immunoprecipitated proteins showed that VP24 and lamin A/C co-immunoprecipitated (figure 15a). Similar results were obtained after co-IP studies carried out in HUH-7 cells (figure 15b), highly susceptible to EBOV infection. To further study the VP24-lamin A interaction, BiFC experiments were carried out. Vero cells were transfected with expression plasmids encoding VP24 or lamin A fused to the two complementary halves of YFP. Cells transfected with YC-lamin A did not show fluorescence signal, as expected (figure 7c). Co-transfection of YC-lamin A and YN-lamin A led to the recovery of YFP fluorescence, indicative of lamin A

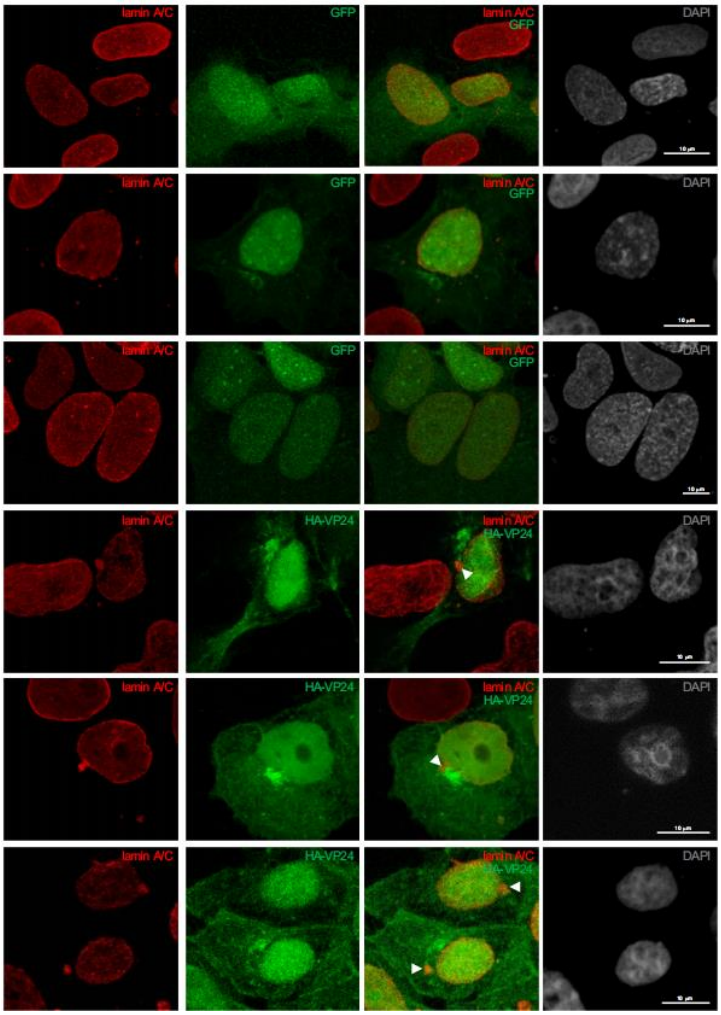

Figure 16. HA-VP24 co-localize with endogenous lamin A/C. a, Vero cells were transfected with GFP or HA-VP24 expression plasmids. 36 h after transfection cells were fixed, permeabilized and stained with anti-lamin A/C and anti-HA primary antibodies. Chromosomes were stained with DAPI (grey). White arrows indicate lamin A/C-HA-VP24 co-localization.

oligomerization. We also detected YFP reconstitution in cells expressing YC-lamin A and YN-VP24 (figure 15c), indicative of

VP24-lamin A interaction. We then decided to evaluate the co-localization between endogenous lamin A/C and HA-VP24 using immunofluorescence assays. Vero cells transfected with GFP or HA-VP24 were immunostained using anti-lamin A/C and anti-HA antibodies. After confocal analysis we observed partial co-localization between lamin A and VP24 (figure 15d and figure 16). Interestingly, we also observed the presence of cytoplasmic lamin A/C aggregates in those cells expressing VP24 protein (figure 15d and figure 16). Then we evaluated the putative interaction between VP24 and lamin B. Vero cells were transfected with pcDNA or HA-VP24. 36 h after transfection protein extracts were immunoprecipitated with anti-HA or anti-lamin B antibodies. Finally, immunoprecipitated proteins were analyzed by Western blot with the same antibodies. As shown in figure 17a, lamin B and HA-VP24 co-immunoprecipitate. To further characterize this interaction, we performed immunofluorescence staining of endogenous lamin B in cells expressing or not VP24. Vero cells were transfected with GFP or HA-VP24. 36 h after transfection cells were fixed and immunostained with anti-HA and anti-lamin B antibodies, and analyzed using a confocal microscope. Co-localization between HA-VP24 and lamin B was observed (figure 17b and figure 18). In addition, we detected the presence of cytoplasmic aggregates of lamin B in those cells expressing VP24 (figure 17b and figure 18). Altogether these results indicated that VP24 can interact with different nu clear membrane components.

6.2.3. VP24-emerin interaction occurs in a tag-independent manner

It has been reported that tagging proteins can modify their activity, stability or subcellular localization. In the case of VP24 protein, adding a flag tag on its C-terminus alters VP24 ability to form nucleocapsid structures and to inhibit replication and transcription of the EBOV

genome (Watanabe et al., 2007). To address whether VP24 interacts with emerin in a tag-independent manner, the coding region for VP24

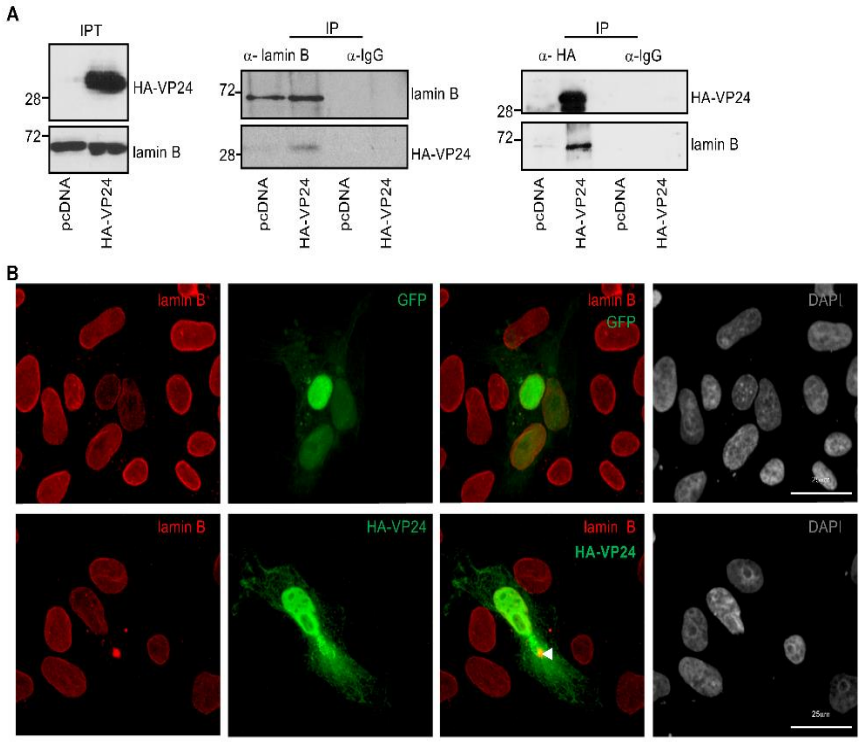

Figure 17. HA-VP24 interacts with lamin B. a, Vero cells were transfected with pcDNA or HA-VP24 expression plasmids. 36 h after transfection protein extracts were immunoprecipitated with anti-lamin B or anti-HA antibodies. Samples were analyzed by Western blot using anti-lamin B or anti-HA antibodies. b, Vero cells were transfected with GFP or HA-VP24 expression plasmids. 36 h after transfection, cells were fixed, permeabilized and stained with anti-lamin B and anti-HA primary antibodies. Chromosomes were stained with DAPI (grey). White arrow indicates lamin B-HA-VP24 co-localization.

was cloned fused to a GFP tag. Confocal analysis of Vero cells that were transfected with GFP-VP24 expression plasmid revealed the cytoplasmic localization of GFP-VP24 protein (figure 19a), in contrast with the nuclear and cytoplasm localization of HA-VP24 protein

(figures 12c, 15d, and 17c). We speculated that passive cytoplasm to nucleus diffusion of the small HA-VP24 protein may be inhibited by the fusion of the 30 kDa GFP tag. To evaluate whether VP24 can be

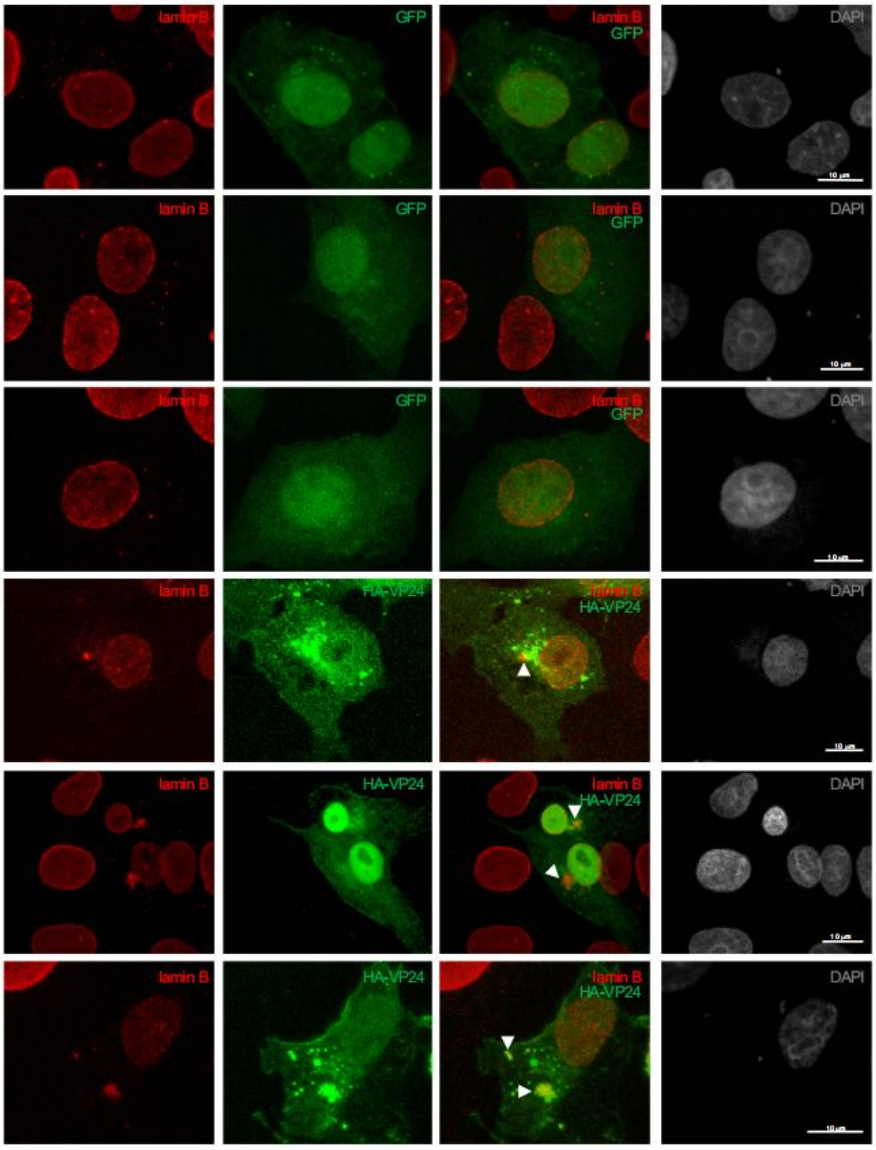

Figure 18. HA-VP24 co-localize with endogenous lamin B. a, Vero cells were transfected with GFP or HA-VP24 expression plasmids. 36 h after transfection cells were fixed, permeabilized and stained with anti-lamin B and anti-HA primary antibodies. Chromosomes were stained with DAPI (grey). White arrows indicate lamin B-HA-VP24 co-localization.

actively transported inside the nucleus we co-transfected Vero cells with GFP-VP24 and KPNA5 expression plasmids. 36 h after

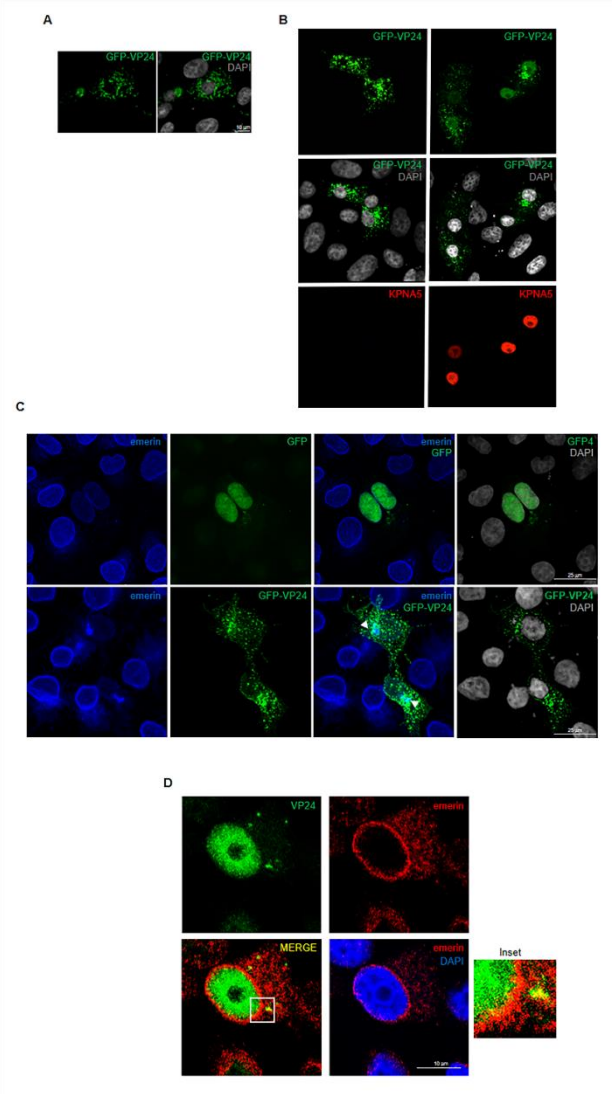

Figure 19. VP24-emerin interaction occurs in a tag independent manner. a, Vero cells were transfected with GFP-VP24 expression plasmid. 36 h after transfection cells were fixed and chromosomes were stained with DAPI (grey). b, Vero cells were transfected with GFP-VP24 or GFP-VP24 and KPNA5 expression plasmids. 36 h after transfection cells were fixed, permeabilized and stained with anti-KPNA5 primary antibody. Chromosomes were stained with DAPI (grey). c, Vero cells were transfected with GFP or GFP-VP24 expression plasmids. 36 h after transfection cells were fixed, permeabilized and stained with anti-emerin primary antibody. Chromosomes were stained with DAPI (grey). White arrow indicates emerin-GFP-VP24 co-localization. d, Vero cells were transfected with VP24 expression plasmid. 36 h after transfection cells were fixed, permeabilized and stained with anti-emerin and anti-VP24 primary antibodies. Chromosomes were stained with DAPI (blue). White square indicates area which is zoomed in inset panel.

transfection cells were fixed and immunostained with anti-KPNA5 antibody. Confocal analysis of the samples revealed that GFP-VP24 was detected in the cytoplasm of cells untransfected with KPNA5 (figure 19b). However, GFP-VP24 was detected in the cytoplasm of those cells co-expressing KPNA5 (figure 19b), indicating that KPNA5 promotes the nuclear translocation of VP24. We then evaluated the co-localization of GFP-VP24 with endogenous emerin by immunofluorescence assays. Vero cells were transfected with GFP or GFP-VP24 and 36 h after transfection cells were fixed, immunostained with anti-emerin antibody and samples were analyzed by confocal microscopy. We observed that GFP-VP24 partially co-localized with emerin in the cell cytoplasm (figure 19c). Then we evaluated the putative interaction of untagged VP24 with emerin. BSR-T7 cells were transfected with VP24 expression plasmid. 36 h after transfection cells were fixed and immunostained with anti-VP24 and anti-emerin antibodies. Confocal analysis revealed that VP24 was detected both in cytoplasm and nucleus, partially co-localizing with emerin (figure 19d).

Altogether these results indicated that emerin-VP24 interaction occurs in a tag-independent manner.

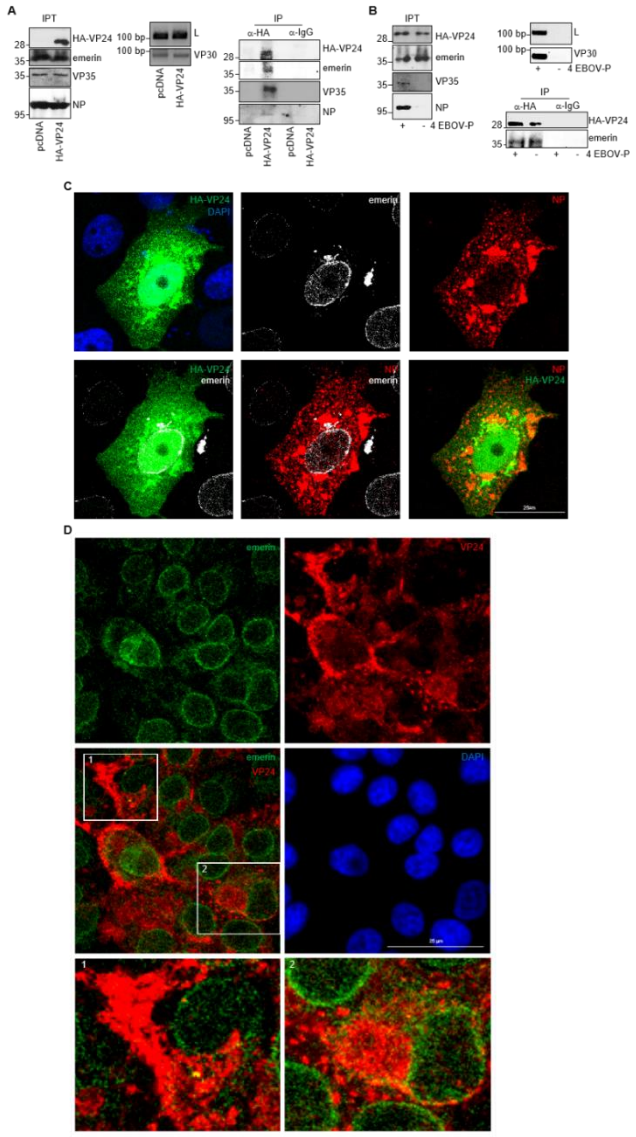

Figure 20. Emerin associates with VP24 in the presence of other EBOV proteins. a, BSR-T7 cells were transfected with EBOV NP, VP30, L, and VP35 together with pcDNA or HA-VP24 expression plasmids. 36 h after transfection protein extracts were immunoprecipitated with anti-HA antibody. Immunoprecipitated proteins were analyzed by Western blot with anti-emerin, anti-HA, anti-NP, and anti-VP35 antibodies. RNA extracts were analyzed by qRT-PCR to demonstrate VP30 and polymerase L expression. b, Vero cells were transfected with NP and HA-VP24 expression plasmids. 36 h after transfection cells were fixed, permeabilized and stained with anti-NP, anti-HA, and anti-emerin antibodies. Chromosomes were stained with DAPI (blue). c, Vero cells were infected with EBOV. 2 d after infection cells were fixed, permeabilized and stained with anti-emerin and anti-VP24 antibodies. Chromosomes were stained with DAPI (blue). White squares show area zoomed in insets 1 and 2.

6.2.4. VP24 interacts with emerin in the presence of other EBOV proteins

To determine whether VP24 interacts with emerin in the presence of other viral components, we performed IP assays in BSR-T7 cells co-transfected with EBOV proteins of Makona strain NP, VP35, VP30, and L, together with pcDNA or HA-VP24. 36 h after transfection protein extracts were immunoprecipitated with an anti-HA antibody. Western blot analysis of the immunoprecipitated proteins revealed that VP24 interacted with NP and VP35 (figure 20a) as expected (Huang et al., 2002). We also detected emerin protein in the immunoprecipitated fraction (figure 20a). We then performed immunofluorescence assays to determine whether NP expression alters the VP24-emerin co-localization. Vero cells were co-transfected with HA-VP24 and NP. 36 h after transfection cells were fixed and immunostained with anti-NP, anti-HA, and anti-emerin antibodies. Co-localization between NP and VP24 was observed (figure 20b and figure 21), as expected. Furthermore, we detected partial emerin-VP24 co-localization (figure 20b). Finally, we evaluated the potential co-localization of VP24 expressed from the virus with endogenous emerin. Vero cells were infected with EBOV and 2 d after infection cells were fixed and immunostained with anti-emerin and anti-VP24 antibodies. As shown in figure 20c, co-localization between VP24 protein and emerin was detected in cells infected with EBOV.

6.2.5. VP24 compromises nuclear membrane integrity

Mislocalization of nuclear envelope components can be associated to disruptions of interactions between emerin and lamin A/C. Therefore, we decided to evaluate whether VP24 alters the interaction between emerin and lamin A/C. We transfected HEK 293 cells with pcDNA or HA-VP24. 36 h after transfection protein extracts were immunoprecipitated with anti-emerin or anti-lamin A/C antibodies and analyzed by Western blot with the indicated antibodies. Emerin and lamin A/C coimmunoprecipitated, as expected (figure 22a). Expression of VP24 reduced the interaction between emerin and lamin A/C (figure 22a). To further evaluate the impact of VP24 expression on emerin-lamin A interaction, we performed BiFC assays. Vero cells were transfected with EYC-lamin A, EYN-emerin, and pcDNA or EYC-lamin A, EYN-emerin, and HA-VP24. 36 h after transfection cells were fixed and immunostained. After confocal analysis we observed that co-expression of YC-lamin A and YN-emerin led to YFP fluorescence reconstitution at the nuclear membrane (figure 22b). An irregular fluorescent signal at the nuclear rim and in cytoplasmic aggregates was observed in those cells expressing HA-VP24, indicating that expression of VP24 alters the interaction between emerin and lamin A (figure 22b and figure 23). Finally, we decided to evaluate whether co-expression of EBOV proteins altered the ability of VP24 to downmodulate emerin-lamin A/C interaction. BSR-T7 cells were transfected with EBOV NP, VP35, VP30, and L together with pcDNA or HA-VP24. 36 h after transfection protein extracts were immunoprecipitated with an anti-lamin A/C antibody and immunoprecipitated proteins were analyzed by Western blot with anti-lamin A/C or anti-emerin antibodies. We observed a clear reduction in the levels of emerin protein co-immunoprecipitating with lamin A/C when VP24 was expressed (figure 22c), indicating that VP24 expression alters emerin-lamin A/C interaction in presence of other EBOV proteins.

An alteration in the lamin A-emerin interaction could trigger the collapse of the nuclear envelope. Therefore, we decided to evaluate whether VP24 expression led to nuclear envelope damage. Vero cells

were transfected with GFP or HA-VP24. 36 h after transfection cells

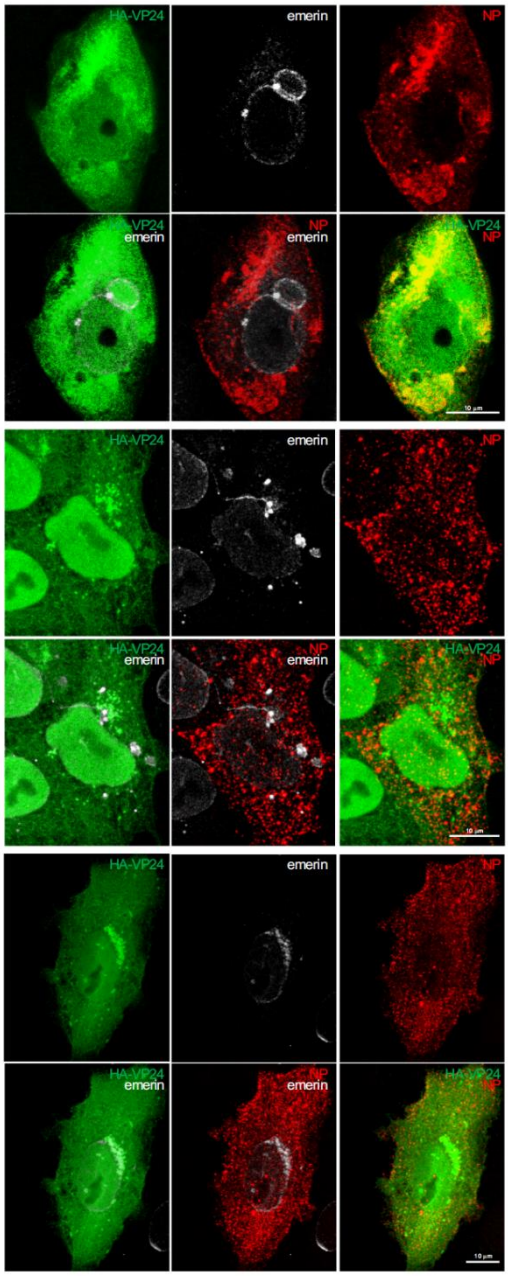

Figure 21. Emerin co-localizes with HA-VP24 in presence of NP. Vero cells were transfected with NP and HA-VP24 expression plasmids. 36 h after transfection cells were fixed, permeabilized and stained with anti-NP, anti-HA and anti-emerin primary antibodies. Chromosomes were stained with DAPI (blue).

were fixed and then permeabilized with digitonin, a detergent that permeabilizes the plasma membrane leaving the nuclear membrane

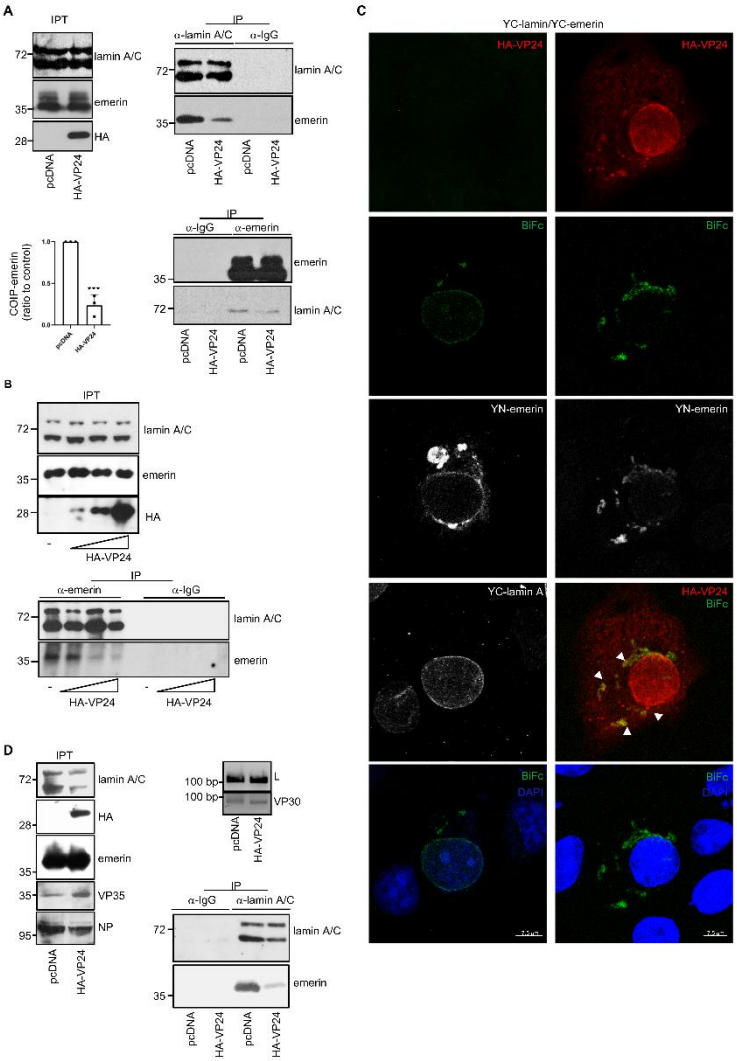

Figure 22. VP24 reduces lamin A/C-emerin interaction. a, HEK 293 cells were transfected with pcDNA or HA-VP24 expression plasmids. 36 h after transfection protein extracts were immunoprecipitated with anti-lamin A/C or anti-emerin antibodies. Immunoprecipitated proteins were analyzed by Western blot with anti-emerin, anti-lamin A/C and anti-HA antibodies. Emerin protein co-immunoprecipitating with lamin A/C in presence or absence of VP24 in three different experiments was quantified and normalized to the total amount of immunoprecipitated Lamin A/C.The emerin/lamin A/C ratio detected in cells transfected with pcDNA was set to 1 and the values found in HA-VP24 expressing cells were calculated relative to it. Statistical analysis was assessed by a Student's t-test. ***, P<0.001. b, Vero cells were transfected with the indicated BiFC constructs together with pcDNA or HA-VP24 expression plasmids. 36 h after transfection cells were fixed, permeabilized and stained with anti-emerin, anti-lamin A/C and anti-HA antibodies. Chromosomes were stained with DAPI (blue). White arrows indicate co-localization between lamin A, emerin and HA-VP24. c, BSR-T7 cells were transfected with EBOV NP, VP30, L, and VP35 together with pcDNA or HA-VP24. 36 h after transfection protein extracts were immunoprecipitated with anti-lamin A/C antibody. Immunoprecipitated proteins were analyzed by Western blot with anti-NP, anti-VP35, anti-HA, anti-lamin A/C, and anti-emerin antibodies. RNA extracts were analyzed by qRT-PCR for VP30 and L expression.

intact and cells were then immunostained with an anti-lamin A/C antibody. Immunofluorescence analysis using a confocal microscope showed that lamin A/C was undetectable in the cells expressing GFP (figure 24a). In contrast, we observed lamin A/C staining in the cells expressing HA-VP24 (figure 24b), indicating that expression of VP24 resulted in damage of the nuclear membrane. To confirm the loss of the nuclear membrane integrity by VP24, we evaluated the subcellular localization of the fluorescent reporter of nuclear membrane rupture, a construct expressing GFP protein fused to a NLS (GFP-NLS), in cells expressing or not VP24. Vero cells were co-transfected with GFP-NLS and pcDNA or HA-VP24, permeabilized with digitonin and immunostained with anti-HA antibody. Confocal analysis revealed that

GFP-NLS was detected inside the nucleus in those cells transfected

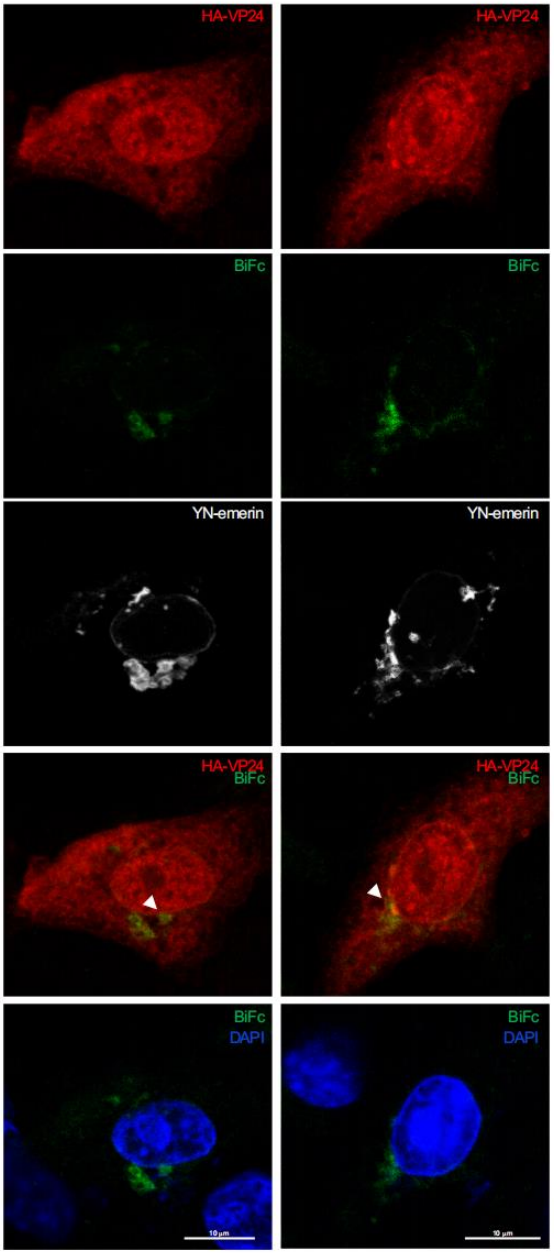

Figure 23. VP24 reduces lamin A/C-emerin interaction. Vero cells were transfected with the indicated BiFC constructs together with pcDNA or HA-VP24 expression plasmids. 36 h after transfection cells were fixed, permeabilized and stained with anti-emerin, anti-lamin A/C, and anti-HA antibodies. Chromosomes were stained with DAPI (blue). White arrows indicate co-localization between lamin A, emerin and HA-VP24.

with pcDNA (figure 24b) In cells expressing HA-VP24, the GFP-NLS signal was detected inside the nucleus and the cytoplasm (figure 24b), suggesting that VP24 expression leads to nuclear membrane disruption. We then decided to analyze the effects of VP24 expression on another

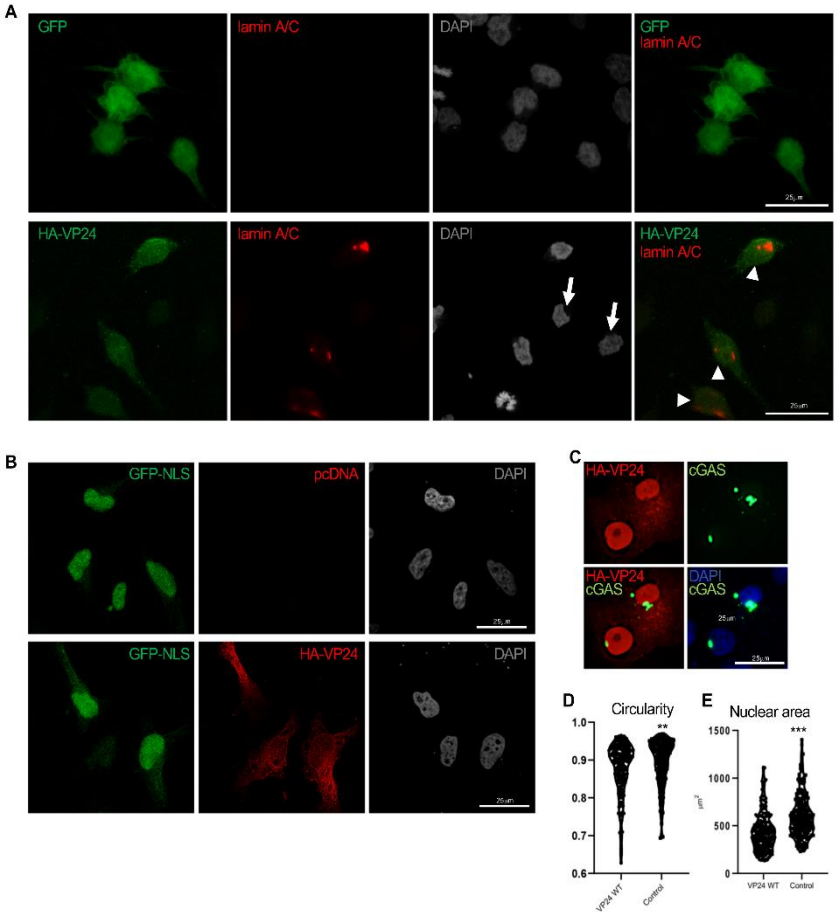

Figure 24. VP24 induces nuclear membrane disruption. a, Vero cells were transfected with GFP or HA-VP24 expression plasmids. 36 h after transfection cells were permeabilized with digitonin, fixed and stained with anti-lamin A/C and anti-HA primary antibodies. Chromosomes were stained with DAPI (grey). White arrows indicate positive cells for lamin A/C staining. b, Vero cells were transfected with GFP-NLS together with pcDNA or HA-VP24 expression plasmids. 36 h after transfection cells were permeabilized with digitonin, fixed and stained with anti-HA primary antibody. Chromosomes were stained with DAPI (grey). c, Vero cells were transfected with GFP-cGAS and HA-VP24. 36 h after transfection cells were fixed, permeabilized and stained with anti-HA primary antibody. Chromosomes were stained with DAPI (blue). d, Shape of the nucleus of Vero cells expressing HA-VP24 or pcDNA. A higher circularity denotes a more circular shape. Graphs show one data point per nucleus analyzed. Statistical analysis was assessed by a Student's t-test. **, P<0.01. e, Size of the nucleus of Vero cells expressing HA-VP24 or pcDNA. Graphs show one data point per nucleus analyzed. Statistical analysis was assessed by a Student's t-test. ***, P<0.001.

nuclear membrane rupture reporter, GFP-cGAS. After nuclear envelope rupture, the cytoplasmic GFP-cGAS has been described to accumulate at the disruption site and bind to exposed genomic DNA. Confocal analysis of Vero cells transfected with GFP-cGAS and HA-VP24 revealed an accumulation of GFP-cGAS in intranuclear foci (figure 24c), suggesting that expression of VP24 promotes the loss of nuclear membrane integrity. Abnormalities in the shape of the nuclei and a reduction in nuclear size are characteristics of cells with nuclear membrane damage. To determine whether VP24 has an impact on the shape and size of the nucleus, we measured the area and analyzed the shape of the nucleus of Vero cells expressing HA-VP24. We observed that the cells expressing VP24 showed more irregular nuclei than the cells transfected with pcDNA (figure 24d). In addition, the nuclear size of those cells expressing VP24 was significantly smaller than that detected in control cells (figure 24e). Altogether these results suggested that HA-VP24 expression compromises nuclear membrane integrity by altering emerin-lamin A interaction.

6.2.6. VP24 activates MAPK pathways

Nuclear membrane disorganization such as the one induced after lamin A downmodulation has been reported to promote ERK phosphorylation (Muchir et al., 2009) (figure 25a). To evaluate

whether VP24 could also induce the activation of the MAPK pathway, Vero cells were transfected with HA-VP24 or pcDNA and 36 h after

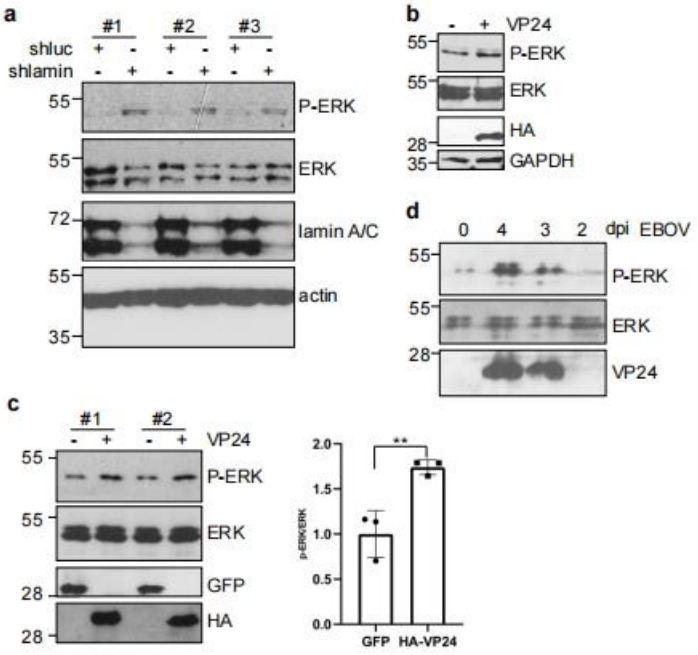

Figure 25. VP24 activates MAPK pathway. a, protein extracts from Hela cells stably transfected with sh-luc or sh-lamin A (shlamin) were analyzed by Western blot with anti-phoshorylated-ERK 1/2 (P-ERK 1/2), anti-ERK 1/2, anti-lamin A/C, or anti-actin antibodies (three different replicas are shown). b, Vero cells were transfected with HA-VP24 or pcDNA expression plasmids. 36 h after transfection whole cell protein extracts were analyzed by Western blot with anti-P-ERK 1/2, anti-ERK 1/2, anti-HA, or anti-GAPDH antibodies. c, A549 cells were transfected with HA-VP24 or GFP expression plasmids. 36 h after transfection whole cell protein extracts were analyzed by Western blot with anti-P-ERK 1/2, anti-ERK 1/2, anti-HA, and anti-GFP antibodies. Phospho-ERK 1/2 and total ERK 1/2 protein levels form three different replicas were quantified. P-ERK/ERK ratio from each replica was calculated and plotted. Data represent the mean and error bars of 3 biological replicates (right panel). Statistical analysis was assessed by a Student's t-test. **, P<0.01. d, Vero cells were infected or not with EBOV. Different days post infection cells were collected directly in loading buffer. Whole cell extracts were analyzed by Western blot with anti-P-ERK 1/2, ERK 1/2 or anti-VP24 antibodies. 0 stands for mock cells cultured for 4 days in the same conditions that EBOV infected cells.

transfection whole cell protein extracts were analyzed by Western blot with anti-phosphorylated-ERK 1/2 antibody. As shown in figure 25b, expression of VP24 promoted the phosphorylation of ERK 1/2. Similar results were observed in Hela cells (figure 25c). Finally, we decided to evaluate whether EBOV infection also induced phosphorylation of ERK 1/2. Vero cells were infected with EBOV and at different days after infection whole cell protein extracts were analyzed by Western blot with anti-phosphorylated ERK 1/2 antibody. We observed a clear increase in the levels of phosphorylated ERK 1/2 protein at 3 and 4 d after infection (figure 25d).

6.2.7. DNA damage and ISG15 induction in VP24 expressing cells

Disruption of nuclear membrane correlates with the accumulation of DNA damage(Schreiber and Kennedy, 2013). To evaluate whether VP24 induces DNA damage we transfected Vero cells with GFP or HA-VP24 and 36 h after transfection cells were fixed and immunostained with anti-phosphorylated-H2AX (gH2AX) antibody. After analysis by confocal microscopy we observed foci of gH2AX in 85% of cells expressing HA-VP24 and in 13% of control cells (figure 26a). We also detected an increase in gH2AX protein levels upon expression of HA-VP24 using Western blot analysis (figure 26b), suggesting that VP24 expression triggers DNA damage. Analysis of gH2AX in EBOV infected cells using both immunofluorescence and Western blot analysis also revealed an increase in gH2AX upon EBOV infection (figure 26c and 26d). DNA damage has been demonstrated to induce the upregulation of ISG15 (Jeon et al., 2017; Park et al., 2016). We then decided to analyze the levels of ISG15 in cells expressing VP24. Vero cells were transfected with HA-VP24 or pcDNA, RNA was isolated and the expression of ISG15 was evaluated by qRT-PCR. A significant increase in the transcript levels of ISG15 was observed after transfection with HA-VP24 (figure 26e). In addition, transfection of A549 or Hela cells with HA-VP24 also induced an increase in ISG15 protein levels in comparison with the levels detected in GFP transfected cells (figure 26f and 26g, respectively). To note, an upregulation in ISG15 protein

levels was also observed after downmodulation of lamin A (figures 26g and 26h).

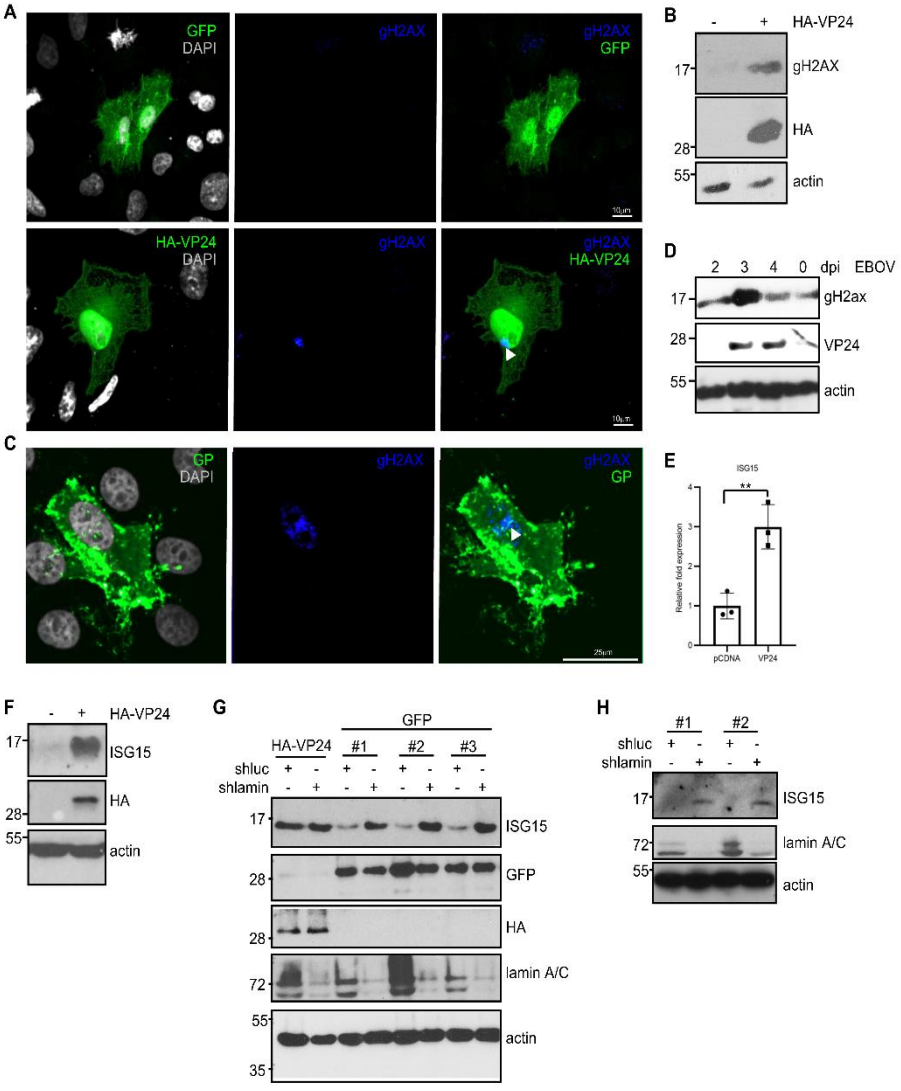

Figure 26. DNA damage and ISG15 induction in VP24 expressing cells. a, Vero cells were transfected with HA-VP24 or GFP expression plasmids. 36 h after transfection cells were fixed, permeabilized and stained with anti-gH2AX and anti-HA primary antibodies. Chromosomes were stained with DAPI (grey). White arrow indicates detection of gH2AX. b, Vero cells were transfected with pcDNA or HA-VP24 and 36 h after transfection whole cell protein extracts were analyzed by Western blot with anti-gH2AX, anti-HA, or anti-actin antibodies. c, Vero cells were infected with EBOV. 2 days after infection, cells were fixed, permeabilized and stained with anti-GP and anti-gH2AX primary antibodies. Chromosomes were stained with DAPI (grey). White arrow indicates positive detection of gH2AX in the infected cells. d, Vero cells were infected or not with EBOV. At different days post-infection cells were collected in SDS-loading buffer. Whole cell extracts were analyzed by Western blot with anti-gH2AX, anti-VP24, or anti-actin antibodies. e, Vero cells were transfected with pcDNA or HA-VP24 expression plasmids. 36 h after transfection RNA was isolated and ISG15 transcript levels were determined by qRT-PCR. Columns are representative of the mean, and error bars represent the standard deviation of 3 biological replicates (right panel). Statistical analysis was assessed by a Student's t-test. **, P<0.01. f, A549 cells were transfected with pcDNA or HA-VP24 expression plasmids. 36 h after transfection whole cell lysates were analyzed by Western blot with anti-ISG15, anti-HA, or anti-actin antibodies. G, Hela cells stably transfected with sh-luciferase (sh-luc) or sh-lamin A (shlamin) were transfected with HA-VP24 or GFP expression plasmids. 36 h after transfection whole cell lysates were analyzed by Western blot with anti-ISG15, anti-GFP, anti-HA, anti-lamin A/C, or anti-actin antibodies. Three different replicas are shown. h, A549 cells stably transfected with sh-luciferase or sh-lamin A were collected in SDS-sample buffer and analyzed by Western blot with anti-ISG15, anti-lamin A/C, or anti-actin antibodies.

6.2.8. RANGAP and RANBP subcellular localization is not affected by VP24

One of the main functions of lamin A is to anchor nuclear pores(Guo and Zheng, 2015). Therefore, we decided to evaluate whether VP24 triggers the mislocalization of the nuclear pore-associated proteins RANGAP and RANBP. Vero cells were transfected with HA-VP24 or GFP and both RANGAP and RANBP were analyzed by immunofluorescence. Confocal analysis revealed that both proteins were located at the nuclear envelope and in cytoplasmic aggregates independently of HA-VP24 expression (figures 27a and 27b), suggesting that nuclear pore complexes are not affected by VP24.

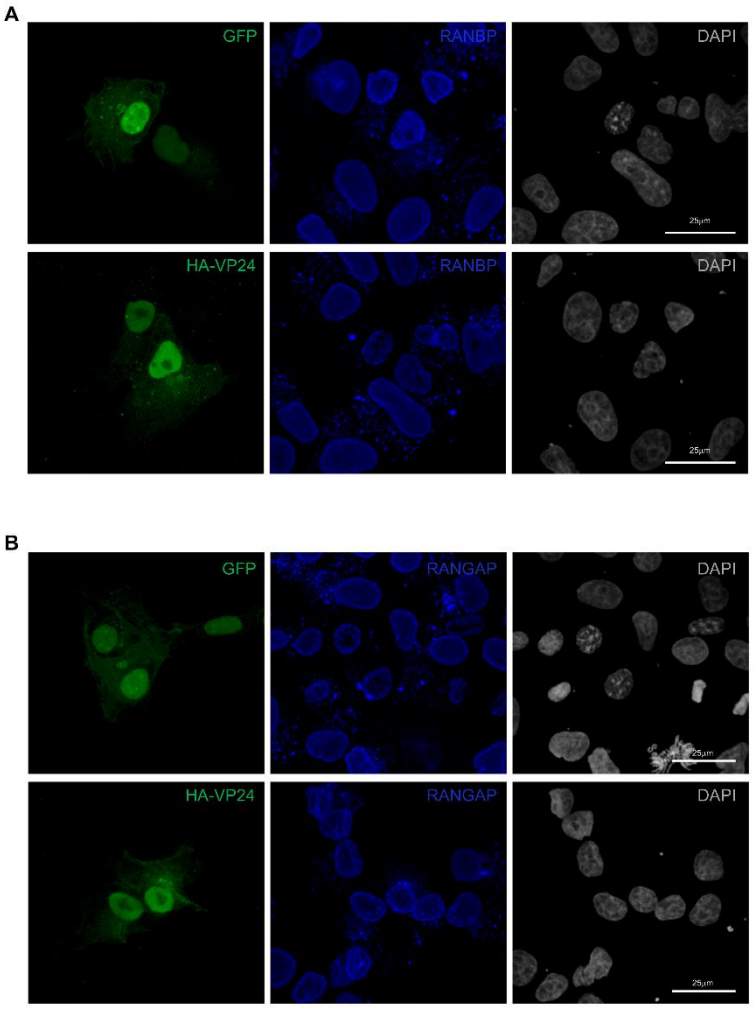

Figure 27. RANGAP and RANBP subcellular localization is not affected by VP24. a, Vero cells were transfected with GFP or HA-VP24 expression plasmids. 36 h after transfection, cells were fixed, permeabilized and stained with anti-RANBP and anti-HA primary antibodies. Chromosomes were stained with DAPI (grey). b, Vero cells were transfected with GFP or HA-VP24 transfection plasmids. 36 h after transfection cells were fixed, permeabilized and stained with anti-RANGAP and anti-HA primary antibodies. Chromosomes were stained with DAPI (grey).

6.2.9. BAF translocation and downmodulation by VP24

Structurally interdependence and interaction between the nuclear

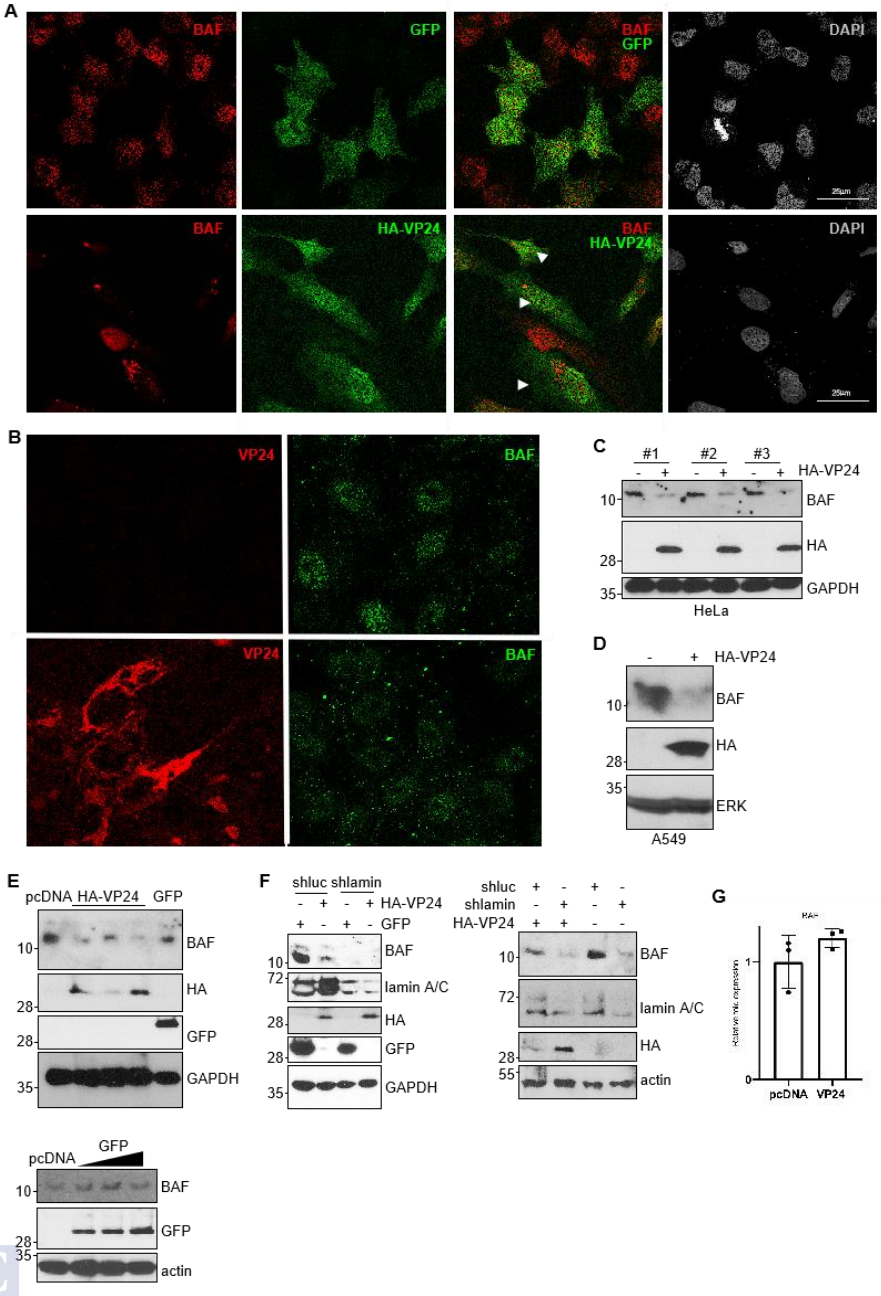

Figure 28. BAF translocation and dowmodulation by VP24. a, Vero cells were transfected with GFP or HA-VP24 plasmids. 36 h after transfection cells were fixed, permeabilized and stained with anti-BAF and anti-HA antibodies. Chromosomes were stained with DAPI (grey). White arrows indicate BAF translocation. b, Vero cells were infected with EBOV. 2 days after infection, cells were fixed, permeabilized and stained with anti-BAF and anti-VP24 antibodies. c, Hela cells were transfected with pcDNA or HA-VP24 expression plasmids. 36 h after transfection whole cell extracts were analyzed by Western blot with anti-BAF, anti-HA, and anti-GAPDH antibodies. Three different replicas are shown. d, A549 cells were transfected with pcDNA or HA-VP24 expression plasmids. 36 h after transfection whole cell extracts were analyzed by Western blot with anti-BAF, anti-HA, and anti-ERK antibodies. e, Hela cells were transfected with pcDNA, GFP or different doses of HA-VP24 (upper panels) or with pcDNA or different doses of GFP (lower panels). 36 h after transfection whole cell extracts were analyzed by Western blot with anti-BAF, anti-HA, anti-GFP, anti-actin, or anti-GAPDH antibodies. f, A549 (left panel) or Hela (right panel) cells stably expressing sh-luciferase (sh-luc) or sh-lamin A (sh-lamin) were transfected with GFP or HA-VP24 expression plasmids. 36 h after transfection whole cell extracts were analyzed by Western blot with anti-BAF, anti-HA, anti-GFP, anti-lamin A/C, anti-actin, or anti-GAPDH antibodies.g, Vero cells were transfected with pcDNA or HA-VP24 expression plasmids. 36 h after transfection RNA was isolated and BAF transcript levels were analyzed by qRT-PCR. The mean and error bars of 3 biological replicates are shown.

membrane components lamin A, emerin, and BAF have been reported (Liu et al., 2003; Qi et al., 2015; Samson et al., 2018). Therefore, we decided to study the localization of BAF in cells expressing VP24. We observed that BAF was located at the nucleus in 90% of untransfected or GFP expressing Hela cells (figure 28a). However, BAF was detected in cytoplasmic granules in 95% of the cells expressing HA-VP24 (figure 28a). To determine whether EBOV infection also alters BAF distribution, Hela cells were infected with EBOV and 2 days after infection, cells were fixed and immunostained with anti-BAF and anti-VP24 antibodies. Confocal analysis revealed that BAF was detected in cytoplasmic dots in infected cells whereas BAF was mainly detected at the nucleus in uninfected cells (figure 28b). It has been reported that phosphorylation of BAF modulates its subcellular localization (Bengtsson and Wilson, 2006; Nichols et al., 2006). Therefore, we evaluated BAF protein using Western blot analysis. Hela and A549 cells were transfected with HA-VP24 or pcDNA and analyzed by Western blot with anti-BAF antibody. We detected a clear decrease in

BAF levels in both cell lines expressing VP24 (figures 28c and 28d), with an inverse correlation between HA-VP24 and BAF protein levels (figure 28e). Furthermore, we observed that downmodulation of lamin A protein induced a decrease in BAF protein levels similar to that observed in cells expressing VP24 (figure28f). We did not detect a significant change in BAF expression in cells expressing HA-VP24 using qRT-PCR (figure 28g) suggesting a post-translational regulation of BAF. BAF is a chromatin-binding protein that can regulate gene expression. In fact, BAF has been shown to limit basal inflammation and ablation of BAF has been reported to upregulate some ISGs such as ISG15 (Ma et al., 2020). The upregulation of ISG15 protein levels upon VP24 expression correlated with the observed BAF downmodulation. To identify additional genes whose expression is

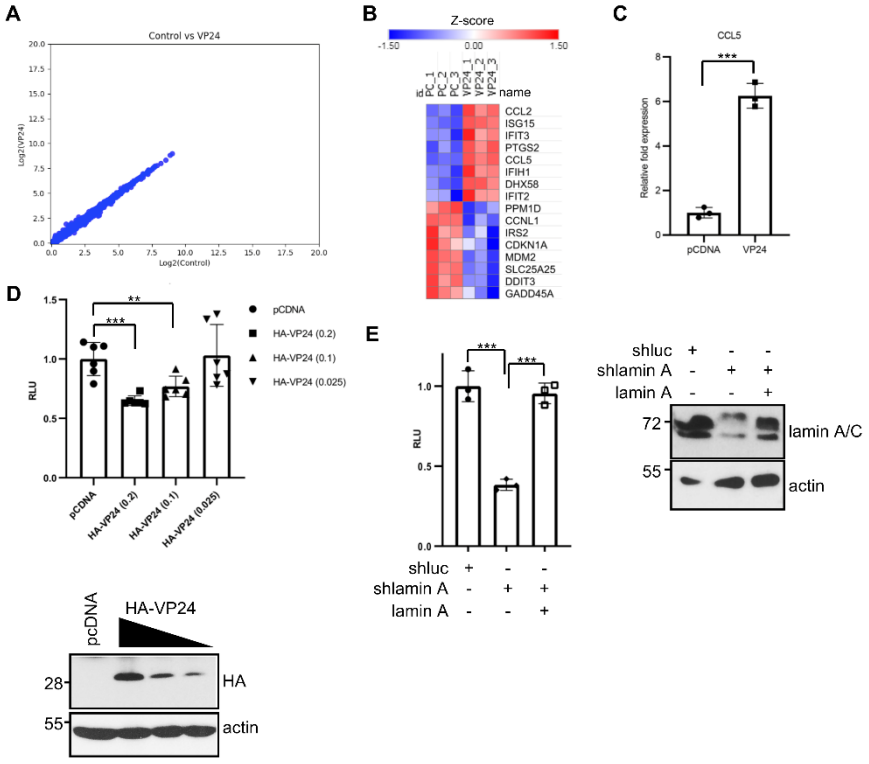

Figure 29. Transcriptional changes upon VP24 expression. a, Vero cells were transfected with pcDNA or HA-VP24 together with GFP at a 10:1 ratio. 24 h after transfection GFP positive cells were sorted. RNA of sorted cells was isolated and RNA-seq analysis was performed. Scatterplots of transcript expression data for Vero cells expressing VP24 are shown. b, Heat map of genes transactivated or downmodulated (>1.3-1.4-fold) in response to HA-VP24 expression. c, Vero cells were transfected with pcDNA or HA-VP24 expression plasmids. 36 h after transfection RNA was isolated and CCL5 transcriptional transactivation was analyzed by qRT-PCR. The mean and error bars of 3 biological replicates are shown (right panel). Statistical analysis was assessed by a Student's t-test. ***, P<0.001. d, Hela cells were co-transfected with the luciferase reporter pREP-CSF1-luc together with pcDNA-beta-gal, and pcDNA or the indicated doses of HA-VP24-WT plasmids. At 36 h after transfection luciferase production was analyzed. Columns are representative of the mean, and error bars represent the standard deviation of six biological replicates. Statistical significance was assessed by a Student's t-test (upper panel). **, P<0.01, ***, P<0.001. Cell lysates were analyzed by Western blot with anti-HA antibody (lower panel). e, Hela cells stably transfected with sh-luciferase (sh-luc) or sh-lamin A (sh-lamin) were co-transfected with the luciferase reporter pREP-CSF1-luc plasmid together with pcDNA-beta-gal, and pcDNA or lamin A/C expression plasmids, as indicated. At 36 h after transfection luciferase production was analyzed. Columns are representative of the mean and error bars represent the standard deviation of three biological replicates. Similar results were obtained twice. Statistical significance was assessed by a Student's t-test (left panel). ***, P<0.001. Cell lysates were analyzed by Western blot with anti-lamin A/C antibody (right panel).

altered by VP24 expression, we studied the transcriptional pattern in cells transfected with VP24. Vero cells were co-transfected with pcDNA or HA-VP24 together with GFP at a 10:1 ratio. 24 h after transfection FACS sorted GFP expressing cells were subjected to RNA-seq analysis. We did not observe genes with >1.5-fold change in transcript levels in VP24 expressing cells (figure 29a). We only detected a small group of genes that were slightly but significantly down or upregulated >1.3-1.4-fold (figure 29b). These results indicated that VP24 expression alone provoked very little changes in steady-state transcript abundance in Vero cells. Most of the downmodulated genes uponVP24 expression belong to the DNA damage response pathway, whereas the transactivated ones are related to inflammatory response (figure 29b). One of the upregulated genes was *ISG15* confirming our previous results. In order to validate the differential expression results, we performed qRT-PCR for CCL5. We

detected a significant upregulation of CCL5 in HA-VP24 expressing cells (figure 29c). It has been reported that BAF complex activates the human colony-stimulation factor 1 (CSF1) (Liu et al., 2001). Therefore, we evaluated the effect of VP24 expression on the transactivation of the CSF1-luciferase reporter. Hela cells were co-transfected with CSF1-luc, pcDNA-beta-gal, and pcDNA or increasing doses of HA-VP24. 36 h after transfection protein extracts were assayed for luciferase and beta-galactosidase activity. We observed that VP24 significantly inhibited luciferase expression in a dose dependent manner (figure 29d). This inhibition was similar to the one observed in cells with downmodulated lamin A (figure 29e). Altogether, these results suggested that downmodulation of BAF by VP24 reduces the expression of BAF-inducible genes.

6.3. VP24 INDUCES TRANSLOCATION OF PML-NBS TO THE CYTOPLASM

6.3.1. EBOV VP24 protein co-localizes with PML and induces its translocation to the cytoplasm

Our results revealed that VP24 expression promotes disruption of nuclear membrane and induces a laminopathy-like phenotype. One of the consequences of nuclear membrane rupture, identified as a marker for diagnosis of laminopathy disease development, is the detection of PML particles in the cytoplasm (Houben et al., 2013). PML is a nuclear protein key in the formation of nuclear macromolecular multiprotein complexes knowns as PML nuclear bodies (PML-NBs) and contributes to cellular antiviral activity. Therefore, we decided to analyze whether VP24 expression modulates PML subcellular localization. HEK 293 cells were co-transfected with GFP-PML together with pcDNA or HA-VP24-WT. 36 h after transfection cells were immunostained with anti-HA antibody. PML was detected in a dot-like pattern inside the nucleus in those cells co-transfected with pcDNA, as expected (figure 30a). However, PML was detected in the cytoplasm in those cells expressing HA-VP24-WT protein (figure 30a). Moreover, we observed a partial co-localization of the cytoplasmic PML particles and HA-VP24 protein (figure 30a). SUMO is necessary for PML-NB formation and it is critical for PML function. Some viral proteins modulate the SUMOylation of PML (Conde et al., n.d.; Everett et al., 2013; Neerukonda, 2021; Sohn and Hearing, 2012). Therefore, we decided to evaluate whether VP24 expression had an impact on PML SUMOylation. We co-transfected HEK 293 cells with GFP-PML and pcDNA, His6-SUMO2 and UBC9 or His6-SUMO2, UBC9, and HA-VP24-WT. 36 h after transfection cells were collected and Histidine-tagged proteins were purified under denaturing conditions using Ni^{2+} columns. Western blot analysis with anti-GFP antibody revealed the presence of SUMOylated PML in those cells expressing SUMO2 (figure 30b). A clear reduction in the SUMOylation of PML was

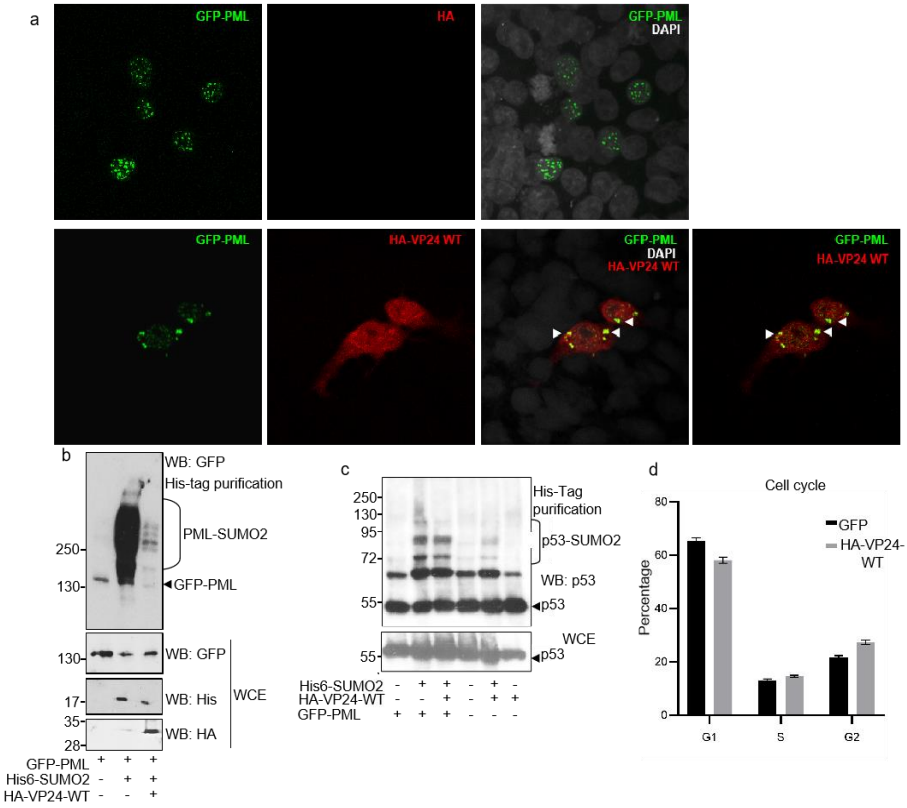

Figure 30. EBOV VP24 protein colocalizes with PML and induces its translocation to the cytoplasm. a, HEK 293 cells were transfected with GFP-PML and pcDNA or HA-VP24 expression plasmids. 36 h after transfection cells were immunostained with anti-HA antibody. Chromosomes were stained with DAPI (grey). White arrowheads indicated cytoplasmic PML-VP24 coloclaization b, HEK 293 cells were transfected with GFP-PML in combination with pcDNA, His6-SUMO2 and UBC9 or His6-SUMO2, UBC9 and HA-VP24, as indicated. 36 h after transfection whole cell lysates and Histidine-tagged purified proteins were analyzed by Western blot with the indicated antibodies. c, HEK 293 cells were transfected with the indicated expression plasmids and 36 h after transfection whole cell lysates and histidine-tagged purified proteins were analyzed by Western blot with anti-p53 antibody. d, U2OS cells were transfected with GFP, HA-VP24. 24 h after transfection cells were stained with propidium iodide and analyzed by flow cytometry. Mean percentage of cells in G1, S and G2 phases of the cell cycle is shown (n=3).

detected in those cells co-transfected with HA-VP24 (figure 30b). SUMO is required for the recruitment of nuclear bodies-related proteins

such as p53 by PML as well as for the induction of their SUMOylation upon PML overexpression (Fogal et al., 2000; Ivanschitz et al., 2015). We then decided to evaluate the increase in the SUMOylation of p53 induced by PML in cells expressing or not VP24. HEK 293 cells were co-transfected with pcDNA, pcDNA and GFP-PML or GFP-PML and HA-VP24 together with pcDNA or His6-SUMO2 and UBC9. 36 h after transfection cells were collected and protein extracts were then purified under denaturing conditions using Ni^{2+} columns. Samples were analyzed by Western blot with anti-p53 antibody. Overexpression of SUMO2 induced the SUMOylation of p53, as expected (figure 30c). Interestingly, expression of VP24 reduced the upregulation in the SUMOylation of p53 induced by PML (figure 30c). The tumor suppressor p53 is involved in the regulation of the cell cycle. Therefore, we decided to analyze whether VP24 expression has an impact on the cell cycle of cycling cells. U2OS cells were transfected with GFP or HA-VP24. 24 h after transfection cells were collected, stained with propidium iodide and analyzed by flow cytometry. We observed a decrease in the percentage of cells in G1 phase in the HA-VP24 expressing cells compared to GFP transfected cells (figure 30d).

6.3.2. SIM domain in VP24 is crucial for cytoplasmic displacement of PML but it is not required for PML-VP24 interaction

PML protein has a positive role in type I IFN response. Therefore, we speculated that the nucleus to cytoplasm translocation of PML upon VP24 expression may be a mechanism that contributes to the inhibition of IFN signaling by the viral protein. Our results revealed that the SIM domain was essential for VP24-mediated counteraction of the IFN signaling. Therefore, we decided to study the subcellular localization of PML upon VP24-SIM expression. U2OS cells were co-transfected with GFP-PML together with pcDNA, HA-VP24-WT or HA-VP24-SIM. 36 h after transfection cells were immunostained with anti-HA antibody. PML was detected in a dot-like pattern inside the nucleus in those cells co-transfected with pcDNA, as expected (figure 31a). In contrast, PML was detected in the cytoplasm of those cells expressing HA-VP24-WT

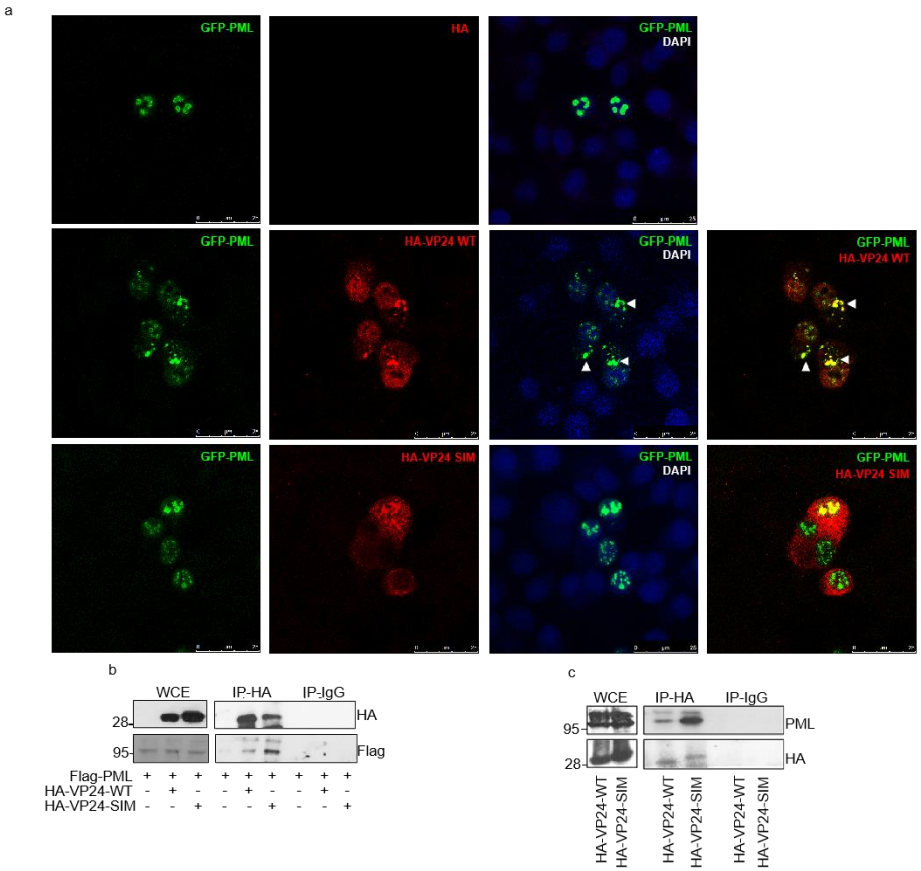

Figure 31. SIM domain in VP24 is crucial for translocation of PML but it is not required for PML-VP24 interaction. a, U2OS cells were transfected with GFP-PML and pcDNA, HA-VP24-WT or HA-VP24-SIM expression plasmids. 36 h after transfection cells were immunostained with anti-HA antibody. Chromosomes were stained with DAPI (blue). White arrow indicated cytoplasmic PML-VP24 co-localization. b, HEK 293 cells were co-transfected with flag-PML and pcDNA, HA-VP24-WT or HA-VP24-SIM expression plasmids. 36 h after transfection protein extracts were immunoprecipitated with anti-HA or anti-IgG antibodies. Immunoprecipitated proteins were analyzed by Western blot with anti-flag or anti-HA antibodies. c, HEK 293 cells were transfected with HA-VP24-WT or HA-VP24-SIM expression plasmids. 36 h after transfection protein extracts were immunoprecipitated with anti-PML or anti-IgG antibodies. Immunoprecipitated proteins were analyzed by Western blot with anti-PML or anti-HA antibodies.

protein (figure 31a), confirming our previous observations. In addition,

we observed a partial co-localization between the cytoplasmic PML and HA-VP24 protein (figure 31a). A clear co-localization between VP24-SIM and PML were also observed (figure 31a). However, PML-VP24-SIM co-localization was detected inside the nucleus (figure 31a), suggesting that SIM domain in VP24 is required for VP24-mediated translocation of PML. In addition, these results suggested that VP24 can interact with PML. To evaluate this hypothesis, we performed IP assays. HEK 293 cells were transfected with flag-PML and pcDNA, HA-VP24-WT or HA-VP24-SIM expression plasmids. 36 h after transfection cells were lysed in RIPA buffer and protein extracts were immunoprecipitated with anti-flag or anti-IgG antibodies. Samples were analyzed by Western blot with anti-flag or anti-HA antibodies.

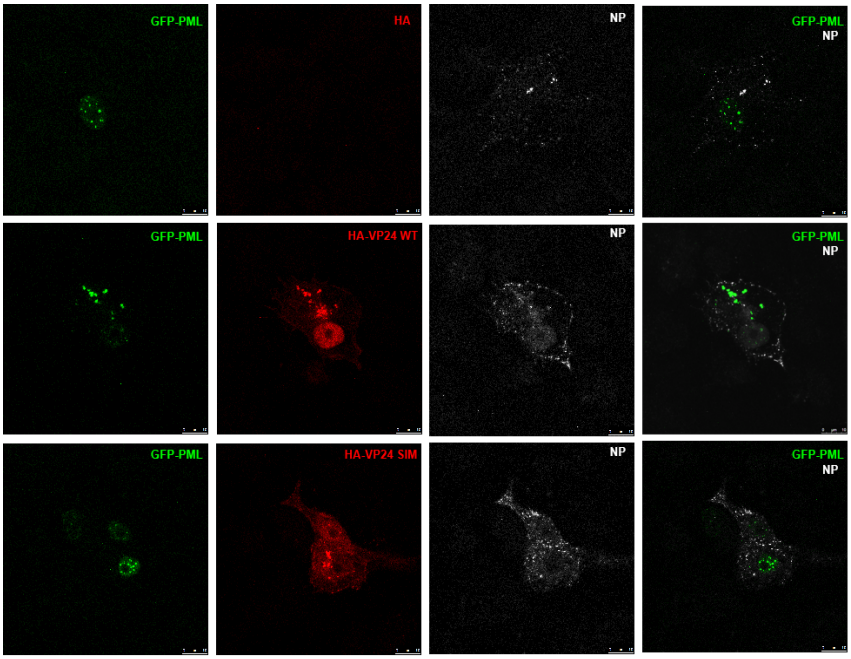

Figure 32. VP24 facilitates the interaction between PML and NP. Vero cells were transfected with GFP-PML and NP or GFP-PML, NP and HA-VP24-WT or GFP-PML, NP and HA-VP24-SIM expression plasmids.36h after transfection cells were fixed, permeabilized and immunostained with anti-HA and anti-NP primary antibodies.

Both HA-VP24-WT and HA-VP24-SIM proteins co-immunoprecipitated with flag-PML (figure 31b). To confirm this result HEK 293 cells were transfected with HA-VP24-WT or HA-VP24-SIM expression plasmids. 36 h after transfection cells were lysed in RIPA buffer and protein extracts were immunoprecipitated with anti-HA or anti-IgG antibodies. Immunoprecipitated proteins were analyzed by Western blot with anti-HA or anti-PML antibodies. As shown in figure 31c, endogenous PML co-immunoprecipitated with VP24. Similarly, co-immunoprecipitation between PML and VP24-SIM protein was observed (figure 31c).

6.3.3. VP24 facilitates the interaction between PML and NP

Our data indicated that VP24 recruited PML to the cytoplasm. It has been reported that VP24 co-localizes with other viral proteins such as NP in cytoplasmic aggregates. Therefore, we decided to analyze the putative co-localization between NP and PML. Vero cells were co-transfected with GFP-PML and NP in the absence or presence of HA-VP24-WT or HA-VP24-SIM. 36 h after transfection cells were immunostained with anti-HA and anti-NP antibodies. NP was detected in cytoplasmic aggregates, partially co-localizing with VP24, as expected (figure 32). GFP-PML was detected in the cytoplams of cells expressing VP24-WT protein but not in VP24-SIM expressing cells (figure 32), confirming our previous results. We did not observe co-localization between NP and PML neither in absence of VP24-WT nor in presence of VP24-SIM. However, we detected co-localization of NP with PML and VP24 in those cells expressing VP24-WT (figure 32). These results suggest that the cytoplasmic translocation of PML by VP24 may play a role in EBOV transcription and/or replication of the EBOV genome.

6.4. SUMO2 REGULATES EBOV VP35 PROTEIN

6.4.1. Covalent and non-covalent interaction of EBOV VP35 with SUMO2

To evaluate whether EBOV VP35 can be modified by SUMO, we first *in vitro* translated VP35 protein using a rabbit reticulocyte

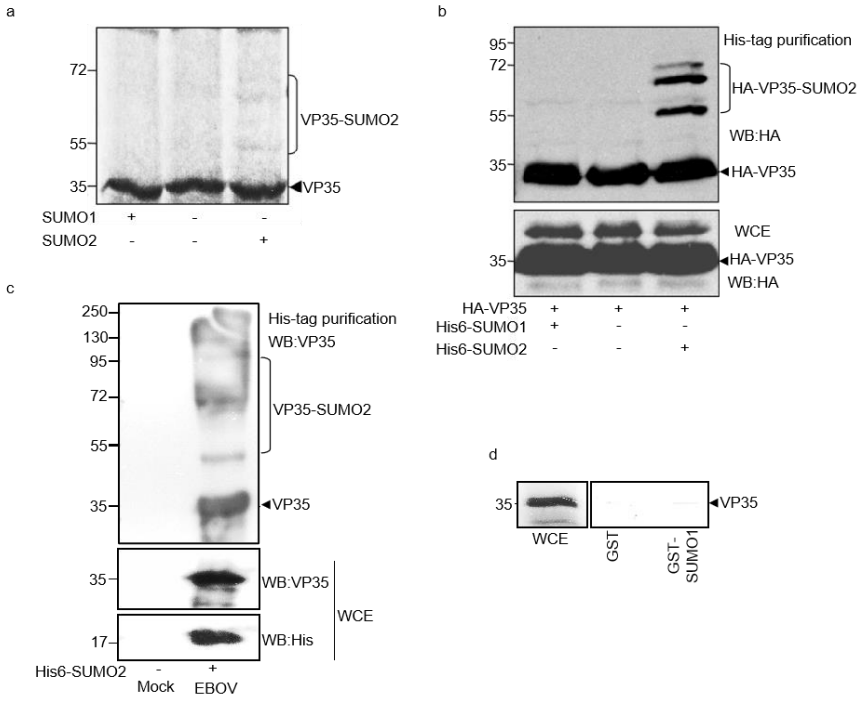

Figure 33 Covalent and non-covalent interaction of EBOV VP35 with SUMO2. a, VP35 is modified by SUMO2 *in vitro*. *In vitro* SUMOylation assay using ^{35}S-methionine-labeled *in vitro* translated VP35 protein and in the presence of SUMO1 or SUMO2. b, VP35 is modified by SUMO2 in transfected cells. HEK 293 cells were co-transfected with HA-VP35 together with pcDNA, His6-SUMO1 and Ubc9 or His6-SUMO2 and Ubc9, and 36 h after transfection whole protein extracts and Histidine-tagged purified proteins were analyzed by Western blot using anti-HA antibody. c, VP35 is modified by SUMO 2 in infected cells. Hela cells were transfected with pcDNA or His6-SUMO2 plasmids and infected or not with Zaire EBOV. 5 days after infection Histidine-tagged purified proteins were analyzed by Western blot using anti-VP35 antibody. d, GST-pulldown assay using ^{35}S methionine labeled *in vitro*-translated VP35-WT and GST or GST-SUMO1.

system and in presence of ^{35}S-methionine. Then, we performed an *in*

vitro SUMOylation assay with ^{35}S-methionine labeled VP35 protein and in presence of SUMO1 or SUMO2. We observed that EBOV VP35 protein was detected as a band of around 37 kDa molecular weight in both the control lane and after incubation with SUMO1 (figure 33a). Incubation with SUMO 2 led to the appearance of at least two additional bands with the predicted molecular weight of VP35-SUMO proteins (around 50 and 65 kDa). These results suggested that VP35 can be modified by SUMO2 but not by SUMO1 *in vitro*. In order to determine whether VP35 can be modified by SUMO in cells, we co-transfected HEK 293 cells with HA-VP35 together with pcDNA, His6-SUMO2 and UBC9 or His6-SUMO1 and Ubc9. 36 h after transfection cells were collected and the Histidine-tagged proteins were purified under denaturing conditions using Ni^{2+} columns. Western blot analysis of the samples revealed that HA-VP35 protein was detected as a band of around 37 kDa molecular weight, as expected. We did not detect additional bands in those cells transfected with SUMO1 (figure 33b). However, at least two additional bands with the expected molecular weight of VP35-SUMO2 were detected in those cells co-transfected with SUMO2, (figure 33b). These results suggested that VP35 is SUMOylated by SUMO2 but not by SUMO1 in cells. We then decided to evaluate whether VP35 can be SUMOylated in EBOV infected cells. Hela cells were transfected with pcDNA or His6-SUMO2 and infected or not with *Zaire ebolavirus.* 5 days after infection cells were collected and Histidine-tagged proteins were then purified under denaturing conditions using Ni^{2+} columns. Western blot analysis using anti-VP35 antibody revealed the presence of a band or around 37 kDa, corresponding with the unmodified viral protein. In addition, we also detected the appearance of higher molecular weight bands with the expected molecular weight of VP35-SUMO2 proteins (figure 33c), suggesting that VP35 protein is modified by SUMO2 when expressed from the virus. As mentioned above, many SUMOylated proteins can interact with SUMO in a non-covalent manner through a SIM domain. To know whether VP35 protein can interact with SUMO in a non-covalent manner, we performed *in vitro* GST-pulldown assay using *in vitro* translated ^{35}S-metionine labeled VP35 protein and GST or GST-SUMO1. We observed that VP35 protein interacted with GST-SUMO1

but did not interact with GST, indicating that VP35 can interact in a non-covalent manner with SUMO1 (figure 33d). Altogether these results indicated that VP35 can interact with SUMO1 and SUMO2 in a non-covalent and covalent manner, respectively.

6.4.2. VP35-SUMO co-localization

To analyze the potential co-localization between VP35 and SUMO we performed immunofluorescence assays. Vero cells were co-transfected with HA-VP35 together with pcDNA, His6-SUMO1 or

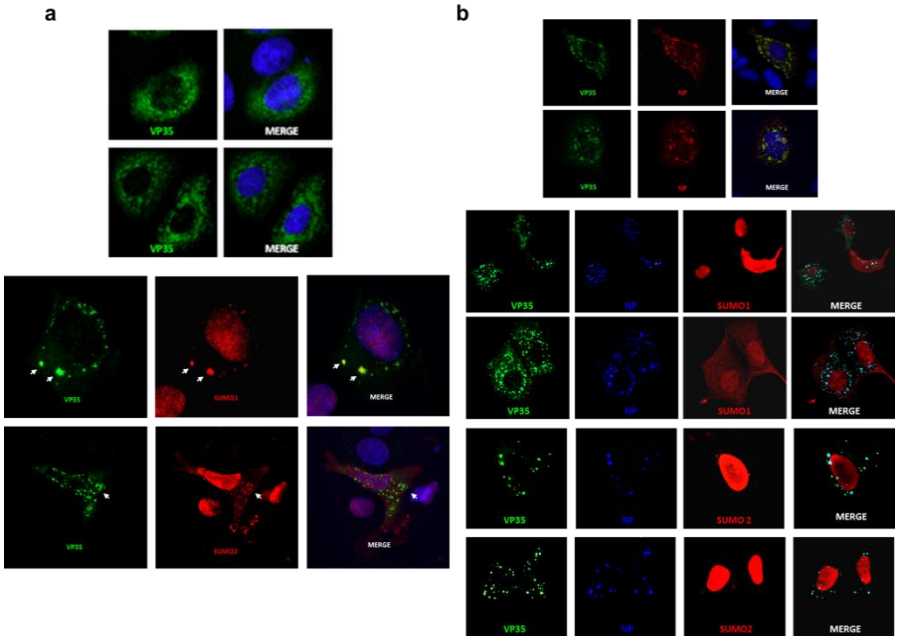

Figure 34. VP35-SUMO co-localization. a, Co-localization of VP35 and SUMO2 or SUMO1 in cells. Vero cells were co-transfected with HA-VP35 and SUMO1 or SUMO2 and 24 h after transfection cells were immunostained with anti-HA and anti-SUMO1 or anti-SUMO2 antibodies, as indicated. White arrows show co-localization of VP35 and SUMO in cytoplasmic aggregates. b, SUMO overexpression does not alter NP-VP35 co-localization. Vero cells were transfected with EBOV NP and HA-VP35 expression plasmids (at a 1:2.5 ratio) together with pcDNA, SUMO1 or SUMO2. 36 h after transfection cells were immunostained with anti-NP, anti-HA and anti-SUMO1 or anti-SUMO2 antibodies.

His6-SUMO2 expression plasmids. 36 h after transfection cells were stained with anti-HA and anti-SUMO1 or anti-SUMO2 antibodies. As

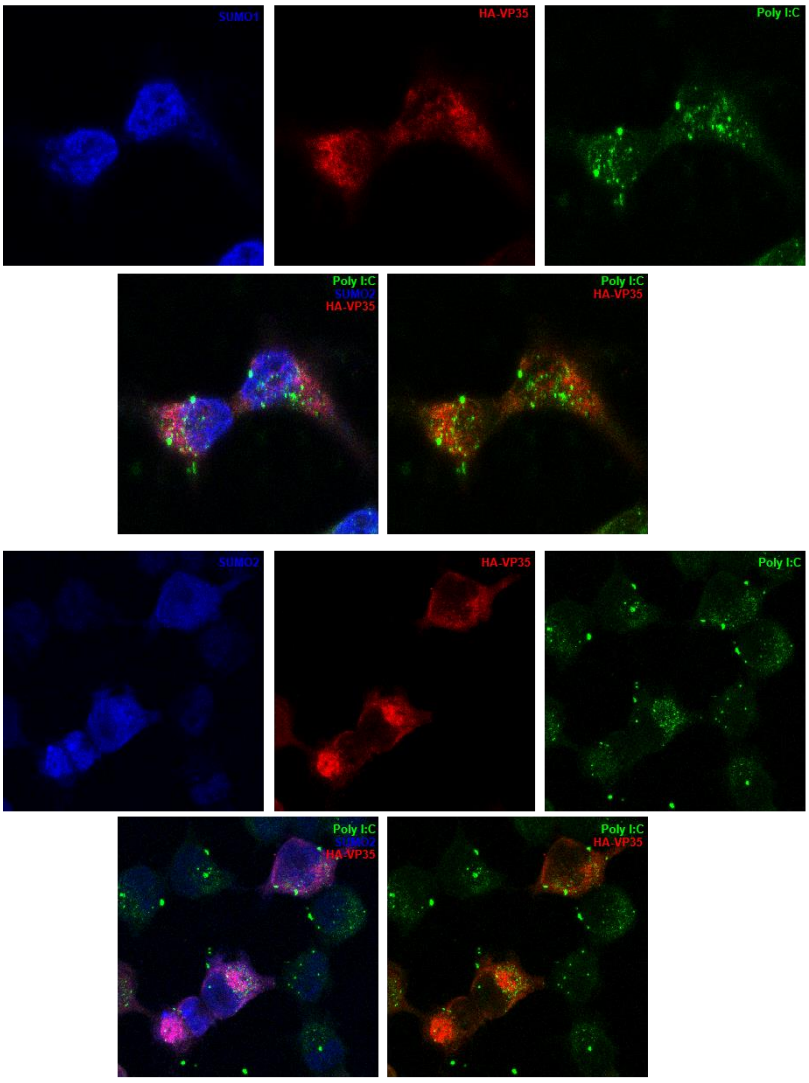

Figure 35. Co-localization of VP35, SUMO and double-stranded RNA in cytoplasmic aggregates. Vero cells were transfected with HA-VP35 and SUMO1 os SUMO2 and 24 h after transfection cell were transfected with Poly I:C. At 16 h after Poly I:C transfection, cells were immunostained with anti-HA, anti-dsRNA and anti-SUMO1 or anti-SUMO2 antibodies.

shown in figure 34a, VP35 localized in cytoplasmic aggregates independently of the co-transfection of SUMO1 or SUMO2. Although

SUMO1 and SUMO2 proteins were mainly detected inside the nucleus (figure 34a) we also observed SUMO1 and SUMO2 proteins colocalizing with VP35 in cytoplasmic aggregates (figure 34a). VP35 associates with several EBOV proteins including NP. Therefore, we decided to evaluate whether SUMO overexpression modulates the VP35-NP co-localization. Vero cells were co-transfected with VP35 and NP expression plasmids at a 1:2.5 ratio together with pcDNA, His6-SUMO1 or His6-SUMO2. 36 h after transfection cells were stained with the indicated antibodies and samples were analyzed using confocal microscope. We observed that VP35 and NP co-localized in cytoplasmic aggregates, as expected (figure 34b). This co-localization was independent of the co-expression of SUMO1 or SUMO2 (figure 34b lower panel). Interestingly, we observed a reduction in the number of cytoplasmic aggregates showing VP35 and SUMO1 or SUMO2 co-staining (figure 34b lower panel), suggesting that NP may negatively modulate the interaction between VP35 and SUMO.

6.4.3. Co-localization of VP35, SUMO and double-stranded RNA in cytoplasmic aggregates

VP35 is a dsRNA-binding protein and the dsRNA-binding domain is critical for the suppression of innate immunity mediated by VP35 (Basler et al., 2003; Cárdenas et al., 2006; Leung et al., 2009). We then decided to evaluate the putative co-localization between VP35, dsRNA and SUMO. We co-transfected cells with HA-VP35 and His6-SUMO1 or His6-SUMO2 and 24 h after transfection, cells were transfected with Polyinosinic:polycytidylic acid (poly I:C), a synthetic analog of dsRNA. 16 h after dsRNA transfection, cells were immunostained with anti-HA, anti-SUMO1 or anti-SUMO2, and anti-dsRNA antibodies. We observed that poly I:C and VP35 co-localized in the cell. In addition, we observed partial co-localization of VP35, SUMO and dsRNA in cytoplasmic aggregates (figure 35).

6.4.4. SUMO promotes the interaction between VP35 and dsRNA

The interaction and co-localization of VP35 with SUMO and dsRNA led us to hypothesize that SUMO may favor the interaction of

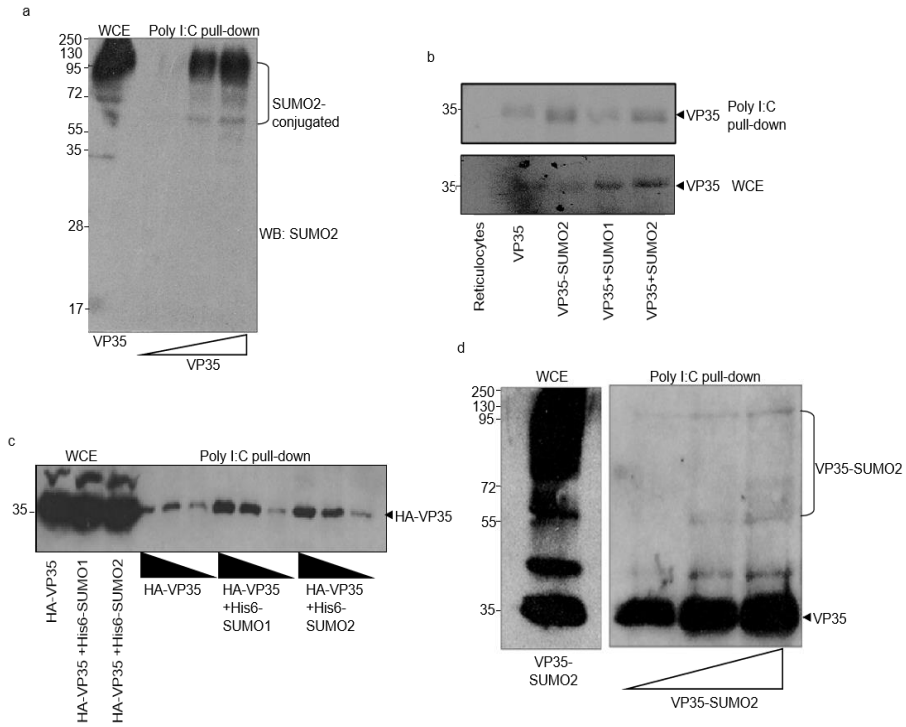

Figure 36. SUMO promotes the interaction between VP35 and dsRNA. a, dsRNA-binding assay using protein extracts obtained from cells co-transfected with HA-VP35 and SUMO2. Samples were analyzed by Westernblot using anti-SUMO2 antibody. White triangle indicates increasing doses of protein extract. b, dsRNA-binding assay using ^{35}S-methionine-labeled *in vitro* translated unmodified VP35 protein, VP35 protein subjected to *in vitro* SUMOylation assay in the presence of SUMO2 or VP35 protein incubated with recombinant SUMO1 or SUMO2, as indicated. C, dsRNA-binding assay using protein extracts obtained from cells co-transfected with HA-VP35 together with pcDNA, His6-SUMO1 or His6-SUMO2, as indicated. Samples were analyzed by Western blot using anti-HA antibody. Black triangles indicate decreasing doses of protein extract. d, dsRNA-binding assay using protein extracts obtained from cells co-transfected with HA-VP35 and SUMO2. Samples were analyzed by Western blot using anti-HA antibody. White triangle indicates increasing doses of protein extracts.

VP35 with dsRNA. To test this hypothesis, we first analyzed the potential interaction between dsRNA and SUMO using dsRNA binding assays. We co-transfected HEK 293 with HA-VP35 and His6-SUMO2

expression plasmids. 36 h after transfection cells were lysed in RNA binding buffer and increasing amounts of protein extracts were then incubated with dsRNA conjugated to agarose beads. Samples were then analyzed by Western blot with anti-SUMO2 antibody. We did not observed free SUMO but we detected SUMO2-conjugated proteins interacting with dsRNA (figure 36a). Then, we analyzed the effect of SUMO on VP35-dsRNA interaction using *in vitro* dsRNA binding assays. First, *in vitro* translated ^{35}S-methionine labeled VP35 protein was subjected to *in vitro* SUMOylation assay in the presence or absence of SUMO2. Then the ^{35}S-methionine labeled VP35 protein resulting from the SUMOylation assay or untreated ^{35}S-methionine labeled VP35 protein were incubated with dsRNA-agarose beads or with dsRNA-agarose beads and recombinant SUMO1 or SUMO2. Samples were analyzed by SDS-PAGE followed by autoradiography. We observed that VP35 interacted with dsRNA, as expected (figure 36b). We did not observe differences in the levels of VP35 interacting with dsRNA in the presence of SUMO1 (figure 36b). Interestingly, the levels of VP35 interacting with dsRNA increased in the presence of both free and conjugated SUMO2 (figure 36b), indicating that SUMO2 promotes the interaction between VP35 and dsRNA *in vitro*. To further evaluate this hypothesis, we co-transfected HEK 293 cells with HA-VP35 and pcDNA, His6-SUMO1 or His6-SUMO2. 36 h after transfection cells were lysed in RNA Binding Buffer and increasing amounts of protein extracts were then incubated with dsRNA-agarose beads. Samples were analyzed by Western blot using anti-HA antibody. We observed that VP35 interacted with dsRNA (figure 36c). In addition, we also observed that the levels of VP35 interacting with dsRNA increased in those cells co-transfected with His6-SUMO1 or His6-SUMO2 (figure 36c), suggesting that both SUMO1 and SUMO2 trigger the interaction of VP35 and dsRNA in cells. Finally, we evaluated the potential interaction of VP35-SUMO2 protein with dsRNA. We transfected HEK 293 cells with HA-VP35, His6-SUMO2 and Ubc9. 24 h after transfection protein extracts were lysed in RNA binding buffer and protein extracts were incubated with dsRNA-agarose beads. Samples were then analyzed by Western blot with anti-HA antibody. We detected both unmodified VP35 and SUMO2-conjugated VP35 protein

interacting with dsRNA (figure 36d). Altogether, these results suggested that SUMO triggers the interaction of VP35 with dsRNA.

7. DISCUSSION

Ebola virus infection causes a severe disease with a high mortality ratio. Recurrent outbreaks affect the population of West and Central Africa, despite having an efficient vaccine approved by the FDA since 2019. Studying the interaction between EBOV and the host cell may highlight novel therapeutic targets and strategies that allow us to develop effective treatments to improve the survival of patients infected with the virus. Our results pointed to SUMO as one of these therapeutic targets. In this work we demonstrate that two different proteins of the virus, VP35 and VP24, are modified by SUMO *in vitro,* in transfected cells, and in the context of viral infection. SUMOylation of these proteins in transfected cells indicates that other EBOV proteins are not essential for their SUMOylation. VP24 can be modified by SUMO1 and SUMO2. However, we only detected modification of VP35 protein with SUMO2 and not with SUMO1. While many studies try to understand the differential role of SUMO1 and SUMO2/3 proteins (Ayaydin and Dasso, 2004; Gareau and Lima, 2010; Saitoh and Hinchey, 2000) few SUMO substrates such as RANGAP1 protein, appears to be specifically modified by one of the paralogs but not by the other (Saitoh and Hinchey, 2000). One possible explanation for this specificity is the SUMO isoform-specific conjugation activity of some E3 ligases. Thus, it has been found that some host cell as well as viral E3 ligases promote the conjugation of exclusively one SUMO paralog (Chang et al., 2010; Tatham et al., 2005). Discovering the E3 ligase for VP35 may help to understand the reasons for this specificity. VP24 and VP35 are not the first EBOV proteins to be identified as SUMO substrates. VP40, the major matrix protein of the virus, is also modified by SUMO (Baz-Martínez et al., 2016). SUMO increases VP40 stability by blocking its ubiquitination. Moreover, electron microscopy analysis demonstrated that SUMO protein can be detected inside the VP40-VLPs (Baz-Martínez et al., 2016). Altogether these results indicate that EBOV extensively exploits the SUMOylation machinery of the cell, as reported for other RNA viruses such as Influenza virus (Domingues et al., 2015; Han et al., 2014; Pal et al., 2011; Sun et al., 2011; Wu et al., 2011) or rotavirus (Campagna et al., 2013). Understanding the regulation of the SUMO modification of EBOV proteins and their

consequences for EBOV pathogenesis is essential to advance in the design of novel therapeutic strategies.

In silico analysis pointed out to K14 in VP24 as a possible SUMO acceptor. *In vitro* and *in vivo* SUMOylation studies revealed that indeed K14 in VP24 is involved in SUMO conjugation. One of the main functions of VP24 is to inhibit interferon signaling pathways (Harrison et al., 2021, p. 3; Reid et al., 2007, 2006). We observed that a mutant of VP24 in K14 had reduced ability to block interferon signaling, suggesting that conjugation of SUMO to VP24 facilitates this activity. VP24 inhibits IFN signaling through its interaction with KPNA (Reid et al., 2007, 2006; Schwarz et al., 2017; Xu et al., 2014). VP24 binds some host KPNA proteins, preventing them from transporting p-STAT1 to the nucleus (Reid et al., 2006). Our results showed that mutation of the SUMOylation site in VP24 reduced the interaction between KPNA5 and VP24 and increased the IFN-induced nuclear accumulation of p-STAT suggesting that SUMO facilitates the interaction of VP24 and KPNA. Interaction of VP24 with KPNA also favors the stabilization of the viral protein (Schwarz et al., 2017). We demonstrated that the VP24 SUMOylation mutant has reduced stability compared to VP24-WT, in agreement with the reduced KPNA-SUMOylation mutant VP24 interaction. Altogether these results suggest that conjugation of SUMO to K14 in VP24 promotes its interaction with KPNA5, thereby facilitating the retention of p-STAT1 in the cytoplasm and the inhibition of the IFN signaling. In the case of VP35 protein, *in silico* analysis point to lysine residues located within the dsRNA-binding domain in VP35 as important for SUMO conjugation. However, additional studies are required in order to confirm this hypothesis.

SUMOylated proteins frequently interact in a non-covalent manner with SUMO or SUMOylated proteins through a SIM domain. In this work we demonstrated that both VP35 and VP24 proteins interact with SUMO in a non-covalent manner. We identified the 198-LVEL-201 residues as the SIM domain in VP24. SIM domains can regulate SUMOylation, localization, stability or activity of the proteins (Saether et al., 2011). Mutation of the SIM domain in VP24 did not alter its SUMOylation but abolished the ability of VP24 to block the

interferon signaling and slightly reduced its interaction with KPNA5. These results suggested that the non-covalent interaction of VP24 with SUMO is essential for the immunomodulatory activity of the viral protein and pointed to the possibility that this interaction may be involved in additional functions of the viral protein. Interestingly, our data also revealed that mutation of the SIM domain in VP24 triggers the mono-ubiquitination of the viral protein, suggesting that non-covalent interaction with SUMO negatively modulates the ubiquitination of VP24. USP7 is a SUMO deubiquitinase (Lecona et al., 2016) that has been reported to interact with several viral proteins and that modulates the replication of different viruses (Chavoshi et al., 2016; Jäger et al., 2012). We demonstrate that USP7 interacts with VP24-WT but not with the mutant of VP24 in the SIM domain. Furthermore, we also demonstrated that USP7 decreases the mono-ubiquitination of VP24-WT. These results indicate that USP7 interacts with VP24 through its SIM domain and promotes its deubiquitination. Moreover, these results led us to hypothesize that USP7 can be modified by SUMO. So far, USP7 has not been reported to be SUMOylated although proteomic studies have pointed to USP7 as a putative SUMO substrate (Lumpkin et al., 2017). Evaluation of the potential SUMOylation of USP7 in cells demonstrate that USP7 can interact with SUMO2, opening a new line of research to elucidate the role of SUMO in the regulation of the deubiquitinase USP7.

Since a mutant of VP24 in the SIM domain was monoubiquitinated and lacked the ability to block interferon signaling, we studied the role of ubiquitination on the regulation of VP24 activity. Mutation of the potential ubiquitination site K206 in VP24 led to a reduction in VP24 mono-ubiquitination and a significant higher ability to downmodulate IFN signaling that the VP24-WT protein, suggesting that ubiquitin conjugation to K206 in VP24 plays a negative role on the activity of the viral protein.

VP35 is a dsRNA-binding protein (Cárdenas et al., 2006; Feng et al., 2007) and the dsRNA binding domain in VP35 is required for its immunomodulatory activity (Di Palma et al., 2019; Leung et al., 2009). *In silico* analysis of VP35 pointed to the presence of different putative SIMs inside the dsRNA binding domain. SUMO has been already

reported to regulate proteins containing a dsRNA-binding motif such as the host cellular PKR protein (de la Cruz-Herrera et al., 2014) and the vaccinia virus E3 protein (González-Santamaría et al., 2011) and the identification of RNA-binding E3 ubiquitin ligases has been already reported (Hildebrandt et al., 2017). Therefore, we hypothesized that SUMO may favor the activity of VP35 by promoting the interaction between VP35 and dsRNA. We observed that dsRNA interacted with SUMOylated proteins including VP35-SUMO2. Interestingly, we observed that SUMO was recruited to cytoplasmic VP35 aggregates and that this recruitment was downmodulated by NP. The impact of this modulation on the induction of IRF3 and IRF7 SUMOylation by VP35 (Chang et al., 2009) and the consequences on EBOV replication will be analyzed in future studies.

In summary, here we demonstrated that SUMO is a key regulator of VP24 and VP35 EBOV proteins pointing to modulation of their interaction with SUMO as novel potential strategies to control EBOV replication. Here we also show that ubiquitin conjugation modulates VP24 activity. The regulatory activity of ubiquitin on VP24 as well as on other Ebola proteins (Bharaj et al., 2017), led us to suggest that regulation of ubiquitin conjugation to viral proteins may be also exploited as a therapeutic strategy.

The importance of VP24 for EBOV replication and pathogenesis has led to several groups to carry out proteomic studies in order to identify novel VP24 partners. Two different studies identified emerin as a potential interactor of VP24 (Batra et al., 2018; García-Dorival et al., 2014). Here we confirmed the interaction between VP24 and emerin. Moreover, we also identified other nuclear membrane components including lamin A/C and lamin B as novel VP24 partners. Additionally, our data revealed that VP24 partially mislocalize these proteins to cytoplasmic aggregates, suggesting that VP24 may disturb the nuclear envelope. Indeed, we demonstrate that VP24 diminishes the interaction between lamin A and emerin thereby inducing nuclear membrane disruption and a plethora of molecular markers of nuclear envelope disruption including DNA damage, ISG15 induction, alterations in nuclear size and shape and activation of MAPK pathway (Muchir et al., 2009; Muchir and Worman, 2007; Nikolova et al., 2004). Several

viruses induce the disruption of the nuclear lamin in order to ensure their replication (Walker and Ghildyal, 2017). Disruption of nuclear lamin by VP24 protein may work as an EBOV strategy to gain access to different nuclear components or to modulate cellular signaling such as the ERK pathway. Activation of ERK pathway has been shown to inhibit type I IFN production in several cell types (Dong et al., 2002; Noser et al., 2007; Zhang et al., 2018). Induction of ERK phosphorylation by VP24 may be then an additional mechanism by which VP24 interferes with IFN expression. VP24 is not the only EBOV protein able to induce ERK activation. VLPs containing the viral glycoprotein GP and the major matrix protein VP40 also induce MAPK pathway activation, suggestive of its relevance for EBOV replication (Martinez et al., 2007).

Our data also revealed that VP24 induces the cytoplasmic translocation of BAF, its downmodulation and the repression of BAF-dependent transactivation of CSF1. CSF1 modulates macrophage differentiation, proliferation and survival (Jones and Ricardo, 2013). VP24, cooperatively with VP35, has been reported to modulate maturation of infected human dendritic cells (Jin et al., 2010; Lubaki et al., 2013). Downmodulation of BAF may be then a mechanism involved in the modulation of dendritic cells by VP24.

BAF is also a regulator of inflammation. After nuclear envelope rupture, cGAs protein binds to the exposed genomic DNA to induce an inflammatory state (Denais et al., 2016), a process negatively regulated by BAF (Guey et al., 2020). The downmodulation of BAF by VP24 may explain the transactivation of the proinflammatory genes such as ISG15 or CCL5 detected upon VP24 expression. This transactivation is in agreement with the upregulation of cytokines and chemokines detected at early times after EBOV infection (Ilinykh et al., 2015). It has been proposed that BAF can limit viral replication (Cui et al., 2004). In order to overcome BAF antiviral activity and enhance viral replication, viruses have developed different strategies including regulation of BAF phosphorylation (Nichols et al., 2006) or of its subcellular localization (Jamin et al., 2014). Here we demonstrated for the first time the mislocalization and downmodulation of BAF as a consequence of the expression of a viral protein. Further studies are

needed to identify the molecular mechanism by which VP24 modulates BAF levels.

The RNA-Seq analysis revealed that VP24 also exerts transcriptional repression of several DNA damage response genes already described as c-MYC targets (Barsyte-Lovejoy et al., 2004; Seoane et al., 2002). ERK activation induces phosphorylation of c-MYC in serine 92 and this modification increases the stability of c-MYC protein (Sears et al., 2000). Downmodulation of these transcripts in VP24 expressing cells may then result as a consequence of the activation of ERK by VP24.

One molecular marker of diseases characterized by defects in nuclear lamina organization is the detection of PML aggregates in the cytoplasm (Houben et al., 2013). PML is considered part of the cellular antiviral response. Consequently, viruses have developed multiple strategies to target and control PML (Everett, 2001) including the induction of PML degradation or its mislocalization (Möller and Schmitz, 2003). We demonstrate that VP24 interacts with PML and recruits PML to cytoplasmic aggregates, in agreement with the nuclear envelope disruption caused by VP24 expression. A cytoplasmic translocation of PML has been reported to occur in response to infection with different viruses such as arenavirus (Borden et al., 1998). We also proved that although the VP24-PML interaction does not requires the SIM domain in VP24, this motif is needed for the cytoplasmic recruitment of PML by the viral protein, suggesting that SUMO plays an essential role in this displacement. The consequences of this translocation are still unclear; however, the VP24-mediated interaction between PML and NP led us to propose that it may play a role in EBOV replication or transcription. Sequestering PML in viral replication centers is an adenovirus strategy to improve viral replication (Stubbe et al., 2020). However, a negative correlation between PML levels and EBOV infectivity in Vero cells has been reported (Björndal et al., 2003). Additional experiments are required in order to identify the consequences of the cytoplasmic translocation of PML in EBOV pathogenesis.

In summary, in this work we have demonstrated the relevance of SUMO and ubiquitin in order to modulate EBOV proteins. We have

also identified a novel mechanism involved in the pathogenesis of the virus, the interaction of VP24 with nuclear membrane components and the disruption of the nuclear envelope. VP24 expression induces a laminopathy-like phenotype characterized by the induction of DNA damage, a pro-inflammatory state and de-regulation of BAF. These VP24 activities could potentially be linked with the inflammatory phenotype observed in infected EBOV patients as well as with the lack of maturation of EBOV-infected dendritic cells. PML-VP24 interaction also emerges as an important player in EBOV infection. Some of the partners and pathways identified in this study are promising therapeutic targets. In addition, these findings have help us to increase our understanding of EBOV infection and infectivity.

8. CONCLUSIONS

- VP24 is modified by SUMO1 and SUMO2 *in vitro*, in transfected cells, and in EBOV infected cells. Lysine 14 is a SUMO acceptor site in VP24 and it is required for proper downmodulation of interferon signaling and VP24 stability.
- VP24 interacts with SUMO in a non-covalent way through the 198-LVEL-201 SIM domain. Non-covalent interaction of VP24 with SUMO is essential for the VP24-mediated downmodulation of interferon signaling.
- Non-covalent interaction of VP24 with SUMO negatively regulates VP24 mono-ubiquitination by modulating its interaction with the deubiquitinase USP7.
- Lysine 206 is an ubiquitin acceptor site in VP24.
- Ubiquitin conjugation to K206 in VP24 negatively modulates the inhibition of the interferon signaling by VP24.
- VP24 protein interacts with the nuclear membrane components emerin, lamin A/C and lamin B and downmodulates the lamin A/C-emerin interaction, leading to a nuclear membrane disruption and to a laminopathy-like phenotype characterized by increased expression of proinflammatory genes.
- VP24 protein is actively transported to the cellular nucleus by KPNA.
- VP24 expression induces mislocalization and downmodulation of Barrier to autointegration Factor (BAF) and represses the BAF-mediated transactivation of CSF1.
- VP24-WT interacts with PML, induces its cytoplasmic translocation, and reduces its SUMOylation as well as the PML-mediated upregulation of p53 SUMOylation.
- Non-covalent interaction of VP24 with SUMO is required for the induction of cytoplasmic translocation of PML by the viral protein but not for VP24-PML interaction.
- VP24 protein promotes EBOV NP-PML interaction.
- VP35 protein is modified by SUMO2 *in vitro*, in transfected cells and upon EBOV infection
- VP35 protein interacts with SUMO in a non-covalent manner and this interaction promotes its interaction with dsRNA

9. TABLES

Table 1: Oligonucleotides used in cloning and mutagenesis

Name	Sequence
VP24-BglII-F	5' GGGAGATCTGCTAAAGCTACGGGACG 3'
VP24-PstI-R	5' GGGCTGCAGTTAGATAGCAAGAGAGC 3'
VP24-K14R-F	5'CAATCTAATATCGCCCAGAAAGGACCTGGAGAAAG-3'
VP24-K14R-R	5'CTTTCTCCAGGTCCTTTCTGGGCGATATTAGATTG-3'
VP24-K142R	5'GCGAACACAACGTGTCAGGGAACAATTGAGCC-3'
VP24-K142R-R	5'-GGCTCAATTGTTCCCTGACACGTTGTGTTCGC-3'
VP24-LSLI-ASAA-F	5'CAATTGAGCCTAAAAATGGCGTCGGCGGCTCGATCCAATATTCTC-3'
VP24-LSLI-ASA-R	5'GAGAATATTGGATCGAGCCGCCGACGCCATTTTTAGGCTCAATTG-3'
VP24-LGLI-AGAA-F	5'CCCTTAGCAGGAGCCGCTGGTGCGGCCTCTGATTGGCTGCTAAC-3'
VP24-LGLI-AGAA-R	5'GTTAGCAGCCAATCAGAGGCCGCACCAGCGGCTCCTGCTAAGGG-3'
VP24-LRVI-ARAA-F	5'GAATCACCGCTGTGGGCAGCGAGAGCGGCCCTTGCAGCAGGGATAC-3'
VP24-LRVI-ARAA-R	5'GTATCCCTGCTGCAAGGGCCGCTCTCGCTGCCCACAGCGGTGATTC-3'
VP24-LVEL-AAEA-F	5'GAACTAACATGGGTTTTGCGGCGGAGGCCCAAGAACCCGACAA-3'
VP24-LVEL-AAEA-R	5'TTGTCGGGTTCTTGGGCCTCCGCCGCAAAACCCATGTTAGTTC-3

VP24-LHVV-AHAA-F	5’AACAAATTGGATGCTGCACATGCCGCGAACTACAACGGATTG-3’
VP24-LHVV-AHAA-R	5’CAATCCGTTGTAGTTCGCGGCATGTGCAGCATCCAATTTGTT-3’
VP24-K206R-F	5’CTCCAAGAACCCGACAGATCGGCAATGAACCGC-3’
VP24-K206R-R	5’GCGGTTCATTGCCGATCTGTCGGGTTCTTGGAG-3’
VP24-LVEL-K206R-F	5’GCCCAAGAACCCGACAGATCGGCAATGAACCGC-3’
VP24-LVEL-K206-R	5’GCGGTTCATTGCCGATCTGTCGGGTTCTTGGGC-3’
Xho-link-VP24-R	5’ GGCCCTCGAGCTCAAGCTTCGAATTCTATGGCTAAAGCTACGGGACGATAC-3′
NheI-VP24-R	5’ GCTAGCTCAGATAGCAAGAGAGCTA-3′
Xho-link-emerin-F	5’ GGCCCTCGAGCTCAAGCTTCGAATTCTATGGACAACTACGCAGATCTTTCGG-3′
NheI-emerin-R	5’ GCTAGCTCAGAAGGGGTTGCCTTCTTC-3′
Xho-link-laminA-F	5’ GGCCCTCGAGCTCAAGCTTCGAATTCTATGGAGACCCCGTCCCAGCGGCGCGC-3′
NheI-laminA-R	5’ GCTAGCTCACATGATGCTGCAGTTCTGGGG-3′

Table 2: Oligonucleotides used in RT-PCR

GAPDH-Vero-qRT-F	5'GTGAAGGTCGGAGTCAACGG-3'
GAPDH-Vero-qRT-R	5'AAGACGCCAGTGGACTCCA-3'
ISG15-Vero-qRT-F	5'GAGAGGCAGCGAACTCATCT-3'
ISG15-Vero-qRT-R	5'CTTCAGCTCTGACACCGACA-3'
CCL5-Vero-qRT-F	5'GCTGTCATCCTCATTGCTACAG-3'
CCL5-Vero-qRT-R	5'TGGTGTAGAAATACTCCTTGATGTG-3'
EBOV L-qRT-F	5'CCATCTACATCGGTGGAGCC-3'
EBOV L-qRT-R	5'GTGGTCGTTGATGGTGGTCT-3'
EBOV VP30-qRT-F	5'CTCGCCAAAGGAATGCAAGG-3'
EBOV VP30-qRT-R	5'AAAGGGTCGCTACAGACGTT-3'
BANF-Vero-qRT-F	5' TGGCTGGGATTGGTGAAGTCCT-3'
BANF-Vero-qRT-R	5' CGCCACACGTGTCCTTCAGCCA-3'

10. BIBLIOGRAPHY

Al-Eidan, A., Wang, Y., Skipp, P., Ewing, R.M., 2020. The USP7 protein interaction network and its roles in tumorigenesis. Genes & Diseases

Alvarez, C.P., Lasala, F., Carrillo, J., Muñiz, O., Corbí, A.L., Delgado, R., 2002. C-type lectins DC-SIGN and L-SIGN mediate cellular entry by Ebola virus in cis and in trans. J Virol 76, 6841–6844.

Ayaydin, F., Dasso, M., 2004. Distinct In Vivo Dynamics of Vertebrate SUMO Paralogues. Mol Biol Cell 15, 5208–5218.

Barsyte-Lovejoy, D., Mao, D.Y.L., Penn, L.Z., 2004. c-Myc represses the proximal promoters of GADD45a and GADD153 by a post-RNA polymerase II recruitment mechanism. Oncogene 23, 3481–3486.

Basler, C.F., Mikulasova, A., Martinez-Sobrido, L., Paragas, J., Mühlberger, E., Bray, M., Klenk, H.-D., Palese, P., García-Sastre, A., 2003. The Ebola virus VP35 protein inhibits activation of interferon regulatory factor 3. J Virol 77, 7945–7956.

Basler, C.F., Wang, X., Muhlberger, E., Volchkov, V., Paragas, J., Klenk, H.-D., Garcia-Sastre, A., Palese, P., 2000. The Ebola virus VP35 protein functions as a type I IFN antagonist. Proceedings of the National Academy of Sciences 97, 12289–12294.

Batra, J., Hultquist, J.F., Liu, D., Shtanko, O., Von Dollen, J., Satkamp, L., Jang, G.M., Luthra, P., Schwarz, T.M., Small, G.I., Arnett, E., Anantpadma, M., Reyes, A., Leung, D.W., Kaake, R., Haas, P., Schmidt, C.B., Schlesinger, L.S., LaCount, D.J., Davey, R.A., Amarasinghe, G.K., Basler, C.F., Krogan, N.J., 2018. Protein Interaction Mapping Identifies RBBP6 as a Negative Regulator of Ebola Virus Replication. Cell 175, 1917-1930.e13.

Baz-Martínez, M., El Motiam, A., Ruibal, P., Condezo, G.N., de la Cruz-Herrera, C.F., Lang, V., Collado, M., San Martín, C., Rodríguez, M.S., Muñoz-Fontela, C., Rivas, C., 2016. Regulation of Ebola virus VP40 matrix protein by SUMO. Scientific Reports 6.

Begitt, A., Droescher, M., Knobeloch, K.-P., Vinkemeier, U., 2011. SUMO conjugation of STAT1 protects cells from hyperresponsiveness to IFNγ. Blood 118, 1002–1007.

Bengtsson, L., Wilson, K.L., 2006. Barrier-to-autointegration factor phosphorylation on Ser-4 regulates emerin binding to lamin A in vitro and emerin localization in vivo. Mol Biol Cell 17, 1154–1163.

Berk, J.M., Simon, D.N., Jenkins-Houk, C.R., Westerbeck, J.W., Grønning-Wang, L.M., Carlson, C.R., Wilson, K.L., 2014. The molecular basis of emerin-emerin and emerin-BAF interactions. J Cell Sci 127, 3956–3969.

Bernardi, R., Pandolfi, P.P., 2007. Structure, dynamics and functions of promyelocytic leukaemia nuclear bodies. Nat Rev Mol Cell Biol 8, 1006–1016.

Bernardi, R., Papa, A., Pandolfi, P.P., 2008. Regulation of apoptosis by PML and the PML-NBs. Oncogene 27, 6299–6312.

Bharaj, P., Atkins, C., Luthra, P., Giraldo, M.I., Dawes, B.E., Miorin, L., Johnson, J.R., Krogan, N.J., Basler, C.F., Freiberg, A.N., Rajsbaum, R., 2017. The Host E3-Ubiquitin Ligase TRIM6 Ubiquitinates the Ebola Virus VP35 Protein and Promotes Virus Replication. J Virol 91, e00833-17.

Björndal, A.S., Szekely, L., Elgh, F., 2003. Ebola virus infection inversely correlates with the overall expression levels of promyelocytic leukaemia (PML) protein in cultured cells. BMC Microbiol 3, 6.

Blondel, D., Regad, T., Poisson, N., Pavie, B., Harper, F., Pandolfi, P.P., de Thé, H., Chelbi-Alix, M.K., 2002. Rabies virus P and small P products interact directly with PML and reorganize PML nuclear bodies. Oncogene 21, 7957–7970.

Bohren, K.M., Nadkarni, V., Song, J.H., Gabbay, K.H., Owerbach, D., 2004. A M55V polymorphism in a novel SUMO gene (SUMO-4) differentially activates heat shock transcription factors and is associated with susceptibility to type I diabetes mellitus. J Biol Chem 279, 27233–27238.

Bonilla, W.V., Pinschewer, D.D., Klenerman, P., Rousson, V., Gaboli, M., Pandolfi, P.P., Zinkernagel, R.M., Salvato, M.S., Hengartner, H., 2002. Effects of Promyelocytic Leukemia Protein on Virus-Host Balance. J Virol 76, 3810–3818.

Borden, K.L., Campbell Dwyer, E.J., Salvato, M.S., 1998. An arenavirus RING (zinc-binding) protein binds the oncoprotein

promyelocyte leukemia protein (PML) and relocates PML nuclear bodies to the cytoplasm. J Virol 72, 758–766.

Bowen, E.T., Lloyd, G., Harris, W.J., Platt, G.S., Baskerville, A., Vella, E.E., 1977. Viral haemorrhagic fever in southern Sudan and northern Zaire. Preliminary studies on the aetiological agent. Lancet 1, 571–573.

Brisse, M., Ly, H., 2019. Comparative Structure and Function Analysis of the RIG-I-Like Receptors: RIG-I and MDA5. Frontiers in Immunology 10, 1586.

Campagna, M., Marcos-Villar, L., Arnoldi, F., de la Cruz-Herrera, C.F., Gallego, P., González-Santamaría, J., González, D., Lopitz-Otsoa, F., Rodriguez, M.S., Burrone, O.R., Rivas, C., 2013. Rotavirus viroplasm proteins interact with the cellular SUMOylation system: implications for viroplasm-like structure formation. J Virol 87, 807–817.

Cárdenas, W.B., Loo, Y.-M., Gale, M., Hartman, A.L., Kimberlin, C.R., Martínez-Sobrido, L., Saphire, E.O., Basler, C.F., 2006. Ebola virus VP35 protein binds double-stranded RNA and inhibits alpha/beta interferon production induced by RIG-I signaling. J Virol 80, 5168–5178.

Carette, J.E., Raaben, M., Wong, A.C., Herbert, A.S., Obernosterer, G., Mulherkar, N., Kuehne, A.I., Kranzusch, P.J., Griffin, A.M., Ruthel, G., Cin, P.D., Dye, J.M., Whelan, S.P., Chandran, K., Brummelkamp, T.R., 2011. Ebola virus entry requires the cholesterol transporter Niemann-Pick C1. Nature 477, 340–343.

Chang, P.-C., Izumiya, Y., Wu, C.-Y., Fitzgerald, L.D., Campbell, M., Ellison, T.J., Lam, K.S., Luciw, P.A., Kung, H.-J., 2010. Kaposi's Sarcoma-associated Herpesvirus (KSHV) Encodes a SUMO E3 ligase That Is SIM-dependent and SUMO-2/3-specific. J Biol Chem 285, 5266–5273.

Chang, T.-H., Kubota, T., Matsuoka, M., Jones, S., Bradfute, S.B., Bray, M., Ozato, K., 2009. Ebola Zaire Virus Blocks Type I Interferon Production by Exploiting the Host SUMO Modification Machinery. PLoS Pathogens 5, e1000493.

Chavoshi, S., Egorova, O., Lacdao, I.K., Farhadi, S., Sheng, Y., Saridakis, V., 2016. Identification of Kaposi Sarcoma Herpesvirus

(KSHV) vIRF1 Protein as a Novel Interaction Partner of Human Deubiquitinase USP7. J Biol Chem 291, 6281–6291.

Chen, H., Engelman, A., 1998. The barrier-to-autointegration protein is a host factor for HIV type 1 integration. Proc Natl Acad Sci U S A 95, 15270–15274.

Cohen, S., Au, S., Panté, N., 2011. How viruses access the nucleus. Biochimica et Biophysica Acta (BBA) - Molecular Cell Research, Regulation of Signaling and Cellular Fate through Modulation of Nuclear Protein Import 1813, 1634–1645.

Conde, J.N., Schutt, W.R., Mladinich, M., Sohn, S.-Y., Hearing, P., Mackow, E.R., n.d. NS5 Sumoylation Directs Nuclear Responses That Permit Zika Virus To Persistently Infect Human Brain Microvascular Endothelial Cells. Journal of Virology 94, e01086-20.

Côté, M., Misasi, J., Ren, T., Bruchez, A., Lee, K., Filone, C.M., Hensley, L., Li, Q., Ory, D., Chandran, K., Cunningham, J., 2011. Small molecule inhibitors reveal Niemann-Pick C1 is essential for ebolavirus infection. Nature 477, 344–348.

Cuchet-Lourenço, D., Vanni, E., Glass, M., Orr, A., Everett, R.D., 2012. Herpes Simplex Virus 1 Ubiquitin Ligase ICP0 Interacts with PML Isoform I and Induces Its SUMO-Independent Degradation. Journal of Virology 86, 11209–11222.

Cui, K., Tailor, P., Liu, H., Chen, X., Ozato, K., Zhao, K., 2004. The chromatin-remodeling BAF complex mediates cellular antiviral activities by promoter priming. Mol Cell Biol 24, 4476–4486.

Day, P.M., Roden, R.B., Lowy, D.R., Schiller, J.T., 1998. The papillomavirus minor capsid protein, L2, induces localization of the major capsid protein, L1, and the viral transcription/replication protein, E2, to PML oncogenic domains. J Virol 72, 142–150.

de la Cruz-Herrera, C.F., Campagna, M., García, M.A., Marcos-Villar, L., Lang, V., Baz-Martínez, M., Gutiérrez, S., Vidal, A., Rodríguez, M.S., Esteban, M., Rivas, C., 2014. Activation of the double-stranded RNA-dependent protein kinase PKR by small ubiquitin-like modifier (SUMO). J Biol Chem 289, 26357–26367.

Dechat, T., Adam, S.A., Goldman, R.D., 2009. Nuclear lamins and chromatin: When structure meets function. Advances in Enzyme Regulation 49, 157–166.

Dechat, T., Pfleghaar, K., Sengupta, K., Shimi, T., Shumaker, D.K., Solimando, L., Goldman, R.D., 2008. Nuclear lamins: major factors in the structural organization and function of the nucleus and chromatin. Genes Dev 22, 832–853.

Denais, C.M., Gilbert, R.M., Isermann, P., McGregor, A.L., te Lindert, M., Weigelin, B., Davidson, P.M., Friedl, P., Wolf, K., Lammerding, J., 2016. Nuclear envelope rupture and repair during cancer cell migration. Science 352, 353–358.

Desbois, C., Rousset, R., Bantignies, F., Jalinot, P., 1996. Exclusion of Int-6 from PML Nuclear Bodies by Binding to the HTLV-I Tax Oncoprotein. Science 273, 951–953.

Desterro, J.M., Rodriguez, M.S., Hay, R.T., 1998. SUMO-1 modification of IkappaBalpha inhibits NF-kappaB activation. Mol Cell 2, 233–239.

Di Palma, F., Daino, G.L., Ramaswamy, V.K., Corona, A., Frau, A., Fanunza, E., Vargiu, A.V., Tramontano, E., Ruggerone, P., 2019. Relevance of Ebola virus VP35 homo-dimerization on the type I interferon cascade inhibition. Antivir Chem Chemother 27, 2040206619889220.

Domingues, P., Golebiowski, F., Tatham, M.H., Lopes, A.M., Taggart, A., Hay, R.T., Hale, B.G., 2015. Global Reprogramming of Host SUMOylation during Influenza Virus Infection. Cell Reports 13, 1467–1480.

Dong, C., Davis, R.J., Flavell, R.A., 2002. MAP kinases in the immune response. Annu Rev Immunol 20, 55–72. https://doi.org/10.1146/annurev.immunol.20.091301.131133

El Motiam, A., Vidal, S., Seoane, R., Bouzaher, Y.H., González-Santamaría, J., Rivas, C., 2020. SUMO and Cytoplasmic RNA Viruses: From Enemies to Best Friends, in: Barrio, R., Sutherland, J.D., Rodriguez, M.S. (Eds.), Proteostasis and Disease : From Basic Mechanisms to Clinics, Advances in Experimental Medicine and Biology. Springer International Publishing, Cham, pp. 263–277.

Emond, R.T., Evans, B., Bowen, E.T., Lloyd, G., 1977. A case of Ebola virus infection. Br Med J 2, 541–544.

Everett, R.D., 2001. DNA viruses and viral proteins that interact with PML nuclear bodies. Oncogene 20, 7266–7273.

Everett, R.D., Boutell, C., Hale, B.G., 2013. Interplay between viruses and host sumoylation pathways. Nat Rev Microbiol 11, 400–411.

Everett, R.D., Meredith, M., Orr, A., Cross, A., Kathoria, M., Parkinson, J., 1997. A novel ubiquitin-specific protease is dynamically associated with the PML nuclear domain and binds to a herpesvirus regulatory protein. EMBO J 16, 1519–1530.

Everett, R.D., Rechter, S., Papior, P., Tavalai, N., Stamminger, T., Orr, A., 2006. PML contributes to a cellular mechanism of repression of herpes simplex virus type 1 infection that is inactivated by ICP0. J Virol 80, 7995–8005.

Feldherr, C.M., Feldherr, A.B., 1960. The Nuclear Membrane as a Barrier to the Free Diffusion of Proteins. Nature 185, 250–251.

Feng, Z., Cerveny, M., Yan, Z., He, B., 2007. The VP35 Protein of Ebola Virus Inhibits the Antiviral Effect Mediated by Double-Stranded RNA-Dependent Protein Kinase PKR. J Virol 81, 182–192.

Flather, D., Semler, B.L., 2015. Picornaviruses and nuclear functions: targeting a cellular compartment distinct from the replication site of a positive-strand RNA virus. Front Microbiol 6, 594.

Flotho, A., Melchior, F., 2013. Sumoylation: a regulatory protein modification in health and disease. Annu Rev Biochem 82, 357–385.

Fogal, V., Gostissa, M., Sandy, P., Zacchi, P., Sternsdorf, T., Jensen, K., Pandolfi, P.P., Will, H., Schneider, C., Del Sal, G., 2000. Regulation of p53 activity in nuclear bodies by a specific PML isoform. EMBO J 19, 6185–6195.

Fu, J., Xiong, Y., Xu, Y., Cheng, G., Tang, H., 2011. MDA5 is SUMOylated by PIAS2β in the upregulation of Type I interferon signaling. Mol Immunol 48, 415–422.

García-Dorival, I., Wu, W., Armstrong, S.D., Barr, J.N., Carroll, M.W., Hewson, R., Hiscox, J.A., 2016. Elucidation of the Cellular Interactome of Ebola Virus Nucleoprotein and Identification of Therapeutic Targets. J Proteome Res 15, 4290–4303.

García-Dorival, I., Wu, W., Dowall, S., Armstrong, S., Touzelet, O., Wastling, J., Barr, J.N., Matthews, D., Carroll, M., Hewson, R., Hiscox, J.A., 2014. Elucidation of the Ebola virus VP24 cellular

interactome and disruption of virus biology through targeted inhibition of host-cell protein function. J Proteome Res 13, 5120–5135.

Gareau, J.R., Lima, C.D., 2010. The SUMO pathway: emerging mechanisms that shape specificity, conjugation and recognition. Nat Rev Mol Cell Biol 11, 861–871.

Geisbert, T.W., 2015. Marburg and Ebola Hemorrhagic Fevers (Filoviruses). Mandell, Douglas, and Bennett's Principles and Practice of Infectious Diseases 1995-1999.e1.

Geiss-Friedlander, R., Melchior, F., 2007. Concepts in sumoylation: a decade on. Nature Reviews Molecular Cell Biology 8, 947–956.

González-Santamaría, J., Campagna, M., García, M.A., Marcos-Villar, L., González, D., Gallego, P., Lopitz-Otsoa, F., Guerra, S., Rodríguez, M.S., Esteban, M., Rivas, C., 2011. Regulation of Vaccinia Virus E3 Protein by Small Ubiquitin-Like Modifier Proteins. Journal of Virology 85, 12890–12900.

Grönholm, J., Vanhatupa, S., Ungureanu, D., Väliaho, J., Laitinen, T., Valjakka, J., Silvennoinen, O., 2012. Structure-function analysis indicates that sumoylation modulates DNA-binding activity of STAT1. BMC Biochem 13, 20.

Guey, B., Wischnewski, M., Decout, A., Makasheva, K., Kaynak, M., Sakar, M.S., Fierz, B., Ablasser, A., 2020. BAF restricts cGAS on nuclear DNA to prevent innate immune activation. Science 369, 823–828.

Guito, J.C., Albariño, C.G., Chakrabarti, A.K., Towner, J.S., 2017. Novel activities by ebolavirus and marburgvirus interferon antagonists revealed using a standardized in vitro reporter system. Virology 501, 147–165.

Guo, D., Han, J., Adam, B.-L., Colburn, N.H., Wang, M.-H., Dong, Z., Eizirik, D.L., She, J.-X., Wang, C.-Y., 2005. Proteomic analysis of SUMO4 substrates in HEK293 cells under serum starvation-induced stress. Biochem Biophys Res Commun 337, 1308–1318.

Guo, Y., Zheng, Y., 2015. Lamins position the nuclear pores and centrosomes by modulating dynein. Mol Biol Cell 26, 3379–3389.

Gupta, M., Mahanty, S., Ahmed, R., Rollin, P.E., 2001. Monocyte-derived human macrophages and peripheral blood mononuclear cells

infected with ebola virus secrete MIP-1alpha and TNF-alpha and inhibit poly-IC-induced IFN-alpha in vitro. Virology 284, 20–25.

Han, Q., Chang, C., Li, L., Klenk, C., Cheng, J., Chen, Y., Xia, N., Shu, Y., Chen, Z., Gabriel, G., Sun, B., Xu, K., 2014. Sumoylation of Influenza A Virus Nucleoprotein Is Essential for Intracellular Trafficking and Virus Growth. J Virol 88, 9379–9390.

Han, Z., Boshra, H., Sunyer, J.O., Zwiers, S.H., Paragas, J., Harty, R.N., 2003. Biochemical and functional characterization of the Ebola virus VP24 protein: implications for a role in virus assembly and budding. J Virol 77, 1793–1800.

Haraguchi, T., Koujin, T., Segura-Totten, M., Lee, K.K., Matsuoka, Y., Yoneda, Y., Wilson, K.L., Hiraoka, Y., 2001. BAF is required for emerin assembly into the reforming nuclear envelope. Journal of Cell Science 114, 4575–4585.

Harcourt, B.H., Sanchez, A., Offermann, M.K., 1998. Ebola Virus Inhibits Induction of Genes by Double-Stranded RNA in Endothelial Cells. Virology 252, 179–188. https://doi.org/10.1006/viro.1998.9446

Harrison, A.R., Todd, S., Dearnley, M., David, C.T., Green, D., Rawlinson, S.M., Au, G.G., Marsh, G.A., Moseley, G.W., 2021. Antagonism of STAT3 signalling by Ebola virus. PLOS Pathogens 17, e1009636.

Hay, R.T., 2005. SUMO. Molecular Cell 18, 1–12. https://doi.org/10.1016/j.molcel.2005.03.012

He, F., Melén, K., Maljanen, S., Lundberg, R., Jiang, M., Österlund, P., Kakkola, L., Julkunen, I., 2017. Ebolavirus protein VP24 interferes with innate immune responses by inhibiting interferon-λ1 gene expression. Virology 509, 23–34.

Hildebrandt, A., Alanis-Lobato, G., Voigt, A., Zarnack, K., Andrade-Navarro, M.A., Beli, P., König, J., 2017. Interaction profiling of RNA-binding ubiquitin ligases reveals a link between posttranscriptional regulation and the ubiquitin system. Sci Rep 7, 16582.

Hjerpe, R., Aillet, F., Lopitz-Otsoa, F., Lang, V., England, P., Rodriguez, M.S., 2009. Efficient protection and isolation of ubiquitylated proteins using tandem ubiquitin-binding entities. EMBO Rep 10, 1250–1258.

Hochstrasser, M., 2009. Origin and function of ubiquitin-like proteins. Nature 458, 422–429. https://doi.org/10.1038/nature07958

Hoenen, T., Biedenkopf, N., Zielecki, F., Jung, S., Groseth, A., Feldmann, H., Becker, S., 2010. Oligomerization of Ebola virus VP40 is essential for particle morphogenesis and regulation of viral transcription. J Virol 84, 7053–7063.

Hoenen, T., Groseth, A., Kolesnikova, L., Theriault, S., Ebihara, H., Hartlieb, B., Bamberg, S., Feldmann, H., Ströher, U., Becker, S., 2006. Infection of Naïve Target Cells with Virus-Like Particles: Implications for the Function of Ebola Virus VP24. J Virol 80, 7260–7264.

Horvath, C.M., 2004. The Jak-STAT Pathway Stimulated by Interferon γ. Sci. Signal. 2004, tr8.

Houben, F., De Vos, W.H., Krapels, I.P.C., Coorens, M., Kierkels, G.J.J., Kamps, M.A.F., Verstraeten, V.L.R.M., Marcelis, C.L.M., van den Wijngaard, A., Ramaekers, F.C.S., Broers, J.L.V., 2013. Cytoplasmic localization of PML particles in laminopathies. Histochem Cell Biol 139, 119–134.

Huang, Y., Xu, L., Sun, Y., Nabel, G.J., 2002. The Assembly of Ebola Virus Nucleocapsid Requires Virion-Associated Proteins 35 and 24 and Posttranslational Modification of Nucleoprotein. Molecular Cell 10, 307–316.

Ilinykh, P.A., Lubaki, N.M., Widen, S.G., Renn, L.A., Theisen, T.C., Rabin, R.L., Wood, T.G., Bukreyev, A., 2015. Different Temporal Effects of Ebola Virus VP35 and VP24 Proteins on Global Gene Expression in Human Dendritic Cells. J Virol 89, 7567–7583.

Ishov, A.M., Sotnikov, A.G., Negorev, D., Vladimirova, O.V., Neff, N., Kamitani, T., Yeh, E.T., Strauss, J.F., Maul, G.G., 1999. PML is critical for ND10 formation and recruits the PML-interacting protein daxx to this nuclear structure when modified by SUMO-1. J Cell Biol 147, 221–234.

Ito, H., Watanabe, S., Takada, A., Kawaoka, Y., 2001. Ebola Virus Glycoprotein: Proteolytic Processing, Acylation, Cell Tropism, and Detection of Neutralizing Antibodies. J Virol 75, 1576–1580.

Ivanschitz, L., Takahashi, Y., Jollivet, F., Ayrault, O., Bras, M.L., Thé, H. de, 2015. PML IV/ARF interaction enhances p53 SUMO-1 conjugation, activation, and senescence. PNAS 112, 14278–14283.

Jacque, J.-M., Stevenson, M., 2006. The inner-nuclear-envelope protein emerin regulates HIV-1 infectivity. Nature 441, 641–645.

Jäger, W., Santag, S., Weidner-Glunde, M., Gellermann, E., Kati, S., Pietrek, M., Viejo-Borbolla, A., Schulz, T.F., 2012. The ubiquitin-specific protease USP7 modulates the replication of Kaposi's sarcoma-associated herpesvirus latent episomal DNA. J Virol 86, 6745–6757.

Jamin, A., Thunuguntla, P., Wicklund, A., Jones, C., Wiebe, M.S., 2014. Barrier to auto integration factor becomes dephosphorylated during HSV-1 Infection and Can Act as a host defense by impairing viral DNA replication and gene expression. PLoS One 9, e100511.

Jasenosky, L.D., Neumann, G., Lukashevich, I., Kawaoka, Y., 2001. Ebola virus VP40-induced particle formation and association with the lipid bilayer. J Virol 75, 5205–5214.

Jeon, Y.J., Park, J.H., Chung, C.H., 2017. Interferon-Stimulated Gene 15 in the Control of Cellular Responses to Genotoxic Stress. Mol Cells 40, 83–89.

Jin, H., Yan, Z., Prabhakar, B.S., Feng, Z., Ma, Y., Verpooten, D., Ganesh, B., He, B., 2010. The VP35 protein of Ebola virus impairs dendritic cell maturation induced by virus and lipopolysaccharide. J Gen Virol 91, 352–361.

Johnson, K.M., Lange, J.V., Webb, P.A., Murphy, F.A., 1977. Isolation and partial characterisation of a new virus causing acute haemorrhagic fever in Zaire. Lancet 1, 569–571.

Johnson, R.F., Bell, P., Harty, R.N., 2006. Effect of Ebola virus proteins GP, NP and VP35 on VP40 VLP morphology. Virol J 3, 31.

Jones, C.V., Ricardo, S.D., 2013. Macrophages and CSF-1. Organogenesis 9, 249–260.

Jounai, N., Kobiyama, K., Takeshita, F., Ishii, K.J., 2013. Recognition of damage-associated molecular patterns related to nucleic acids during inflammation and vaccination. Front Cell Infect Microbiol 2, 168.

Katano, H., Ogawa-Goto, K., Hasegawa, H., Kurata, T., Sata, T., 2001. Human-herpesvirus-8-encoded K8 protein colocalizes with the

promyelocytic leukemia protein (PML) bodies and recruits p53 to the PML bodies. Virology 286, 446–455.

Kerscher, O., 2007. SUMO junction—what's your function? New insights through SUMO-interacting motifs. EMBO Rep 8, 550–555.

Kerscher, O., Felberbaum, R., Hochstrasser, M., 2006. Modification of Proteins by Ubiquitin and Ubiquitin-Like Proteins. Annual Review of Cell and Developmental Biology 22, 159–180.

Kiley, M.P., Cox, N.J., Elliott, L.H., Sanchez, A., DeFries, R., Buchmeier, M.J., Richman, D.D., McCormick, J.B., 1988. Physicochemical properties of Marburg virus: evidence for three distinct virus strains and their relationship to Ebola virus. J Gen Virol 69 (Pt 8), 1957–1967.

Kobiler, O., Drayman, N., Butin-Israeli, V., Oppenheim, A., 2012. Virus strategies for passing the nuclear envelope barrier. Nucleus 3, 526–539.

Komander, D., Rape, M., 2012. The Ubiquitin Code. Annu. Rev. Biochem. 81, 203–229.

Kondratowicz, A.S., Lennemann, N.J., Sinn, P.L., Davey, R.A., Hunt, C.L., Moller-Tank, S., Meyerholz, D.K., Rennert, P., Mullins, R.F., Brindley, M., Sandersfeld, L.M., Quinn, K., Weller, M., McCray, P.B., Chiorini, J., Maury, W., 2011. T-cell immunoglobulin and mucin domain 1 (TIM-1) is a receptor for Zaire Ebolavirus and Lake Victoria Marburgvirus. Proc Natl Acad Sci U S A 108, 8426–8431.

Kubota, T., Matsuoka, M., Chang, T.-H., Tailor, P., Sasaki, T., Tashiro, M., Kato, A., Ozato, K., 2008. Virus Infection Triggers SUMOylation of IRF3 and IRF7, Leading to the Negative Regulation of Type I Interferon Gene Expression. Journal of Biological Chemistry 283, 25660–25670.

Kuhn, J.H., Amarasinghe, G.K., Basler, C.F., Bavari, S., Bukreyev, A., Chandran, K., Crozier, I., Dolnik, O., Dye, J.M., Formenty, P.B.H., Griffiths, A., Hewson, R., Kobinger, G.P., Leroy, E.M., Mühlberger, E., Netesov (Нетёсов Сергей Викторович), S.V., Palacios, G., Pályi, B., Pawęska, J.T., Smither, S.J., Takada (高田礼人), A., Towner, J.S., Wahl, V., ICTV Report Consortium, 2019. ICTV Virus Taxonomy Profile: Filoviridae. Journal of General Virology 100, 911–912.

Leach, N., Bjerke, S.L., Christensen, D.K., Bouchard, J.M., Mou, F., Park, R., Baines, J., Haraguchi, T., Roller, R.J., 2007. Emerin is hyperphosphorylated and redistributed in herpes simplex virus type 1-infected cells in a manner dependent on both UL34 and US3. J Virol 81, 10792–10803.

Lecona, E., Rodriguez-Acebes, S., Specks, J., Lopez-Contreras, A.J., Ruppen, I., Murga, M., Muñoz, J., Mendez, J., Fernandez-Capetillo, O., 2016. USP7 is a SUMO deubiquitinase essential for DNA replication. Nat Struct Mol Biol 23, 270–277.

Leroy, E.M., Kumulungui, B., Pourrut, X., Rouquet, P., Hassanin, A., Yaba, P., Délicat, A., Paweska, J.T., Gonzalez, J.-P., Swanepoel, R., 2005. Fruit bats as reservoirs of Ebola virus. Nature 438, 575–576.

Leung, D.W., Amarasinghe, G.K., 2012. Structural insights into RNA recognition and activation of RIG-I-like receptors. Curr Opin Struct Biol 22, 297–303.

Leung, D.W., Ginder, N.D., Fulton, D.B., Nix, J., Basler, C.F., Honzatko, R.B., Amarasinghe, G.K., 2009. Structure of the Ebola VP35 interferon inhibitory domain. Proc Natl Acad Sci U S A 106, 411–416.

Licata, J.M., Johnson, R.F., Han, Z., Harty, R.N., 2004. Contribution of Ebola Virus Glycoprotein, Nucleoprotein, and VP24 to Budding of VP40 Virus-Like Particles. J Virol 78, 7344–7351.

Lin, D.H., Hoelz, A., 2019. The Structure of the Nuclear Pore Complex (An Update). Annu Rev Biochem 88, 725–783.

Lin, F., Blake, D.L., Callebaut, I., Skerjanc, I.S., Holmer, L., McBurney, M.W., Paulin-Levasseur, M., Worman, H.J., 2000. MAN1, an Inner Nuclear Membrane Protein That Shares the LEM Domain with Lamina-associated Polypeptide 2 and Emerin*. Journal of Biological Chemistry 275, 4840–4847.

Liu, J., Lee, K.K., Segura-Totten, M., Neufeld, E., Wilson, K.L., Gruenbaum, Y., 2003. MAN1 and emerin have overlapping function(s) essential for chromosome segregation and cell division in Caenorhabditis elegans. PNAS 100, 4598–4603.

Liu, R., Liu, H., Chen, X., Kirby, M., Brown, P.O., Zhao, K., 2001. Regulation of CSF1 promoter by the SWI/SNF-like BAF complex. Cell 106, 309–318.

Liu, Y., Zheng, Z., Shu, B., Meng, J., Zhang, Y., Zheng, C., Ke, X., Gong, P., Hu, Q., Wang, H., 2016. SUMO Modification Stabilizes Enterovirus 71 Polymerase 3D To Facilitate Viral Replication. Journal of Virology 90, 10472–10485.

Lowrey, A.J., Cramblet, W., Bentz, G.L., 2017. Viral manipulation of the cellular sumoylation machinery. Cell Commun Signal 15, 27.

Lubaki, N.M., Ilinykh, P., Pietzsch, C., Tigabu, B., Freiberg, A.N., Koup, R.A., Bukreyev, A., 2013. The Lack of Maturation of Ebola Virus-Infected Dendritic Cells Results from the Cooperative Effect of at Least Two Viral Domains. J Virol 87, 7471–7485.

Lumpkin, R.J., Gu, H., Zhu, Y., Leonard, M., Ahmad, A.S., Clauser, K.R., Meyer, J.G., Bennett, E.J., Komives, E.A., 2017. Site-specific identification and quantitation of endogenous SUMO modifications under native conditions. Nat Commun 8, 1171.

Luthra, P., Ramanan, P., Mire, C.E., Weisend, C., Tsuda, Y., Yen, B., Liu, G., Leung, D.W., Geisbert, T.W., Ebihara, H., Amarasinghe, G.K., Basler, C.F., 2013. Mutual Antagonism between the Ebola Virus VP35 Protein and the RIG-I Activator PACT Determines Infection Outcome. Cell Host & Microbe 14, 74–84.

Ma, H., Qian, W., Bambouskova, M., Collins, P.L., Porter, S.I., Byrum, A.K., Zhang, R., Artyomov, M., Oltz, E.M., Mosammaparast, N., Miner, J.J., Diamond, M.S., 2020. Barrier-to-Autointegration Factor 1 Protects against a Basal cGAS-STING Response. mBio 11.

Maarifi, G., Maroui, M.A., Dutrieux, J., Dianoux, L., Nisole, S., Chelbi-Alix, M.K., 2015. Small Ubiquitin-like Modifier Alters IFN Response. The Journal of Immunology 195, 2312–2324.

Maertens, G.N., El Messaoudi-Aubert, S., Elderkin, S., Hiom, K., Peters, G., 2010. Ubiquitin-specific proteases 7 and 11 modulate Polycomb regulation of the INK4a tumour suppressor. EMBO J 29, 2553–2565.

Margalit, A., Brachner, A., Gotzmann, J., Foisner, R., Gruenbaum, Y., 2007. Barrier-to-autointegration factor – a BAFfling little protein. Trends in Cell Biology 17, 202–208.

Martell, H.J., Masterson, S.G., McGreig, J.E., Michaelis, M., Wass, M.N., 2019. Is the Bombali virus pathogenic in humans? Bioinformatics 35, 3553–3558.

Martinez, O., Valmas, C., Basler, C.F., 2007. Ebola virus-like particle-induced activation of NF-kappaB and Erk signaling in human dendritic cells requires the glycoprotein mucin domain. Virology 364, 342–354.

Matsuno, K., Nakayama, E., Noyori, O., Marzi, A., Ebihara, H., Irimura, T., Feldmann, H., Takada, A., 2010. C-type lectins do not act as functional receptors for filovirus entry into cells. Biochem Biophys Res Commun 403, 144–148.

Mayo, C.B., Cole, J.L., 2017. Interaction of PKR with single-stranded RNA. Sci Rep 7, 3335.

McBride, K.M., Banninger, G., McDonald, C., Reich, N.C., 2002. Regulated nuclear import of the STAT1 transcription factor by direct binding of importin-alpha. EMBO J 21, 1754–1763.

McBride, K.M., McDonald, C., Reich, N.C., 2000. Nuclear export signal located within theDNA-binding domain of the STAT1transcription factor. EMBO J 19, 6196–6206.

McCormick, J.B., Bauer, S.P., Elliott, L.H., Webb, P.A., Johnson, K.M., 1983. Biologic differences between strains of Ebola virus from Zaire and Sudan. J Infect Dis 147, 264–267.

McNab, F., Mayer-Barber, K., Sher, A., Wack, A., O'Garra, A., 2015. Type I interferons in infectious disease. Nat Rev Immunol 15, 87–103.

Minty, A., Dumont, X., Kaghad, M., Caput, D., 2000. Covalent modification of p73alpha by SUMO-1. Two-hybrid screening with p73 identifies novel SUMO-1-interacting proteins and a SUMO-1 interaction motif. J Biol Chem 275, 36316–36323.

Mohan, G.S., Li, W., Ye, L., Compans, R.W., Yang, C., 2012. Antigenic subversion: a novel mechanism of host immune evasion by Ebola virus. PLoS Pathog 8, e1003065.

Möller, A., Schmitz, M.L., 2003. Viruses as hijackers of PML nuclear bodies. Arch Immunol Ther Exp (Warsz) 51, 295–300.

Muchir, A., Shan, J., Bonne, G., Lehnart, S.E., Worman, H.J., 2009. Inhibition of extracellular signal-regulated kinase signaling to

prevent cardiomyopathy caused by mutation in the gene encoding A-type lamins. Hum Mol Genet 18, 241–247.

Muchir, A., Worman, H.J., 2007. Emery-Dreifuss muscular dystrophy. Curr Neurol Neurosci Rep 7, 78–83.

Müller, S., Dejean, A., 1999. Viral immediate-early proteins abrogate the modification by SUMO-1 of PML and Sp100 proteins, correlating with nuclear body disruption. J Virol 73, 5137–5143.

Nanbo, A., Imai, M., Watanabe, S., Noda, T., Takahashi, K., Neumann, G., Halfmann, P., Kawaoka, Y., 2010. Ebolavirus Is Internalized into Host Cells via Macropinocytosis in a Viral Glycoprotein-Dependent Manner. PLoS Pathog 6.

Neerukonda, S.N., 2021. Interplay between RNA Viruses and Promyelocytic Leukemia Nuclear Bodies. Veterinary Sciences 8, 57.

Nichols, R.J., Wiebe, M.S., Traktman, P., 2006. The vaccinia-related kinases phosphorylate the N' terminus of BAF, regulating its interaction with DNA and its retention in the nucleus. Mol Biol Cell 17, 2451–2464.

Nikolova, V., Leimena, C., McMahon, A.C., Tan, J.C., Chandar, S., Jogia, D., Kesteven, S.H., Michalicek, J., Otway, R., Verheyen, F., Rainer, S., Stewart, C.L., Martin, D., Feneley, M.P., Fatkin, D., 2004. Defects in nuclear structure and function promote dilated cardiomyopathy in lamin A/C-deficient mice. J Clin Invest 113, 357–369.

Nisole, S., Maroui, M.A., Mascle, X.H., Aubry, M., Chelbi-Alix, M.K., 2013. Differential Roles of PML Isoforms. Front Oncol 3, 125.

Noser, J.A., Mael, A.A., Sakuma, R., Ohmine, S., Marcato, P., Lee, P.W., Ikeda, Y., 2007. The RAS/Raf1/MEK/ERK Signaling Pathway Facilitates VSV-mediated Oncolysis: Implication for the Defective Interferon Response in Cancer Cells. Molecular Therapy 15, 1531–1536.

Owerbach, D., McKay, E.M., Yeh, E.T.H., Gabbay, K.H., Bohren, K.M., 2005. A proline-90 residue unique to SUMO-4 prevents maturation and sumoylation. Biochem Biophys Res Commun 337, 517–520.

Pal, S., Santos, A., Rosas, J.M., Ortiz-Guzman, J., Rosas-Acosta, G., 2011. Influenza A virus interacts extensively with the cellular SUMOylation system during infection. Virus Research 158, 12–27.

Park, J.H., Yang, S.W., Park, J.M., Ka, S.H., Kim, J.-H., Kong, Y.-Y., Jeon, Y.J., Seol, J.H., Chung, C.H., 2016. Positive feedback regulation of p53 transactivity by DNA damage-induced ISG15 modification. Nat Commun 7, 12513.

Piekarowicz, K., Machowska, M., Dzianisava, V., Rzepecki, R., 2019. Hutchinson-Gilford Progeria Syndrome—Current Status and Prospects for Gene Therapy Treatment. Cells 8, 88.

Pindel, A., Sadler, A., 2011. The Role of Protein Kinase R in the Interferon Response. Journal of Interferon & Cytokine Research 31, 59–70.

Platanias, L.C., 2005. Mechanisms of type-I- and type-II-interferon-mediated signalling. Nat Rev Immunol 5, 375–386.

Prins, K.C., Cárdenas, W.B., Basler, C.F., 2009. Ebola virus protein VP35 impairs the function of interferon regulatory factor-activating kinases IKKepsilon and TBK-1. J Virol 83, 3069–3077.

Proud, C.G., 2005. eIF2 and the control of cell physiology. Seminars in Cell & Developmental Biology 16, 3–12.

Qi, R., Xu, N., Wang, G., Ren, H., Li, S., Lei, J., Lin, Q., Wang, L., Gu, X., Zhang, H., Jiang, Q., Zhang, C., 2015. The lamin-A/C–LAP2α–BAF1 protein complex regulates mitotic spindle assembly and positioning. Journal of Cell Science 128, 2830–2841.

Raab, M., Gentili, M., de Belly, H., Thiam, H.R., Vargas, P., Jimenez, A.J., Lautenschlaeger, F., Voituriez, R., Lennon-Duménil, A.M., Manel, N., Piel, M., 2016. ESCRT III repairs nuclear envelope ruptures during cell migration to limit DNA damage and cell death. Science 352, 359–362.

Ran, Y., Liu, T.-T., Zhou, Q., Li, S., Mao, A.-P., Li, Y., Liu, L.-J., Cheng, J.-K., Shu, H.-B., 2011. SENP2 negatively regulates cellular antiviral response by deSUMOylating IRF3 and conditioning it for ubiquitination and degradation. Journal of Molecular Cell Biology 3, 283–292.

Redwood, A.B., Perkins, S.M., Vanderwaal, R.P., Feng, Z., Biehl, K.J., Gonzalez-Suarez, I., Morgado-Palacin, L., Shi, W., Sage, J., Roti-

Roti, J.L., Stewart, C.L., Zhang, J., Gonzalo, S., 2011. A dual role for A-type lamins in DNA double-strand break repair. Cell Cycle 10, 2549–2560.

Rehwinkel, J., Gack, M.U., 2020. RIG-I-like receptors: their regulation and roles in RNA sensing. Nat Rev Immunol 20, 537–551.

Reid, S.P., Leung, L.W., Hartman, A.L., Martinez, O., Shaw, M.L., Carbonnelle, C., Volchkov, V.E., Nichol, S.T., Basler, C.F., 2006. Ebola Virus VP24 Binds Karyopherin α1 and Blocks STAT1 Nuclear Accumulation. Journal of Virology 80, 5156–5167.

Reid, S.P., Valmas, C., Martinez, O., Sanchez, F.M., Basler, C.F., 2007. Ebola Virus VP24 Proteins Inhibit the Interaction of NPI-1 Subfamily Karyopherin α Proteins with Activated STAT1. Journal of Virology 81, 13469–13477.

Richman, D.D., Cleveland, P.H., McCormick, J.B., Johnson, K.M., 1983. Antigenic analysis of strains of Ebola virus: identification of two Ebola virus serotypes. J Infect Dis 147, 268–271.

Rodriguez, J.A., Au, W.W.Y., Henderson, B.R., 2004. Cytoplasmic mislocalization of BRCA1 caused by cancer-associated mutations in the BRCT domain. Experimental Cell Research 293, 14–21.

Rodriguez, K.R., Bruns, A.M., Horvath, C.M., 2014. MDA5 and LGP2: Accomplices and Antagonists of Antiviral Signal Transduction. J Virol 88, 8194–8200.

Rodriguez, M.S., Dargemont, C., Hay, R.T., 2001. SUMO-1 conjugation in vivo requires both a consensus modification motif and nuclear targeting. J Biol Chem 276, 12654–12659.

Rodriguez, M.S., Desterro, J.M., Lain, S., Midgley, C.A., Lane, D.P., Hay, R.T., 1999. SUMO-1 modification activates the transcriptional response of p53. EMBO J 18, 6455–6461.

Saeed, M.F., Kolokoltsov, A.A., Albrecht, T., Davey, R.A., 2010. Cellular Entry of Ebola Virus Involves Uptake by a Macropinocytosis-Like Mechanism and Subsequent Trafficking through Early and Late Endosomes. PLoS Pathog 6.

Saether, T., Pattabiraman, D.R., Alm-Kristiansen, A.H., Vogt-Kielland, L.T., Gonda, T.J., Gabrielsen, O.S., 2011. A functional

SUMO-interacting motif in the transactivation domain of c-Myb regulates its myeloid transforming ability. Oncogene 30, 212–222.

Saitoh, H., Hinchey, J., 2000. Functional Heterogeneity of Small Ubiquitin-related Protein Modifiers SUMO-1 versus SUMO-2/3*. Journal of Biological Chemistry 275, 6252–6258.

Samson, C., Petitalot, A., Celli, F., Herrada, I., Ropars, V., Le Du, M.-H., Nhiri, N., Jacquet, E., Arteni, A.-A., Buendia, B., Zinn-Justin, S., 2018. Structural analysis of the ternary complex between lamin A/C, BAF and emerin identifies an interface disrupted in autosomal recessive progeroid diseases. Nucleic Acids Research 46, 10460–10473.

Samuel, C.E., 2001. Antiviral Actions of Interferons. Clin Microbiol Rev 14, 778–809.

Sanchez, A., Trappier, S.G., Mahy, B.W., Peters, C.J., Nichol, S.T., 1996. The virion glycoproteins of Ebola viruses are encoded in two reading frames and are expressed through transcriptional editing. Proc Natl Acad Sci U S A 93, 3602–3607.

Sánchez-Aparicio, M.T., Ayllón, J., Leo-Macias, A., Wolff, T., García-Sastre, A., 2017. Subcellular Localizations of RIG-I, TRIM25, and MAVS Complexes. J Virol 91, e01155-16.

Schmidt, N., Domingues, P., Golebiowski, F., Patzina, C., Tatham, M.H., Hay, R.T., Hale, B.G., 2019. An influenza virus-triggered SUMO switch orchestrates co-opted endogenous retroviruses to stimulate host antiviral immunity. PNAS 116, 17399–17408.

Schreiber, K.H., Kennedy, B.K., 2013. When Lamins Go Bad: Nuclear Structure and Disease. Cell 152, 1365–1375.

Schwarz, T.M., Edwards, M.R., Diederichs, A., Alinger, J.B., Leung, D.W., Amarasinghe, G.K., Basler, C.F., 2017. VP24-Karyopherin Alpha Binding Affinities Differ between Ebolavirus Species, Influencing Interferon Inhibition and VP24 Stability. J Virol 91.

Sears, R., Nuckolls, F., Haura, E., Taya, Y., Tamai, K., Nevins, J.R., 2000. Multiple Ras-dependent phosphorylation pathways regulate Myc protein stability. Genes Dev 14, 2501–2514.

Segura-Totten, M., Wilson, K.L., 2004. BAF: roles in chromatin, nuclear structure and retrovirus integration. Trends Cell Biol 14, 261–266.

Sekimoto, T., Imamoto, N., Nakajima, K., Hirano, T., Yoneda, Y., 1997. Extracellular signal-dependent nuclear import of Stat1 is mediated by nuclear pore-targeting complex formation with NPI-1, but not Rch1. EMBO J 16, 7067–7077.

Seoane, J., Le, H.-V., Massagué, J., 2002. Myc suppression of the p21(Cip1) Cdk inhibitor influences the outcome of the p53 response to DNA damage. Nature 419, 729–734.

Shabman, R.S., Gulcicek, E.E., Stone, K.L., Basler, C.F., 2011. The Ebola Virus VP24 Protein Prevents hnRNP C1/C2 Binding to Karyopherin α1 and Partially Alters its Nuclear Import. The Journal of Infectious Diseases 204, S904–S910.

Shen, T.H., Lin, H.-K., Scaglioni, P.P., Yung, T.M., Pandolfi, P.P., 2006. The mechanisms of PML-nuclear body formation. Mol Cell 24, 331–339.

Shimojima, M., Takada, A., Ebihara, H., Neumann, G., Fujioka, K., Irimura, T., Jones, S., Feldmann, H., Kawaoka, Y., 2006. Tyro3 family-mediated cell entry of Ebola and Marburg viruses. J Virol 80, 10109–10116.

Simmons, G., Reeves, J.D., Grogan, C.C., Vandenberghe, L.H., Baribaud, F., Whitbeck, J.C., Burke, E., Buchmeier, M.J., Soilleux, E.J., Riley, J.L., Doms, R.W., Bates, P., Pöhlmann, S., 2003. DC-SIGN and DC-SIGNR bind ebola glycoproteins and enhance infection of macrophages and endothelial cells. Virology 305, 115–123.

Sohn, S.-Y., Hearing, P., 2012. Adenovirus regulates sumoylation of Mre11-Rad50-Nbs1 components through a paralog-specific mechanism. J Virol 86, 9656–9665.

Stark, G.R., Kerr, I.M., Williams, B.R.G., Silverman, R.H., Schreiber, R.D., 1998. How Cells Respond to Interferons. Annual Review of Biochemistry 67, 227–264.

Stubbe, M., Mai, J., Paulus, C., Stubbe, H.C., Berscheminski, J., Karimi, M., Hofmann, S., Weber, E., Hadian, K., Hay, R., Groitl, P., Nevels, M., Dobner, T., Schreiner, S., 2020. Viral DNA Binding Protein SUMOylation Promotes PML Nuclear Body Localization Next to Viral Replication Centers. mBio 11, e00049-20.

Su, Y., Stahelin, R.V., 2020. The Minor Matrix Protein VP24 from Ebola Virus Lacks Direct Lipid-Binding Properties. Viruses 12.

Sun, D., Xu, P., He, B., 2011. Sumoylation of the P Protein at K254 Plays an Important Role in Growth of Parainfluenza Virus 5 ▿ . J Virol 85, 10261–10268.

Swatek, K.N., Komander, D., 2016. Ubiquitin modifications. Cell Res 26, 399–422.

Szostecki, C., Guldner, H.H., Netter, H.J., Will, H., 1990. Isolation and characterization of cDNA encoding a human nuclear antigen predominantly recognized by autoantibodies from patients with primary biliary cirrhosis. J Immunol 145, 4338–4347.

Tatham, M.H., Kim, S., Jaffray, E., Song, J., Chen, Y., Hay, R.T., 2005. Unique binding interactions among Ubc9, SUMO and RanBP2 reveal a mechanism for SUMO paralog selection. Nat Struct Mol Biol 12, 67–74.

Timmins, J., Scianimanico, S., Schoehn, G., Weissenhorn, W., 2001. Vesicular release of ebola virus matrix protein VP40. Virology 283, 1–6.

Turelli, P., Doucas, V., Craig, E., Mangeat, B., Klages, N., Evans, R., Kalpana, G., Trono, D., 2001. Cytoplasmic recruitment of INI1 and PML on incoming HIV preintegration complexes: interference with early steps of viral replication. Mol Cell 7, 1245–1254.

Ungureanu, D., Vanhatupa, S., Grönholm, J., Palvimo, J.J., Silvennoinen, O., 2005. SUMO-1 conjugation selectively modulates STAT1-mediated gene responses. Blood 106, 224–226.

van der Veen, A.G., Ploegh, H.L., 2012. Ubiquitin-Like Proteins. Annual Review of Biochemistry 81, 323–357.

Vertegaal, A.C.O., Andersen, J.S., Ogg, S.C., Hay, R.T., Mann, M., Lamond, A.I., 2006. Distinct and overlapping sets of SUMO-1 and SUMO-2 target proteins revealed by quantitative proteomics. Mol Cell Proteomics 5, 2298–2310.

Volchkov, V.E., Becker, S., Volchkova, V.A., Ternovoj, V.A., Kotov, A.N., Netesov, S.V., Klenk, H.D., 1995. GP mRNA of Ebola virus is edited by the Ebola virus polymerase and by T7 and vaccinia virus polymerases. Virology 214, 421–430.

Volchkov, V.E., Volchkova, V.A., Dolnik, O., Feldmann, H., Klenk, H.-D., 2005. Polymorphism of filovirus glycoproteins. Adv Virus Res 64, 359–381.

Walker, E.J., Ghildyal, R. (Eds.), 2017. Viral Interactions with the Nucleus, Frontiers Research Topics. Frontiers Media SA.

Wang, H., Shi, Y., Song, J., Qi, J., Lu, G., Yan, J., Gao, G.F., 2016. Ebola Viral Glycoprotein Bound to Its Endosomal Receptor Niemann-Pick C1. Cell 164, 258–268.

Watanabe, S., Noda, T., Halfmann, P., Jasenosky, L., Kawaoka, Y., 2007. Ebola Virus (EBOV) VP24 Inhibits Transcription and Replication of the EBOV Genome. J Infect Dis 196, S284–S290.

Wiebe, M.S., Jamin, A., 2016. The Barrier to Autointegration Factor: Interlocking Antiviral Defense with Genome Maintenance. J Virol 90, 3806–3809.

Wilkinson, K.A., Henley, J.M., 2010. Mechanisms, regulation and consequences of protein SUMOylation. Biochem J 428, 133–145.

Wilson, K.L., Foisner, R., 2010. Lamin-binding Proteins. Cold Spring Harb Perspect Biol 2, a000554.

Wilson, V.G., 2016. Viral Interplay with the Host Sumoylation System. SUMO Regulation of Cellular Processes 963, 359–388.

Wu, C.-Y., Jeng, K.-S., Lai, M.M.-C., 2011. The SUMOylation of Matrix Protein M1 Modulates the Assembly and Morphogenesis of Influenza A Virus. Journal of Virology 85, 6618–6628.

Xu, K., Klenk, C., Liu, B., Keiner, B., Cheng, J., Zheng, B.-J., Li, L., Han, Q., Wang, C., Li, T., Chen, Z., Shu, Y., Liu, J., Klenk, H.-D., Sun, B., 2011. Modification of Nonstructural Protein 1 of Influenza A Virus by SUMO1. Journal of Virology 85, 1086–1098.

Xu, W., Edwards, M.R., Borek, D.M., Feagins, A.R., Mittal, A., Alinger, J.B., Berry, K.N., Yen, B., Hamilton, J., Brett, T.J., Pappu, R.V., Leung, D.W., Basler, C.F., Amarasinghe, G.K., 2014. Ebola Virus VP24 Targets a Unique NLS Binding Site on Karyopherin Alpha 5 to Selectively Compete with Nuclear Import of Phosphorylated STAT1. Cell Host & Microbe 16, 187–200.

Xu, Y., Ahn, J.-H., Cheng, M., apRhys, C.M., Chiou, C.-J., Zong, J., Matunis, M.J., Hayward, G.S., 2001. Proteasome-Independent Disruption of PML Oncogenic Domains (PODs), but Not Covalent Modification by SUMO-1, Is Required for Human Cytomegalovirus Immediate-Early Protein IE1 To Inhibit PML-Mediated Transcriptional Repression. Journal of Virology 75, 10683–10695.

Yadav, S., Libotte, F., Buono, E., Valia, S., Farina, G.A., Faggioni, A., Farina, A., 2017. EBV early lytic protein BFRF1 alters emerin distribution and post-translational modification. Virus Res 232, 113–122.

Zhang, A.P.P., Abelson, D.M., Bornholdt, Z.A., Liu, T., Woods, Jr, V.L., Saphire, E.O., 2012. The ebolavirus VP24 interferon antagonist. Virulence 3, 440–445.

Zhang, Y., Chen, Y., Liu, Z., Lai, R., 2018. ERK is a negative feedback regulator for IFN-γ/STAT1 signaling by promoting STAT1 ubiquitination. BMC Cancer 18, 613.

Zimnik, S., Gaestel, M., Niedenthal, R., 2009. Mutually exclusive STAT1 modifications identified by Ubc9/substrate dimerization-dependent SUMOylation. Nucleic Acids Res 37, e30.

11. ANNEX

11.1. COPYRIGHT LICENSE

Lifetime Unit Quantity Up to 499
Rights Requested Main product
Distribution Worldwide
Translation Original language of publication
Copies for the disabled? No
Minor editing privileges? No
Incidental promotional use? No
Currency EUR

NEW WORK DETAILS

Title Contribution of SUMO to the replication of Ebola virus
Instructor name M. Carmen Rivas Vázquez
Institution name Universidade de Santiago de Compostela
Expected presentation date 2021-10-15

ADDITIONAL DETAILS

Order reference number N/A
The requesting person / organization to appear on the license Santiago Vidal Freire, Universidade de Santiago de Compostela

REUSE CONTENT DETAILS

Title, description or numeric reference of the portion(s) Regulation of the Ebola Virus VP24 Protein by SUMO.
Editor of portion(s) Vidal, Santiago
Volume of serial or monograph 94
Page or page range of portion 1-16
Title of the article/chapter the portion is from Regulation of the Ebola Virus VP24 Protein by SUMO.
Author of portion(s) Vidal, Santiago
Issue, if republishing an article from a serial 1
Publication date of portion 2019-12-12

Order Date 14-Oct-2021
Order License ID 1154431-2
ISSN 2150-7511
Type of Use Republish in a thesis/dissertation
Publisher American Society for Microbiology
Portion Chapter/article

LICENSED CONTENT

Publication Title mBio
Article Title Expression of the Ebola Virus VP24 Protein Compromises the Integrity of the Nuclear Envelope and Induces a Laminopathy-Like Cellular Phenotype
Author/Editor American Society for Microbiology.
Date 01/01/2010
Language English
Country United States of America
Rightsholder American Society for Microbiology - Journals
Publication Type e-Journal
Issue 4
Volume 12
URL https://journals.asm.org/journal/mbio

REQUEST DETAILS

Portion Type Chapter/article
Page range(s) 1-25
Total number of pages 25
Format (select all that apply) Print, Electronic
Who will republish the content? Author of requested content
Duration of Use Life of current edition
Lifetime Unit Quantity Up to 499

Rights Requested Main product
Distribution Worldwide
Translation Original language of publication
Copies for the disabled? No
Minor editing privileges? No
Incidental promotional use? No
Currency EUR

NEW WORK DETAILS

Title Contribution of SUMO to the replication of Ebola virus
Instructor name M. Carmen Rivas Vázquez
Institution name Universidade de Santiago de Compostela
Expected presentation date 2021-10-15

ADDITIONAL DETAILS

Order reference number N/A
The requesting person / organization to appear on the license Santiago Vidal Freire, Universidade de Santiago de Compostela

REUSE CONTENT DETAILS

Title, description or numeric reference of the portion(s) Expression of the Ebola Virus VP24 Protein Compromises the Integrity of the Nuclear Envelope and Induces a Laminopathy-Like Cellular Phenotype
Editor of portion(s) Vidal, Santiago
Volume of serial or monograph 12
Page or page range of portion 1-25
Title of the article/chapter the portion is from Expression of the Ebola Virus VP24 Protein Compromises the Integrity of the Nuclear Envelope and Induces a Laminopathy-Like Cellular Phenotype
Author of portion(s) Vidal, Santiago
Issue, if republishing an article from a serial 4
Publication date of portion 2021-08-31

AMERICAN SOCIETY FOR MICROBIOLOGY | Journal of Virology®

VIRUS-CELL INTERACTIONS

Regulation of the Ebola Virus VP24 Protein by SUMO

Santiago Vidal,[a,b] Ahmed El Motiam,[a,b] Rocío Seoane,[a,b] Viktorija Preitakaite,[a] Yanis Hichem Bouzaher,[a,b] Sergio Gómez-Medina,[c,d] Carmen San Martín,[e] Dolores Rodríguez,[f] María Teresa Rejas,[g] Maite Baz-Martínez,[a,b,c] Rosa Barrio,[h] James D. Sutherland,[h] Manuel S. Rodríguez,[i,j] César Muñoz-Fontela,[c,d] Carmen Rivas[a,b,f]

[a]Centro de Investigación en Medicina Molecular (CIMUS), Universidade de Santiago de Compostela, Santiago de Compostela, Spain
[b]Instituto de Investigaciones Sanitarias (IDIS), Santiago de Compostela, Spain
[c]Berhard Nocht Institute for Tropical Medicine, Hamburg, Germany
[d]German Center for Infection Research (DZIF), Partner Site Hamburg, Hamburg, Germany
[e]Departamento de Estructura de Macromoléculas, Centro Nacional de Biotecnología-CSIC, Madrid, Spain
[f]Departamento de Biología Molecular y Celular, Centro Nacional de Biotecnología-CSIC, Madrid, Spain
[g]Centro de Biología Molecular Severo Ochoa (CSIC-UAM), Universidad Autónoma de Madrid, Madrid, Spain
[h]CIC bioGUNE, Derio, Spain
[i]Advanced Technology Institute in Life Sciences (ITAV) CNRS-USR3505, Toulouse, France
[j]IPBS-University of Toulouse III-Paul Sabatier, Toulouse, France

ABSTRACT Some viruses take advantage of conjugation of ubiquitin or ubiquitin-like proteins to enhance their own replication. One example is Ebola virus, which has evolved strategies to utilize these modification pathways to regulate the viral proteins VP40 and VP35 and to counteract the host defenses. Here, we show a novel mechanism by which Ebola virus exploits the ubiquitin and SUMO pathways. Our data reveal that minor matrix protein VP24 of Ebola virus is a bona fide SUMO target. Analysis of a SUMOylation-defective VP24 mutant revealed a reduced ability to block the type I interferon (IFN) pathway and to inhibit IFN-mediated STAT1 nuclear translocation, exhibiting a weaker interaction with karyopherin 5 and significantly diminished stability. Using glutathione *S*-transferase (GST) pulldown assay, we found that VP24 also interacts with SUMO in a noncovalent manner through a SIM domain. Mutation of the SIM domain in VP24 resulted in a complete inability of the protein to downmodulate the IFN pathway and in the monoubiquitination of the protein. We identified SUMO deubiquitinating enzyme ubiquitin-specific-processing protease 7 (USP7) as an interactor and a negative modulator of VP24 ubiquitination. Finally, we show that mutation of one ubiquitination site in VP24 potentiates the IFN modulatory activity of the viral protein and its ability to block IFN-mediated STAT1 nuclear translocation, pointing to the ubiquitination of VP24 as a negative modulator of the VP24 activity. Altogether, these results indicate that SUMO interacts with VP24 and promotes its USP7-mediated deubiquitination, playing a key role in the interference with the innate immune response mediated by the viral protein.

IMPORTANCE The Ebola virus VP24 protein plays a critical role in escape of the virus from the host innate immune response. Therefore, deciphering the molecular mechanisms modulating VP24 activity may be useful to identify potential targets amenable to therapeutics. Here, we identify the cellular proteins USP7, SUMO, and ubiquitin as novel interactors and regulators of VP24. These interactions may represent novel potential targets to design new antivirals with the ability to modulate Ebola virus replication.

KEYWORDS SUMO, USP7, VP24, Ebola virus, ubiquitin

Ebola virus (species *Zaire ebolavirus*; EBOV) is a highly pathogenic agent causing hemorrhagic fever with a high case fatality rate in humans. One of the mechanisms that contribute to the pathogenesis of the virus is the inhibition of signaling cascades

Citation Vidal S, El Motiam A, Seoane R, Preitakaite V, Bouzaher YH, Gómez-Medina S, San Martín C, Rodríguez D, Rejas MT, Baz-Martínez M, Barrio R, Sutherland JD, Rodríguez MS, Muñoz-Fontela C, Rivas C. 2020. Regulation of the Ebola virus VP24 protein by SUMO. J Virol 94:e01687-19. https://doi.org/10.1128/JVI.01687-19.

Editor Susana López, Instituto de Biotecnologia/UNAM

Address correspondence to Carmen Rivas, mcarmen.rivas@usc.es.

Received 1 October 2019
Accepted 2 October 2019
Accepted manuscript posted online 9 October 2019
Published 12 December 2019

of the interferon (IFN) system by EBOV protein VP24. The minor matrix VP24 protein has been reported to exert its inhibitory activity by competing with tyrosine-phosphorylated STAT1 for interaction with the importins alpha karyopherin 1 (KPNA1), KPNA5, and KPNA6, inhibiting the import of phosphorylated STAT1 into the nucleus (1–3). So far, whether the IFN-signaling modulatory activity of VP24 can be regulated at the posttranslational level has not been investigated. Identification of molecular mechanisms controlling the antagonistic activity of VP24 may be useful to identify potential targets amenable to therapeutics.

Posttranslational modifications by ubiquitin and ubiquitin-like proteins play a key role in the regulation of protein-protein interactions, being essential in the control of multiple processes (4). SUMOylation consists in the covalent attachment of the small ubiquitin-like modifier (SUMO) to a lysine residue in the target protein by an enzymatic process that requires an E1 activating enzyme, a ubiquitin E2 conjugating enzyme (Ubc9), and a SUMO E3 ligase (5). This modification may promote or inhibit binding to other proteins. Importantly, many SUMOylated proteins also contain SUMO-interacting motifs (SIM) that mediate the noncovalent interaction between the target protein and SUMO or SUMOylated proteins (6). In addition, ubiquitin, through its numerous connections with SUMO, may alter the properties of the SUMO substrate (7). Many viruses have developed strategies to manipulate these modification pathways to favor virus replication either by modulating global or specific cellular protein modifications or by exploiting the modification machinery of the cell to regulate their own proteins (8, 9). One example is EBOV, which can exploit the SUMOylation machinery of the cell using both strategies. The EBOV VP35 protein induces SUMOylation of IRF7 and therefore inhibits the production of type I interferon (IFN) (10), and the EBOV major matrix VP40 protein is modified by SUMO, which contributes to its stability (11). Furthermore, EBOV can also exploit the ubiquitination pathway. Thus, promotion of EBOV replication by conjugation of VP35 or VP40 proteins to ubiquitin has been reported previously (12, 13).

Here, we identify a novel mechanism by which EBOV exploits both the ubiquitin and the SUMO pathways. Our data demonstrate that VP24 can interact with SUMO in both covalent and noncovalent manners. Inhibition of the covalent and noncovalent interactions between VP24 and SUMO modulated the ability of the protein to interact with karyopherin 5 (KPNA5) and to inhibit the IFN-mediated STAT1 nuclear translocation and diminished and totally blocked, respectively, the ability of the viral protein to inhibit the IFN signaling. In addition, inhibition of the noncovalent VP24-SUMO interaction promoted the monoubiquitination of the viral protein, a modification regulated through its interaction with the SUMO deubiquitinase ubiquitin-specific-processing protease 7 (USP7). Interestingly, mutation of a ubiquitination site in VP24 potentiated the IFN downmodulation activity of the viral protein. In summary, we have identified a novel mechanism by which EBOV exploits the SUMOylation machinery of the cell and demonstrate that this strategy contributes to viral control of the immune response.

RESULTS

EBOV VP24 is modified by SUMO. We wondered whether VP24 protein could be modified by SUMO. To evaluate whether EBOV VP24 was modified *in vitro*, we carried out an *in vitro* SUMOylation assay with ^{35}S-methionine-labeled *in vitro*-translated VP24 in the presence of SUMO1 or SUMO2. The molecular weight of the *in vitro*-translated VP24 was around 28 kDa, as expected (14) (Fig. 1a). Incubation with SUMO1 induced the appearance of a double band of around 40 kDa (Fig. 1a), indicating that VP24 can be SUMOylated by SUMO1 *in vitro* and suggesting that the VP24-SUMO1 protein may be additionally modified (Fig. 1a). A band of around 40 kDa was detected also after incubation of the protein with SUMO2 (Fig. 1a), indicating that VP24 can be modified by SUMO2 *in vitro*. To prove that the 40-kDa band corresponds to SUMOylated VP24 protein, the VP24-SUMO1 and VP24-SUMO2 proteins were incubated with the SUMO-specific protease SENP1. The 40-kDa-molecular-weight bands disappeared after incubation with SENP1, demonstrating that EBOV VP24 protein is modified by SUMO1 and SUMO2 *in vitro* (Fig. 1b). To confirm that the protein can be modified also in living cells,

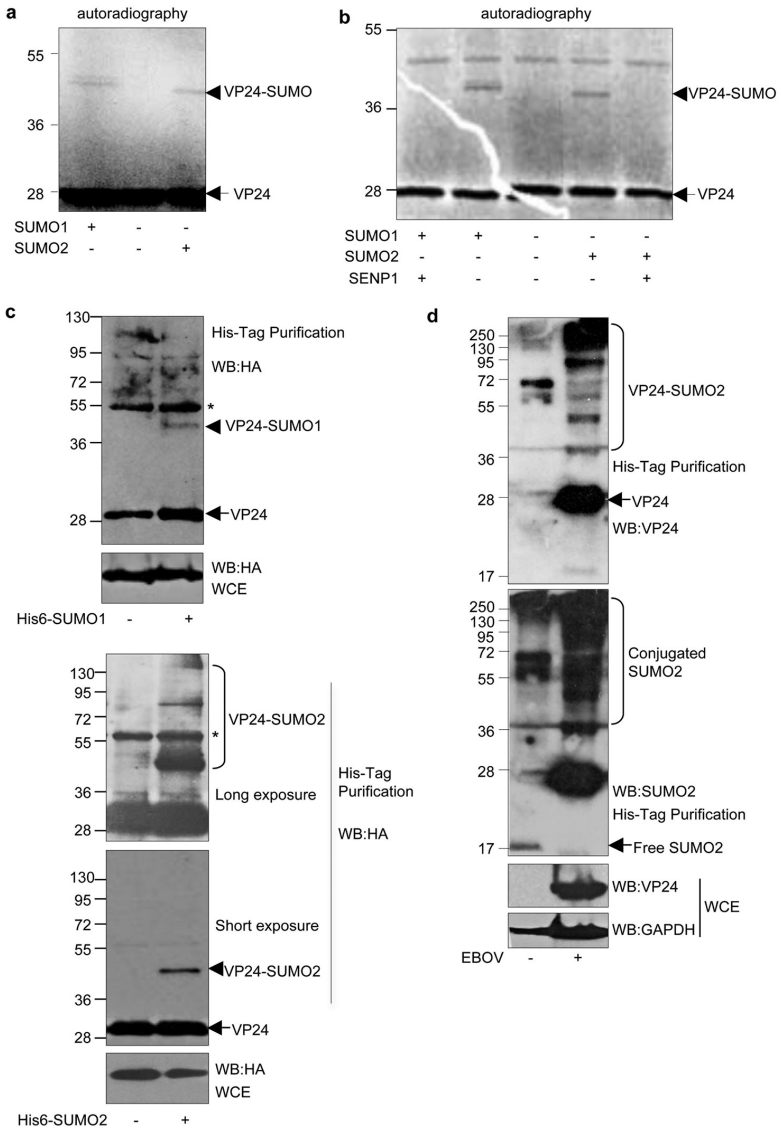

FIG 1 EBOV VP24 protein is modified by SUMO. (a) *In vitro* SUMOylation assay in the presence of SUMO1 or SUMO2 using ^{35}S-methionine-labeled *in vitro*-translated VP24 protein. (b) SUMO1-VP24 or SUMO2-modified VP24 proteins were incubated with SENP1. (c) HEK-293 cells were transfected with HA-VP24 in combination with either pcDNA, Ubc9 and His6-SUMO1-expressing plasmids (upper panel) or His6-SUMO2-expressing plasmids (lower panel), and 36 h after transfection, whole-protein extracts and histidine-tagged purified proteins were analyzed by Western blotting with anti-HA antibody. The asterisk indicates an unspecific band. (d) HeLa cells stably expressing His6-SUMO2 were infected with Ebola virus or left uninfected. At 5 days after infection, whole-protein extracts or histidine-tagged purified proteins were then analyzed by Western blotting (WB) with the indicated antibodies. WCE, whole-cell extracts.

we transfected HEK-293 cells with hemagglutinin-VP24 (HA-VP24) in combination either with pcDNA-, Ubc9-, and His6-SUMO1-expressing plasmids or with Ubc9- and His6-SUMO2-expressing plasmids and, at 36 h after transfection, whole-protein extracts and histidine-tagged proteins purified under denaturing conditions using nickel col-

umns were analyzed by Western blotting with anti-HA antibody. As shown in Fig. 1c, analysis of the purified proteins revealed a 40-kDa band exclusively in those cells transfected with His6-SUMO1 (upper panel) or His6-SUMO2 (lower panel). Also, additional higher-molecular-weight bands corresponding to VP24 protein conjugated to SUMO2 chains were observed in the His6-SUMO2-transfected cells (Fig. 1c, lower panel). These results indicated that VP24 protein is modified by SUMO1 and SUMO2 in transfected cells. Finally, we decided to evaluate whether VP24 protein is SUMOylated in cells infected with authentic EBOV. HeLa cells stably expressing His6-SUMO2 were infected with EBOV, and at 5 days after infection, the histidine-tagged proteins were purified under denaturing conditions. Western blot analysis of the purified proteins by the use of anti-VP24 antibody revealed the appearance of multiple bands corresponding to VP24-SUMO2 protein, indicating that VP24 is modified in infected cells (Fig. 1d). Interestingly, subsequent incubation with anti-SUMO2 antibody also revealed that EBOV infection triggers an increase in the levels of SUMOylated proteins whereas the level of unconjugated SUMO2 protein decreases (Fig. 1d). Altogether, these results indicate that the VP24 protein was modified by SUMO1 and SUMO2 *in vitro* and *in vivo*.

Mutation of the SUMOylation site in VP24 slightly reduces its stability and its ability to both block IFN-I signaling and interact with KPNA5. *In silico* analysis of the VP24 amino acid sequence using the SUMOsp2.0 program revealed lysine residue K142 to be the most probable residue involved in SUMO conjugation and K14 as the second most probable SUMO conjugation site in VP24. We then generated single mutants in lysine K14 (VP24-K14R) or K142 (VP24-K142R) or the double mutant VP24-K14RK142R, and then we carried out an *in vitro* SUMOylation assay with ^{35}S-methionine-labeled *in vitro*-translated VP24 wild-type (VP24-WT), VP24-K14R, VP24-K142R, or VP24-K14RK142R proteins in the presence of SUMO1. We did not observe a reduction in the level of *in vitro* SUMOylation of the VP24-K142R mutant in comparison with the WT protein (Fig. 2a). However, we observed a reduction in the SUMOylation of the K14R or K14RK142R VP24 mutants, indicating that lysine residue K14 is involved in SUMO conjugation. To confirm this result, we then evaluated the relevance of these residues for the SUMOylation of VP24 *in vivo*. We cotransfected HEK-293 cells with HA-VP24-WT or the indicated mutants together with pcDNA or Ubc9 and His6-SUMO2, and 36 h after transfection, whole-protein extracts and histidine-tagged proteins purified under denaturing conditions using nickel columns were analyzed by Western blotting with anti-HA antibody. We observed a clear reduction in the SUMOylation of both the VP24-K14R and VP24-K14RK142R mutants relative to the WT protein (Fig. 2b), indicating that lysine residue K14 in VP24 is indeed involved in SUMO conjugation.

One of the main functions of VP24 is to inhibit IFN-I signaling (2). Therefore, we decided to evaluate whether mutation of the SUMOylation site in VP24 would alter the ability of the viral protein to inhibit IFN-I signaling. We cotransfected HEK-293 cells with ISG54-luc together with beta-galactosidase and pcDNA, HA-VP24-WT, or HA-VP24-K14R, as indicated, and 24 h after transfection, cells were treated with IFN-α for 16 h. Cell extracts were then harvested and assayed for luciferase and beta-galactosidase activity. We observed that IFN induced transactivation of the reporter, as expected, and that VP24-WT significantly abolished this transactivation, as previously reported (Fig. 2c, upper panel) (2). The luciferase levels observed in cells transfected with the VP24-K14R mutant were significantly lower than the levels detected in pcDNA-transfected cells but significantly higher than the levels observed in the VP24-WT-transfected cells (Fig. 2c, upper panel), suggesting that conjugation of SUMO to lysine K14 in VP24 contributes to the inhibition of IFN signaling by the viral protein. Evaluation of the ability of the protein to inhibit IFN-I signaling was also carried out in Vero cells. We cotransfected Vero cells with ISG54-luc together with beta-galactosidase and pcDNA, HA-VP24-WT, HA-VP24-K14R, HA-VP24-K142R, or HA-VP24-K14RK142R, and 24 h after transfection, cells were treated with IFN-α for 16 h. Cells were then harvested, and extracts were assessed for luciferase and beta-galactosidase activity. We observed that IFN induced transactivation of the reporter and that VP24-WT significantly abolished this transactivation, as expected (Fig. 2c, lower panel). We did not detect significant differences in

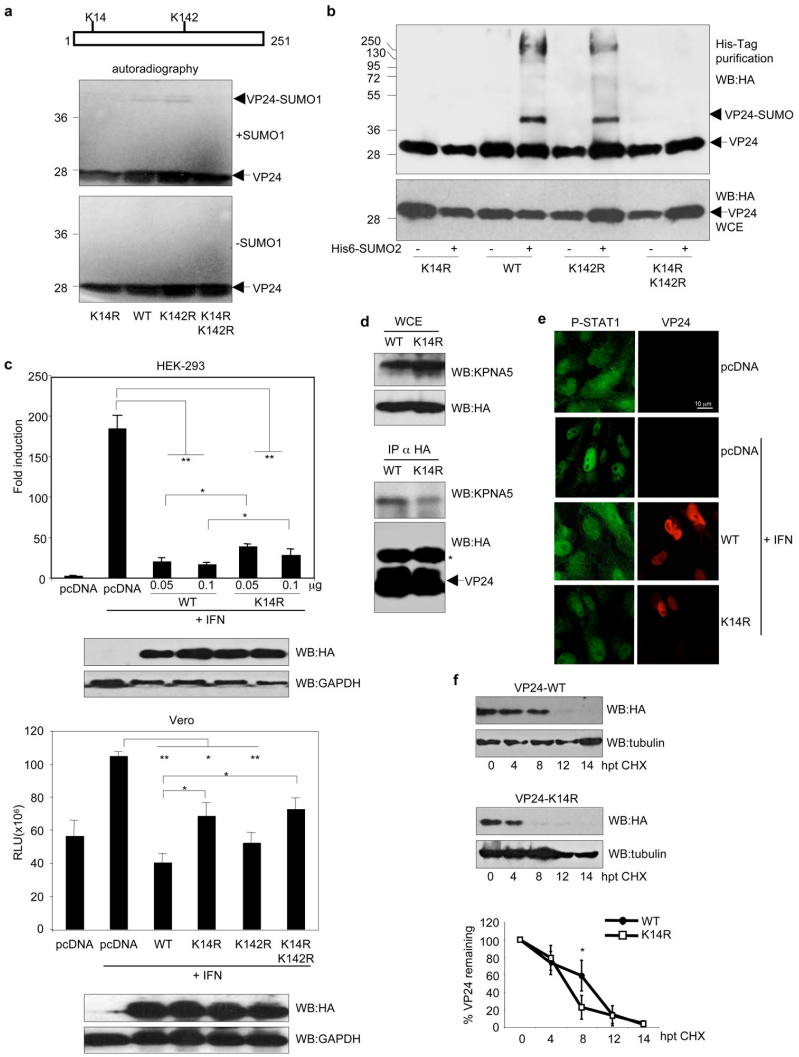

FIG 2 Mutation of the SUMOylation site in VP24 slightly reduces its stability and its ability to block interferon. (a) *In vitro* SUMOylation assay performed with SUMO1 using ^{35}S-methionine-labeled *in vitro*-translated VP24-WT, VP24-K14R, VP24-K142R or VP24-K14RK142R proteins. (b) HEK-293 cells were transfected with a plasmid encoding HA-tagged VP24-WT, VP24-K14R, VP24-K142R, or VP24-K14RK142R together with pcDNA or with Ubc9 and His6-SUMO2, and 36 h after transfection, whole-protein extracts and histidine-tagged purified proteins were analyzed by Western blotting with anti-HA antibody. (c) HEK-293 cells (upper panel) were cotransfected with the luciferase reporter ISG54-luc and the pcDNA-beta-galactosidase plasmids together with the indicated doses of HA-VP24-WT or HA-VP24-K14R. Cells were treated with IFN-α 24 h after transfection, and luciferase production was analyzed 16 h after treatment. Columns are representative of means of results, and error bars represent standard deviations of results from three biological replicates. Similar results were obtained at least twice. Statistical significance was assessed by a Student's *t* test. Cell lysates from the experiment were analyzed by Western blotting for HA-VP24 expression (bottom panel). Vero cells (lower panel) were cotransfected with the luciferase reporter ISG54-luc and the pcDNA-beta-galactosidase plasmids together with the indicated plasmids. Cells were treated with IFN-α 24 h after transfection, and luciferase production was analyzed 16 h after treatment. Columns are representative of means of results, and error bars represent standard deviations of results from three biological replicates. Statistical significance was assessed by a Student's *t* test. Cell lysates from the experiment were analyzed by Western blotting for HA-VP24 expression (lower panel). (d) HEK-293 cells were transfected with HA-VP24 WT or HA-VP24-K14R, and 36 h after transfection, immunoprecipitations (IP) were performed with anti-HA antibody, and the precipitated proteins were analyzed by Western blotting with anti-HA or anti-KPNA5 antibodies, as indicated.

(Continued on next page)

the abilities of VP24-K142R and VP24-WT to inhibit the transactivation of the reporter (Fig. 2c, lower panel). We also observed that VP24-K14R inhibited ISG54 reporter activity but that this reduction was significantly lower than that caused by the WT protein (Fig. 2c, lower panel). In addition, we observed that VP24-K14RK142R was unable to block the IFN pathway (Fig. 2c, lower panel). These results suggest that conjugation of SUMO to lysine K14 in VP24 contributes to the inhibition of IFN signaling by the viral protein.

Inhibition of the IFN activity by VP24 has been reported to be mediated, at least partially, by its binding to karyopherin alpha 1, 5, and 6 (2, 3, 15). Therefore, we decided to evaluate the binding between VP24-K14R and karyopherin. HEK-293 cells were transfected with HA-VP24-WT or HA-VP24-K14R expression plasmids. At 36 h after transfection, immunoprecipitations (IP) were performed with anti-HA antibody, and the precipitated proteins were analyzed by Western blotting with anti-HA or anti-KPNA5 antibodies. As shown in Fig. 2d, the levels of KPNA5 coimmunoprecipitating with HA-VP24-K14R were lower than the levels of KPNA5 protein interacting with VP24-WT, indicating that lysine residue K14R contributes to the VP24-KPNA5 interaction.

Interaction of VP24 with karyopherin blocks the nuclear accumulation of phosphorylated STAT1 in response to interferon treatment (2). We therefore carried out immunofluorescence analysis of phosphorylated STAT1 in Vero cells expressing VP24-WT or VP24-K14R protein after treatment with IFN. Treatment with IFN of cells transfected with an empty vector (pcDNA) induced the translocation of STAT1 to the nucleus in 88% of the cells ($n = 69$), whereas only 4% of the cells expressing VP24-WT ($n = 72$) exhibited nuclear STAT1 protein (Fig. 2e). This percentage increased to 36% in cells expressing VP24-K14R ($n = 79$) (Fig. 2e). These observations suggest that the covalent interaction of VP24 with SUMO has a positive impact on the ability of VP24 to block STAT1 nuclear accumulation in response to IFN treatment.

Interaction of EBOV VP24 protein with karyopherin has also been reported to increase the stability of the viral protein (16). We thus decided to evaluate the stability of the VP24-K14R mutant. HEK-293 cells transfected with WT or K14R mutant VP24 proteins were treated with cycloheximide, and at different times after treatment, HA-VP24 protein was analyzed by Western blotting using anti-HA antibody, and levels were quantified and plotted. As shown in Fig. 2f, the stability of VP24-K14R was significantly reduced compared with the stability of the VP24-WT protein, suggesting that conjugation of SUMO to lysine residue K14 in VP24 contributes to its stability.

The SIM domain in VP24 mediates its noncovalent interaction with SUMO and is essential for the control of IFN activity by the viral protein. Many SUMOylated proteins can interact with SUMO in a noncovalent manner through a SUMO-interacting motif (SIM), which has been reported to consist of a hydrophobic core with the consensus sequence V/I/L-X-V/I/L-V/I/L or V/I/L-V/I/L-X-V/I/L (17). *In silico* analysis of EBOV VP24 using the SUMOsp2.0 program revealed the presence of 5 putative SIM domains in VP24. We then generated single mutants of VP24 in the different putative SIM domains and carried out a glutathione *S*-transferase (GST) pulldown assay using ^{35}S-methionine-labeled *in vitro*-translated VP24 proteins and GST-SUMO1. As shown in Fig. 3a, we observed that VP24-WT interacted with SUMO1 in a noncovalent manner. Similarly, we observed interactions of VP24-94LRVI97-94ARAA97, VP24-119LGLI122-119AGAA122, VP24-150LSLI153-150ASAA153, and VP24-167LHVV170-167AHAA170

FIG 2 Legend (Continued)

The asterisk indicates the immunoglobulin. (e) Vero cells were transfected with the indicated plasmids, and 24 h after transfection, cells were serum starved for 4 h and then treated with 1,000 U/ml of human IFN-alpha for 30 min or left untreated. Cells were then fixed and immunostained using primary goat anti-HA and mouse anti-phosphorylated STAT1 (P-STAT1) antibodies and secondary Alexa 488 chicken anti-mouse and Alexa 594 donkey anti-goat antibodies. (f) HEK-293 cells were transfected with HA-VP24-WT or HA-VP24-K14R, and 24 h after transfection, cells were treated with cycloheximide (CHX). At the indicated hours after CHX treatment, protein extracts were analyzed by Western blotting with anti-HA antibody. VP24 protein intensity bands were quantified using ImageJ software. VP24 band intensity was normalized to tubulin from each respective time point and plotted. Data represent means and error bars of results from 3 independent experiments and 2 biological replicas. Statistical analysis was assessed by a Student's *t* test.

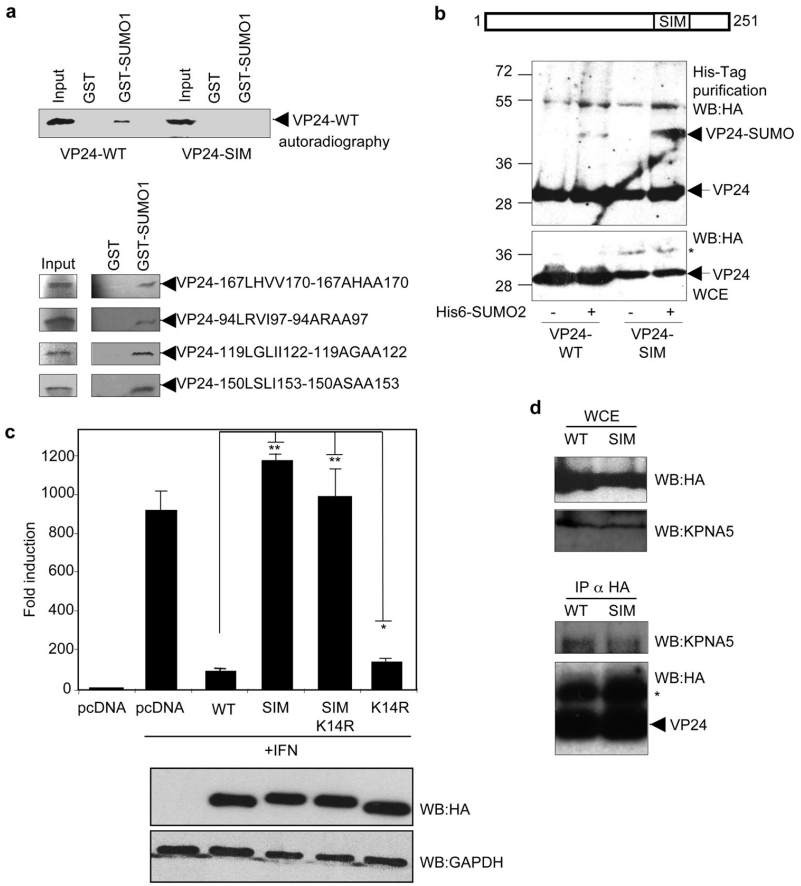

FIG 3 VP24 protein interacts with SUMO in a noncovalent manner, and this interaction is required for the control of IFN activity by the viral protein. (a) GST pulldown assay using ^{35}S-methionine-labeled *in vitro*-translated VP24-WT or the indicated VP24 mutants and GST or GST-SUMO1. (b) HEK-293 cells were transfected with a plasmid encoding HA-VP24-WT or HA-VP24-SIM together with pcDNA or Ubc9 and His6-SUMO2, and 36 h after transfection, whole-protein extracts and histidine-tagged purified proteins were analyzed by Western blotting with anti-HA antibody. The asterisk indicates a band of around 10-kDa-higher molecular weight than VP24 detected in the cells transfected with VP24-SIM. (c) HEK293 cells were cotransfected with the luciferase reporter ISG54-luc together with pcDNA, HA-VP24-WT, or the indicated mutants. Cells were treated with IFN-α 24 h after transfection, and luciferase production was analyzed 16 h after treatment. Columns are representative of means of results, and error bars represent standard deviations of results from three biological replicates. Similar results were obtained at least twice. Statistical significance was assessed by a Student's *t* test. Cell lysates from the experiment were analyzed by Western blotting for HA-VP24 expression (lower panel). (d) HEK-293 cells were transfected with HA-VP24 WT or HA-VP24-SIM, and 36 h after transfection, immunoprecipitations (IP) were performed with anti-HA antibody, and the precipitated proteins were analyzed by Western blotting with anti-HA or anti-KPNA5 antibodies, as indicated. The asterisk indicates the immunoglobulin.

mutants with GST-SUMO1 (Fig. 3a). However, we detected a clear reduction in the level of the interaction between VP24-198LVEL201-198AAEA201 (VP24-SIM) and GST-SUMO1 (Fig. 3a), indicating that the 198LVEL201 SIM domain is involved in noncovalent conjugation of VP24 with SUMO1.

The presence of a SIM motif in the SUMOylation substrate can contribute to its conjugation to SUMO. We then decided to evaluate whether mutation of the SIM domain in VP24 inhibited its SUMO conjugation. HEK-293 cells were cotransfected with HA-VP24-WT or HA-VP24-SIM and with pcDNA or Ubc9 and His6-SUMO2, and 48 h after

transfection, whole-protein extracts and histidine-tagged purified proteins were analyzed by Western blotting with anti-HA antibody. As shown in Fig. 3b, we observed SUMOylation of the VP24-SIM protein, suggesting that conjugation of SUMO to VP24 did not require the SIM domain.

We then decided to evaluate whether the mutation of the SIM domain in VP24 had a role in the modulation of the IFN-signaling pathway by the viral protein. We cotransfected HEK-293 cells with ISG54-luc together with beta-galactosidase and pcDNA, HA-VP24-WT, HA-VP24-K14R, HA-VP24-SIM or the double mutant HA-VP24-SIMK14R, as indicated, and 24 h after transfection, cells were treated with IFN-α for 16 h. Cell extracts were then harvested and assayed for luciferase and beta-galactosidase activity. IFN treatment induced transactivation of the reporter, and statistically significant results showed that VP24-WT abolished this transactivation, as expected (Fig. 3c). The ability of a mutant of VP24 with a mutation in lysine residue K14 to block the IFN response was significantly reduced relative to the WT protein, as shown above (Fig. 3c). Interestingly, both VP24-SIM and VP24-SIMK14R proteins were totally unable to block the IFN pathway (Fig. 3c), indicating that the SIM motif in VP24 was essential for its IFN downmodulation activity.

We then evaluated the coimmunoprecipitation between VP24-SIM and KPNA5. As shown in Fig. 3d, the levels of KPNA5 that coimmunoprecipitated with HA-VP24-SIM were lower than the levels of KPNA5 protein interacting with VP24-WT protein, indicating that the SIM domain in VP24 contributes to the interaction with KPNA5.

Mutation of the SIM domain in VP24 inhibits its interaction with ubiquitin-specific-processing protease 7 (USP7) and promotes its monoubiquitination. Of note, Western blotting of the cells transfected with HA-VP24-SIM revealed the appearance of a band of the expected VP24-WT molecular weight, as well as an additional band of around 38 kDa (Fig. 3b; band marked by an asterisk). We wondered whether this 10-kDa-higher-molecular-weight band might correspond to monoubiquitin-modified VP24 protein. To evaluate the putative monoubiquitination of VP24-SIM, we first transfected HEK-293 cells with pcDNA or HA-VP24-SIM, and 24 h after transfection, VP24-SIM protein was immunoprecipitated using anti-HA antibody and analyzed by Western blotting using anti-ubiquitin antibody. As shown in Fig. 4a, the anti-ubiquitin antibody recognized a band of the expected 38-kDa molecular weight in the lane corresponding to the HA-VP24-SIM protein, identified also with the anti-HA antibody, indicating that mutation of the SIM domain in VP24 promoted its monoubiquitination. Therefore, we then decided to study the putative monoubiquitination of the WT protein. We first carried out an *in vitro* ubiquitination assay using ^{35}S-methionine-labeled *in vitro*-translated VP24-WT protein in the presence of recombinant ubiquitin protein in which all the lysine residues had been mutated to arginine (ubiquitin knockout [UbKO]). As shown in Fig. 4b (left panel), incubation of VP24 protein with UbKO led to the appearance of two additional bands of around 38 and 48 kDa, indicating that monoubiquitin could be conjugated to at least two lysine residues in VP24 *in vitro*. To determine whether VP24 protein could be monoubiquitinated also in cells, we transfected HEK-293 cells with HA-VP24-WT together with pcDNA or His6-UbKO. Analysis of the histidine-tagged purified proteins using anti-HA antibody revealed the appearance of two bands of around 38 and 48 kDa in the lane corresponding to His-UbKO-transfected cells (Fig. 4b, right panel), indicating that VP24 could be monoubiquitinated in cells. The results shown here suggested that inhibition of the SIM-mediated noncovalent interaction between VP24 and SUMO or SUMOylated proteins promoted the covalent interaction between VP24 and ubiquitin. Therefore, we decided to evaluate whether an increase in SUMO levels would negatively modulate the ubiquitination of VP24. HEK-293 cells were cotransfected with HA-VP24-WT together with pcDNA, His6-UbKO, and pcDNA, with SUMO2 and pcDNA, or with SUMO2 and His6-UbKO, and 48 h after transfection, whole-protein extracts and histidine-tagged purified proteins were analyzed by Western blotting with anti-HA antibody. Western blotting of the purified proteins revealed the appearance of bands corresponding to monoubiquitinated VP24 protein in cells transfected with His6-UbKO and

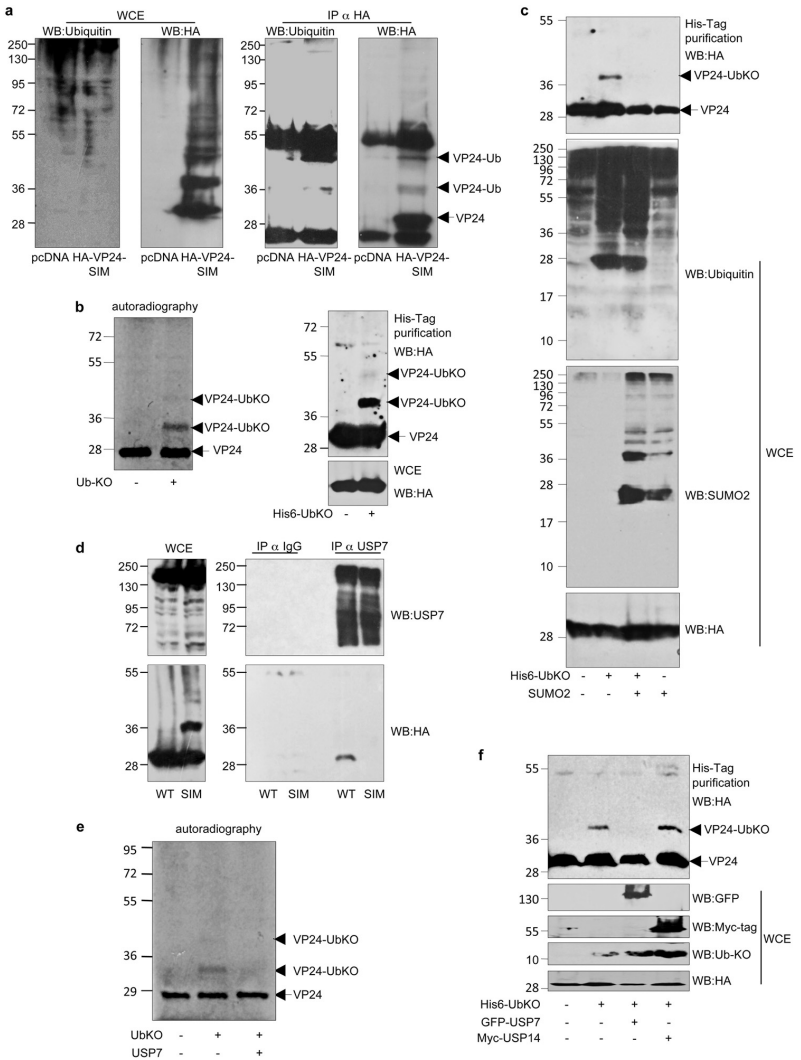

FIG 4 Mutation of the SIM domain in VP24 inhibits its interaction with the ubiquitin-specific-processing protease 7 (USP7) and promotes its monoubiquitination. (a) HEK-293 cells were transfected with pcDNA or HA-VP24-SIM, and 24 h after transfection, protein extracts of transfected cells were immunoprecipitated using anti-HA antibody. Immunoprecipitated proteins were analyzed using anti-ubiquitin antibody. (b) *In vitro* ubiquitination assay with UbKO using ^{35}S-methionine-labeled *in vitro*-translated VP24-WT protein (left panel). HEK-293 cells were cotransfected with VP24-WT and pcDNA or His6-ubiquitin KO. At 36 h after transfection, total cell extracts and histidine-purified proteins were analyzed by Western blotting using anti-HA antibody (right panel). (c) HEK-293 cells were cotransfected with VP24-WT and pcDNA, His6-ubiquitin KO and pcDNA, SUMO2 or SUMO2, and His6-ubiquitin KO, as indicated. At 36 h after transfection, total cell extracts and histidine-purified proteins were analyzed by Western blotting using anti-HA antibody. (d) HEK-293 cells were transfected with HA-VP24-WT or HA-VP24-SIM, and 24 h after transfection, protein extracts of transfected cells were immunoprecipitated using anti-USP7 antibody. Immunoprecipitated proteins were analyzed using anti-HA antibody. (e) Incubation of *in vitro*-ubiquitinated ^{35}S-methionine-labeled *in vitro*-translated VP24-WT protein with UbKO in presence or absence of recombinant USP7. (f) HEK-293 cells were cotransfected with VP24-WT and pcDNA, His6-ubiquitin KO, His6-ubiquitin KO and GFP-USP7, or His6-ubiquitin KO and Myc-USP14. At 36 h after transfection, total cell extracts and histidine-purified proteins were analyzed by Western blotting using anti-HA antibody.

pcDNA that were almost undetectable in cells cotransfected with His6-UbKO and SUMO2 (Fig. 4c). These findings suggested that SUMO2 had a negative impact on the monoubiquitination of VP24. One possible explanation for these results could be that mutation of the SIM domain in VP24 might disrupt the interaction between VP24 and a deubiquitinase enzyme. It has been recently demonstrated that ubiquitin-specific protease USP7 interacts with SUMOylated proteins, probably through a SIM domain, and reverses its ubiquitination (18). In addition, USP7 has been reported to be involved in virus-host interaction processes (19–22). Therefore, we decided to study the putative interaction between VP24-WT or VP24-SIM and USP7. Endogenous USP7 was immunoprecipitated from HEK-293 cells transfected with HA-VP24-WT or HA-VP24-SIM, and immunoprecipitated proteins were then analyzed by Western blotting using anti-HA antibody. As shown in Fig. 4d, VP24-WT protein interacted with USP7. However, we could not detect an interaction between VP24-SIM and USP7 (Fig. 4d). We then decided to evaluate the putative deubiquitination of VP24 by USP7. First, we evaluated the deubiquitination of *in vitro*-monoubiquitinated ^{35}S-methionine-labeled *in vitro*-translated VP24 protein incubated or not incubated with recombinant USP7. As shown in Fig. 4e, incubation with USP7 led to a reduction in the intensity of the VP24-UbKO band *in vitro*. To further evaluate this possibility, we cotransfected HEK-293 cells together with HA-VP24 and pcDNA, His6-UbKO and pcDNA, His6-UbKO and GFP-USP7, or His6-UbKO and Myc-USP14, and 48 h after transfection, whole-protein extracts and histidine-tagged purified proteins were analyzed by Western blotting with anti-HA antibody. The band corresponding to the monoubiquitinated VP24 protein detected in the lane transfected with His6-UbKO and pcDNA was almost undetectable in those cells cotransfected with His6-UbKO and GFP-USP7 (Fig. 4f). However, we did not observe any alteration in the intensity of the monoubiquitinated VP24 band in those cells expressing USP14 (Fig. 4f). Altogether, these results indicated that USP7 interacted with VP24 through the SIM domain and downmodulated the conjugation of ubiquitin to VP24.

Mutation of lysine residue K206 in VP24 potentiates its IFN-signaling inhibitory activity. Interestingly, *in silico* analysis of VP24 protein using the Ubpred program pointed to lysine residue K206 in VP24, just five amino acids away from the SIM domain, as the unique putative ubiquitin conjugation site in VP24. To determine whether lysine K206 had a role in the ubiquitination of VP24, lysine residue K206 in VP24-SIM was mutated to arginine followed by evaluation for the presence of the VP24-UbKO band in cells transfected with VP24-SIM or VP24-SIM-K206R by Western blotting. As shown in Fig. 5a (left panel), the intensity of the band corresponding to VP24 conjugated to ubiquitin was reduced in the SIM-K206R mutant relative to that of the band observed in the VP24-SIM-transfected cells, suggesting that K206 is one of the lysine residues involved in ubiquitin conjugation in VP24. To further evaluate this possibility, we generated a VP24 mutant in lysine residue K206 (VP24-K206R) and then evaluated its monoubiquitination in cells. We cotransfected HEK-293 cells with HA-VP24-WT or HA-VP24-K206R together with pcDNA or His6-UbKO, and 36 h after transfection, whole-protein extracts and histidine-tagged proteins purified under denaturing conditions using nickel columns were analyzed by Western blotting with anti-HA antibody. We observed a slight reduction in the monoubiquitination of VP24-K206R relative to the WT protein (Fig. 5a, right panel), suggesting that lysine residue K206 in VP24 is involved in ubiquitin conjugation. Finally, to determine whether ubiquitin conjugation had a role in the antagonistic activity of VP24, we evaluated the ability of the mutants of VP24 with mutations in lysine residue K206 to inhibit IFN signaling. We cotransfected HEK-293 or Vero cells with ISG54-luc together with beta-galactosidase and pcDNA, HA-VP24-WT, HA-VP24-K206R, HA-VP24-SIM, or HA-VP24-SIMK206R as indicated, and 24 h after transfection, cells were treated with IFN-α for 16 h. Cell extracts were then harvested and assayed for luciferase and beta-galactosidase activity. Interferon treatment induced transactivation of the reporter, and VP24-WT significantly abolished this transactivation (Fig. 5b). The VP24-SIM mutant was not able to inhibit the transactivation of the reporter, as shown above (Fig. 5b). Interestingly, the VP24-K206R mutant had a stronger inhibitory effect on IFN response than the WT protein (Fig. 5b), suggesting

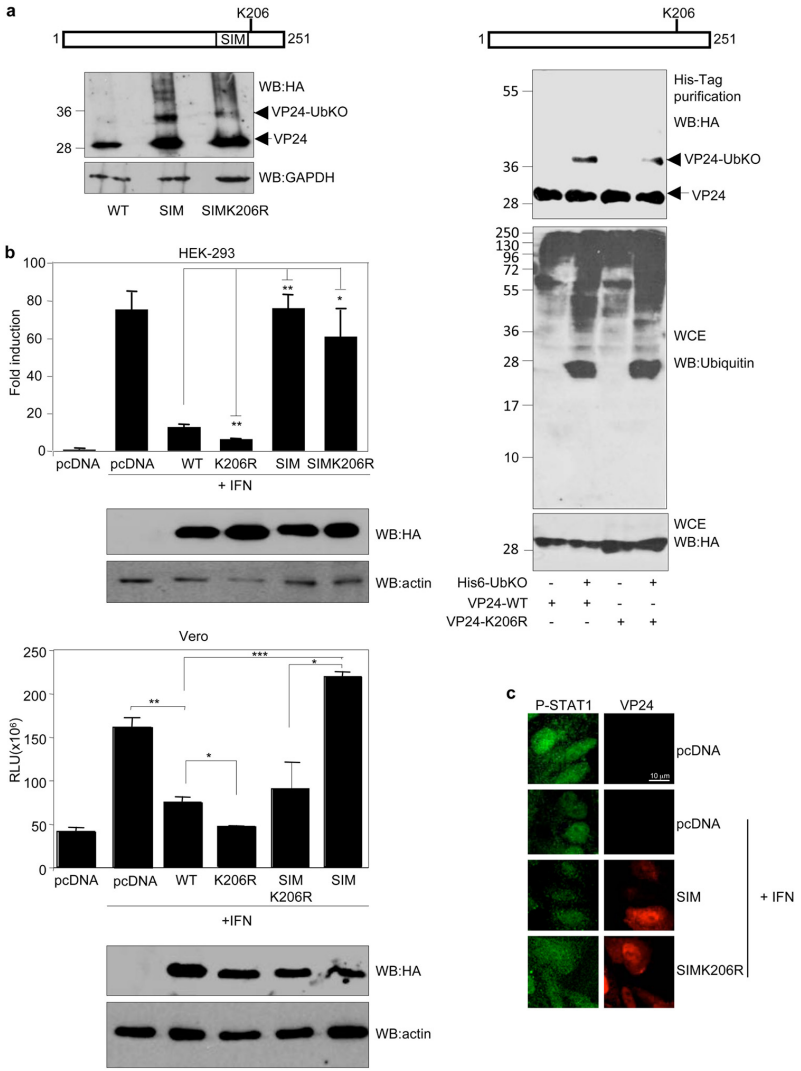

FIG 5 Mutation of lysine residue K206 in VP24 potentiates its IFN-signaling inhibitory activity. (a) HEK-293 cells were transfected with HA-VP24-SIM or HA-VP24-SIMK206R, and 24 h after transfection, protein extracts of transfected cells were analyzed using anti-HA antibody (left panel). HEK-293 cells were transfected with a plasmid encoding HA-VP24-WT or HA-VP24-K206R together with pcDNA or His6-UbKO and 36 h after transfection whole-protein extracts and histidine-tagged purified proteins were analyzed by Western blotting with anti-HA antibody (right panel). (b) HEK-293 cells (upper panels) or Vero cells (lower panels) were cotransfected with the luciferase reporter ISG54-luc together with pcDNA, HA-VP24-WT, or the indicated mutants. Cells were treated with IFN-β 24 h after transfection, and luciferase production was analyzed 16 h after treatment. Columns are representative of means of results, and error bars represent standard deviations of results from three biological replicates. Similar results were obtained at least twice. Statistical significance was assessed by a Student's *t* test. Cell lysates from the experiments were analyzed by Western blotting for HA-VP24 expression (lower panels). (c) Vero cells were transfected with the indicated plasmids, and 24 h after transfection, cells were serum starved for 4 h and then treated with 1,000 U/ml of human IFN-alpha for 30 min or left untreated. Cells were then fixed and immunostained using primary goat anti-HA and mouse anti-phosphorylated STAT1 antibodies and secondary Alexa 488 chicken anti-mouse and Alexa 594 donkey anti-goat antibodies.

that conjugation of ubiquitin to K206 in VP24 had a negative role on the IFN inhibitory activity of the viral protein. Immunofluorescence analysis of phosphorylated STAT1 supported this hypothesis. Among the cells expressing VP24-SIM, 90% ($n = 96$) were observed to have nuclear phosphorylated STAT1, and in those cells expressing VP24-SIMK206R, the percentage was lower (73%) ($n = 49$) (Fig. 5c). Taken together, these observations suggest that the interaction of VP24 with SUMO has a positive impact on the ability of VP24 to block STAT1 nuclear accumulation in response to IFN treatment whereas interaction with ubiquitin negatively modulates such activity.

DISCUSSION

Here, we show that EBOV exploits the SUMOylation machinery of infected cells to regulate the immune antagonistic function of the minor matrix protein VP24. Our results demonstrate that VP24 is modified by SUMO *in vitro* and *in vivo* in both transfected and EBOV-infected cells. In addition, the SUMOylation of VP24 in transfected cells indicates that its posttranslational modification does not require additional EBOV proteins. Moreover, the appearance of a unique double band in the *in vitro* SUMOylation assay with SUMO1 suggests that only one SUMO molecule is conjugated to VP24 at a time and that the SUMOylated protein may be additionally modified. *In silico* analysis of the putative SUMOylation sites pointed to lysine residue K14 as one of the lysine residues in VP24 involved in SUMO conjugation. One of the best well-known functions of VP24 is to inhibit the IFN activity (2). This immunomodulatory activity of VP24 has been reported to be mediated at least partially by the interaction with STAT1 (23) and with karyopherin, an interaction that also increases the stability of VP24 (2, 3, 15). We show that a mutant of VP24 in lysine residue K14 has a significantly reduced ability to interact with KPNA5 and to block the IFN activity, exhibits decreased stability, and shows a reduced capacity to inhibit IFN-induced nuclear translocation of phosphorylated STAT1. These results suggest that SUMOylation of VP24 at lysine residue K14 has a role in its interaction with karyopherin contributing to blocking the IFN signaling.

SUMOylated proteins frequently contain SUMO interaction domains (SIM) that allow the noncovalent interaction between the SUMO substrates and SUMO or SUMOylated proteins (6). Here, we show that VP24 also interacts with SUMO in a noncovalent manner and that mutation of the 198LVEL201 domain in VP24 reduces this interaction, indicating that the SIM domain located at positions 198 to 201 in VP24 has a role in the noncovalent interaction between SUMO and VP24. A SIM domain may have an impact on the SUMOylation, subcellular localization, stability, or activity of a protein (6). We did not observe an effect of the SIM domain in the SUMOylation of VP24. However, our data revealed that the SIM domain was essential for the IFN inhibitory activity of VP24, suggesting that the noncovalent interaction with SUMO is indispensable for the immunomodulatory activity of VP24. Although the SIM domain seems to contribute to the VP24-KPNA5 interaction, mutation of the SIM domain did not totally abolish the coimmunoprecipitation of VP24 and KPNA5, suggesting that the noncovalent interaction of SUMO with VP24 may be involved in additional functions of the viral protein. Interestingly, mutation of the SIM domain in VP24 also led to the appearance of a band that is 10 kDa higher than that corresponding to the VP24 protein that was identified as VP24-UbKO protein, suggesting that the interaction of SUMO or a SUMOylated protein with the SIM domain in VP24 negatively modulates the ubiquitination of VP24, a hypothesis that was also supported by the inhibition of VP24 ubiquitination in response to SUMO overexpression.

USP7 is a SUMO deubiquitinase that has been shown to interact with different viral proteins and to regulate the replication of some viruses (18–22). We then hypothesized that USP7 may be the ubiquitin protease that, by interacting with the SIM domain of VP24, induces its deubiquitination. Although, so far, USP7 has not been reported to be SUMOylated, recently, proteomic studies have pointed to USP7 as a putative SUMOylation substrate (24), reinforcing our hypothesis. Furthermore, coimmunoprecipitation studies revealed that VP24-WT protein but not a mutant with a mutation in the SIM domain can interact with USP7, demonstrating the involvement of the SIM domain in VP24-USP7

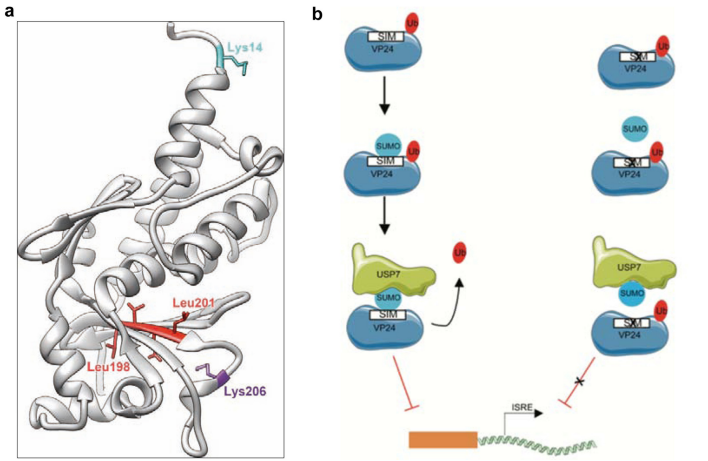

FIG 6 (a) Structure of VP24 (gray ribbon) with the key residues discussed in this work highlighted. The crystal structure of Zaire Ebolavirus VP24 (PDB ID 4m0q) (15) is depicted. Residues proposed to form a SIM domain are colored in red. The figure was composed using UCSF Chimera (30). (b) Proposed model to explain the regulatory role of ubiquitination and noncovalent SUMO interaction in the IFN-inhibitory activity of VP24.

interaction. Finally, we showed that USP7 decreases the levels of the monoubiquitinated VP24 protein *in vitro* and *in vivo*, supporting the idea of a newly recognized form of cooperative SUMO and ubiquitin signaling.

We show that a mutant of VP24 with a mutation in the SIM domain that did not interact with SUMO in a noncovalent manner but covalently interacted with ubiquitin was not able to inhibit IFN signaling, had weaker interaction with KPNA5 than with VP24-WT protein, and had lost its ability to block phosphorylated STAT1 nuclear translocation. Therefore, the noncovalent interaction with SUMO and/or the conjugation to ubiquitin may play a role in the IFN inhibitory activity of VP24. *In silico* analysis of VP24 pointed to the K206 lysine residue as one ubiquitin conjugation site in VP24. Mutation of this residue did not abolish the conjugation of VP24 to ubiquitin, likely due to the interaction of ubiquitin with additional lysine residues in VP24, as suggested by the two monoubiquitinated bands detected in the monoubiquitination assays. However, we detected a decrease in the levels of the monoubiquitinated protein, suggesting that K206, a lysine residue conserved in all species of the genus *Ebolavirus*, has a role in the ubiquitin conjugation. Interestingly, mutation of lysine residue K206 in VP24 significantly potentiated the IFN downmodulation activity of the viral protein, indicative of a negative impact of ubiquitin conjugation on the activity of VP24.

Location of the SUMOylation or ubiquitination sites in the VP24 structure reveals that both lysine residues are on the protein surface (Fig. 6a). Regarding the SIM domain (Fig. 6a), some of the residues that conform to it have been proposed to constitute part of a cavity in the Sudan EBOV VP24 structure (23). In addition, according to X-ray structures of Sudan EBOV VP24 and H/D exchange assays previously reported (23), the VP24 peptidic region adjacent to the SIM domain (residues 181 to 198) is probably involved in flexibility/conformational change under specific conditions. Therefore, we speculate that SUMO may interact with the SIM domain in VP24 through this cavity or in response to a conformational change in the SIM region.

In summary, these results identify SUMO and ubiquitin as positive and negative regulators of the ability of VP24 to inhibit the signaling cascades of the interferon system, respectively (Fig. 6b), and point to modulation of the VP24-SUMO and VP24-ubiquitin interactions as a novel strategy that may help in the design of new antivirals with the ability to modulate EBOV replication.

TABLE 1 Oligonucleotides used in VP24 protein mutagenesis

Name	Sequence
VP24-K14R-F	5′-CAATCTAATATCGCCCAGAAAGGACCTGGAGAAAG-3′
VP24-K14R-R	5′-CTTTCTCCAGGTCCTTTCTGGGCGATATTAGATTG-3′
VP24-K142R-F	5′-GCGAACACAACGTGTCAGGGAACAATTGAGCC-3′
VP24-K142R-R	5′-GGCTCAATTGTTCCCTGACACGTTGTGTTCGC-3′
VP24-LSLI-ASAA-F	5′-CAATTGAGCCTAAAAATGGCGTCGGCGGCTCGATCCAATATTCTC-3′
VP24-LSLI-ASAA-R	5′-GAGAATATTGGATCGAGCCGCCGACGCCATTTTTAGGCTCAATTG-3′
VP24-LGLI-AGAA-F	5′-CCCTTAGCAGGAGCCGCTGGTGCGGCCTCTGATTGGCTGCTAAC-3′
VP24-LGLI-AGAA-R	5′-GTTAGCAGCCAATCAGAGGCCGCACCAGCGGCTCCTGCTAAGGG-3′
VP24-LRVI-ARAA-F	5′-GAATCACCGCTGTGGGCAGCGAGAGCGGCCCTTGCAGCAGGGATAC-3′
VP24-LRVI-ARAA-R	5′-GTATCCCTGCTGCAAGGGCCGCTCTCGCTGCCCACAGCGGTGATTC-3′
VP24-LVEL-AAEA-F	5′-GAACTAACATGGGTTTTGCGGCGGAGGCCCAAGAACCCGACAA-3′
VP24-LVEL-AAEA-R	5′-TTGTCGGGTTCTTGGGCCTCCGCCGCAAAACCCATGTTAGTTC-3′
VP24-LHVV-AHAA-F	5′-AACAAATTGGATGCTGCACATGCCGCGAACTACAACGGATTG-3′
VP24-LHVV-AHAA-R	5′-CAATCCGTTGTAGTTCGCGGCATGTGCAGCATCCAATTTGTT-3′
VP24-K206R-F	5′-CTCCAAGAACCCGACAGATCGGCAATGAACCGC-3′
VP24-K206R-R	5′-GCGGTTCATTGCCGATCTGTCGGGTTCTTGGAG-3′
VP24-LVEL-K206R-F	5′-GCCCAAGAACCCGACAGATCGGCAATGAACCGC-3′
VP24-LVEL-K206R-R	5′-GCGGTTCATTGCCGATCTGTCGGGTTCTTGGGC-3′

MATERIALS AND METHODS

Cells and plasmids. HeLa cells stably expressing His6-SUMO2, HEK-293, and Vero cells were cultured in Dulbecco's modified Eagle's medium (DMEM) supplemented with 10% fetal bovine serum (FBS) and 1% penicillin/streptomycin. Transfection experiments were performed using polyethylenimine (PEI), according to the manufacturer's instructions.

The plasmid encoding HA-tagged VP24 (HA-VP24) was generated by subcloning of the VP24 coding cDNA into the pcMV5-HA plasmid. Site-directed mutagenesis was carried out using the primers listed in Table 1 and HA-VP24. All mutations were verified by sequencing. Expression plasmids pcDNA-His6-SUMO1, pcDNA-Hi6-SUMO2, pcDNA-Ubc9-SV5, and pcDNA-His6-UbKO have been previously reported (25–27).

***In vitro* transcription/translation.** The *in vitro* transcription/translation of proteins was performed by using 1 μg of plasmid DNA and a rabbit reticulocyte-coupled transcription/translation system following the instructions of the manufacturer (Promega).

Stability assay. HEK-293 cells were transfected with the indicated plasmids, and 24 h after transfection, cells were treated with cycloheximide (100 μg/ml). At different times after treatment, cells were analyzed by Western blotting with anti-HA antibody. Band intensities were measured using ImageJ software. VP24 band intensity was normalized to tubulin from each respective time.

***In vitro* SUMOylation assay.** *In vitro* SUMO conjugation assays were performed on ^{35}S-methionine-labeled *in vitro*-transcribed/translated proteins as described previously (28) using recombinant E1 (Biomol, Lausen, Switzerland), Ubc9, and SUMO1 or SUMO2.

***In vitro* deSUMOylation assay.** *In vitro* deSUMOylation assays with recombinant GST-SENP1 (Biomol) were performed on VP24-SUMO1 or VP24-SUMO2 as described previously (11).

Histidine purification. The purification of His-tagged conjugates using Ni^{2+}-nitrilotriacetic acid (NTA)-agarose beads was performed as described previously (11).

GST pulldown assay. Pulldown experiments were performed with GST-SUMO1 as described previously (29), using ^{35}S-methionine-labeled *in vitro*-transcribed/translated VP24 WT or mutant proteins.

Reporter assay. HEK-293 cells were cotransfected with ISG54-luc plasmid, the pcDNA-beta-galactosidase plasmid, and pcDNA, VP24-WT, or mutated VP24 expression plasmids. At 24 h after transfection, cells were treated with 1,500 U/ml human IFN-α for 16 h. Then, the cells were harvested and analyzed. Firefly luciferase values were normalized to beta-galactosidase values. Fold induction for each sample was then determined relative to the normalized luciferase activity value for untreated cells. Statistical significance was assessed using a Student's *t* test.

Western blotting and antibodies. For Western blotting, cells were washed in phosphate-buffered saline (PBS), resuspended in SDS-gel loading buffer, and boiled for 5 min. Proteins of total extracts were separated by SDS-PAGE and transferred to a nitrocellulose membrane. Monoclonal antibody against HA (901503) was purchased from BioLegend. Goat anti-HA (A190-138A) antibody was purchased from Bethyl Laboratories. Anti-tubulin (2146), anti-myc tag (2276S), and anti-SUMO2 (4971) antibodies were from Cell Signaling. Anti-GAPDH (anti-glyceraldehyde-3-phosphate dehydrogenase) (32233), anti-phosphorylated STAT1 (8394), and anti-ubiquitin (8017) antibodies were from Santa Cruz Biotechnology. Anti-VP24 antibody (362919) was from Biorbyt. Anti-GFP was from Abcam (1218) or from BioLegend (902601). Anti-USP7 antibody (A300-034A) was purchased from Bethyl Laboratories or from Sigma (PLA0009). Anti-KPNA5 antibody (PA529460) and Alexa 488 chicken anti-mouse antibody (A21200) were from Invitrogen. Alexa 594 donkey anti-goat antibody (ab150136) was from Abcam.

Immunofluorescence assay. Vero cells were transfected with the indicated plasmids, and 24 h after transfection, cells were serum starved for 4 h and then treated or not with 1,000 U/ml of human IFN-alpha for 30 min. Cells were then fixed and immunostained as previously described (11).

Infection. HeLa cells at 90% confluence were infected with EBOV (Ebola virus/*H. sapiens*-tc/COD/Yambuku-Mayinga) at a multiplicity of infection (MOI) of 1. All infection experiments were carried out by experienced personnel wearing positive-pressure protection suits at the biosafety level 4 (BSL4) laboratory of the Bernhard Nocht Institute for Tropical Medicine in Hamburg.

***In vitro* ubiquitylation assay.** ^{35}S-methionine-labeled *in vitro*-transcribed/translated VP24 were incubated in a 10-μl reaction mixture (50 mM Tris [pH 7.6], 5 mM $MgCl_2$, 2 mM ATP, 10 mM creatine phosphate, 3.5 U/ml of creatine kinase, 0.6 U/ml of inorganic pyrophosphatase), 10 ng human E1, 12 ng E2 (UbcH5), and 10 μg recombinant ubiquitin-KO in an apparatus that included an ATP regenerating system. After incubation at 37°C for 120 min, the reaction products were separated by SDS-PAGE and analyzed by autoradiography.

Immunoprecipitation assay. Cells were lysed in radioimmunoprecipitation assay (RIPA) or BC-100 buffer at 4°C, centrifuged at 15,800 $\times$ *g* for 10 min, and immunoprecipitated overnight at 4°C after addition of the specified antibody and 30 μl of 50% protein G-Sepharose (Life Technologies). Beads were then washed four times with lysis buffer and resuspended in 30 μl of loading buffer.

Data availability. The data sets generated during the present study are available from C. Rivas upon request.

ACKNOWLEDGMENTS

Funding at the laboratory of C.R. is provided by Ministry of Science, Innovation and Universities and FEDER (BFU-2017-88880-P). C.R. also acknowledges grants GRC GI-2119 (Xunta de Galicia) and SAF2017-90900-REDT (UBIRed Program). S.V. is a predoctoral fellow funded by Xunta de Galicia. M.B.-M. is a postdoctoral fellow funded by Xunta de Galicia (Consellería de Cultura, Educación e Ordenación Universitaria). A.E.M. is the recipient of a fellowship of the Spanish FPI program. This work was partially funded by the German Center for Infection Research (DZIF TTU 01.702_00 to C.M.-F.). R.B. and J.D.S. acknowledge grants BFU2017-84653-P (MINECO/FEDER, EU), SEV-2016-0644 (Severo Ochoa Excellence Program), 765445-EU (UbiCODE Program), and SAF2017-90900-REDT (UBIRed Program). C.S.M. acknowledges grant BFU2016-74868-P.

We declare that we have no competing financial interests.

S.V., A.E.M., R.S., V.P., S.G.-M., Y.H.B., D.R., M.T.R., and M.B.-M. conducted the experiments. S.V., C.M.-F., and C.R. designed the experiments. C.R. wrote the paper. S.V., C.S.M., M.S.R., R.B., D.R., J.D.S., and C.R. analyzed the data. D.R., M.S.R., R.B., J.D.S., C.S.M., and C.M.-F. provided critical revisions of the article.

REFERENCES

1. Mateo M, Reid SP, Leung LW, Basler CF, Volchkov VE. 2010. Ebolavirus VP24 binding to karyopherins is required for inhibition of interferon signaling. J Virol 84:1169–1175. https://doi.org/10.1128/JVI.01372-09.
2. Reid SP, Leung LW, Hartman AL, Martinez O, Shaw ML, Carbonnelle C, Volchkov VE, Nichol ST, Basler CF. 2006. Ebola virus VP24 binds karyopherin alpha1 and blocks STAT1 nuclear accumulation. J Virol 80:5156–5167. https://doi.org/10.1128/JVI.02349-05.
3. Reid SP, Valmas C, Martinez O, Sanchez FM, Basler CF. 2007. Ebola virus VP24 proteins inhibit the interaction of NPI-1 subfamily karyopherin alpha proteins with activated STAT1. J Virol 81:13469–13477. https://doi.org/10.1128/JVI.01097-07.
4. Hochstrasser M. 2009. Origin and function of ubiquitin-like proteins. Nature 458:422–429. https://doi.org/10.1038/nature07958.
5. Flotho A, Melchior F. 2013. Sumoylation: a regulatory protein modification in health and disease. Annu Rev Biochem 82:357–385. https://doi.org/10.1146/annurev-biochem-061909-093311.
6. Gareau JR, Reverter D, Lima CD. 2012. Determinants of small ubiquitin-like modifier 1 (SUMO1) protein specificity, E3 ligase, and SUMO-RanGAP1 binding activities of nucleoporin RanBP2. J Biol Chem 287:4740–4751. https://doi.org/10.1074/jbc.M111.321141.
7. Praefcke GJ, Hofmann K, Dohmen RJ. 2012. SUMO playing tag with ubiquitin. Trends Biochem Sci 37:23–31. https://doi.org/10.1016/j.tibs.2011.09.002.
8. Calistri A, Munegato D, Carli I, Parolin C, Palu G. 2014. The ubiquitin-conjugating system: multiple roles in viral replication and infection. Cells 3:386–417. https://doi.org/10.3390/cells3020386.
9. Lowrey AJ, Cramblet W, Bentz GL. 2017. Viral manipulation of the cellular sumoylation machinery. Cell Commun Signal 15:27. https://doi.org/10.1186/s12964-017-0183-0.
10. Chang TH, Kubota T, Matsuoka M, Jones S, Bradfute SB, Bray M, Ozato K. 2009. Ebola Zaire virus blocks type I interferon production by exploiting the host SUMO modification machinery. PLoS Pathog 5:e1000493. https://doi.org/10.1371/journal.ppat.1000493.
11. Baz-Martínez M, El Motiam A, Ruibal P, Condezo GN, de la Cruz-Herrera CF, Lang V, Collado M, San Martín C, Rodríguez MS, Muñoz-Fontela C, Rivas C. 2016. Regulation of Ebola virus VP40 matrix protein by SUMO. Sci Rep 6:37258. https://doi.org/10.1038/srep37258.
12. Bharaj P, Atkins C, Luthra P, Giraldo MI, Dawes BE, Miorin L, Johnson JR, Krogan NJ, Basler CF, Freiberg AN, Rajsbaum R. 24 August 2017, posting date. The host E3-ubiquitin ligase TRIM6 ubiquitinates the Ebola virus VP35 protein and promotes virus replication. J Virol. https://doi.org/10.1128/JVI.00833-17.
13. Han Z, Sagum CA, Takizawa F, Ruthel G, Berry CT, Kong J, Sunyer JO, Freedman BD, Bedford MT, Sidhu SS, Sudol M, Harty RN. 27 September 2017, posting date. Ubiquitin ligase WWP1 interacts with Ebola virus VP40 to regulate egress. J Virol. https://doi.org/10.1128/JVI.00812-17.
14. Han Z, Boshra H, Sunyer JO, Zwiers SH, Paragas J, Harty RN. 2003. Biochemical and functional characterization of the Ebola virus VP24 protein: implications for a role in virus assembly and budding. J Virol 77:1793–1800. https://doi.org/10.1128/jvi.77.3.1793-1800.2003.
15. Xu W, Edwards MR, Borek DM, Feagins AR, Mittal A, Alinger JB, Berry KN, Yen B, Hamilton J, Brett TJ, Pappu RV, Leung DW, Basler CF, Amarasinghe GK. 2014. Ebola virus VP24 targets a unique NLS binding site on karyopherin alpha 5 to selectively compete with nuclear import of phosphorylated STAT1. Cell Host Microbe 16:187–200. https://doi.org/10.1016/j.chom.2014.07.008.
16. Schwarz TM, Edwards MR, Diederichs A, Alinger JB, Leung DW, Amarasinghe GK, Basler CF. 31 January 2017, posting date. VP24-karyopherin alpha binding affinities differ between ebolavirus species, influencing interferon inhibition and VP24 stability. J Virol. https://doi.org/10.1128/JVI.01715-16.
17. Kerscher O. 2007. SUMO junction—what's your function? New insights

through SUMO-interacting motifs. EMBO Rep 8:550–555. https://doi.org/10.1038/sj.embor.7400980.
18. Lecona E, Rodriguez-Acebes S, Specks J, Lopez-Contreras AJ, Ruppen I, Murga M, Muñoz J, Mendez J, Fernandez-Capetillo O. 2016. USP7 is a SUMO deubiquitinase essential for DNA replication. Nat Struct Mol Biol 23:270–277. https://doi.org/10.1038/nsmb.3185.
19. Chavoshi S, Egorova O, Lacdao IK, Farhadi S, Sheng Y, Saridakis V. 2016. Identification of Kaposi sarcoma herpesvirus (KSHV) vIRF1 protein as a novel interaction partner of human deubiquitinase USP7. J Biol Chem 291:6281–6291. https://doi.org/10.1074/jbc.M115.710632.
20. Everett RD, Meredith M, Orr A, Cross A, Kathoria M, Parkinson J. 1997. A novel ubiquitin-specific protease is dynamically associated with the PML nuclear domain and binds to a herpesvirus regulatory protein. EMBO J 16:1519–1530. https://doi.org/10.1093/emboj/16.7.1519.
21. Holowaty MN, Zeghouf M, Wu H, Tellam J, Athanasopoulos V, Greenblatt J, Frappier L. 2003. Protein profiling with Epstein-Barr nuclear antigen-1 reveals an interaction with the herpesvirus-associated ubiquitin-specific protease HAUSP/USP7. J Biol Chem 278:29987–29994. https://doi.org/10.1074/jbc.M303977200.
22. Jager W, Santag S, Weidner-Glunde M, Gellermann E, Kati S, Pietrek M, Viejo-Borbolla A, Schulz TF. 2012. The ubiquitin-specific protease USP7 modulates the replication of Kaposi's sarcoma-associated herpesvirus latent episomal DNA. J Virol 86:6745–6757. https://doi.org/10.1128/JVI.06840-11.
23. Zhang AP, Bornholdt ZA, Liu T, Abelson DM, Lee DE, Li S, Woods VL, Jr, Saphire EO. 2012. The Ebola virus interferon antagonist VP24 directly binds STAT1 and has a novel, pyramidal fold. PLoS Pathog 8:e1002550. https://doi.org/10.1371/journal.ppat.1002550.
24. Lumpkin RJ, Gu H, Zhu Y, Leonard M, Ahmad AS, Clauser KR, Meyer JG, Bennett EJ, Komives EA. 2017. Site-specific identification and quantitation of endogenous SUMO modifications under native conditions. Nat Commun 8:1171. https://doi.org/10.1038/s41467-017-01271-3.
25. Desterro JM, Rodriguez MS, Hay RT. 1998. SUMO-1 modification of IkappaBalpha inhibits NF-kappaB activation. Mol Cell 2:233–239. https://doi.org/10.1016/s1097-2765(00)80133-1.
26. Hjerpe R, Aillet F, Lopitz-Otsoa F, Lang V, England P, Rodriguez MS. 2009. Efficient protection and isolation of ubiquitylated proteins using tandem ubiquitin-binding entities. EMBO Rep 10:1250–1258. https://doi.org/10.1038/embor.2009.192.
27. Vertegaal AC, Andersen JS, Ogg SC, Hay RT, Mann M, Lamond AI. 2006. Distinct and overlapping sets of SUMO-1 and SUMO-2 target proteins revealed by quantitative proteomics. Mol Cell Proteomics 5:2298–2310. https://doi.org/10.1074/mcp.M600212-MCP200.
28. González-Santamaría J, Campagna M, García MA, Marcos-Villar L, González D, Gallego P, Lopitz-Otsoa F, Guerra S, Rodríguez MS, Esteban M, Rivas C. 2011. Regulation of vaccinia virus E3 protein by small ubiquitin-like modifier proteins. J Virol 85:12890–12900. https://doi.org/10.1128/JVI.05628-11.
29. Marcos-Villar L, Lopitz-Otsoa F, Gallego P, Muñoz-Fontela C, González-Santamaría J, Campagna M, Shou-Jiang G, Rodriguez MS, Rivas C. 2009. Kaposi's sarcoma-associated herpesvirus protein LANA2 disrupts PML oncogenic domains and inhibits PML-mediated transcriptional repression of the survivin gene. J Virol 83:8849–8858. https://doi.org/10.1128/JVI.00339-09.
30. Pettersen EF, Goddard TD, Huang CC, Couch GS, Greenblatt DM, Meng EC, Ferrin TE. 2004. UCSF Chimera–a visualization system for exploratory research and analysis. J Comput Chem 25:1605–1612. https://doi.org/10.1002/jcc.20084.

AMERICAN SOCIETY FOR MICROBIOLOGY | mBio®

RESEARCH ARTICLE

Expression of the Ebola Virus VP24 Protein Compromises the Integrity of the Nuclear Envelope and Induces a Laminopathy-Like Cellular Phenotype

Santiago Vidal,[a] Maite Sánchez-Aparicio,[b,c] Rocío Seoane,[a] Ahmed El Motiam,[a] Emily V. Nelson,[d,e] Yanis H. Bouzaher,[a] Maite Baz-Martínez,[a,d] Isabel García-Dorival,[f] Susana Gonzalo,[g] Enrique Vázquez,[h] Anxo Vidal,[a] César Muñoz-Fontela,[d,e] Adolfo García-Sastre,[b,c,i,j] Carmen Rivas[a,k]

[a]Centro de Investigación en Medicina Molecular (CIMUS), Universidade de Santiago de Compostela, Instituto de Investigaciones Sanitarias (IDIS), Santiago de Compostela, Spain
[b]Department of Microbiology, Icahn School of Medicine at Mount Sinai, New York, New York, USA
[c]Global Health and Emerging Pathogens Institute, Icahn School of Medicine at Mount Sinai, New York, New York, USA
[d]Bernhard Nocht Institute for Tropical Medicine, Hamburg, Germany
[e]German Center for Infection Research (DZIF), Partner Site Hamburg, Germany
[f]Institute of Infection, Veterinary and Ecological Sciences, University of Liverpool, Liverpool, UK
[g]Department of Biochemistry and Molecular Biology, Saint Louis University, School of Medicine, Saint Louis, Missouri, USA
[h]Centro Nacional de Investigaciones Cardiovasculares (CNIC) Carlos III, Madrid, Spain
[i]Division of Infectious Diseases, Department of Medicine, Icahn School of Medicine at Mount Sinai, New York, New York, USA
[j]The Tisch Cancer Institute, Icahn School of Medicine at Mount Sinai, New York, New York, USA
[k]Centro Nacional de Biotecnología, CSIC, Cantoblanco, Madrid, Spain

ABSTRACT Ebola virus (EBOV) VP24 protein is a nucleocapsid-associated protein that inhibits interferon (IFN) gene expression and counteracts the IFN-mediated antiviral response, preventing nuclear import of signal transducer and activator of transcription 1 (STAT1). Proteomic studies to identify additional EBOV VP24 partners have pointed to the nuclear membrane component emerin as a potential element of the VP24 cellular interactome. Here, we have further studied this interaction and its impact on cell biology. We demonstrate that VP24 interacts with emerin but also with other components of the inner nuclear membrane, such as lamin A/C and lamin B. We also show that VP24 diminishes the interaction between emerin and lamin A/C and compromises the integrity of the nuclear membrane. This disruption is associated with nuclear morphological abnormalities, activation of a DNA damage response, the phosphorylation of extracellular signal-regulated kinase (ERK), and the induction of interferon-stimulated gene 15 (ISG15). Interestingly, expression of VP24 also promoted the cytoplasmic translocation and downmodulation of barrier-to-autointegration factor (BAF), a common interactor of lamin A/C and emerin, leading to repression of the BAF-regulated *CSF1* gene. Importantly, we found that EBOV infection results in the activation of pathways associated with nuclear envelope damage, consistent with our observations in cells expressing VP24. In summary, here we demonstrate that VP24 acts at the nuclear membrane, causing morphological and functional changes in cells that recapitulate several of the hallmarks of laminopathy diseases.

IMPORTANCE The Ebola virus (EBOV) VP24 protein is a nucleocapsid-associated protein with multiple functions. Proteomic studies have identified the cellular nuclear membrane component emerin as a potential VP24 interactor. Here, we demonstrate that VP24 not only interacts with emerin but also with lamin A/C and lamin B, prompting nuclear membrane disruption. This disruption is associated with nuclear morphological abnormalities, activation of a DNA damage response, the

Citation Vidal S, Sánchez-Aparicio M, Seoane R, El Motiam A, Nelson EV, Bouzaher YH, Baz-Martínez M, García-Dorival I, Gonzalo S, Vázquez E, Vidal A, Muñoz-Fontela C, García-Sastre A, Rivas C. 2021. Expression of the Ebola virus VP24 protein compromises the integrity of the nuclear envelope and induces a laminopathy-like cellular phenotype. mBio 12: e00972-21. https://doi.org/10.1128/mBio.00972-21.

Editor Thomas Shenk, Princeton University

Address correspondence to Adolfo García-Sastre, adolfo.garcia-sastre@mssm.edu, or Carmen Rivas, mcarmen.rivas@usc.es.

This article is a direct contribution from Adolfo García-Sastre, a Fellow of the American Academy of Microbiology, who arranged for and secured reviews by Slobodan Paessler, University of Texas Medical Branch, and Stephan Ludwig, Westfaelische-Wilhelms-University.

Received 23 May 2021
Accepted 1 June 2021
Published 6 July 2021

phosphorylation of extracellular signal-regulated kinase (ERK), and the induction of interferon-stimulated gene 15 (ISG15). Interestingly, VP24 also promotes the cytoplasmic translocation and downmodulation of barrier-to-autointegration factor (BAF), leading to repression of the BAF-regulated *CSF1* gene. Finally, we show that EBOV infection also results in the activation of pathways associated with nuclear envelope damage, consistent with our observations in cells expressing VP24. These results reveal novel activities of EBOV VP24 protein, resulting in a cell phenotype similar to that of most laminopathies, with potential impact on EBOV replication.

KEYWORDS Ebola virus, laminopathies, nuclear envelope, virus-host interactions

Ebola virus (Zaire ebolavirus, EBOV) is a highly pathogenic virus that causes hemorrhagic fever with a high case fatality rate in humans. EBOV VP24 is known as the minor viral matrix protein and may have a role in nucleocapsid assembly and virus budding (1–4). In addition, VP24 inhibits type I and II interferon (IFN) signaling by both directly interacting with signal transducer and activator of transcription 1 (STAT1) and binding to karyopherin alpha (KPNA) proteins involved in nuclear import, preventing their interaction with tyrosine-phosphorylated STAT1 and therefore inhibiting its nuclear translocation (5–9). Furthermore, VP24 inhibits IFN production and diminishes the interaction between KPNA1 and heterogeneous nuclear ribonuclear protein complex C1/C2 (hnRNP C1/C2), redistributing it from the nucleus to the cytoplasm (8, 10). Interestingly, roles of VP24 in both the aberrant expression of cytokines and chemokines and dendritic cell maturation impairment by unknown mechanisms have been reported (11). The importance of VP24 during virus replication is highlighted by the fact that all the attempts to generate recombinant EBOV without VP24 have failed (12). Proteomic studies to discover novel EBOV VP24 partners have identified the nuclear membrane constituent emerin as a potential component of the VP24 cellular interactome (13, 14).

Emerin is a component of the nuclear membrane that localizes predominantly at the nuclear envelope inner membrane. Emerin belongs to the LEM (LAP2, emerin, MAN1) family of nuclear proteins. These proteins are characterized by the presence of an LEM domain (15), which consists of approximately 40 amino acids that allow them to directly bind to lamins and barrier-to-autointegration factor (BAF), a mobile lamin-binding protein that can bridge DNA and interact with histones. Heterochromatin at the nuclear periphery (16, 17) and a wide range of transcription factors (18–21) also interact with emerin. There are two types of lamin proteins, A-type (lamins A and C from the *LMNA* gene) and B-type (lamins B1 and B2 encoded by *LMNB1* and *LMNB2* genes). Lamin filaments are important for the assembly, structure, shape, and mechanical stability of metazoan nuclei but also regulate chromatin organization and gene expression and influence signaling (22, 23). Importantly, lamins, emerin, and BAF are structurally interdependent, and if any one component is missing, the other two fail to coassemble (19, 24–26). Therefore, mutations in lamin A or in lamin-binding proteins result in nuclear envelope disorganization, nuclear morphological abnormalities, accumulation of DNA damage, and an altered pattern of heterochromatin distribution and signaling abnormalities, including those affecting the mitogen-activated protein kinase (MAPK) pathway, features of many diseases collectively known as laminopathies.

The critical roles of the nuclear envelope as both a cellular barrier and a regulator of gene expression explain why many viral pathogens have evolved to modulate its permeability (27). Here, we show that EBOV VP24 interacts with emerin, lamin A, and lamin B. VP24 reduces the interaction between emerin and lamin A/C, prompts nuclear membrane disruption, and induces the activation of the DNA damage response. In addition, the expression of VP24 was associated with nuclear morphological alterations, extracellular signal-regulated kinase (ERK) pathway activation, and transcriptional changes. Finally, we demonstrate that VP24 expression leads to BAF relocation and downmodulation. In summary, here we reveal a novel activity of EBOV VP24 that results in nuclear

membrane disruption and that may contribute to its critical role in virus replication and in virus pathogenesis.

RESULTS

VP24 interacts with emerin. Two proteomic reports have identified the nuclear membrane constituent emerin as a component of the VP24 interactome (13, 14). Here, we verified the interaction between VP24 and emerin by coimmunoprecipitation assays. Vero cells were transfected with pcDNA or a hemagglutinin (HA)-tagged VP24 expression plasmid, and 36 h after transfection, immunoprecipitations were performed using anti-emerin or anti-HA antibodies. The precipitated proteins were then analyzed by Western blotting with anti-HA or anti-emerin antibodies. Coimmunoprecipitation analysis revealed that VP24 coimmunoprecipitated with emerin (Fig. 1A). To further evaluate the VP24-emerin interaction, a biomolecular fluorescence complementation (BiFc) system assay was developed as described in Materials and Methods. Vero cells cotransfected with plasmids encoding a fusion of emerin to the two complementary halves (the N-terminal end [YN] and the C-terminal end [YC]) of the yellow fluorescent protein (YFP) led to the recovery of YFP fluorescence, indicative of oligomerization of the protein, as previously demonstrated (28, 29) (Fig. 1B). Cotransfection of Vero cells with the VP24 fusion plasmids with the YN and YC halves of YFP also led to the recovery of YFP fluorescence (Fig. 1B), indicative of its oligomerization, as previously reported (2). However, a significant component of the VP24 signal was also present without reconstitution of YFP. Finally, when Vero cells were cotransfected with YN-VP24 and YC-emerin, YFP fluorescence was recovered, indicative of the emerin-VP24 interaction (Fig. 1B). We then evaluated whether EBOV VP24 colocalizes with endogenous emerin. Vero cells were transfected with green fluorescent protein (GFP) or HA-VP24, and 36 h after transfection, immunostaining of HA-VP24 and endogenous emerin was carried out. VP24 protein was detected both in the nucleus and cytoplasm of transfected cells, as reported previously (30). Whereas endogenous emerin was mainly localized to the nuclear rim in GFP-transfected cells (Fig. 1C), it was observed lining the nuclear membrane and in cytoplasmic aggregates in HA-VP24-expressing cells (Fig. 1C and Fig. S1 in the supplemental material). We observed partial colocalization between VP24 and emerin (Fig. 1C and Fig. S1). Western blotting revealed that the overall level of emerin was identical independent of the expression of VP24 (Fig. 1D).

VP24 interacts with both lamin A and lamin B. Emerin localization at the nuclear envelope has been shown to depend on lamin A (31–35). Therefore, we decided to study the putative interaction between transfected HA-VP24 and endogenous lamin A/C protein by coimmunoprecipitation assays. Vero cells were transfected with pcDNA or HA-VP24, and 36 h after transfection, immunoprecipitations were performed using anti-lamin A/C or anti-HA antibodies. The precipitated proteins were then analyzed by Western blotting with anti-HA or anti-lamin A/C antibodies. We observed coimmunoprecipitation between lamin A/C and VP24 (Fig. 2A). Similar experiments carried out in HUH-7 cells revealed that lamin A/C also coimmunoprecipitated with VP24 when expressed in these cells (Fig. 2B). Interaction between VP24 and lamin A was also evaluated using a BiFc system assay. Vero cells cotransfected with the plasmids encoding a fusion of lamin A to the two complementary halves of YFP led to the recovery of YFP fluorescence, indicative of oligomerization of the protein, as previously demonstrated (36) (Fig. 2C). We also observed reconstitution of YFP fluorescence in Vero cells cotransfected with YC-lamin A and YN-VP24 plasmids, indicative of an interaction between lamin A and VP24 (Fig. 2C). Colocalization between endogenous lamin A/C and HA-VP24 was then analyzed by immunofluorescence staining and confocal analysis. Vero cells were transfected with GFP or HA-VP24, and 36 h after transfection, cells were fixed and immunostained with anti-lamin A/C and anti-HA antibodies. Endogenous lamin A/C was detected as a nuclear rim stain, indicating its location at the nuclear envelope in cells expressing or not expressing HA-VP24 (Fig. 2D and Fig. S2). Colocalization between VP24 and lamin A was detected both at the nuclear

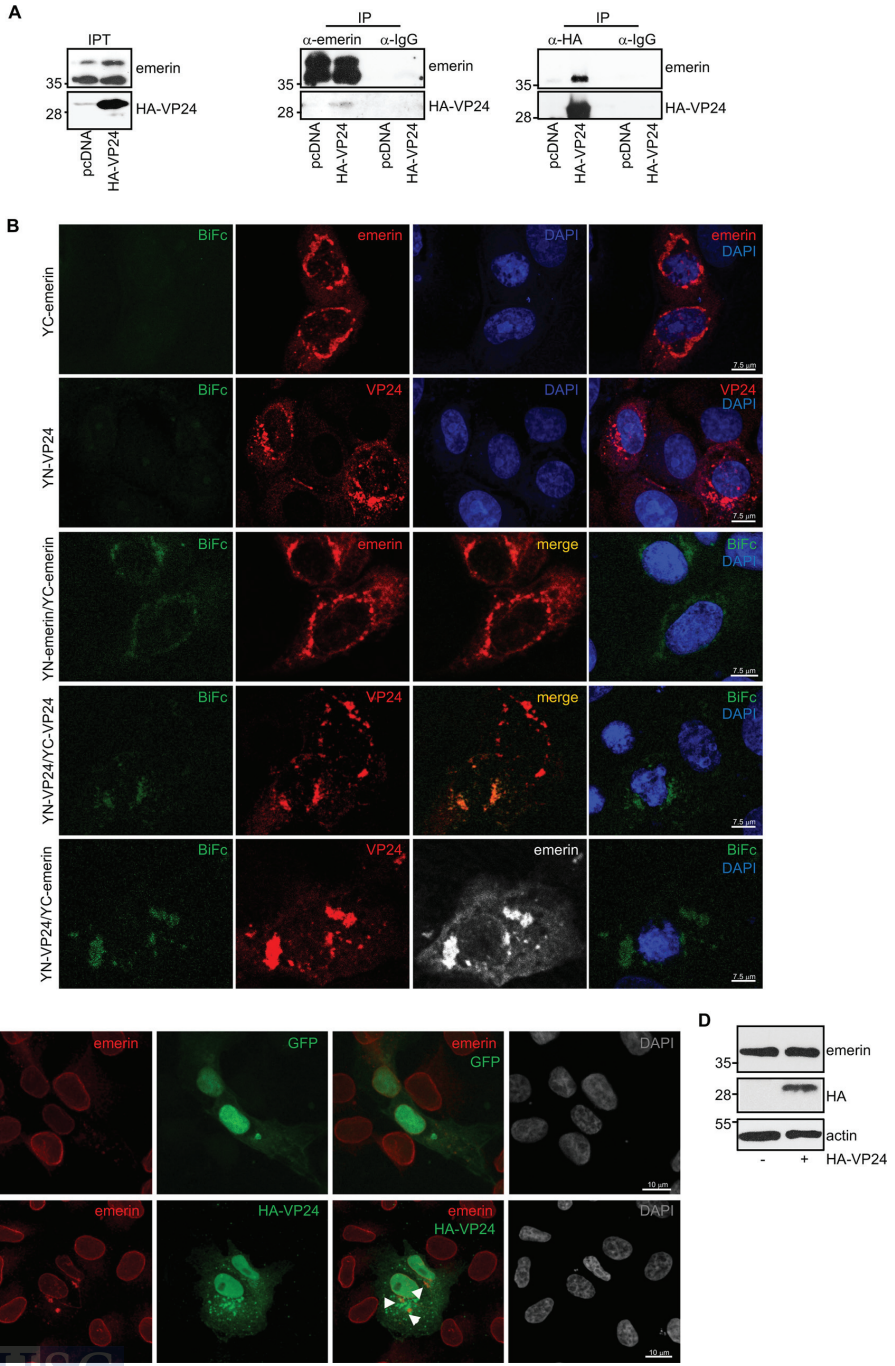

FIG 1 Interaction of EBOV VP24 protein with emerin. (A) Coimmunoprecipitation between VP24 and emerin. Vero cells seeded in 100-mm plates were transfected with 5 μg of pcDNA or HA-VP24, and 36 h after transfection, protein extracts of transfected cells were immunoprecipitated using anti-emerin, anti-HA, or anti-IgG antibodies. Immunoprecipitated proteins were analyzed by

(Continued on next page)

membrane as well as in some lamin A cytoplasmic aggregates, which were only present in VP24-expressing cells (Fig. 2D and Fig. S2).

Emerin also binds B-type lamins (32, 34). In addition, lamin B has been identified as a component of the VP24 interactome in a proteomic study (13). Therefore, we investigated the interaction between endogenous lamin B and HA-VP24. Vero cells were transfected with pcDNA or HA-VP24, and 36 h after transfection, immunoprecipitations were performed using anti-lamin B or anti-HA antibodies. The precipitated proteins were then analyzed by Western blotting with anti-HA or anti-lamin B antibodies. Coimmunoprecipitation analysis revealed that both proteins interact (Fig. 3A). We next analyzed the colocalization of endogenous lamin B with HA-VP24. Vero cells were transfected with GFP or HA-VP24, and 36 h after transfection, cells were fixed and immunostained with anti-lamin B and anti-HA antibodies. Endogenous lamin B was detected mainly at the nuclear envelope (Fig. 3B and Fig. S3). Colocalization between VP24 and lamin B was detected both at the nuclear rim as well as in some lamin B cytoplasmic aggregates (Fig. 3B and Fig. S3). Altogether, these data indicate that VP24 interacts with both lamin A/C and B, and VP24 appears to displace a fraction of these proteins from the nuclear envelope to the cytoplasm.

VP24 interacts with emerin in a tag-independent manner. Tagging proteins may alter subcellular localization, stability, activity, or interaction with binding partners. Thus, fusion of VP24 with a Flag-tag at its C terminus inhibits the ability of VP24 to form nucleocapsid-like structures and inhibits transcription and replication of the EBOV genome (37). Therefore, we decided to evaluate whether the HA-tagged VP24 protein employed in this study shares the main characteristics previously described for the viral protein. First, we analyzed the ability of HA-VP24 to inhibit IFN signaling. HEK-293 cells were cotransfected with ISG54-luciferase together with beta-galactosidase and pcDNA, HA-VP24, YN-VP24, or a GFP-tagged VP24 construct, and 24h after transfection, cells were treated with IFN-α for 16 h. Cell extracts were then harvested and analyzed for luciferase and beta-galactosidase activities. As shown in Figure 4A, IFN induces transactivation of the reporter, as expected, and all VP24 constructs significantly reduced this transactivation, indicating their ability to inhibit IFN signaling. Then, we evaluated the ability of HA-VP24 to modulate luciferase expression from an EBOV minigenome. HEK-293 cells were cotransfected with plasmids for the expression of the T7 polymerase, nucleoprotein (NP), VP30, VP35, and L protein of the Zaire EBOV minigenome strain Mayinga, as previously described (38), together with pcDNA or HA-VP24. At 48 h after transfection, luciferase activity was analyzed. Transfection of HA-VP24 inhibited luciferase expression from the minigenome, as previously reported (37, 39–41) (Fig. 4B). Another function of VP24 is its ability to interact with NP to facilitate nucleocapsid assembly and genome packaging (42). We then evaluated the coimmunoprecipitation between HA-VP24 and NP. We cotransfected Vero cells with HA-VP24 together with the NP expression plasmid or the empty vector pcDNA. At 36 h after transfection, immunoprecipitation was performed using anti-HA antibody. The precipitated proteins were then analyzed by Western blotting with anti-HA or anti-NP antibodies. We observed coimmunoprecipitation between NP and VP24 (Fig. 4C).

FIG 1 Legend (Continued)
Western blotting using the indicated antibodies. The anti-emerin antibody detected a major band of around 37 kDa and a higher molecular weight band of around 39 kDa, probably corresponding to phosphorylated emerin. The experiments were repeated twice, and representative images of one experiment are shown; IP, immunoprecipitated samples; IPT, input cell extract. (B) VP24-emerin colocalization using the BiFc system. Vero cells were transfected with the indicated combination of the BiFc constructs (YC-emerin, C-terminal part of the yellow fluorescent protein [YFP] fused to the N terminus of full-length emerin; YN-emerin, N-terminal part of YFP fused to the N terminus of full-length emerin; YN-VP24, N-terminal part of YFP fused to the N-terminal part of full-length VP24; YC-VP24, C-terminal part of YFP fused to the N-terminal part of full-length VP24). Cells were fixed, permeabilized, and stained with anti-emerin and/or anti-VP24 primary antibodies. Chromosomes were stained with DAPI (blue). Coexpression of YC- and YN-emerin, YC- and YN-VP24, or YN-VP24 and YC-emerin led to the reconstitution of YFP signal (BiFc). The data represent more than three biological replicates. (C) Localization of endogenous emerin in Vero cells transfected with 0.3 μg of GFP or HA-VP24 or in untransfected cells. Emerin and HA-tagged VP24 are shown. Chromosomes were stained with DAPI. Arrowheads indicate colocalization of HA-VP24 and emerin. (D) Western blotting analysis using anti-emerin antibody of Vero cells at 36 h after transfection with 0.3 μg of pcDNA or HA-VP24 expression plasmids.

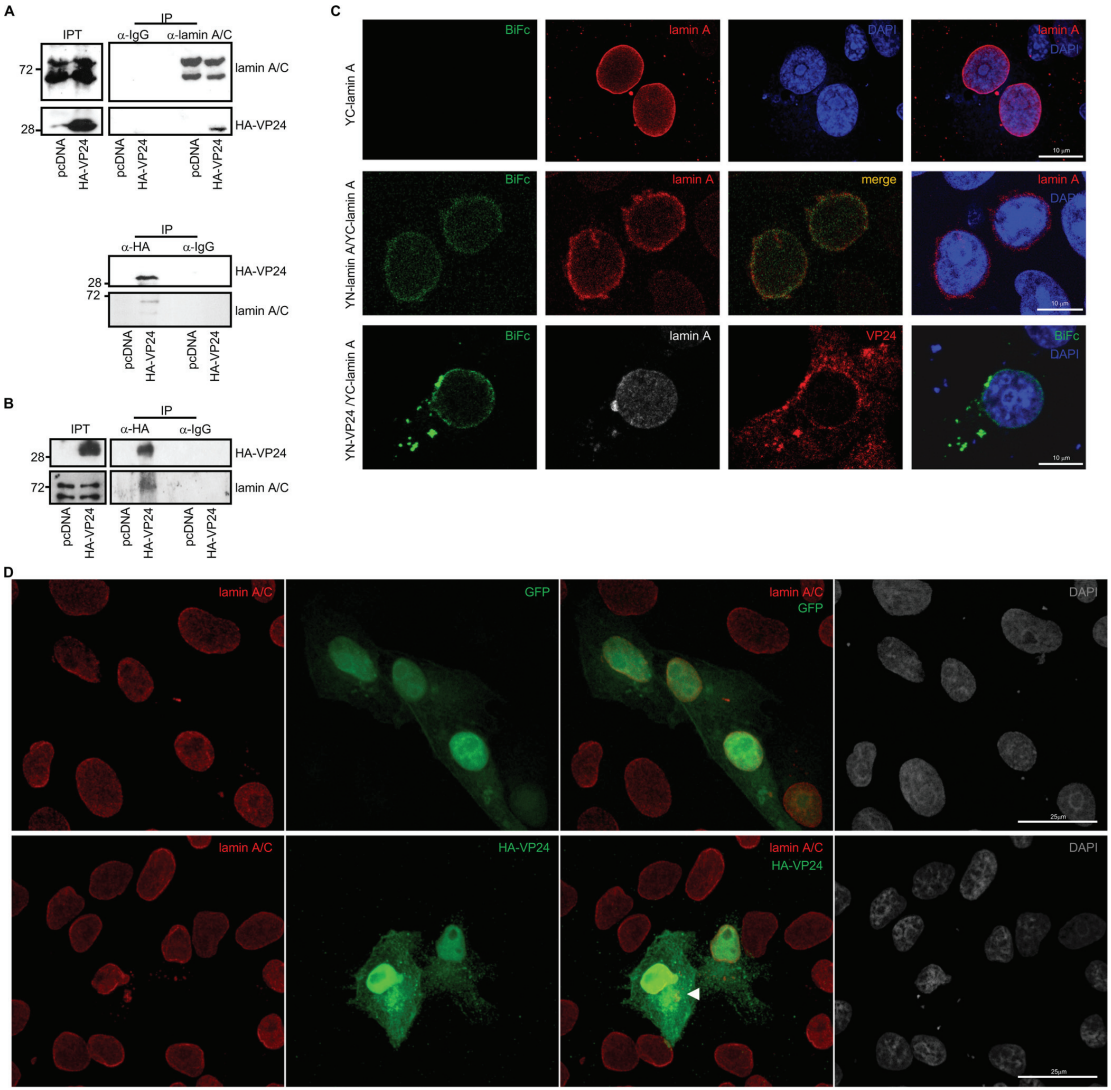

FIG 2 VP24 interacts with lamin A/C. (A) Coimmunoprecipitation between VP24 and lamin A/C. Vero cells were transfected with 5 μg of HA-VP24 in a 100-mm dish, and 36 h after transfection, protein extracts of transfected cells were immunoprecipitated using anti-HA, anti-lamin A/C, or anti-IgG antibodies. Immunoprecipitated proteins were analyzed by Western blotting using the indicated antibodies. The experiments were repeated twice, and representative images of one experiment are shown; IP, immunoprecipitated samples; IPT, input cell extract. (B) HUH-7 cells were transfected with 5 μg of HA-VP24 in a 100-mm dish, and 36 h after transfection, protein extracts of transfected cells were immunoprecipitated using anti-HA antibody. Immunoprecipitated proteins were analyzed by Western blotting using anti-lamin A/C antibody; IP, immunoprecipitated samples; IPT, input cell extract. (C) VP24-lamin A colocalization using the BiFc system. Vero cells were transfected with the indicated combination of the BiFc constructs (YC-lamin A, C-terminal part of the yellow fluorescent protein [YFP] fused to the N terminus of full-length lamin A; YN-lamin A, N-terminal part of YFP fused to the N terminus of full-length lamin A; YN-VP24, N-terminal part of YFP fused to the N-terminal part of full-length VP24). Cells were fixed, permeabilized, and stained with anti-lamin A/C and/or anti-VP24 primary antibodies. Chromosomes were stained with DAPI (blue). Coexpression of YC- and YN-lamin or YN-VP24 and YC-lamin A led to the reconstitution of YFP signal (BiFc). The data represent more than three biological replicates. Chromosomes were stained with DAPI (blue). (D) Localization of lamin A/C in Vero cells transfected with 0.3 μg of GFP or HA-VP24 or in untransfected cells. Lamin A/C and HA-tagged VP24 are shown. Chromosomes were stained with DAPI. Arrowhead indicates colocalization of HA-VP24 and lamin A/C.

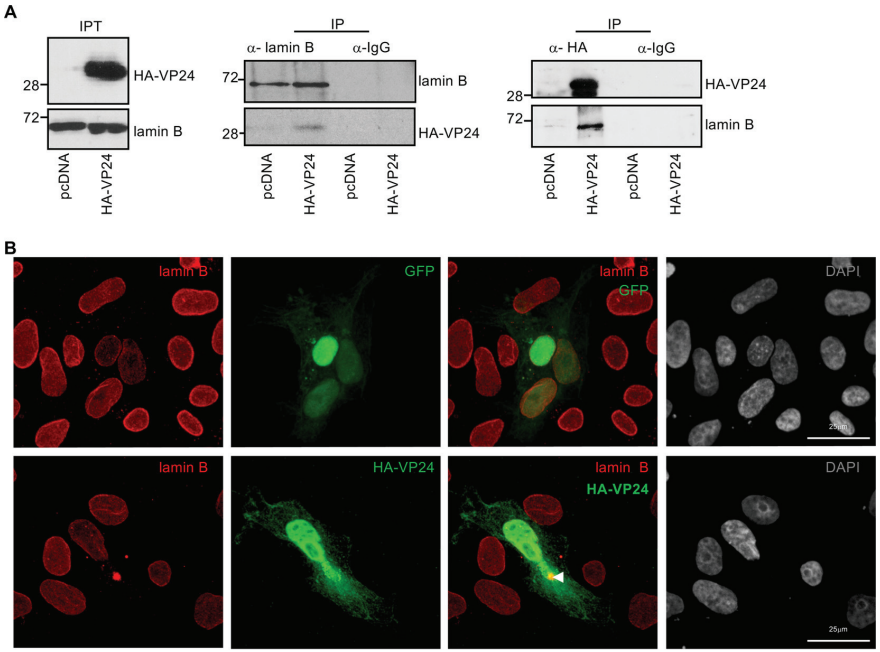

FIG 3 VP24 interacts with lamin B. (A) Coimmunoprecipitation between VP24 and lamin B. Vero cells were transfected with 5 μg of HA-VP24 in a 100-mm dish, and 36 h after transfection, protein extracts of transfected cells were immunoprecipitated using anti-lamin B, anti-HA, or anti-IgG antibodies. Immunoprecipitated proteins were analyzed by Western blotting using the indicated antibodies. The experiments were repeated twice, and representative images of one experiment are shown; IP, immunoprecipitated samples; IPT, input cell extract. (B) Localization of lamin B in Vero cells transfected with 0.3 μg of GFP or HA-VP24 or in untransfected cells. Lamin B and HA-tagged VP24 are shown. Chromosomes were stained with DAPI. Arrowhead indicates colocalization of HA-VP24 and lamin B.

Altogether, these results indicated that the fusion of HA-tag to the N terminus of VP24 does not alter the main functions of the viral protein.

However, one feature of the HA-VP24 protein is not consistent with some previous VP24 descriptions. Ebola VP24 protein has been initially described as a cytoplasmic protein in both infected and transfected cells (2), similar to the subcellular localization of the protein fused to YC or YN of YFP, as shown in Figure 1B. However, HA-VP24 protein was detected both in the nucleus and cytoplasm of Vero cells, as recently reported (30). The small size of the VP24 protein could facilitate a passive cytoplasm-to-nucleus translocation of the protein. Cytoplasmic proteins with a molecular mass larger than 40 to 45 kDa are unable to enter the nucleus unless they provide a signal for nuclear import (43). Therefore, we decided to evaluate the subcellular localization of the VP24 protein after fusing to a 30-kDa GFP tag. As shown in Figure 4D, confocal analysis revealed that GFP-VP24 protein was detected mainly at the cell cytoplasm, suggesting that HA-VP24 protein entered into the nucleus by passive diffusion. Although VP24 does not have a classical targeting signal to go inside the nucleus, it interacts with members of the importin superfamily of nuclear import transporters (6). To evaluate whether this interaction can facilitate the entry of the viral protein inside the nucleus, we analyzed the localization of GFP-VP24 protein after karyopherin overexpression. Confocal analysis showed that GFP-VP24 protein localized in the nucleus of cells overexpressing karyopherin (Fig. 4E), suggesting that the interaction with the nuclear import transporter may promote its nuclear translocation. We then decided to evaluate whether the mainly cytoplasmic GFP-VP24 protein was still able to colocalize with emerin. Vero cells were transfected with GFP-VP24, and 36 h after transfection, cells were fixed and immunostained with anti-emerin antibody. A fraction of endogenous

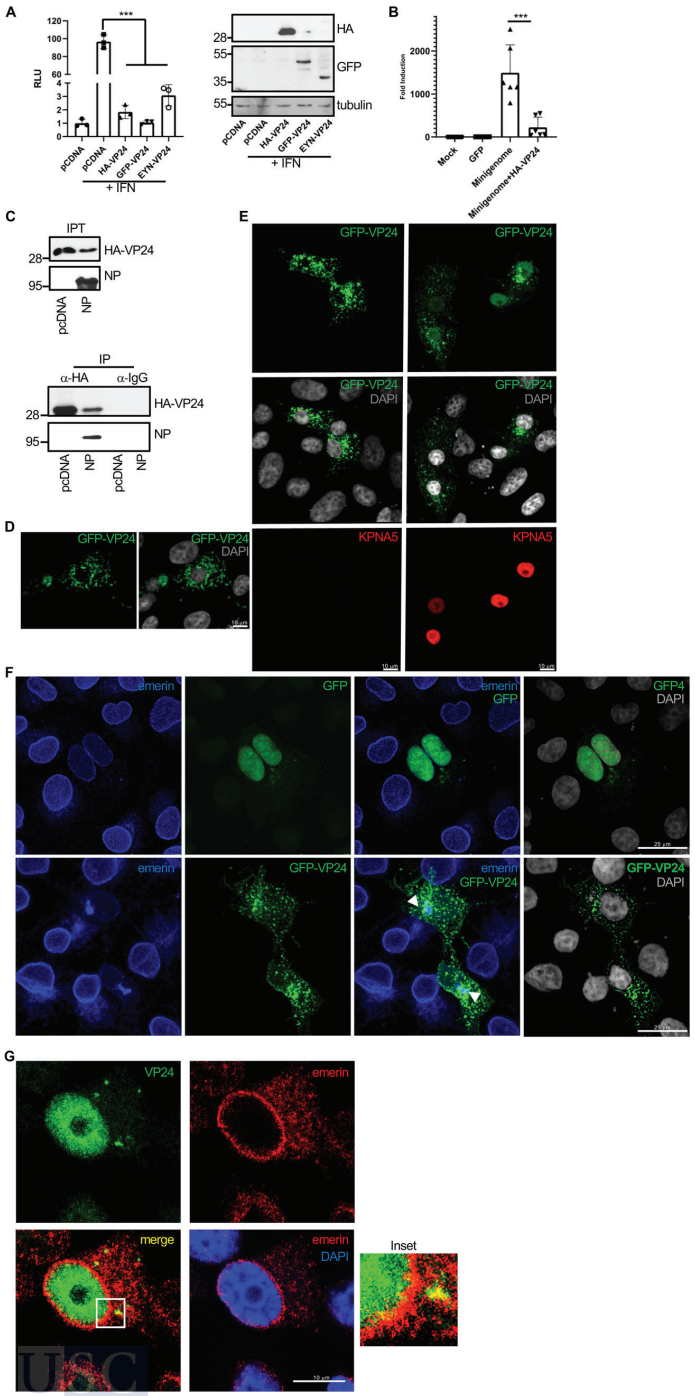

FIG 4 EBOV VP24 protein interacts with emerin in a tag-independent manner. (A) HEK-293 cells were cotransfected with ISG54-luciferase together with pcDNA or the indicated VP24 expression plasmids.

(Continued on next page)

emerin was detected in cytoplasmic aggregates, partially colocalizing with GFP-VP24 protein (Fig. 4F), indicating the interaction of GFP-VP24 and emerin. Finally, we decided to evaluate the colocalization between untagged VP24 protein and emerin. BSR-T7 cells were transfected with a plasmid encoding untagged VP24, and 36 h after transfection, cells were stained with anti-VP24 and anti-emerin antibodies. VP24 was detected both at the nucleus and in cytoplasmic aggregates, and a partial colocalization with emerin was observed (Fig. 4G). Altogether, these results indicate that VP24 interacts with emerin in a tag-independent manner.

VP24 associates with emerin in the presence of other EBOV proteins. Our results indicate that VP24 protein, in the absence of other EBOV proteins, interacts with emerin. Previous studies have shown that VP24 colocalizes with NP in a time-dependent manner in the course of EBOV infection in Vero cells (40). Therefore, we decided to evaluate whether HA-VP24 protein expressed together with EBOV proteins involved in RNA replication still interacted with emerin. We cotransfected 1×10^5 BSR-T7 cells with the expression plasmids for the EBOV Makona proteins NP (0.059 μg), VP35 (0.029 μg), VP30 (0.029 μg), and L (0.029 μg), and in the presence or absence of HA-VP24 (0.041 μg). At 36 h after transfection, immunoprecipitations were performed using anti-HA antibody. The precipitated proteins were then analyzed by Western blotting with antibodies against HA-tag, emerin, or the EBOV proteins NP and VP35. We observed that HA-VP24 coimmunoprecipitated with NP and VP35. Moreover, we also observed that HA-VP24 coimmunoprecipitated with emerin when coexpressed with EBOV NP, VP35, VP30, and L (Fig. 5A). In addition, coimmunoprecipitation analysis between HA-VP24 and emerin in cells cotransfected with HA-VP24 and pcDNA or the EBOV NP, VP35, VP30, and L expression plasmids did not reveal differences in the VP24-emerin interaction (Fig. 5B). We also analyzed the putative colocalization of VP24 and emerin in the presence of NP. Vero cells were cotransfected with HA-VP24 and NP expression plasmids, and 36 h after transfection, we fixed the cells and immunostained using anti-HA, anti-emerin, and anti-NP antibodies. NP was detected in cytoplasmic inclusions, whereas HA-VP24 localized both in the nucleus and in some cytoplasmic aggregates where it partially colocalized with NP (Fig. 5C and Fig. S4). Emerin was detected at the nuclear rim and in some cytoplasmic aggregates, and a partial colocalization with VP24 was observed (Fig. 5C and Fig. S4), indicating that VP24 can associate with emerin in the presence of NP. Finally, we evaluated the putative VP24-emerin colocalization in Vero cells infected with EBOV. Emerin was observed lining the nuclear membrane, diffused in the cytoplasm, and in some small cytoplasmic aggregates. Colocalization between emerin and VP24 was observed both at the nuclear membrane as well as in cytoplasmic aggregates (Fig. 5D). Altogether, these results indicate that VP24 interacts with emerin independent of the expression of other EBOV proteins.

Loss of nuclear membrane integrity upon EBOV VP24 expression. Mutations in nuclear envelope components blocking the interaction between emerin and lamins

FIG 4 Legend (Continued)
At 24 h after transfection, cells were treated with IFN-α, and at 16 h after treatment, luciferase production was analyzed. Columns are representative of the mean, and error bars represent the standard deviation of three biological replicates (left). Cell lysates from the experiment were analyzed by Western blotting for VP24 expression (right). (B) Minigenome assay in cells cotransfected with HA-VP24. Columns are representative of the mean, and error bars represent the standard deviation of three biological replicates. (C) Coimmunoprecipitation between HA-VP24 and NP. Vero cells were cotransfected with 2.5 μg of HA-VP24 and 2.5 μg of pcDNA or NP expression plasmids in a 100-mm dish, and 36 h after transfection, protein extracts of transfected cells were immunoprecipitated using anti-HA antibody. Immunoprecipitated proteins were analyzed by Western blotting using the indicated antibodies. The experiments were repeated twice, and representative images of one experiment are shown; IP, immunoprecipitated samples; IPT, input cell extract. (D) Localization of GFP-VP24 protein in Vero cells. Chromosomes were stained with DAPI. (E) Localization of GFP-VP24 protein in cells cotransfected with pcDNA or karyopherin 5 (KPNA5) expression plasmid. Chromosomes were stained with DAPI. (F) Colocalization of emerin and GFP-VP24 in Vero cells cotransfected with GFP or GFP-VP24. Chromosomes are stained with DAPI. Arrowheads indicate colocalization of GFP-VP24 and emerin. (G) Colocalization of emerin and VP24 in Vero cells transfected with untagged VP24 expression plasmid. Chromosomes are stained with DAPI. Inset shows higher magnification of the boxed area.

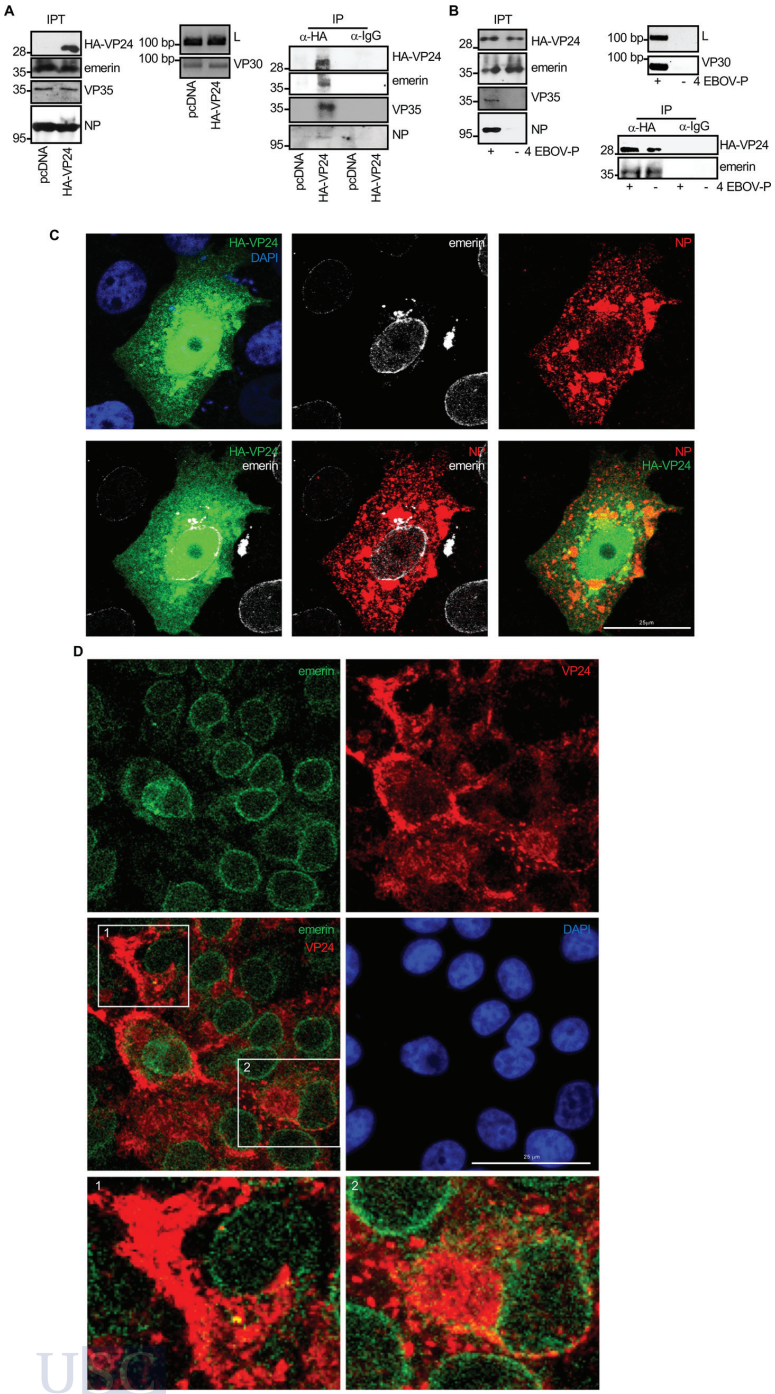

FIG 5 VP24 associates with emerin in the presence of other EBOV proteins. (A) Coimmunoprecipitation between VP24 and emerin in BSR-T7 cells cotransfected with the plasmids from the EBOV minigenome, NP,

(Continued on next page)

are associated with the mislocalization of nuclear envelope components (44–46). We then decided to evaluate whether VP24 modulates the interaction between emerin and lamin A/C. First, we analyzed the coimmunoprecipitation between emerin and lamin A/C in cells expressing VP24. HEK-293 cells transfected with HA-VP24 or pcDNA were subjected to immunoprecipitation with anti-emerin or anti-lamin A/C antibodies. Immunoprecipitated proteins were then analyzed by Western blotting with the same antibodies. As shown in Figure 6A, emerin coimmunoprecipitated with lamin A/C in pcDNA-transfected cells, as expected. We observed a clear reduction in the coimmunoprecipitation between both proteins in those cells expressing VP24 (Fig. 6A). Quantification of the emerin protein that coimmunoprecipitated with lamin A/C in three independent experiments revealed that expression of VP24 significantly reduced the amount of emerin interacting with lamin A/C ($P < 0.001$; Fig. 6A). Additionally, we evaluated the emerin-lamin A/C coimmunoprecipitation in HEK-293 cells transfected with different doses (0, 1.25, 2.5, or 5 μg per 100-mm dish) of HA-VP24 expression vector. A clear reduction in the coimmunoprecipitation between both proteins was observed in the cells transfected with the two highest doses of HA-VP24 (Fig. 6B). To further evaluate the consequences of VP24 expression on emerin-lamin interaction, we analyzed the emerin/lamin A complexes using the BiFc system in cells expressing VP24. Confocal analysis revealed that cells cotransfected with YN-emerin and YC-lamin A showed a fluorescent signal mainly at the nuclear rim, indicating the interaction of emerin and lamin A at the inner nuclear membrane, as expected. An uneven fluorescent signal located both at the nuclear envelope and in some cytoplasmic aggregates was observed in the VP24-expressing cells (Fig. 6C and Fig. S5), indicating that the remaining interactions between emerin and lamin A are not happening at the right compartment, the nuclear rim. An association between the BiFc signal and VP24 cytoplasmic protein was also observed (Fig. 6C and Fig. S5). Finally, we decided to evaluate whether the expression of VP24 in the context of the EBOV replicative proteins also altered the emerin-lamin A/C interaction. We cotransfected 1×10^5 BSR-T7 cells with the expression plasmids for the EBOV Makona proteins NP (0.059 μg), VP35 (0.029 μg), VP30 (0.029 μg), and L (0.029 μg) and in presence or absence of HA-VP24 (0.041 μg). At 36 h after transfection, immunoprecipitations were performed using anti-lamin antibody. The precipitated proteins were then analyzed by Western blotting with anti-lamin A/C or anti-emerin antibodies. We observed a clear reduction in the coimmunoprecipitation between both proteins in those cells expressing VP24 (Fig. 6D).

Since nuclear envelope disorganization triggers its collapse (47), we hypothesized that VP24 expression could lead to nuclear envelope damage. To address this hypothesis, we carried out immunofluorescence analysis using anti-lamin A/C antibody of cells transfected with HA-VP24 after permeabilization with digitonin, a compound that permeabilizes the plasma membrane but leaves the nuclear envelope intact (48, 49). Consequently, antibodies to lamin A/C, located at the inner nuclear membrane, can bind their antigens in digitonin-permeabilized cells only if nuclear membranes are damaged (50). As shown in Figure 7A, lamin A/C was virtually undetectable in digitonin-treated GFP-transfected or untransfected cells; however, a lamin A/C signal was clearly observed in those cells expressing VP24 (Fig. 7A), suggesting that the nuclear

FIG 5 Legend (Continued)
L, VP30, and VP35 (strain Makona), and in the presence or absence of HA-VP24. Expression of VP35, NP, and HA-VP24 was confirmed by Western blotting with the indicated antibodies. Expression of VP30 and L protein was verified by reverse-transcription-PCR (RT-PCR). Coimmunoprecipitation of both VP35 and NP with HA-VP24 was also confirmed; IP, immunoprecipitated samples; IPT, input cell extract. (B) Coimmunoprecipitation between VP24 and emerin in BSR-T7 cells cotransfected with HA-VP24 and pcDNA or the plasmids from the EBOV minigenome NP, L, VP30, and VP35 (strain Makona) (4 EBOV-P). Expression of VP35, NP, and HA-VP24 was confirmed by Western blotting with the indicated antibodies. Expression of VP30 and L protein was verified by RT-PCR; IP, immunoprecipitated samples; IPT, input cell extract. (C) Colocalization of HA-VP24 and emerin in Vero cells cotransfected with HA-VP24 and NP. Emerin, NP, and HA-VP24 localization are shown. Chromosomes were stained with DAPI. (D) Colocalization of VP24 and emerin in Vero cells infected with EBOV. Emerin and VP24 localization are shown. Chromosomes were stained with DAPI. Images 1 and 2 show higher magnification views of the indicated boxed areas.

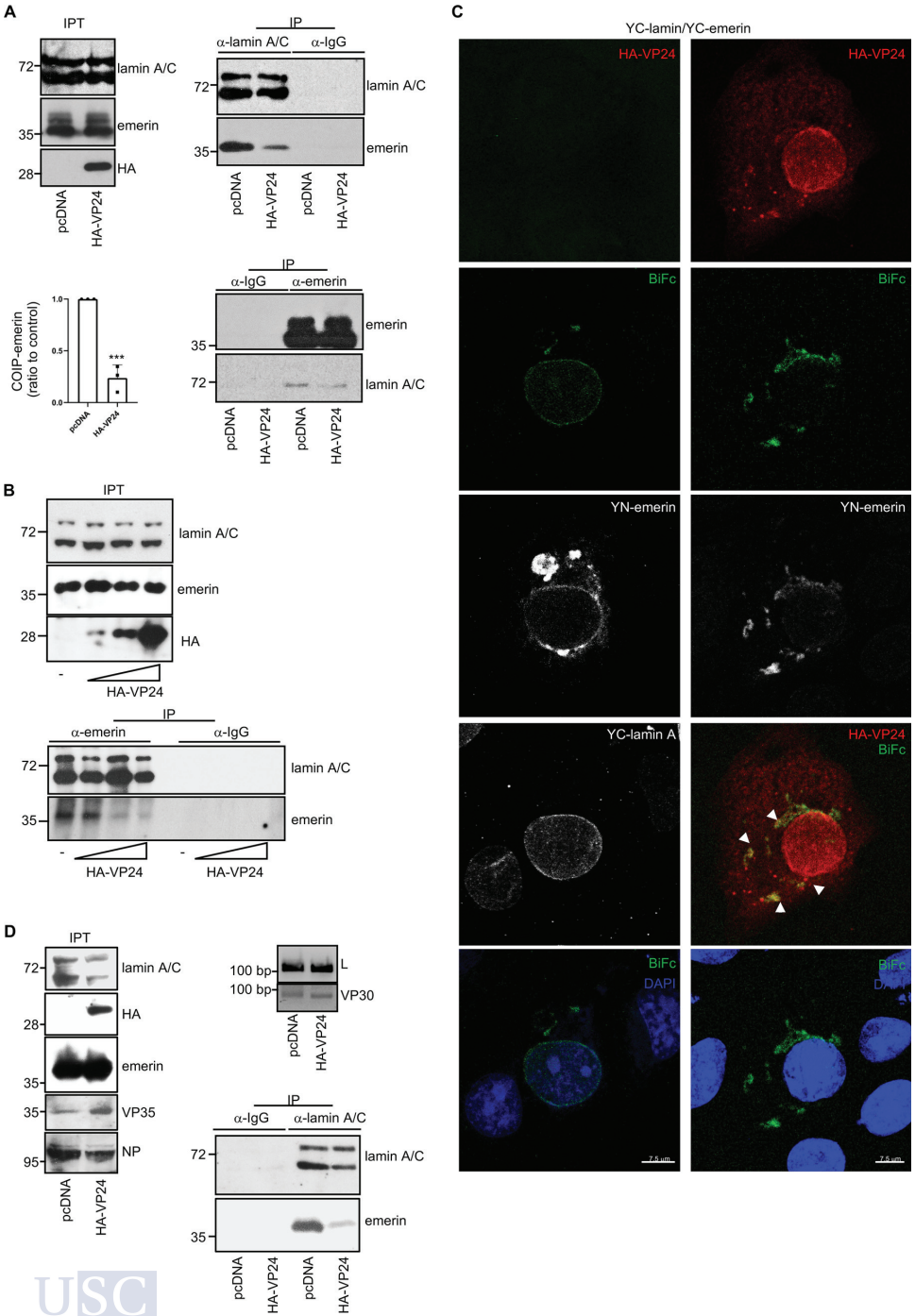

FIG 6 VP24 reduces the interaction between emerin and lamin A/C. (A) Coimmunoprecipitation between emerin and lamin A/C in nontransfected cells and in cells transfected with 2.5 μg of HA-VP24 in a 100-mm dish. Representative blots of one experiment are

(Continued on next page)

membrane is damaged. To ascertain whether nuclear membrane was damaged by VP24 protein, we analyzed the distribution of the fluorescent nuclear envelope rupture reporter GFP-nuclear localization signal (NLS) in cells expressing VP24. GFP-NLS localized to the nucleus in cells cotransfected with pcDNA, whereas it localized to the nucleus but also spilled into the cytoplasm in those cells expressing VP24 (Fig. 7B). Finally, we analyzed the subcellular localization of another fluorescent nuclear envelope rupture reporter, GFP-cyclic GMP-AMP synthase (cGAS). After nuclear membrane breakdown, the GFP-cGAS located at the cytoplasm has been reported to bind to exposed genomic DNA and accumulate at the break site (51). As shown in Figure 7C, GFP-cGAS was detected in discrete intranuclear foci in cells expressing VP24. Altogether, these results indicate that VP24 expression induces the loss of nuclear membrane integrity.

Nuclear shape is linked to the structure of the lamina (52). Therefore, we analyzed the shape and area of the nucleus of cells expressing VP24. Whereas nuclei of control cells are roughly circular or slightly ovoid, those cells expressing VP24 are often irregular (Fig. 7D). We also observed that the median nuclear size of cells transfected with VP24 was significantly smaller than that observed in control cells (Fig. 7E). Altogether, these results indicated that expression of VP24 altered the nuclear morphology of the cells.

Activation of MAPK pathways. Nuclear envelope disorganization detected in laminopathies has been shown to stimulate the phosphorylation of ERK (53–55). In addition, downmodulation of lamin A/C also induces ERK phosphorylation (Fig. 8A). To determine whether expression of VP24 also activates MAPK signaling, we measured phosphorylation of ERK1/2 (pERK1/2) in transiently transfected Vero cells expressing VP24. We observed that the expression of VP24 significantly increased the amount of phosphorylated protein, indicating that VP24 activates MAPK cascades (Fig. 8B). Increased ERK1/2 phosphorylation was also observed in HeLa cells after transfection with VP24 expression plasmid (Fig. 8C). Interestingly, we also observed induction of ERK phosphorylation in response to infection with authentic EBOV (Fig. 8D).

Induction of DNA damage and upregulation of ISG15 by VP24. Nuclear membrane disruption has been shown to correlate with DNA damage accumulation (56, 57). To assess levels of DNA damage, we analyzed the presence of foci of H2A histone family member X (gH2AX) in cells expressing VP24. We found foci of gH2AX in around 85% of VP24-expressing cells and in 13% of control cells (Fig. 9A). Western blotting also revealed an increase in gH2AX levels in those cells transfected with HA-VP24 (Fig. 9B), suggesting that expression of VP24 protein triggers DNA damage. Analysis of the presence of gH2AX foci in EBOV-infected cells was also analyzed. Both immunofluorescent gH2AX foci (Fig. 9C) and an increase in gH2AX levels were detected in those cells infected with EBOV (Fig. 9D).

DNA damage has been shown to induce ISG15 expression (57–60). Therefore, we decided to study the transcript and protein levels of ISG15 in cells expressing VP24. The transcript levels of ISG15 were significantly higher in cells transfected with VP24 than in pcDNA-transfected cells (Fig. 9E). In addition, Western blotting analysis of A549 or HeLa cells transfected with VP24 also revealed a significant increase in ISG15 protein levels (Fig. 9F and G, respectively), similar to that observed after downmodulation of lamin A/C (Fig. 9G and H).

FIG 6 Legend (Continued)
shown. Results obtained from three independent coimmunoprecipitation experiments were quantified. The amount of coimmunoprecipitated emerin was normalized to the amount of lamin A/C protein immunoprecipitated in each experiment; IP, immunoprecipitated samples; IPT, input cell extract. The emerin/lamin detected in the pcDNA-transfected cells was set to 1, and the values found in VP24-expressing cells were calculated relative to it. Statistical analysis was assessed by a Student's *t* test. ***, $P < 0.001$. (B) Coimmunoprecipitation between emerin and lamin A/C in cells transfected with different amounts (0, 1.2, 2.5, or 5 μg per 100-mm dish) of HA-VP24 expression plasmid. IP, immunoprecipitated samples; IPT, input cell extract. (C) Emerin-lamin A colocalization using the BiFc system in cells expressing VP24. Chromosomes were stained with DAPI (blue). Arrowheads indicate colocalization of V24 with the BiFc signal. (D) Coimmunoprecipitation between emerin and lamin A/C in BSR-T7 cells cotransfected with the plasmids L, NP, VP30, and VP35 of the EBOV minigenome system and in presence or absence or HA-VP24. Expression of VP35, NP, and HA-VP24 was confirmed by Western blotting with the indicated antibodies. Expression of VP30 and L protein was verified by reverse-transcription-PCR (RT-PCR). Representative blots of one experiment are shown; IP, immunoprecipitated samples; IPT, input cell extract.

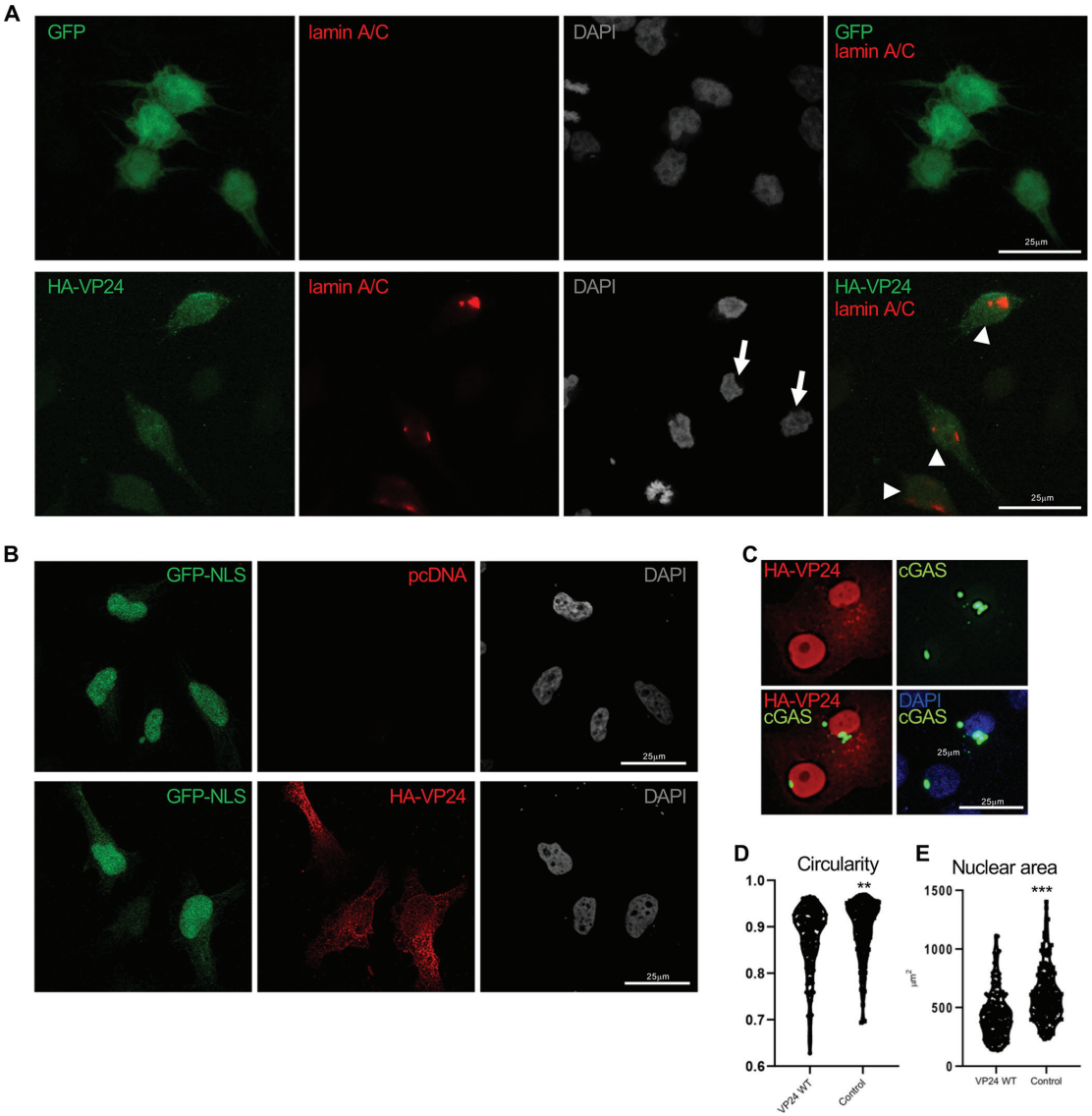

FIG 7 VP24 induces nuclear membrane disruption. (A) Immunofluorescence staining using anti-lamin A/C antibody of cells transfected with 0.3 μg of GFP or VP24 and permeabilized with digitonin. Chromosomes were stained with DAPI. Arrowheads indicate positive detection of lamin A/C in cells expressing VP24, and arrows indicate untransfected cells. (B) Localization of GFP-NLS in cells cotransfected with 0.3 μg of pcDNA or HA-VP24 and permeabilized with digitonin. Chromosomes were stained with DAPI. (C) Localization of GFP-cGAS in Vero cells transfected with 0.3 μg of HA-VP24. (D) Shape of the nucleus of Vero cells expressing HA-VP24 or control cells. A higher circularity denotes a more circular shape. (E) Size of the nucleus of Vero cells expressing HA-VP24 or control cells. Graphs show one data point per nucleus analyzed. Statistical analysis was assessed by a Student's *t* test. **, $P < 0.01$; ***, $P < 0.001$.

RanGAP and RanBP localization is not altered in VP24-expressing cells. One of the functions of lamins is to anchor nuclear pores (61–63). VP24 disruption of lamins might then also trigger the mislocalization of proteins associated with the nuclear pore, such as Ran GTPase-activating protein (RanGAP) and Ran binding protein

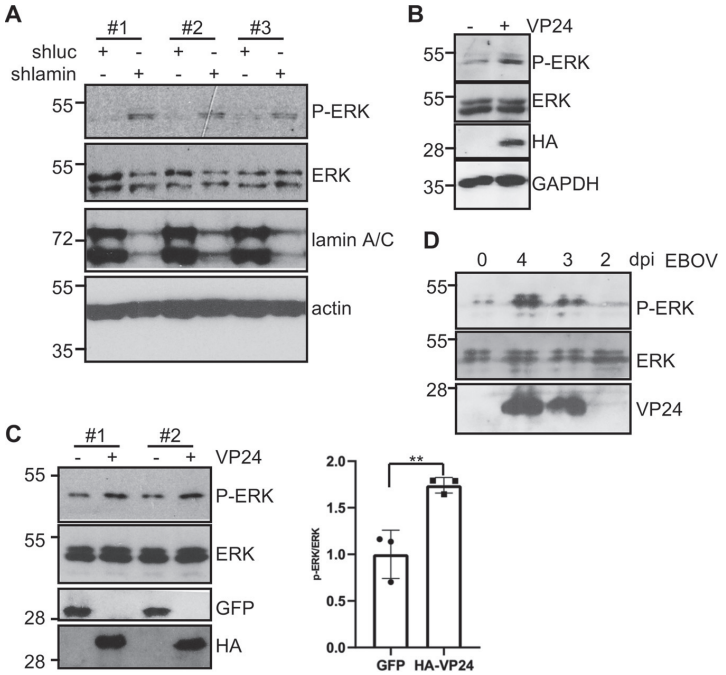

FIG 8 VP24 protein activates ERK1/2. (A) HeLa cells stably transfected with short hairpin RNA specific to luciferase (shluc) or (short hairpin RNA specific to lamin A shlamin A) plasmids were analyzed by Western blotting with the indicated antibodies. Three replicates are shown. (B) Vero cells were transfected with pcDNA or HA-VP24, and 36 h after transfection, cells were tested for the presence of phosphorylated ERK1/2 (P-ERK) and total ERK1/2, as indicated. (C) HeLa cells were transfected with the indicated plasmids, and 36 h after transfection, cells were tested for the presence of phosphorylated ERK1/2 and total ERK1/2, as indicated. Results from two different transfections are shown (left). Phospho-ERK and ERK protein intensity bands from three biological replicates were quantified using ImageJ software. The P-ERK/ERK ratios from each respective time were plotted. Data represent the mean and error bars of 3 biological replicates (right). Statistical analysis was assessed by a Student's *t* test. **, $P < 0.01$. (D) Western blotting analysis with anti-phospho-ERK, anti-ERK, and anti-VP24 antibodies in Vero cells at different times after infection with EBOV. The 0 time corresponds to mock-infected cells that were in culture for 4 days.

(RanBP). We analyzed Vero cells transfected with GFP or HA-VP24 using immunofluorescence staining with anti-RanGAP or anti-RanBP antibodies. Both RanGAP and RanBP were located at the nuclear envelope and in cytoplasmic aggregates independent of the expression of VP24 (Fig. 10A and B), suggesting that nuclear pore complexes are not altered by VP24.

Translocation and downmodulation of BAF by VP24. The interaction and structural interdependence of the nuclear envelope components lamin A, emerin, and BAF have been reported (24). Therefore, we decided to examine the distribution of BAF in cells expressing VP24. BAF was mainly detected inside the nucleus of 90% of untransfected or GFP-transfected HeLa cells, whereas BAF was mainly located in cytoplasmic granules rather than in the nucleus in 95% of those cells expressing VP24 (Fig. 11A). To evaluate whether BAF is also altered in response to EBOV infection, we carried out immunofluorescence staining using anti-BAF and anti-VP24 antibodies in HeLa cells infected with EBOV. BAF was mainly detected at the nucleus of the uninfected cells, whereas cytoplasmic dots were observed in those cells infected with EBOV (Fig. 11B). Together with the partners impact on BAF subcellular localization, phosphorylation has been also reported to influence BAF distribution (64). Therefore, we decided to analyze BAF protein in cells transfected with HA-VP24 by Western blotting. Interestingly,

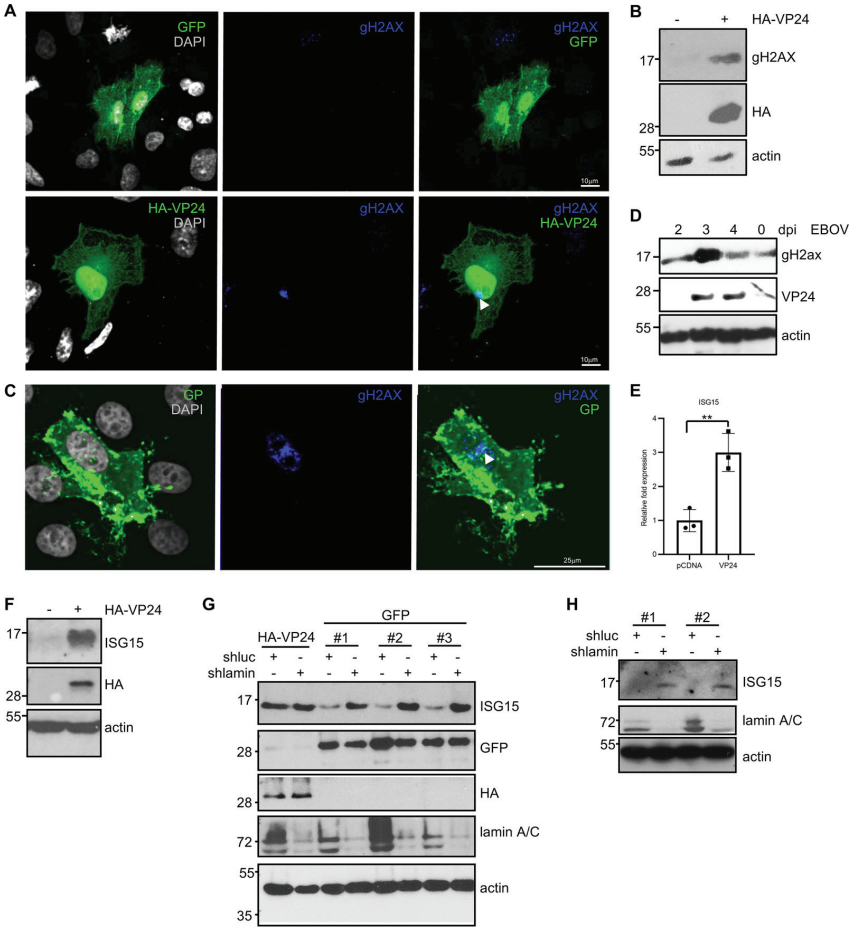

FIG 9 Induction of DNA damage and upregulation of ISG15 by VP24. (A) Immunofluorescence staining using anti-gH2AX antibody of Vero cells transfected with 0.3 μg of HA-VP24. Arrowhead indicates positive detection of gH2AX in cells expressing VP24. (B) Western blotting using anti-gH2AX antibody in Vero cells transfected with 0.3 μg of HA-VP24. (C) Immunofluorescence staining using anti-gH2AX antibody in uninfected cells (EBOV GP negative) and in cells infected with EBOV (EBOV GP positive). (D) Western blotting using anti-VP24 and anti-gH2AX antibodies in HeLa cells at different times after infection with EBOV. The 0 time corresponds to mock-infected cells that were in culture for 4 days. (E) Transcriptional transactivation of *ISG15* in response to VP24 expression by quantitative real-time PCR analysis. Columns are representative of the mean, and error bars represent the standard deviation of three biological replicates. Statistical significance was assessed by a Student's *t* test. **, $P < 0.01$. (F) A549 cells transfected with 0.3 μg of pcDNA or HA-VP24 plasmids were analyzed by Western blotting with anti-ISG15 antibody. (G) HeLa cells stably transfected with shluc or shlamin A plasmids were transfected as indicated and analyzed by Western blotting with anti-ISG15 antibody. Three replicates of HeLa cells transfected with shluc or shlamin are shown. (H) A549 cells stably transfected with shluc or shlamin A plasmids were analyzed by Western blotting with anti-ISG15 antibody. Two replicates are shown.

we also observed a clear decrease in the levels of BAF protein in HeLa (Fig. 11C) or A549 (Fig. 11D) cells transfected with VP24. We found an inverse correlation between VP24 and BAF protein levels (Fig. 11E). Furthermore, VP24 expression caused a decrease in BAF protein levels similar to that observed in cells with downmodulated lamin A/C protein (Fig. 11F). Reverse-transcription quantitative PCR (qRT-PCR) did not reveal any change in BAF expression between cells expressing or not expressing VP24 (data not shown), suggesting a posttranslational reduction of BAF.

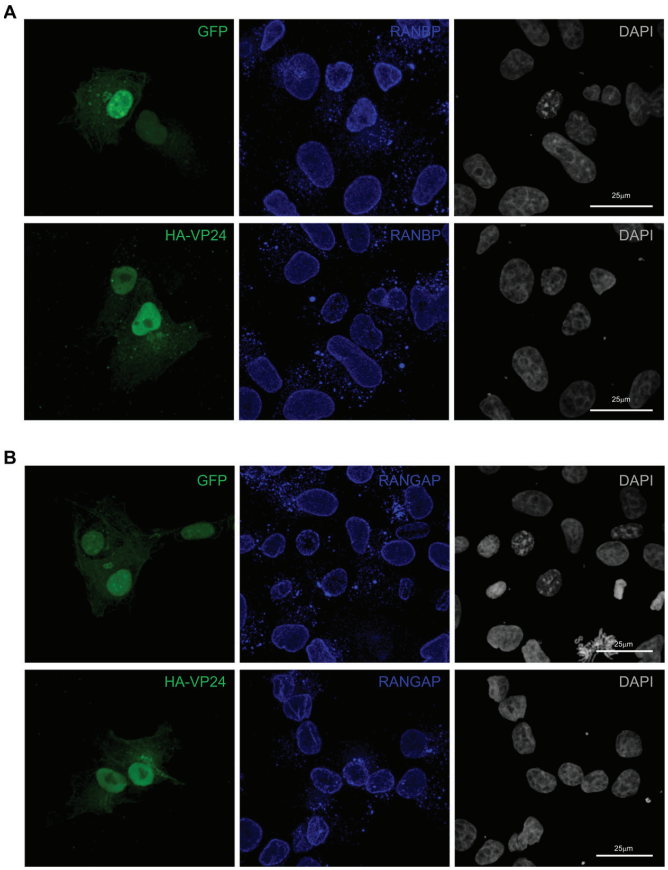

FIG 10 RanBP and RanGAP staining in VP24-expressing cells. Immunofluorescence staining using anti-RanBP (A) or anti-RanGAP (B) antibodies in Vero cells transfected with 0.3 μg GFP or HA-VP24. Chromosomes were stained with DAPI.

BAF is a chromatin-binding protein, and it has a variety of functions, including the regulation of gene expression. It has been proposed that BAF limits basal inflammation, whereas ablation of BAF results in increased expression of some ISGs, including ISG15 (65, 66). ISG15 induction upon VP24 expression is then consistent with the observed BAF downmodulation. In order to identify additional host genes whose expression is altered by VP24 expression, we investigated the transcriptional pattern of cells expressing VP24 protein. Vero cells were cotransfected with VP24 or pcDNA together with GFP at a 10:1 ratio. At 24 h after transfection, fluorescence-activated cell sorter (FACS)-sorted GFP-expressing cells were subjected to RNA sequencing (RNA-seq) analysis. We did not observe genes with a >1.5-fold change (FC) in transcript levels in VP24-expressing cells (Fig. 12A). We only detected a small group of genes slightly, but significantly, upregulated or downmodulated (>1.3- to 1.4-fold) (Fig. 12B), indicating that VP24 expression alone provoked very little change in steady-state transcript abundance in Vero cells. Most of the downmodulated genes upon VP24 expression belong to the DNA damage response pathway, whereas the transactivated genes are related to the inflammatory response (Fig. 12B). Interestingly, one of the upregulated genes was *ISG15*, confirming our previous observations. In addition, to validate the differential expression results, qRT-PCR for another upregulated gene, *CCL5*, was performed.

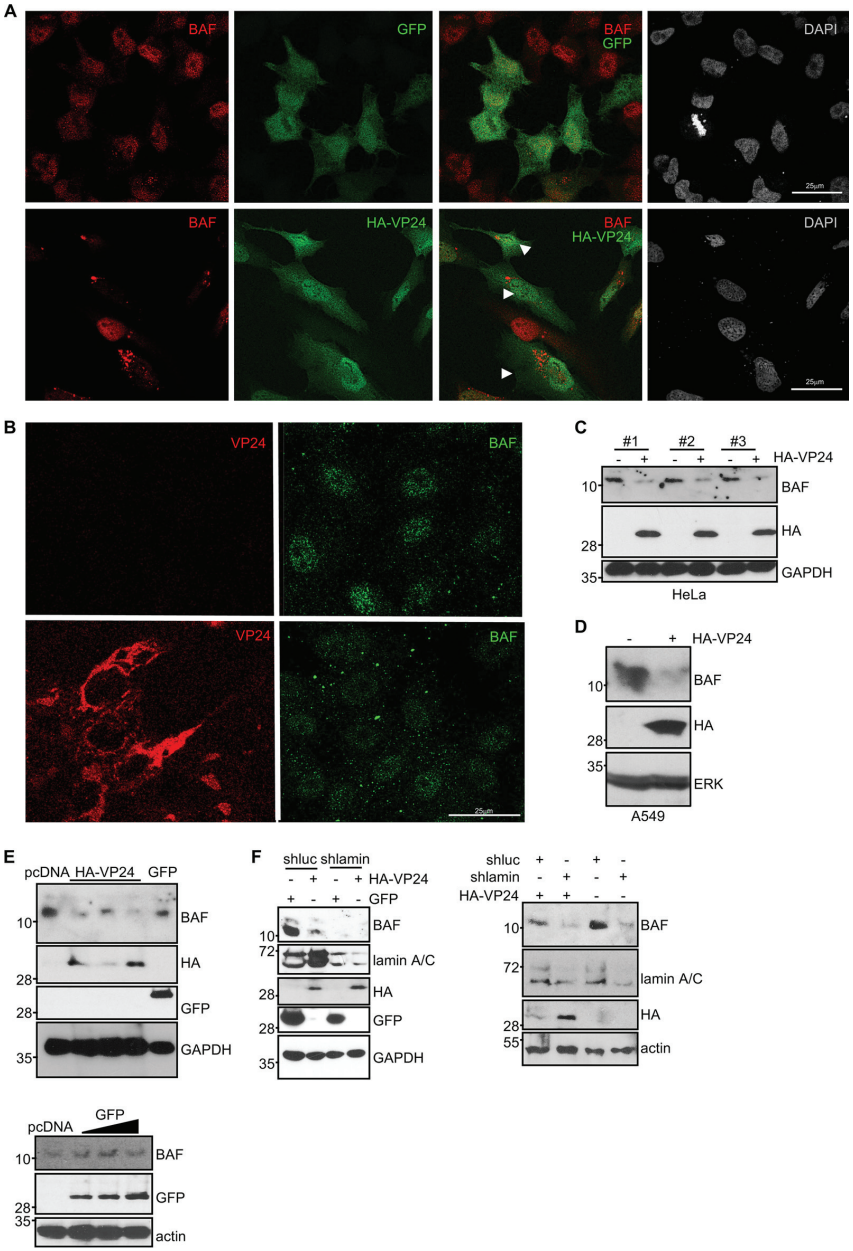

FIG 11 VP24 induces translocation and degradation of BAF. (A) Immunofluorescence staining using anti-BAF antibody in HeLa cells plated in 24-well plates and transfected with 0.3 μg of GFP or HA-VP24. Chromosomes were stained with DAPI. Arrowheads indicate cells expressing VP24. (B) Immunofluorescence staining using anti-BAF and anti-VP24 antibodies of cells infected with EBOV. (C) Western blotting of HeLa cells plated in 24-well plates and transfected with 0.3 μg of pcDNA or HA-VP24 using anti-BAF antibody. Three biological replicates are shown. (D) Western blotting of A549 cells plated in 24-well plates and transfected with 0.3 μg of pcDNA or HA-VP24 using anti-BAF antibody. (E) Western blotting of HeLa cells plated in 24-well plates and transfected with 0.3 μg of pcDNA or expressing different levels of HA-VP24 (top) or GFP (bottom) using anti-BAF antibody. (F) Western blotting of A549 cells stably transfected with shluc or shlamin plated in 24-well plates and transfected with 0.3 μg of GFP or HA-VP24 using anti-BAF antibody (left). Western blotting of HeLa cells stably transfected with shluc or shlamin plated in 24-well plates and transfected with 0.3 μg of GFP or HA-VP24 using anti-BAF antibody (right).

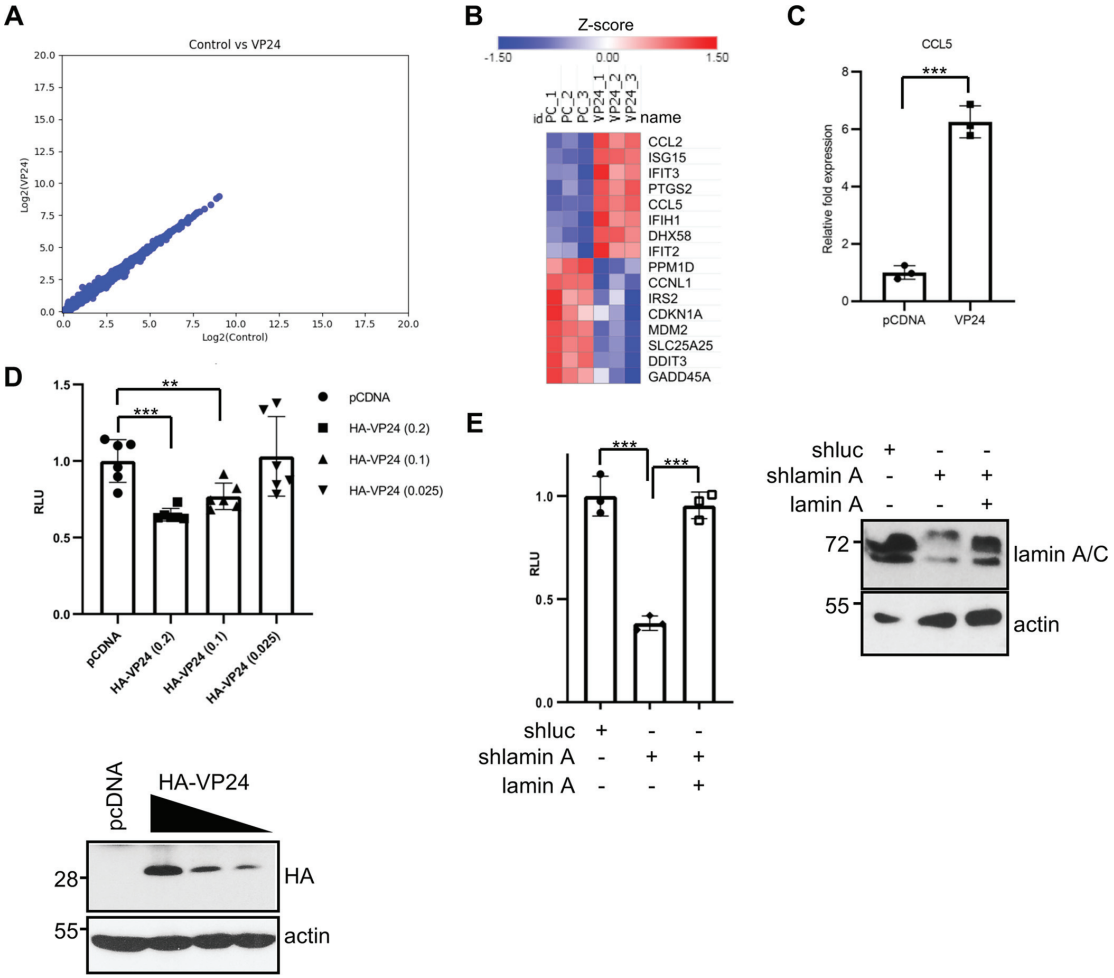

FIG 12 Transcriptional changes in response to VP24 expression. (A) Scatterplots of transcript expression data for Vero cells expressing VP24 obtained after RNA-seq analysis. (B) Heat map of genes transactivated or downmodulated (>1.3- to 1.4-fold) in response to HA-VP24 expression. (C) Transcriptional transactivation of *CCL5* in response to VP24 expression by quantitative real-time PCR analysis. Columns are representative of the mean, and error bars represent the standard deviation of three biological replicates. Statistical significance was assessed by a Student's *t* test. ***, $P < 0.001$. (D) HeLa cells were cotransfected with the luciferase reporter pREP-CSF1-luciferase plasmid together with pcDNA-beta-gal and pcDNA or the indicated doses of HA-VP24 plasmids. At 36 h after transfection, luciferase production was analyzed. Columns are representative of the mean, and error bars represent the standard deviation of six biological replicates. Statistical significance was assessed by a Student's *t* test (top). **, $P < 0.01$, ***, $P < 0.001$. Cell lysates from the experiment were analyzed by Western blotting for HA-VP24 expression (bottom). (E) HeLa cells stably transfected with shluc or shlamin were cotransfected with the luciferase reporter pREP-CSF1-luciferase plasmid together with pcDNA-beta-gal and pcDNA or a lamin A/C expression plasmid, as indicated. At 36 h after transfection, luciferase production was analyzed. Columns are representative of the mean, and error bars represent the standard deviation of three biological replicates. Similar results were obtained twice. Statistical significance was assessed by a Student's *t* test (left). ***, $P < 0.001$. Cell lysates from the experiment were analyzed by Western blotting for lamin A/C expression (right).

Results of the qRT-PCR assay confirmed the upregulation of the inflammatory cytokine *CCL5* in response to VP24 expression (Fig. 12C).

One of the genes activated by the BAF complex is the human colony-stimulating factor 1 (*CSF1*) gene (67). We then analyzed the transactivation of the CSF1-luciferase reporter in cells expressing VP24. HeLa cells were cotransfected with CSF1-luciferase together with beta-galactosidase and pcDNA or increasing doses of HA-VP24 plasmids, and 24 h after transfection, cells were harvested and assayed for luciferase and beta-galactosidase activity. We observed that VP24 inhibits luciferase expression in a dose-

dependent manner (Fig. 12D). Similar inhibition of luciferase expression was observed after lamin downmodulation (Fig. 12E). Altogether, these results suggest that downregulation of BAF by VP24 reduces the expression of BAF-inducible genes.

DISCUSSION

Here, we demonstrate that the EBOV VP24 protein interacts with emerin, lamin A/C, and lamin B, decreasing lamin A/C-emerin interaction and, consequently, inducing loss of nuclear membrane integrity. In agreement with a nuclear envelope disruption, cells expressing VP24 display several characteristics previously reported to be associated with a loss of integrity of the nuclear membrane, such as accumulation of DNA damage, alterations in nuclear size and shape, induction of ISG15, and MAPK pathway activation (53–60). Some viruses require nuclear proteins for replication; therefore, they have evolved mechanisms to overcome the barrier of the nuclear lamin (68). We propose that the lamin disruption by VP24 may facilitate access to some nuclear components or it may serve as a way to modulate signaling pathways. The MAPK pathway governs a wide range of cellular functions, including the regulation of innate immunity (69). Thus, ERK activation inhibits type I interferon production in different cell types (70–72). Consequently, many viruses usurp the pathway to their own benefit and enhance virus replication thanks to the induction of ERK phosphorylation (73–81). Induction of ERK phosphorylation may then be an additional mechanism by which VP24 interferes with IFN gene expression. But VP24 is not the unique EBOV protein able to activate ERK. Virus-like particles (VLPs) containing the viral matrix protein VP40 and the viral glycoprotein GP have also been reported to induce the activation of ERK1/2 (82), suggestive of the relevance of the MAPK pathway for EBOV replication.

Moreover, we show that expression of VP24 induces the translocation of BAF to the cytoplasm, its downmodulation, and repression of the BAF-dependent transactivation of CSF1, a regulator of the proliferation, differentiation, and survival of macrophages (83). VP24-mediated downmodulation of BAF may then be a mechanism by which VP24, cooperatively with EBOV VP35, suppresses maturation of infected human dendritic cells (11). BAF is also involved in the regulation of interferon-stimulated genes (ISGs). Upon nuclear envelope rupture, cGAS binds to the exposed genomic DNA and accumulates at the rupture site (51, 84), leading to proinflammatory activation, and its activity is prevented by BAF (65). Therefore, its downregulation as a consequence of VP24 expression may explain the counterintuitive transactivation of several proinflammatory genes also induced by IFN, such as ISG15. These results are in agreement with the VP24-mediated stimulation of the expression of cytokines, chemokines, and IFN detected at early times after EBOV infection (85). We then propose that, in addition to its well-known inhibitory activity of the IFN pathway, VP24 can still induce the transactivation of ISG15 and a subset of other ISGs in an IFN-independent manner, as previously reported (86, 87). Importantly, we also observed an alteration in BAF distribution in EBOV-infected cells. Overall, our data suggest that alterations in BAF localization and levels play a role in the inflammatory response activated by the virus.

RNA-seq experiments revealed that VP24 not only induces the upregulation of genes but also exerts transcriptional repression of several DNA damage response genes, such as *GADD45A*, *DDIT3*, or *CDKN1A*, reported previously as c-myc-regulated genes (88–90). Given the known association between ERK activation and the stabilization of c-myc mediated by its Ser62 phosphorylation (91), repression of these transcripts in response to VP24 expression may be mediated by ERK activation.

BAF has been previously shown to have antiviral activity, preventing vaccinia virus and herpes simplex type 1 (HSV-1) DNA replication (64), inhibiting retrovirus integration, and working as an epigenetic regulator of HSV lytic infection (92, 93). To counteract its antiviral effect, some viruses have evolved different strategies, such as inducing its phosphorylation (94) or altering its subcellular localization (64). To our knowledge, this study shows for the first time the downmodulation and mislocalization of BAF protein as a consequence of the expression of a viral protein, providing a likely

TABLE 1 Oligonucleotides for cloning

Oligonucleotide	Sequence
Xho-link-VP24-F	5′-GGCCCTCGAGCTCAAGCTTCGAATTCTATGGCTAAAGCTACGGGACGATAC-3′
NheI-VP24-R	5′-GCTAGCTCAGATAGCAAGAGAGCTA-3′
Xho-link-emerin-F	5′-GGCCCTCGAGCTCAAGCTTCGAATTCTATGGACAACTACGCAGATCTTTCGG-3′
NheI-emerin-R	5′-GCTAGCTCAGAAGGGGTTGCCTTCTTC-3′
Xho-link-laminA-F	5′-GGCCCTCGAGCTCAAGCTTCGAATTCTATGGAGACCCCGTCCCAGCGGCGCGC-3′
NheI-laminA-R	5′-GCTAGCTCACATGATGCTGCAGTTCTGGGG-3′

mechanistic explanation for the displacement of BAF observed in Ebola virus-infected cells (Fig. 8B).

In summary, here we identify novel activities for EBOV VP24 protein with potential impact on EBOV replication to perturb the emerin-lamin interaction and to promote BAF downmodulation, leading to the activation of the MAPK pathway, DNA damage, and dysregulation of gene expression, hallmarks for most laminopathies (95). Even though BAF carries out essential functions for the cell, little is known about its regulation. Further studies will be necessary to identify the exact molecular mechanism by which BAF levels are modulated.

MATERIALS AND METHODS

Immunofluorescence. Cells were fixed in 2% paraformaldehyde/phosphate-buffered saline (PBS) and incubated with 0.25% Triton X-100/PBS or digitonin in PBS to permeabilize the plasma and nuclear membrane or the plasma membrane, as indicated. Upon permeabilization, nonspecific binding sites were blocked with 2% bovine serum albumin (BSA)/PBS, and samples were incubated overnight with primary antibodies. Coverslips were extensively washed with PBS and further incubated with the appropriate Alexa-conjugated secondary antibodies for 1 h at room temperature. Nuclei were stained with 4′,6′-diamidino-2-phenylindole (DAPI), and preparations were mounted with ProLong Diamond antifade mounting medium (P36970) and visualized with a confocal Leica microscope.

Biomolecular fluorescence complementation assay. Cells grown on cover slides were transfected, and at 36 h, they were incubated for 3 h at 30°C. Then, cells were fixed and permeabilized with cold 100% methanol, blocked with 2% BSA/PBS, and incubated overnight with primary antibodies. Coverslips were washed extensively with PBS and further incubated with appropriate Alexa-conjugated secondary antibodies for 1 h at room temperature. Nuclei were stained with DAPI, and preparations were mounted with ProLong Diamond antifade mounting medium (P36970) and visualized with a confocal Leica microscope.

Cells, plasmids, and reagents. HEK-293, HeLa, Vero, HUH-7, and A549 cells were cultured in Dulbecco's modified Eagle's medium (DMEM) supplemented with 10% fetal bovine serum (FBS), 1% L-glutamine, and 1% penicillin/streptomycin. Transfection experiments were performed using polyethylenimine (PEI), according to the manufacturer's instructions. The plasmid encoding HA-tagged Mayinga EBOV VP24 (HA-VP24) has been previously reported (96). The plasmid encoding GFP-VP24 was generated by subcloning of the cDNA coding VP24 into the pEGFP-C1 vector (Clontech). The plasmids pTRIP-SFFV-EGFP-NLS and pTRIP-CMV-GFP-Flag-cGAS were kindly provided by Nicolas Manel (Addgene plasmids 86677 and 86675, respectively) (97). pLKO-sh-lamin A and PLKO-sh-luciferase were previously described (98). The plasmids YN-VP24, YC-laminA, YC-emerin, and YN-emerin were obtained by cloning of the coding region in the plasmids pCAGGS-eYN and pCAGGS-eYC (99) with the oligonucleotides listed in Table 1. PREP4-CSF1-luciferase plasmid was kindly provided by Keji Zhao (67). The EBOV minigenome luciferase reporter and the pcAGGS expression plasmids for Zaire EBOV strain Mayinga L, VP30, VP35, and NP (38) were kind gifts from Christopher Basler. Plasmids of the Zaire EBOV Makona minigenome system, VP35, NP, VP30, and L, were previously reported (100). Plasmids used in this study, unless specified otherwise, are derived from the Mayinga strain.

Quantitative PCR. Total RNA was purified with the RNeasy minikit (Qiagen), and reverse transcription (RT-PCR) was performed using the reverse transcription system kit (Promega). qRT-PCR was performed using SYBR green power PCR master mix in a RealPlex 4 thermocycler (Eppendorf). The oligonucleotides used are listed in Table 2.

Reporter assay. HeLa cells were cotransfected with PREP4-CSF1-luciferase plasmid, the pcDNA-beta-galactosidase plasmid, and the indicated plasmids. At 36 h after transfection, cells were harvested and analyzed. An interferon reporter assay was done as reported previously (96). Firefly luciferase values were normalized to beta-galactosidase values. Fold induction for each sample was then determined relative to the normalized luciferase activity value for pcDNA-transfected cells. Statistical significance was assessed using a Student's *t* test.

Western blotting analysis and antibodies. For Western blotting, cells were washed in PBS, scraped in SDS gel-loading buffer, and boiled for 5 min. Proteins of total extracts were separated by SDS-PAGE and transferred to nitrocellulose membranes. Monoclonal antibody against HA was purchased from BioLegend. Anti-HA goat was from Bethyl Laboratories. Anti-emerin and anti-lamin A/C antibodies were from Abcam and Cell Signaling. Anti-tubulin, anti-gH2AX, and anti-ERK were from Cell Signaling. Anti-

TABLE 2 Oligonucleotides for RT-PCR

Oligonucleotide	Sequence
GAPDH-Vero-qRT-F	5′-GTGAAGGTCGGAGTCAACGG-3′
GAPDH-Vero-qRT-R	5′-AAGACGCCAGTGGACTCCA-3′
ISG15-Vero-qRT-F	5′-GAGAGGCAGCGAACTCATCT-3′
ISG15-Vero-qRT-R	5′-CTTCAGCTCTGACACCGACA-3′
CCL5-Vero-qRT-F	5′-GCTGTCATCCTCATTGCTACAG-3′
CCL5-Vero-qRT-R	5′-TGGTGTAGAAATACTCCTTGATGTG-3′
EBOV L-qRT-F	5′-CCATCTACATCGGTGGAGCC-3′
EBOV L-qRT-R	5′-GTGGTCGTTGATGGTGGTCT-3′
EBOV VP30-qRT-F	5′-CTCGCCAAAGGAATGCAAGG-3′
EBOV VP30-qRT-R	5′-AAAGGGTCGCTACAGACGTT-3′

GAPDH, anti-actin, anti-lamin B, anti-RanGAP, anti-RanBP, and anti-phospho-ERK antibodies were from Santa Cruz Biotechnology. Anti-VP24 was from Biorbyt. Anti-VP35 and anti-NP were from Genetex. Anti-BAF antibody was from Abcam.

Infection. HeLa cells at 90% confluence were infected with EBOV (NC_002549.1) at a multiplicity of infection (MOI) of 1. All infection experiments were carried out by experienced personnel wearing positive pressure protection suits at the biosafety level 4 (BSL4) laboratory of the Bernhard Nocht Institute for Tropical Medicine in Hamburg.

Immunoprecipitation assay. Cells were lysed in radioimmunoprecipitation assay (RIPA) or BC-100 buffer at 4°C, centrifuged at 15,800 × *g* for 10 min, and immunoprecipitated overnight at 4°C after addition of the specified antibody and 30 μl of 50% protein G-sepharose (Life Technologies). Beads were then washed four times with lysis buffer and resuspended in 30 μl of loading buffer.

Minigenome assay. This assay was performed as previously described (38). Briefly, 1×10^6 HEK-293 cells were cotransfected with plasmids for the expression of the T7 polymerase (0.4 μg), pCAGGS-NP (0.49 μg), pCAGGS-VP30 (0.2 μg), pCAGGS-VP35 (0.25), pCAGGS-L (1 μg), and GFP or pTM1-eMGLuc (0.5 mg) of the EBOV Mayinga minigenome (38) together with pcDNA or HA-VP24. At 48 h after transfection, luciferase activity was analyzed.

RNA-seq. RNA-seq was carried out at the CNIC Genomics Unit. RNA quantity was measured using a Nanodrop (Thermo Scientific), and RNA integrity was measured with an Agilent 6000 Pico kit and Bioanalyzer. Total RNA (200 ng) was used to generate barcoded RNA-seq libraries using the NEBNext Ultra RNA library preparation kit (New England Biolabs). Briefly, poly A+ RNA was purified using poly T oligo-attached magnetic beads followed by fragmentation and then first and second cDNA strand synthesis. Next, cDNA 3′ ends were adenylated, and the adapters were ligated followed by PCR library amplification. Finally, the size of the libraries was checked using the Agilent 2100 Bioanalyzer DNA 1000 chip, and library concentration was determined using the Qubit fluorometer (Life Technologies). Libraries were sequenced on a HiSeq2500 (Illumina) to generate 60 bases single reads and processed with RTA v1.18.66.3. FastQ files for each sample were obtained using bcl2fastq v2.20.0.422 software (Illumina). Sequencing reads were trimmed of Illumina adapters using cutadapt 1.16 and then aligned to the African green monkey reference transcriptome (ChlSab1 v92) and quantified with RSem v1.3.1 (101, 102). Raw counts were normalized with transcripts per million (TPM) and trimmed mean of M values (TMM) methods, transformed into $\log_2$ expression ($\log_2$ [rawCount + 1]), and compared to calculate fold change (FC) and corrected *P* values. Two groups were too similar, so we could not detect any significant differential expressed with the limits of a $\log_2$ FC of >1 (2×) and a corrected *P* value of <0.05. We reduced the limits to a $\log_2$ FC of >0.4 (1.32×) and a *P* value of <0.05 and tested some of the candidates by qRT-PCR. Only mRNAs detected in almost 3 samples were used in the analysis. Heat maps were created with the Morpheus web app from the Broad Institute.

Image processing. Confocal images were analyzed for nuclear area and circularity (= 4 π [area/perimeter^2]) using ImageJ software.

Data availability. The data sets generated during the current study are available in the following link https://www.ncbi.nlm.nih.gov/geo/query/acc.cgi?acc=GSE155936.

SUPPLEMENTAL MATERIAL

Supplemental material is available online only.

FIG S1, PDF file, 0.1 MB.

FIG S2, PDF file, 0.4 MB.

FIG S3, PDF file, 2.9 MB.

FIG S4, PDF file, 0.3 MB.

FIG S5, PDF file, 1.8 MB.

ACKNOWLEDGMENTS

We thank Richard Cadagan for excellent technical support. We also thank the Microscopy CoRE at the Icahn School of Medicine at Mount Sinai for help with some of

the fluorescence microscopy studies and image analysis. We thank Christopher Basler for the plasmids of the minigenome system. We thank Keji Zhao for the pREP-CSF1-luciferase plasmid. Funding at the laboratory of C.R. is provided by Ministry of Science, Innovation and Universities and FEDER (BFU-2017-88880-P), and Xunta de Galicia (ED431G 2019/02). S.V. and R.S. are predoctoral fellows funded by Xunta de Galicia-Consellería de Cultura, Educación y Ordenación Universitaria (ED481A-2018/110 ED481A-2020/160, respectively). The funders had no role in study design, data collection and interpretation, or the decision to submit the work for publication.

REFERENCES

1. Noda T, Halfmann P, Sagara H, Kawaoka Y. 2007. Regions in Ebola virus VP24 that are important for nucleocapsid formation. J Infect Dis 196: S247–S250. https://doi.org/10.1086/520596.
2. Han Z, Boshra H, Sunyer JO, Zwiers SH, Paragas J, Harty RN. 2003. Biochemical and functional characterization of the Ebola virus VP24 protein: implications for a role in virus assembly and budding. J Virol 77:1793–1800. https://doi.org/10.1128/JVI.77.3.1793-1800.2003.
3. Huang Y, Xu L, Sun Y, Nabel GJ. 2002. The assembly of Ebola virus nucleocapsid requires virion-associated proteins 35 and 24 and posttranslational modification of nucleoprotein. Mol Cell 10:307–316. https://doi.org/10.1016/S1097-2765(02)00588-9.
4. Elliott LH, Kiley MP, McCormick JB. 1985. Descriptive analysis of Ebola virus proteins. Virology 147:169–176. https://doi.org/10.1016/0042-6822(85)90236-3.
5. Reid SP, Valmas C, Martinez O, Sanchez FM, Basler CF. 2007. Ebola virus VP24 proteins inhibit the interaction of NPI-1 subfamily karyopherin alpha proteins with activated STAT1. J Virol 81:13469–13477. https://doi.org/10.1128/JVI.01097-07.
6. Reid SP, Leung LW, Hartman AL, Martinez O, Shaw ML, Carbonnelle C, Volchkov VE, Nichol ST, Basler CF. 2006. Ebola virus VP24 binds karyopherin alpha1 and blocks STAT1 nuclear accumulation. J Virol 80:5156–5167. https://doi.org/10.1128/JVI.02349-05.
7. Mateo M, Reid SP, Leung LW, Basler CF, Volchkov VE. 2010. Ebolavirus VP24 binding to karyopherins is required for inhibition of interferon signaling. J Virol 84:1169–1175. https://doi.org/10.1128/JVI.01372-09.
8. Guito JC, Albariño CG, Chakrabarti AK, Towner JS. 2017. Novel activities by ebolavirus and marburgvirus interferon antagonists revealed using a standardized in vitro reporter system. Virology 501:147–165. https://doi.org/10.1016/j.virol.2016.11.015.
9. Zhang AP, Bornholdt ZA, Liu T, Abelson DM, Lee DE, Li S, Woods VL, Saphire EO. 2012. The Ebola virus interferon antagonist VP24 directly binds STAT1 and has a novel, pyramidal fold. PLoS Pathog 8:e1002550. https://doi.org/10.1371/journal.ppat.1002550.
10. Shabman RS, Gulcicek EE, Stone KL, Basler CF. 2011. The Ebola virus VP24 protein prevents hnRNP C1/C2 binding to karyopherin α1 and partially alters its nuclear import. J Infect Dis 204:S904–S910. https://doi.org/10.1093/infdis/jir323.
11. Lubaki NM, Ilinykh P, Pietzsch C, Tigabu B, Freiberg AN, Koup RA, Bukreyev A. 2013. The lack of maturation of Ebola virus-infected dendritic cells results from the cooperative effect of at least two viral domains. J Virol 87:7471–7485. https://doi.org/10.1128/JVI.03316-12.
12. Mateo M, Carbonnelle C, Martinez MJ, Reynard O, Page A, Volchkova VA, Volchkov VE. 2011. Knockdown of Ebola virus VP24 impairs viral nucleocapsid assembly and prevents virus replication. J Infect Dis 204: S892–S896. https://doi.org/10.1093/infdis/jir311.
13. García-Dorival I, Wu W, Dowall S, Armstrong S, Touzelet O, Wastling J, Barr JN, Matthews D, Carroll M, Hewson R, Hiscox JA. 2014. Elucidation of the Ebola virus VP24 cellular interactome and disruption of virus biology through targeted inhibition of host-cell protein function. J Proteome Res 13:5120–5135. https://doi.org/10.1021/pr500556d.
14. Batra J, Hultquist JF, Liu D, Shtanko O, Von Dollen J, Satkamp L, Jang GM, Luthra P, Schwarz TM, Small GI, Arnett E, Anantpadma M, Reyes A, Leung DW, Kaake R, Haas P, Schmidt CB, Schlesinger LS, LaCount DJ, Davey RA, Amarasinghe GK, Basler CF, Krogan NJ. 2018. Protein interaction mapping identifies RBBP6 as a negative regulator of Ebola virus replication. Cell 175:1917–1930. https://doi.org/10.1016/j.cell.2018.08.044.
15. Lin F, Blake DL, Callebaut I, Skerjanc IS, Holmer L, McBurney MW, Paulin-Levasseur M, Worman HJ. 2000. MAN1, an inner nuclear membrane protein that shares the LEM domain with lamina-associated polypeptide 2 and emerin. J Biol Chem 275:4840–4847. https://doi.org/10.1074/jbc.275.7.4840.
16. Paddy MR, Belmont AS, Saumweber H, Agard DA, Sedat JW. 1990. Interphase nuclear envelope lamins form a discontinuous network that interacts with only a fraction of the chromatin in the nuclear periphery. Cell 62:89–106. https://doi.org/10.1016/0092-8674(90)90243-8.
17. Solovei I, Wang AS, Thanisch K, Schmidt CS, Krebs S, Zwerger M, Cohen TV, Devys D, Foisner R, Peichl L, Herrmann H, Blum H, Engelkamp D, Stewart CL, Leonhardt H, Joffe B. 2013. LBR and lamin A/C sequentially tether peripheral heterochromatin and inversely regulate differentiation. Cell 152:584–598. https://doi.org/10.1016/j.cell.2013.01.009.
18. Lloyd DJ, Trembath RC, Shackleton S. 2002. A novel interaction between lamin A and SREBP1: implications for partial lipodystrophy and other laminopathies. Hum Mol Genet 11:769–777. https://doi.org/10.1093/hmg/11.7.769.
19. Margalit A, Vlcek S, Gruenbaum Y, Foisner R. 2005. Breaking and making of the nuclear envelope. J Cell Biochem 95:454–465. https://doi.org/10.1002/jcb.20433.
20. Rodríguez S, Eriksson M. 2010. Evidence for the involvement of lamins in aging. Curr Aging Sci 3:81–89. https://doi.org/10.2174/1874609811003020081.
21. Wilson KL, Foisner R. 2010. Lamin-binding proteins. Cold Spring Harb Perspect Biol 2:a000554. https://doi.org/10.1101/cshperspect.a000554.
22. Gruenbaum Y, Margalit A, Goldman RD, Shumaker DK, Wilson KL. 2005. The nuclear lamina comes of age. Nat Rev Mol Cell Biol 6:21–31. https://doi.org/10.1038/nrm1550.
23. Dechat T, Adam SA, Goldman RD. 2009. Nuclear lamins and chromatin: when structure meets function. Adv Enzyme Regul 49:157–166. https://doi.org/10.1016/j.advenzreg.2008.12.003.
24. Qi R, Xu N, Wang G, Ren H, Li S, Lei J, Lin Q, Wang L, Gu X, Zhang H, Jiang Q, Zhang C. 2015. The lamin-A/C-LAP2α-BAF1 protein complex regulates mitotic spindle assembly and positioning. J Cell Sci 128:2830–2841. https://doi.org/10.1242/jcs.164566.
25. Liu J, Lee KK, Segura-Totten M, Neufeld E, Wilson KL, Gruenbaum Y. 2003. MAN1 and emerin have overlapping function(s) essential for chromosome segregation and cell division in *Caenorhabditis elegans*. Proc Natl Acad Sci USA 100:4598–4603. https://doi.org/10.1073/pnas.0730821100.
26. Samson C, Petitalot A, Celli F, Herrada I, Ropars V, Le Du MH, Nhiri N, Jacquet E, Arteni AA, Buendia B, Zinn-Justin S. 2018. Structural analysis of the ternary complex between lamin A/C, BAF and emerin identifies an interface disrupted in autosomal recessive progeroid diseases. Nucleic Acids Res 46:10460–10473. https://doi.org/10.1093/nar/gky736.
27. Hennig T, O'Hare P. 2015. Viruses and the nuclear envelope. Curr Opin Cell Biol 34:113–121. https://doi.org/10.1016/j.ceb.2015.06.002.
28. Herrada I, Samson C, Velours C, Renault L, Östlund C, Chervy P, Puchkov D, Worman HJ, Buendia B, Zinn-Justin S. 2015. Muscular dystrophy mutations impair the nuclear envelope emerin self-assembly properties. ACS Chem Biol 10:2733–2742. https://doi.org/10.1021/acschembio.5b00648.
29. Berk JM, Simon DN, Jenkins-Houk CR, Westerbeck JW, Grønning-Wang LM, Carlson CR, Wilson KL. 2014. The molecular basis of emerin-emerin and emerin-BAF interactions. J Cell Sci 127:3956–3969.
30. He F, Melén K, Maljanen S, Lundberg R, Jiang M, Österlund P, Kakkola L, Julkunen I. 2017. Ebolavirus protein VP24 interferes with innate immune responses by inhibiting interferon-λ1 gene expression. Virology 509:23–34. https://doi.org/10.1016/j.virol.2017.06.002.
31. Sullivan T, Escalante-Alcalde D, Bhatt H, Anver M, Bhat N, Nagashima K, Stewart CL, Burke B. 1999. Loss of A-type lamin expression compromises nuclear envelope integrity leading to muscular dystrophy. J Cell Biol 147:913–920. https://doi.org/10.1083/jcb.147.5.913.

32. Fairley EA, Kendrick-Jones J, Ellis JA. 1999. The Emery-Dreifuss muscular dystrophy phenotype arises from aberrant targeting and binding of emerin at the inner nuclear membrane. J Cell Sci 112:2571–2582. https://doi.org/10.1242/jcs.112.15.2571.
33. Tsuchiya Y, Hase A, Ogawa M, Yorifuji H, Arahata K. 2001. Distinct regions specify the nuclear membrane targeting of emerin, the responsible protein for Emery-Dreifuss muscular dystrophy. Eur J Biochem 259:859–865. https://doi.org/10.1046/j.1432-1327.1999.00112.x.
34. Clements L, Manilal S, Love DR, Morris GE. 2000. Direct interaction between emerin and lamin A. Biochem Biophys Res Commun 267:709–714. https://doi.org/10.1006/bbrc.1999.2023.
35. Vaughan A, Alvarez-Reyes M, Bridger JM, Broers JL, Ramaekers FC, Wehnert M, Morris GE, Whitfield WGF, Hutchison CJ. 2001. Both emerin and lamin C depend on lamin A for localization at the nuclear envelope. J Cell Sci 114:2577–2590. https://doi.org/10.1242/jcs.114.14.2577.
36. Kolb T, Maaß K, Hergt M, Aebi U, Herrmann H. 2011. Lamin A and lamin C form homodimers and coexist in higher complex forms both in the nucleoplasmic fraction and in the lamina of cultured human cells. Nucleus 2:425–433. https://doi.org/10.4161/nucl.2.5.17765.
37. Watanabe S, Noda T, Halfmann P, Jasenosky L, Kawaoka Y. 2007. Ebola virus (EBOV) VP24 inhibits transcription and replication of the EBOV genome. J Infect Dis 196:S284–S290. https://doi.org/10.1086/520582.
38. Edwards MR, Pietzsch C, Vausselin T, Shaw ML, Bukreyev A, Basler CF. 2015. High-throughput minigenome system for identifying small-molecule inhibitors of Ebola virus replication. ACS Infect Dis 1:380–387. https://doi.org/10.1021/acsinfecdis.5b00053.
39. Hoenen T, Jung S, Herwig A, Groseth A, Becker S. 2010. Both matrix proteins of Ebola virus contribute to the regulation of viral genome replication and transcription. Virology 403:56–66. https://doi.org/10.1016/j.virol.2010.04.002.
40. Nanbo A, Watanabe S, Halfmann P, Kawaoka Y. 2013. The spatio-temporal distribution dynamics of Ebola virus proteins and RNA in infected cells. Sci Rep 3:1206. https://doi.org/10.1038/srep01206.
41. Watt A, Moukambi F, Banadyga L, Groseth A, Callison J, Herwig A, Ebihara H, Feldmann H, Hoenen T. 2014. A novel life cycle modeling system for Ebola virus shows a genome length-dependent role of VP24 in virus infectivity. J Virol 88:10511–10524. https://doi.org/10.1128/JVI.01272-14.
42. Banadyga L, Hoenen T, Ambroggio X, Dunham E, Groseth A, Ebihara H. 2017. Ebola virus VP24 interacts with NP to facilitate nucleocapsid assembly and genome packaging. Sci Rep 7:7698. https://doi.org/10.1038/s41598-017-08167-8.
43. Weis K. 2003. Regulating access to the genome: nucleocytoplasmic transport throughout the cell cycle. Cell 112:441–451. https://doi.org/10.1016/S0092-8674(03)00082-5.
44. Raharjo WH, Enarson P, Sullivan T, Stewart CL, Burke B. 2001. Nuclear envelope defects associated with LMNA mutations cause dilated cardiomyopathy and Emery-Dreifuss muscular dystrophy. J Cell Sci 114:4447–4457. https://doi.org/10.1242/jcs.114.24.4447.
45. Östlund C, Bonne G, Schwartz K, Worman HJ. 2001. Properties of lamin A mutants found in Emery-Dreifuss muscular dystrophy, cardiomyopathy and Dunnigan-type partial lipodystrophy. J Cell Sci 114:4435–4445. https://doi.org/10.1242/jcs.114.24.4435.
46. Holt I, Östlund C, Stewart CL, Man Nt, Worman HJ, Morris GE. 2003. Effect of pathogenic mis-sense mutations in lamin A on its interaction with emerin in vivo. J Cell Sci 116:3027–3035. https://doi.org/10.1242/jcs.00599.
47. Hatch EM, Fischer AH, Deerinck TJ, Hetzer MW. 2013. Catastrophic nuclear envelope collapse in cancer cell micronuclei. Cell 154:47–60. https://doi.org/10.1016/j.cell.2013.06.007.
48. Adam SA, Marr RS, Gerace L. 1990. Nuclear protein import in permeabilized mammalian cells requires soluble cytoplasmic factors. J Cell Biol 111:807–816. https://doi.org/10.1083/jcb.111.3.807.
49. Plutner H, Davidson HW, Saraste J, Balch WE. 1992. Morphological analysis of protein transport from the ER to Golgi membranes in digitonin-permeabilized cells: role of the P58 containing compartment. J Cell Biol 119:1097–1116. https://doi.org/10.1083/jcb.119.5.1097.
50. Barrowman J, Hamblet C, George CM, Michaelis S. 2008. Analysis of prelamin A biogenesis reveals the nucleus to be a CaaX processing compartment. Mol Biol Cell 19:5398–5408. https://doi.org/10.1091/mbc.e08-07-0704.
51. Denais CM, Gilbert RM, Isermann P, McGregor AL, te Lindert M, Weigelin B, Davidson PM, Friedl P, Wolf K, Lammerding J. 2016. Nuclear envelope rupture and repair during cancer cell migration. Science 352:353–358. https://doi.org/10.1126/science.aad7297.
52. Nikolova V, Leimena C, McMahon AC, Tan JC, Chandar S, Jogia D, Kesteven SH, Michalicek J, Otway R, Verheyen F, Rainer S, Stewart CL, Martin D, Feneley MP, Fatkin D. 2004. Defects in nuclear structure and function promote dilated cardiomyopathy in lamin A/C-deficient mice. J Clin Invest 113:357–369. https://doi.org/10.1172/JCI200419448.
53. Muchir A, Shan J, Bonne G, Lehnart SE, Worman HJ. 2008. Inhibition of extracellular signal-regulated kinase signaling to prevent cardiomyopathy caused by mutation in the gene encoding A-type lamins. Hum Mol Genet 18:241–247. https://doi.org/10.1093/hmg/ddn343.
54. Muchir A, Worman HJ. 2007. Emery-Dreifuss muscular dystrophy. Curr Neurol Neurosci Rep 7:78–83. https://doi.org/10.1007/s11910-007-0025-3.
55. Muchir A, Pavlidis P, Bonne G, Hayashi YK, Worman HJ. 2007. Activation of MAPK in hearts of EMD null mice: similarities between mouse models of X-linked and autosomal dominant Emery Dreifuss muscular dystrophy. Hum Mol Genet 16:1884–1895. https://doi.org/10.1093/hmg/ddm137.
56. Chen NY, Kim P, Weston TA, Edillo L, Tu Y, Fong LG, Young SG. 2018. Fibroblasts lacking nuclear lamins do not have nuclear blebs or protrusions but nevertheless have frequent nuclear membrane ruptures. Proc Natl Acad Sci USA 115:10100–10105. https://doi.org/10.1073/pnas.1812622115.
57. Kreienkamp R, Graziano S, Coll-Bonfill N, Bedia-Diaz G, Cybulla E, Vindigni A, Dorsett D, Kubben N, Batista LFZ, Gonzalo S. 2018. A cell-intrinsic interferon-like response links replication stress to cellular aging caused by progerin. Cell Rep 22:2006–2015. https://doi.org/10.1016/j.celrep.2018.01.090.
58. Gentile M, Latonen L, Laiho M. 2003. Cell cycle arrest and apoptosis provoked by UV radiation-induced DNA damage are transcriptionally highly divergent responses. Nucleic Acids Res 31:4779–4790. https://doi.org/10.1093/nar/gkg675.
59. Liu M, Hummer BT, Li X, Hassel BA. 2004. Camptothecin induces the ubiquitin-like protein, ISG15, and enhances ISG15 conjugation in response to interferon. J Interferon Cytokine Res 24:647–654. https://doi.org/10.1089/jir.2004.24.647.
60. Park JH, Yang SW, Park JM, Ka SH, Kim JH, Kong YY, Jeon YJ, Seol JH, Chung CH. 2016. Positive feedback regulation of p53 transactivity by DNA damage-induced ISG15 modification. Nat Commun 7:12513. https://doi.org/10.1038/ncomms12513.
61. Smythe C, Jenkins HE, Hutchison CJ. 2000. Incorporation of the nuclear pore basket protein nup153 into nuclear pore structures is dependent upon lamina assembly: evidence from cell-free extracts of *Xenopus* eggs. EMBO J 19:3918–3931. https://doi.org/10.1093/emboj/19.15.3918.
62. Al-Haboubi T, Shumaker DK, Köser J, Wehnert M, Fahrenkrog B. 2011. Distinct association of the nuclear pore protein Nup153 with A- and B-type lamins. Nucleus 2:500–509. https://doi.org/10.4161/nucl.2.5.17913.
63. Lussi YC, Hügi I, Laurell E, Kutay U, Fahrenkrog B. 2011. The nucleoporin Nup88 is interacting with nuclear lamin A. Mol Biol Cell 22:1080–1090. https://doi.org/10.1091/mbc.e10-05-0463.
64. Jamin A, Thunuguntla P, Wicklund A, Jones C, Wiebe MS. 2014. Barrier to auto integration factor becomes dephosphorylated during HSV-1 infection and can act as a host defense by impairing viral DNA replication and gene expression. PLoS One 9:e100511. https://doi.org/10.1371/journal.pone.0100511.
65. Guey B, Wischnewski M, Decout A, Makasheva K, Kaynak M, Sakar MS, Fierz B, Ablasser A. 2020. BAF restricts cGAS on nuclear DNA to prevent innate immune activation. Science 369:823–828. https://doi.org/10.1126/science.aaw6421.
66. Ma H, Qian W, Bambouskova M, Collins PL, Porter SI, Byrum AK, Zhang R, Artyomov M, Oltz EM, Mosammaparast N, Miner JJ, Diamond MS. 2020. Barrier-to-autointegration factor 1 protects against a basal cGAS-STING response. mBio 11:e00136-20. https://doi.org/10.1128/mBio.00136-20.
67. Liu R, Liu H, Chen X, Kirby M, Brown PO, Zhao K. 2001. Regulation of CSF1 promoter by the SWI/SNF-like BAF complex. Cell 106:309–318. https://doi.org/10.1016/S0092-8674(01)00446-9.
68. Walker EJ, Ghildyal R. 2017. Editorial: viral interactions with the nucleus. Front Microbiol 8:951. https://doi.org/10.3389/fmicb.2017.00951.
69. Dong C, Davis RJ, Flavell RA. 2002. MAP kinases in the immune response. Annu Rev Immunol 20:55–72. https://doi.org/10.1146/annurev.immunol.20.091301.131133.
70. Janovec V, Aouar B, Font-Haro A, Hofman T, Trejbalova K, Weber J, Chaperot L, Plumas J, Olive D, Dubreuil P, Nunès JA, Stranska R, Hirsch I. 2018. The MEK1/2-ERK pathway inhibits type I IFN production in plasmacytoid dendritic cells. Front Immunol 9:364. https://doi.org/10.3389/fimmu.2018.00364.
71. Christian SL, Zu D, Licursi M, Komatsu Y, Pongnopparat T, Codner DA, Hirasawa K. 2012. Suppression of IFN-induced transcription underlies

IFN defects generated by activated Ras/MEK in human cancer cells. PLoS One 7:e44267. https://doi.org/10.1371/journal.pone.0044267.
72. Chen Y, Chen J, Wang H, Shi J, Wu K, Liu S, Liu Y, Wu J. 2013. HCV-induced miR-21 contributes to evasion of host immune system by targeting MyD88 and IRAK1. PLoS Pathog 9:e1003248. https://doi.org/10.1371/journal.ppat.1003248.
73. Zhao LJ, Wang L, Ren H, Cao J, Li L, Ke JS, Qi ZT. 2005. Hepatitis C virus E2 protein promotes human hepatoma cell proliferation through the MAPK/ERK signaling pathway via cellular receptors. Exp Cell Res 305:23–32. https://doi.org/10.1016/j.yexcr.2004.12.024.
74. Schümann M, Dobbelstein M. 2006. Adenovirus-induced extracellular signal-regulated kinase phosphorylation during the late phase of infection enhances viral protein levels and virus progeny. Cancer Res 66:1282–1288. https://doi.org/10.1158/0008-5472.CAN-05-1484.
75. Liao B, Zhou H, Liang H, Li C. 2017. Regulation of ERK and AKT pathways by hepatitis B virus X protein via the Notch1 pathway in hepatocellular carcinoma. Int J Oncol 51:1449–1459. https://doi.org/10.3892/ijo.2017.4126.
76. Woodson EN, Kedes DH. 2012. Distinct roles for extracellular signal-regulated kinase 1 (ERK1) and ERK2 in the structure and production of a primate gammaherpesvirus. J Virol 86:9721–9736. https://doi.org/10.1128/JVI.00695-12.
77. Colao I, Pennisi R, Venuti A, Nygårdas M, Heikkilä O, Hukkanen V, Sciortino MT. 2017. The ERK-1 function is required for HSV-1-mediated G1/S progression in HEP-2 cells and contributes to virus growth. Sci Rep 7:9176. https://doi.org/10.1038/s41598-017-09529-y.
78. Rodems SM, Spector DH. 1998. Extracellular signal-regulated kinase activity is sustained early during human cytomegalovirus infection. J Virol 72:9173–9180. https://doi.org/10.1128/JVI.72.11.9173-9180.1998.
79. Sharma-Walia N, Krishnan HH, Naranatt PP, Zeng L, Smith MS, Chandran B. 2005. ERK1/2 and MEK1/2 induced by Kaposi's sarcoma-associated herpesvirus (human herpesvirus 8) early during infection of target cells are essential for expression of viral genes and for establishment of infection. J Virol 79:10308–10329. https://doi.org/10.1128/JVI.79.16.10308-10329.2005.
80. Pleschka S. 2008. RNA viruses and the mitogenic Raf/MEK/ERK signal transduction cascade. Biol Chem 389:1273–1282. https://doi.org/10.1515/BC.2008.145.
81. Albarnaz JD, De Oliveira LC, Torres AA, Palhares RM, Casteluber MC, Rodrigues CM, Cardozo PL, De Souza AM, Pacca CC, Ferreira PC, Kroon EG, Nogueira ML, Bonjardim CA. 2014. MEK/ERK activation plays a decisive role in yellow fever virus replication: implication as an antiviral therapeutic target. Antiviral Res 111:82–92. https://doi.org/10.1016/j.antiviral.2014.09.004.
82. Martinez O, Valmas C, Basler CF. 2007. Ebola virus-like particle-induced activation of NF-κB and Erk signaling in human dendritic cells requires the glycoprotein mucin domain. Virology 364:342–354. https://doi.org/10.1016/j.virol.2007.03.020.
83. Stanley IJ, Burgess AW. 1983. Granulocyte macrophage-colony stimulating factor stimulates the synthesis of membrane and nuclear proteins in murine neutrophils. J Cell Biochem 23:241–258. https://doi.org/10.1002/jcb.240230121.
84. Earle AJ, Kirby TJ, Fedorchak GR, Isermann P, Patel J, Iruvanti S, Moore SA, Bonne G, Wallrath LL, Lammerding J. 2020. Mutant lamins cause nuclear envelope rupture and DNA damage in skeletal muscle cells. Nat Mater 19:464–473. https://doi.org/10.1038/s41563-019-0563-5.
85. Ilinykh PA, Lubaki NM, Widen SG, Renn LA, Theisen TC, Rabin RL, Wood TG, Bukreyev A. 2015. Different temporal effects of Ebola virus VP35 and VP24 proteins on global gene expression in human dendritic cells. J Virol 89:7567–7583. https://doi.org/10.1128/JVI.00924-15.
86. Barber GN. 2011. Innate immune DNA sensing pathways: STING, AIMII and the regulation of interferon production and inflammatory responses. Curr Opin Immunol 23:10–20. https://doi.org/10.1016/j.coi.2010.12.015.
87. Hiscott J. 2007. Triggering the innate antiviral response through IRF-3 activation. J Biol Chem 282:15325–15329. https://doi.org/10.1074/jbc.R700002200.
88. Seoane J, Le HV, Massagué J. 2002. Myc suppression of the *p21^{Cip1}* Cdk inhibitor influences the outcome of the p53 response to DNA damage. Nature 419:729–734. https://doi.org/10.1038/nature01119.
89. Ciribilli Y, Singh P, Spanel R, Inga A, Borlak J. 2015. Decoding c-Myc networks of cell cycle and apoptosis regulated genes in a transgenic mouse model of papillary lung adenocarcinomas. Oncotarget 6:31569–31592. https://doi.org/10.18632/oncotarget.5035.
90. Barsyte-Lovejoy D, Mao DY, Penn LZ. 2004. c-Myc represses the proximal promoters of GADD45a and GADD153 by a post-RNA polymerase II recruitment mechanism. Oncogene 23:3481–3486. https://doi.org/10.1038/sj.onc.1207487.
91. Sears R, Nuckolls F, Haura E, Taya Y, Tamai K, Nevins JR. 2000. Multiple Ras-dependent phosphorylation pathways regulate Myc protein stability. Genes Dev 14:2501–2514. https://doi.org/10.1101/gad.836800.
92. Wiebe MS, Jamin A. 2016. The barrier to autointegration factor: interlocking antiviral defense with genome maintenance. J Virol 90:3806–3809. https://doi.org/10.1128/JVI.00178-16.
93. Oh HS, Traktman P, Knipe DM. 2015. Barrier-to-autointegration factor 1 (BAF/BANF1) promotes association of the SETD1A histone methyltransferase with herpes simplex virus immediate-early gene promoters. mBio 6:e00345-15. https://doi.org/10.1128/mBio.00345-15.
94. Nichols RJ, Wiebe MS, Traktman P. 2006. The vaccinia-related kinases phosphorylate the N′ terminus of BAF, regulating its interaction with DNA and its retention in the nucleus. Mol Biol Cell 17:2451–2464. https://doi.org/10.1091/mbc.e05-12-1179.
95. Maciejowski J, Hatch EM. 2020. Nuclear Membrane Rupture and Its Consequences. Annu Rev Cell Dev Biol 36:85–114. https://doi.org/10.1146/annurev-cellbio-020520-120627.
96. Vidal S, El Motiam A, Seoane R, Preitakaite V, Bouzaher YH, Gómez-Medina S, San Martín C, Rodríguez D, Rejas MT, Baz-Martínez M, Barrio R, Sutherland JD, Rodríguez MS, Muñoz-Fontela C, Rivas C. 2019. Regulation of the Ebola virus VP24 protein by SUMO. J Virol 94:e01687-19 https://doi.org/10.1128/JVI.01687-19.
97. Raab M, Gentili M, de Belly H, Thiam HR, Vargas P, Jimenez AJ, Lautenschlaeger F, Voituriez R, Lennon-Duménil AM, Manel N, Piel M. 2016. ESCRT III repairs nuclear envelope ruptures during cell migration to limit DNA damage and cell death. Science 352:359–362. https://doi.org/10.1126/science.aad7611.
98. Redwood AB, Perkins SM, Vanderwaal RP, Feng Z, Biehl KJ, Gonzalez-Suarez I, Morgado-Palacin L, Shi W, Sage J, Roti-Roti JL, Stewart CL, Zhang J, Gonzalo S. 2011. A dual role for A-type lamins in DNA double-strand break repair. Cell Cycle 10:2549–2560. https://doi.org/10.4161/cc.10.15.16531.
99. Sánchez-Aparicio MT, Ayllón J, Leo-Macias A, Wolff T, García-Sastre A. 2017. Subcellular localizations of RIG-I, TRIM25, and MAVS complexes. J Virol 91:e01155-16 https://doi.org/10.1128/JVI.01155-16.
100. García-Dorival I, Wu W, Armstrong SD, Barr JN, Carroll MW, Hewson R, Hiscox JA. 2016. Elucidation of the cellular interactome of Ebola virus nucleoprotein and identification of therapeutic targets. J Proteome Res 15:4290–4303. https://doi.org/10.1021/acs.jproteome.6b00337.
101. Li B, Dewey CN. 2011. RSEM: accurate transcript quantification from RNA-seq data with or without a reference genome. BMC Bioinformatics 12:323. https://doi.org/10.1186/1471-2105-12-323.
102. Martin M. 2011. Cutadapt removes adapter sequences from high-throughput sequencing reads. EMBnet J 17:1–10. https://doi.org/10.14806/ej.17.1.200.